



저작자표시-비영리-변경금지 2.0 대한민국

이용자는 아래의 조건을 따르는 경우에 한하여 자유롭게

- 이 저작물을 복제, 배포, 전송, 전시, 공연 및 방송할 수 있습니다.

다음과 같은 조건을 따라야 합니다:



저작자표시. 귀하는 원저작자를 표시하여야 합니다.



비영리. 귀하는 이 저작물을 영리 목적으로 이용할 수 없습니다.



변경금지. 귀하는 이 저작물을 개작, 변형 또는 가공할 수 없습니다.

- 귀하는, 이 저작물의 재이용이나 배포의 경우, 이 저작물에 적용된 이용허락조건을 명확하게 나타내어야 합니다.
- 저작권자로부터 별도의 허가를 받으면 이러한 조건들은 적용되지 않습니다.

저작권법에 따른 이용자의 권리는 위의 내용에 의하여 영향을 받지 않습니다.

이것은 [이용허락규약\(Legal Code\)](#)을 이해하기 쉽게 요약한 것입니다.

[Disclaimer](#)

A THESIS
FOR THE DEGREE OF DOCTOR OF PHILOSOPHY

**Cosmeceutical effect of fucoidan isolated from
brown seaweed, *Hizikia fusiforme* collected from
Jeju Island**

Lei Wang

Department of Marine Life Sciences

GRADUATE SCHOOL

JEJU NATIONAL UNIVERSITY

February, 2019

Cosmeceutical effect of fucoidan isolated from brown seaweed, *Hizikia fusiforme* collected from Jeju Island

Lei Wang

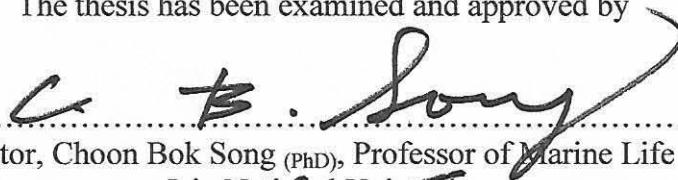
(Supervised by Professor You-Jin Jeon)

A thesis submitted in partial fulfilment of the requirement for the degree of

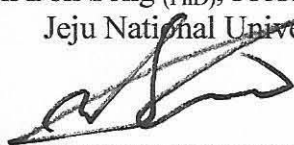
DOCTOR OF PHILOSOPHY

February 2019

The thesis has been examined and approved by



.....
Thesis director, Choon Bok Song (PhD), Professor of Marine Life Sciences,
Jeju National University



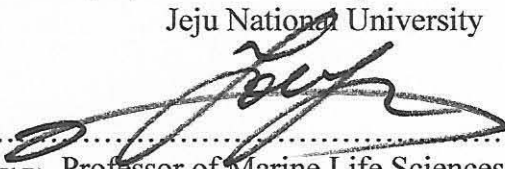
.....
Soo-Jin Heo (PhD), Principle senior scientist, Korea Institute of Ocean Science and
Technology



.....
Gi-Young Kim (PhD), Professor of Marine Life Sciences, Jeju National University



.....
Young-Heun Jee (PhD), Professor of Department of Veterinary Medicine,
Jeju National University



.....
You-Jin Jeon (PhD), Professor of Marine Life Sciences, Jeju National University

02/2019
Date

Department of Marine Life Sciences

Graduate School

Jeju National University

Republic of Korea

CONTENT

SUMMARY	i
LIST OF TABLE	iv
LIST OF FIGURE.....	v
Part I.....	1
Extraction and bioactivity scavenging of seaweeds.....	1
ABSTRACT.....	2
INTRODUCTION	4
1. Materials and Methods.....	7
1.1. Reagents and chemicals	7
1.2. Collection and process of seaweed samples	7
1.3. Water and ethanol extraction	10
1.4. Enzyme-assisted extraction	10
1.5. Determination of chemical composition of seaweed extracts	14
1.5.1. Analysis of polysaccharide content of seaweed extracts.....	14
1.5.2. Analysis of total phenolic content of seaweed extracts.....	14
1.5.3. Analysis of protein content of seaweed extracts	15
1.6. Evaluation of the free radical scavenging activity of seaweed extracts	15

1.7. Measurement of mushroom tyrosinase inhibitory effects of seaweed extracts	15
1.8. Measurement of collagenase inhibitory effects of seaweed extracts.....	15
1.9. Measurement of elastase inhibitory effects of seaweed extracts.....	16
2. Results and Discussion	17
2.1. Extraction yield and proximate composition of seaweed extracts	17
2.2. Free radical scavenging activities of seaweed extracts	23
2.3. Tyrosinase inhibitory effects of seaweed extracts.....	29
2.4. Collagenase inhibitory effects of seaweed extracts.....	31
2.5. Elastase inhibitory effects of seaweed extracts	33
CONCLUSION.....	35
Part II.	37
Preparation of crude polysaccharides of <i>Hizikia fusiforme</i> (HFCPS) and evaluation of its bioactivities	37
ABSTRACT.....	37
INTRODUCTION	38
Section 1: Celluclast-assisted extraction of <i>Hizikia fusiforme</i> and separation of polysaccharides from Celluclast-assisted extract of <i>Hizikia fusiforme</i>	40
Abstract.....	40

1. Materials and Methods.....	41
1.1. Reagents and chemicals.....	41
1.2. Preparation of polysaccharides from <i>H. fusiforme</i>	41
1.3. Chemical analysis of HFC and HFCPS.....	41
2. Results and Discussion	43
2.1. Yield, total carbohydrate, phenolic, and sulfate content of HFC and HFCPS	43
2.2. Natural sugar composition of HFC and HFCPS.....	43
3. Conclusion	47
Section 2: Antioxidant activity of polysaccharides from Celluclast-assisted extract of <i>Hizikia fusiforme</i> <i>in vitro</i> in Vero cells and <i>in vivo</i> in zebrafish	48
Abstract.....	48
1. Materials and methods	49
1.1. Reagents and Chemicals.....	49
1.2. Evaluation of free radical scavenging activities of HFC and HFCPS.....	49
1.3. Cell culture	49
1.4. Determination of the cytotoxicity of HFCPS on Vero cells.....	50
1.5. Determination of the protective effect of HFCPS against H ₂ O ₂ -induced intracellular ROS generation in Vero cells.....	50

1.6. Measurement of the protective effect of HFCPS against H ₂ O ₂ -induced cytotoxicity in Vero cells.....	50
1.7. Nuclear staining with Hoechst 33342.....	50
1.8. Maintenance of zebrafish.....	51
1.9. Application of HFCPS and H ₂ O ₂ to zebrafish embryos	51
1.10. Determination of heart-beating rate, ROS generation, and cell death in zebrafish.....	51
1.11. Statistical analysis.....	52
2. Results and Discussion	53
2.1. Free radical scavenging activities of HFC and HFCPS.....	53
2.2. Cytotoxicity of HFCPS on Vero cells	53
2.3. Protective effect of HFCPS against H ₂ O ₂ -induced oxidative stress in Vero cells.....	56
2.4. Protective effect of HFCPS against H ₂ O ₂ -induced apoptosis	56
2.5. HFCPS improve survival rate and reduce heart-beating rate in H ₂ O ₂ -induced zebrafish.....	59
2.6. Protective effect of HFCPS against H ₂ O ₂ -induced ROS generation and cell death in zebrafish.....	59
3. Conclusion	63

Section 3: Anti-inflammatory effect of polysaccharides from Celluclast-assisted extract of <i>Hizikia fusiforme</i>	64
Abstract.....	64
1. Materials and methods	65
1.1. Reagents and Chemicals.....	65
1.2. Cell culture	65
1.3. Measurement of NO production and cell viability	65
1.4. Measurement of PGE ₂ and pro-inflammatory cytokines (TNF- α , IL-1 β , and IL-6) production	66
1.5. Western blot analysis.....	66
1.6. Statistical analysis.....	67
2. Results and Discussion	68
2.1. The effect of HFCPS on LPS-induced NO generation and cytotoxicity in RAW 264.7 macrophages.....	68
2.2. HFCPS decreased PGE ₂ and pro-inflammatory cytokines release in LPS-induced RAW 264.7 macrophages.....	68
2.3. HFCPS inhibited the expression of iNOS and COX-2 in LPS-induced RAW 264.7 macrophages	71
3. Conclusion	73

Section 4: Whitening effect of polysaccharides from Celluclast-assisted extract of <i>Hizikia fusiforme</i>	74
Abstract.....	74
1. Materials and methods	75
1.1. Reagents and Chemicals.....	75
1.2. Measurement of the mushroom tyrosinase inhibitory effect of HFCPS	75
1.3. Cell culture	75
1.4. Cytotoxicity assay.....	76
1.5. Determination of cellular melanin content	76
1.6. Measurement of intracellular tyrosinase activity.....	76
1.7. Western blot analysis.....	77
1.8. Statistical analysis.....	77
2. Results and Discussion	78
2.1. Tyrosinase inhibitory activity of HFCPS	78
2.2. Cytotoxicity of HFCPS.....	78
2.3. Effect of HFCPS on melanin synthesis in α -MSH-stimulated B16F10 cells	78
2.4. Effect of HFCPS on intracellular tyrosinase activity in α -MSH-stimulated B16F10 cells.....	79

2.5. Effect of HFCPS on tyrosinase, TRP-1, TRP-2, and MITF expression in α -MSH-stimulated B16F10 cells	83
3. Conclusion	85
Section 5: UV protective effect of polysaccharides from Celluclast-assisted extract of <i>Hizikia fusiforme</i>	86
Abstract	86
1. Materials and methods	87
1.1. Reagents and Chemicals	87
1.2. Cell culture and UVB irradiation	87
1.3. Determination of cytotoxicity of HFCPS on HaCaT cells	87
1.4. Measurement of intracellular ROS generation in UVB-irradiated HaCaT cells	88
1.5. Determination of cell viability	88
1.6. Measurement of apoptosis body formation	88
1.7. Maintenance of zebrafish	89
1.8. Application of HFCPS and UVB to zebrafish	89
1.9. Statistical Analysis	90
2. Results and Discussion	91
2.1. Cytotoxicity of HFCPS on HaCaT cells	91

2.2. Effect of HFCPS on intracellular ROS generation and cell death in UVB-irradiated HaCaT cells	91
2.3. Effect of HFCPS on apoptosis formation in UVB-irradiated HaCaT cells.	94
2.4. Effect of HFCPS on ROS generation, cell death, NO production, and lipid peroxidation in UVB-irradiated zebrafish	96
3. Conclusion	101
Section 6: Anti-wrinkle effect of polysaccharides from Celluclast-assisted extract of <i>Hizikia fusiforme</i>	102
Abstract	102
1. Materials and methods	103
1.1. Reagents and Chemicals	103
1.2. Measurement of collagenase inhibitory effect of HFCPS	103
1.3. Measurement of elastase inhibitory effect of HFCPS	104
1.4. Cell culture and UVB-irradiation	104
1.5. Determination of cytotoxicity of HFCPS and UVB irradiation on HDF cells	104
1.6. Determination of the effect of HFCPS against UVB-induced HDF cell damage	105
1.7. Determination of relative intracellular elastase and collagenase activities on UVB-irradiated HDF cells	105

1.8. Determination of collagen synthesis level and MMPs expression levels on UVB-irradiated HDF cells.....	106
1.9. Western blot analysis.....	106
1.10. Statistical Analysis	107
2. Results and Discussion	108
2.1. HFCPS inhibits collagenase from <i>Clostridium Histolyticum</i> and elastase from porcine pancreas	108
2.2. HFCPS promotes HDF cell proliferation and UVB irradiation damages HDF cells.....	110
2.3. HFCPS improves cell viability and reduces intracellular ROS in UVB-irradiated HDF cells.....	112
2.4. HFCPS inhibits intracellular collagenase and elastase activities in UVB-irradiated HDF cells.....	112
2.5. HFCPS protects collagen synthesis and reduces MMPs expression levels in UVB-irradiated HDF cells.....	115
2.6. HFCPS inhibits NF- κ B activation, reduces AP-1 phosphorylation, and suppress MAPKs activation in UVB-induced HDF cells.....	115
3. Conclusion	119
CONCLUSION.....	120
Part III.	122

Isolation of fucoidan from crude polysaccharides of <i>Hizikia fusiforme</i> and evaluation of its bioactivities.....	122
ABSTRACT.....	122
INTRODUCTION	123
Section 1: Isolation fucoidan from crude polysaccharides from Celluclast-assisted extract of <i>Hizikia fusiforme</i>	125
Abstract.....	125
1. Materials and Methods.....	126
1.1. Reagents and chemicals.....	126
1.2. Separation of fucoidan from HFCPS.....	126
1.3. Chemical analysis of fractions separated from HFCPS.....	126
1.4. Evaluation of the free radical scavenging activity of seaweed extracts	127
1.5. Measurement of mushroom tyrosinase inhibitory effects of seaweed extracts	127
1.6. Measurement of collagenase inhibitory effects of seaweed extracts.....	128
1.7. Measurement of elastase inhibitory effects of seaweed extracts.....	128
1.8. Characterization of the purified fucoidan from HFCPS by Fourier transform infrared (FT-IR) spectroscopy	128
2. Results and Discussion	129

2.1. Total carbohydrate, phenolic, and sulfate content of fractions separated from HFCPS	129
2.2. Natural sugar composition of fractions separated from HFCPS	129
2.3. Free radical scavenging activities of fractions separated from HFCPS	132
2.4. Tyrosinase inhibitory effects of fractions from HFCPS	134
2.5. Collagenase inhibitory effects of fractions from HFCPS	134
2.6. Elastase inhibitory effects of fractions from HFCPS	134
2.7. FT-IR analysis of purified fucoidan	135
3. Conclusion	140
Section 2: Antioxidant activity of <i>Hizikia</i> fucoidan <i>in vitro</i> in Vero cells and <i>in vivo</i> in zebrafish.....	141
Abstract.....	141
1. Materials and methods	142
1.1. Reagents and Chemicals.....	142
1.2. Cell culture	142
1.3. Determination of the protective effect of HFCPSF4 against H ₂ O ₂ -induced intracellular ROS generation in Vero cells.....	142
1.4. Measurement of the protective effect of HFCPSF4 against H ₂ O ₂ -induced cytotoxicity in Vero cells.....	143
1.5. Nuclear staining with Hoechst 33342.....	143

1.6. Western blot analysis.....	143
1.7. Application of HFCPSF4 and H ₂ O ₂ to zebrafish embryos.....	144
1.8. Determination of heart-beating rate, ROS generation, cell death, and lipid peroxidation in zebrafish	144
1.9. Statistical analysis.....	144
2. Results and Discussion	145
2.1. Protective effect of HFCPSF4 against H ₂ O ₂ -induced oxidative stress in Vero cells.....	145
2.2. Protective effect of HFCPSF4 against H ₂ O ₂ -induced apoptosis	145
2.3. HFCPSF4 improves the expression of catalase and SOD-1 via regulating Nrf2/HO-1 pathway in H ₂ O ₂ -induced Vero cells.....	148
2.4. HFCPSF4 improves survival rate and reduces heart-beating rate in H ₂ O ₂ -induced zebrafish	152
2.5. Protective effect of HFCPSF4 against H ₂ O ₂ -induced ROS generation, cell death, and lipid peroxidation in zebrafish	152
3. Conclusion	157
Section 3: Anti-inflammatory effect of <i>Hizikia</i> fucoidan <i>in vitro</i> in RAW 264.7 macrophages and <i>in vivo</i> in zebrafish	158
Abstract.....	158
1. Materials and methods	159

1.1. Reagents and Chemicals.....	159
1.2. Cell culture	159
1.3. Measurement of NO production and cell viability	159
1.4. Measurement of PGE ₂ and pro-inflammatory cytokine (TNF- α , IL-1 β , and IL-6) production	160
1.5. Western blot analysis.....	160
1.6. Application of HFCPSF4 and LPS to zebrafish embryos	160
1.7. Determination of heart-beating rate, ROS generation, cell death, and NO generation in zebrafish.....	161
1.8. Statistical analysis.....	161
2. Results and Discussion	162
2.1. The effect of HFCPSF4 on LPS-induced NO generation and cytotoxicity in RAW 264.7 macrophages.....	162
2.2. HFCPSF4 decreased PGE ₂ and pro-inflammatory cytokines release in LPS-induced RAW 264.7 macrophages.....	162
2.3. HFCPSF4 inhibited the expression of iNOS and COX-2 in LPS-induced RAW 264.7 macrophages.....	165
2.4. HFCPSF4 inhibited NF- κ B in LPS-induced RAW 264.7 macrophages...	165
2.5. HFCPSF4 improved survival rate and reduced heart-beating rate in LPS-induced zebrafish.....	169

2.6. Protective effect of HFCPSF4 against LPS-induced ROS generation, cell death, and NO production in zebrafish.....	169
3. Conclusion	174
Section 4: Whitening effect <i>Hizikia</i> fucoidan isolated from HFCPS <i>in vitro</i> in B16F10 melanoma cells.....	175
Abstract.....	175
1. Materials and methods	176
1.1. Reagents and Chemicals	176
1.2. Cell culture	176
1.3. Cytotoxicity assay.....	176
1.4. Determination of cellular melanin contents.....	177
1.5. Western blot analysis	177
1.6. Statistical analysis.....	177
2. Results and Discussion	179
2.1. Cytotoxicity of HFCPSF4	179
2.2. Effect of HFCPSF4 on melanin synthesis in α -MSH-stimulated B16F10 cells	179
2.3. Effect of HFCPSF4 on tyrosinase, TRP-1, TRP-2, and MITF levels and ERK-MAPK phosphorylation in α -MSH-stimulated B16F10 cells.....	182
3. Conclusion	186

Section 5: UV protective effect of <i>Hizikia</i> fucoidan isolated from HFCPS <i>in vitro</i> in HaCaT cells and <i>in vivo</i> in zebrafish	187
Abstract.....	187
1. Materials and methods	188
1.1. Reagents and Chemicals.....	188
1.2. Cell culture and UVB irradiation.....	188
1.3. Measurement of intracellular ROS generation in UVB-irradiated HaCaT cells.....	188
1.4. Determination of cell viability.....	189
1.5. Measurement of apoptosis body formation	189
1.6. Western blot analysis.....	189
1.7. Application of HFCPSF4 and UVB to zebrafish.....	190
1.8. Statistical Analysis	190
2. Results and Discussion	191
2.1. Effect of HFCPSF4 on intracellular ROS generation and cell death in UVB-irradiated HaCaT cells	191
2.2. Effect of HFCPSF4 on apoptosis formation in UVB-irradiated HaCaT cells	191
2.3. Effect of HFCPSF4 on Bax/Bcl-xL, PARP, and cleaved caspass-3 levels in UVB-irradiated HaCaT cells	194

2.4. Effect of HFCPSF4 on ROS generation, cell death, NO production, and lipid peroxidation in UVB-irradiated zebrafish	197
3. Conclusion	202
Section 6: Anti-wrinkle effect of <i>Hizikia</i> fucoidan isolated from HFCPS <i>in vitro</i> in human dermal fibroblasts.....	203
Abstract.....	203
1. Materials and methods	204
1.1. Reagents and Chemicals	204
1.2. Cell culture and UVB-irradiation	204
1.3. Determination of the effect of HFCPSF4 against UVB-induced HDF cell damage.....	205
1.4. Determination of relative intracellular elastase and collagenase activities on UVB-irradiated HDF cells.....	205
1.5. Determination of collagen synthesis level, MMPs expression levels, pro-inflammatory cytokines levels on UVB-irradiated HDF cells.....	206
1.6. Western blot analysis	206
1.7. Statistical Analysis	207
2. Results and Discussion	208
2.1. HFCPSF4 improves cell viability and reduces intracellular ROS in UVB-irradiated HDF cells.....	208

2.2. HFCPSF4 inhibits intracellular collagenase and elastase activities in UVB-irradiated HDF cells.....	208
2.3. HFCPSF4 protects collagen synthesis and reduces MMPs and pro-inflammatory cytokines expression levels in UVB-irradiated HDF cells .	211
2.4. HFCPSF4 inhibits NF- κ B activation, reduces AP-1 phosphorylation, and suppresses MAPKs activation in UVB-irradiated HDF cells.....	211
3. Conclusion	217
CONCLUSION.....	218
REFERENCES	219
ACKNOWLEDGEMENT	235

SUMMARY

In human, skin is the largest organ of the integumentary system. Skin is outer covering of the body and plays an important immunity role because of its protective effect against pathogens. Skin undergoes chronological aging like other organs. In addition, it undergoes aging as a consequence of environmental damage because it is direct exposure to the outside environment. The environmental factors, such as chemicals, air pollution, fine dust particles, and ultraviolet (UV) irradiation, which bring toxicity or stress to human skin and induce skin aging. In these environmental factors, UV irradiation from sunlight is the primary environmental factor that causes human skin aging and results in pigment accumulation and wrinkle formation.

UV can be classified into three subtypes of UVA, UVB, and UVC, based on the wavelength. UVB has a medium wavelength and is thought to bring more cellular stress to humans compared to the other two subtypes. UVB is known to be associated with human health through stimulating reactive oxygen species (ROS) generation. The excessive ROS induce oxidative stress and apoptosis, as well as damage cellular components including proteins, lipids, and DNA. In addition, ROS activate cell signaling pathways including nuclear factor kappa B (NF- κ B), activator protein 1 (AP-1), and mitogen-activated protein kinases (MAPKs). The activated pathways will stimulate the expression of the relative protein including matrix metalloproteinases (MMPs) and pro-inflammatory cytokines, which subsequently lead to skin wrinkling and inflammation. Therefore, a ROS scavenger, NF- κ B, AP-1, and MAPKs blocker, and MMPs inhibitor that can scavenges ROS, blocks NF- κ B, AP-1, and MAPKs pathways, inhibits MMPs without toxicity may potentially against UVB-induced skin inflammatory and photo-damage.

Natural compounds such as vitamins, polysaccharides, polyphenols, and proteins isolated from terrestrial or aquatic natural resources, including plants, animals, and microorganisms, have been used medicinally throughout human history. Compounds isolated from seaweeds, such as polyphenols, polysaccharides, and pigments, possess antioxidant, anti-inflammation, anticancer, UV protection, and anti-wrinkle effect. In particular, polysaccharides isolated from seaweeds have been reported to possess strong bioactivities.

Sargassum fulvellum, *Codium fragile*, and *Hizikia fusiforme* are the most popular edible seaweeds in Asian countries such as Korea, China, and Japan. *S. fulvellum*, *C. fragile*, and *H. fusiforme* are abundantly distributed in Jeju Island. It is a rich and potential natural resource could be used as an ingredient in functional food and medicine, industries. Many reports support that *S. fulvellum*, *C. fragile*, and *H. fusiforme* contain various natural bioactive compounds and possess the potential to develop functional food and medicine. However, the cosmeceutical effects of these seaweeds had not been investigated so far. Therefore, in the present study, the cosmeceutical effects of these three edible seaweeds have been investigated.

In the present study, *S. fulvellum*, *C. fragile*, and *H. fusiforme* had extracted by water, ethanol, and enzymes. The composition of seaweed extracts were analysis. In addition, the free radical scavenging activities and the commercial tyrosinase, collagenase, and elastase inhibitory effects of seaweed extracts were determined. The results indicate that enzyme-assisted extraction could improve the extraction yield comparing to water and ethanol extraction. And all seaweed extracts possess strong free radical scavenging activity, especially on alkyl and hydroxyl radicals. Furthermore, the Celluclast-assisted extract of *H. fusiforme* contains the highest polysaccharides content and possesses strong free radical scavenging activity as well as strong tyrosinase, collagenase, and

elastase inhibitory effects. Therefore, *H. fusiforme* was selected as target seaweed to separate polysaccharides and evaluate the cosmeceutical effects.

The crude polysaccharides from Celluclast-assisted extract of *H. fusiforme* (HFCPS) were prepared by Celluclast-assisted hydrolysis and ethanol precipitation. HFCPS possesses potent cosmeceutical effects including antioxidant, anti-inflammation, whitening, UV protection, and anti-wrinkle effect. Furthermore, the *Hizikia* fucoidan (HFCPSF4) was separated from HFCPS. HFCPSF4 contains $99.01 \pm 0.61\%$ sulfated polysaccharides, which comprise fucose (97.20%), rhamnose (2.09%), mannose (18.32%), and arabinose (0.38%). The cosmeceutical effects of HFCPSF4 were measured including antioxidant activity, anti-inflammatory activity, whitening effect, protective effect, and anti-wrinkle effect. The results indicate that HFCPSF4 significantly reduces hydrogen peroxide (H_2O_2)-induced oxidative stress in monkey kidney fibroblast cells (Vero cells) and in zebrafish; remarkably attenuates lipopolysaccharide (LPS)-induced inflammation in RAW 264.7 macrophages and in zebrafish; inhibits alpha-melanocyte stimulating hormone (α -MSH)-stimulated melanogenesis in B16F10 melanoma cells; against UVB-induced photo-damage in keratinocytes (HaCaT cells) and in zebrafish; protects UVB-induced skin wrinkling in human dermal fibroblasts (HDF cells). These results demonstrate that HFCPSF4 possesses potent cosmeceutical effects, and can be a potential ingredient in the cosmetic industry.

In a conclusion, the present study demonstrates the fucoidan (HFCPSF4) isolated from crude polysaccharides from Celluclast-assisted extract of *Hizikia fusiforme* (HFCPS) possesses strong cosmeceutical effects including antioxidant, anti-inflammation, whitening, UV protection, and anti-wrinkle activity. It can be used as an ingredient in pharmaceutical and cosmeceutical industries.

LIST OF TABLE

Table 1. Korean name and abbreviation of *S. fulvellum*, *C. fragile*, and *H. fusiforme*

Table 2. Optimal reaction condition of enzymes.

Table 3. The yields of water, ethanol, and enzymes extraction of *S. fulvellum*, *C. fragile*, and *H. fusiforme*.

Table 4. Polysaccharide contents of seaweed extracts.

Table 5. Protein contents of seaweed extracts.

Table 6. Phenolic contents of seaweed extracts.

Table 7. DPPH radical scavenging activities of seaweed extracts.

Table 8. Alkyl radical scavenging activities of seaweed extracts.

Table 9. Hydroxyl radical scavenging activities of seaweed extracts.

Table 10. The yields, total carbohydrate contents, total phenolic contents, and sulfate contents of HFC and HFCPS obtained from *H. fusiforme*.

Table 11. The proportion of monosaccharide of HFC and HFCPS obtained from *H. fusiforme*.

Table 12. Free radical scavenging activities of HFC and HFCPS obtained from *H. fusiforme*.

Table 13. Total carbohydrate contents, phenolic contents, sulfate contents, and natural sugar components of polysaccharides separated from HFCPS.

Table 14. Free radical scavenging activities of polysaccharides of polysaccharides separated from HFCPS.

LIST OF FIGURE

- Fig. 1.** The photograph of *S. fulvellum*, *C. fragile*, and *H. fusiforme*.
- Fig. 2.** The procedure of water and ethanol extraction of seaweeds.
- Fig. 3.** The procedure of enzyme extraction of seaweeds.
- Fig. 4.** Tyrosinase inhibitory effects of SF, CF, and HF extracts. (A) Tyrosinase inhibitory effects of SF extracts; (B) tyrosinase inhibitory effects of CF extracts; (C) tyrosinase inhibitory effects of HF extracts.
- Fig. 5.** Collagenase inhibitory effects of SF, CF, and HF extracts. (A) Collagenase inhibitory effects of SF extracts; (B) collagenase inhibitory effects of CF extracts; (C) collagenase inhibitory effects of HF extracts.
- Fig. 6.** Elastase inhibitory effects of SF, CF, and HF extracts. (A) Elastase inhibitory effects of SF extracts; (B) elastase inhibitory effects of CF extracts; (C) elastase inhibitory effects of HF extracts.
- Fig. 7.** The procedure of large-scale extraction and separation polysaccharides from *Hizikia fusiforme*
- Fig. 8.** Cytotoxicity of HFCPS on Vero cells.
- Fig. 9.** The intracellular ROS scavenging effect of HFCPS during H₂O₂-induced oxidative stress in Vero cells (A) and the protective effects of HFCPS against H₂O₂-induced cell death in Vero cells (B).
- Fig. 10.** The protective effect of HFCPS against H₂O₂-induced apoptosis in Vero cells. (A) Nuclear morphology of non H₂O₂-treated cells. (B) Nuclear morphology of

H₂O₂-treated cells. (C) Nuclear morphology of cells treated with 25 µg/mL of HFCPS and H₂O₂. (D) Nuclear morphology of cells treated with 50 µg/mL of HFCPS and H₂O₂. (E) Nuclear morphology of cells treated with 100 µg/mL of HFCPS and H₂O₂. (F) Reactive apoptotic body formation.

Fig. 11. The survival rate and heart-beating rate of zebrafish after treatment with HFCPS and/or treatment with H₂O₂. (A) Survival rate; (B) heart-beating rate.

Fig. 12. The protective effect of HFCPS during H₂O₂-induced ROS production in zebrafish embryos. (A) Zebrafish embryo under fluorescence microscope; (B) the levels of ROS generation.

Fig. 13. The protective effect of HFCPS during H₂O₂-induced cell death in zebrafish embryos. (A) Zebrafish embryo under fluorescence microscope; (B) the measured levels of cell death.

Fig. 14. The effect of HFCPS on LPS-induced NO generation and cytotoxicity in RAW 264.7 macrophages. (A) NO production in LPS-induced RAW 264.7 macrophages and (B) Cell viability in LPS-induced RAW 264.7 macrophages.

Fig. 15. The effect of HFCPS on the production of PGE₂, TNF-α, IL-1β, and IL-6 in LPS stimulated RAW 264.7 macrophages. (A) The production of PGE₂; (B) the production of TNF-α; (C) the production of IL-1β; (D) the production of IL-6.

Fig. 16. The effect of HFCPS on the expression of iNOS and COX-2 in RAW 264.7 macrophages stimulated with LPS. (A) The inhibitory effect of HFCPS on iNOS and COX-2 expression; (B) the relative amount of iNOS and COX-2 levels.

Fig. 17. Tyrosinase inhibitory effects of HFCPS.

Fig. 18. Cytotoxicity of HFCPS on B16F10 cells.

Fig. 19. Melanin synthesis and intracellular tyrosinase inhibitory effect of HFCPS in α -MSH-stimulated B16F10 cells. (A) Melanin synthesis levels in α -MSH-stimulated B16F10 cells; relative intracellular tyrosinase activity of α -MSH-stimulated B16F10 cells.

Fig. 20. Effect of HFCPS on MITF, tyrosinase, TRP-1, and TRP-2 expression in α -MSH-stimulated B16F10 cells.

Fig. 21. Cytotoxicity of HFCPS on HaCaT cells.

Fig. 22. Protective effect of HFCPS against UVB-induced HaCaT cells damage. (A) Intracellular ROS level of UVB-irradiated HaCaT cells; (B) the viability UVB-irradiated HaCaT cells.

Fig. 23. The apoptotic body formation levels in UVB-irradiated HaCaT cells. (A) Nuclear morphology of non UVB-irradiated HaCaT cells; (B) nuclear morphology of UVB-irradiated HaCaT cells; (C) nuclear morphology of cells treated with 25 μ g/mL of HFCPS and irradiated with UVB; (D) nuclear morphology of cells treated with 50 μ g/mL of HFCPS and irradiated with UVB; (E) nuclear morphology of cells treated with 100 μ g/mL of HFCPS and irradiated with UVB; (F) reactive apoptotic body formation.

Fig. 24. The protective effect of HFCPS against on UVB-induced ROS production in zebrafish. (A) Zebrafish under fluorescence microscope; (B) the levels of ROS generation.

Fig. 25. The protective effect of HFCPS against UVB-induced cell death in zebrafish. (A) Zebrafish under fluorescence microscope; (B) the levels of cell death.

Fig. 26. The protective effect of HFCPS against UVB-induced NO production in zebrafish. (A) Zebrafish under fluorescence microscope; (B) NO production levels.

Fig. 27. The protective effect of HFCPS against UVB-induced lipid peroxidation in zebrafish. (A) Zebrafish under fluorescence microscope; (B) lipid peroxidation levels.

Fig. 28. HFCPS inhibits commercial collagenase and elastase. (A) Collagenase inhibitory activity of HFCPS; (B) elastase inhibitory activity of HFCPS.

Fig. 29. HFCPS promotes HDF cell proliferation and UVB irradiation damages HDF cells. (A) Cytotoxicity of UVB irradiation on HDF cells; (B) proliferation effect of HFCPS on HDF cells.

Fig. 30. Protective effects of HFCPS against UVB-induced HDF cell damage. (A) Intracellular ROS scavenging effect of HFCPS in UVB-induced HDF cells; (B) protective effects of HFCPS against UVB-induced HDF cell death.

Fig. 31. HFCPS inhibits cellular collagenase and elastase activities in UVB-irradiated HDF Cells. (A) Relative collagenase activity; (B) relative elastase activity.

Fig. 32. HFCPS improves collagen synthesis and reduces MMPs expression in UVB-irradiated HDF cells. (A) Collagen synthesis level in UVB-irradiated HDF cells; (B) MMP-1 expression level in UVB-irradiated HDF cells; (C) MMP-2 expression level in UVB-irradiated HDF cells; (D) MMP-8 expression level in UVB-irradiated HDF cells; (E) MMP-9 expression level in UVB-irradiated HDF cells; (F) MMP-13 expression level in UVB-irradiated HDF cells.

Fig. 33. HFCPS blocks UVB-induced NF- κ B activation and reduces AP-1 phosphorylation in UVB-induced HDF cells.

Fig. 34. HFCPS suppresses MAPKs activation in UVB-induced HDF cells.

Fig. 35. DEAE-cellulose chromatogram of the polysaccharides separated from HFCPS.

Fig. 36. Tyrosinase inhibitory effects of fractions from HFCPS.

Fig. 37. Collagenase inhibitory effects of the fractions form HFCPS.

Fig. 38. Elastase inhibitory effects of the fractions form HFCPS.

Fig. 39. Spectroscopic analysis of the purified fucoidan from HFCPS.

Fig. 40. The intracellular ROS scavenging effect of HFCPSF4 during H₂O₂-induced oxidative stress in Vero cells (A) and the protective effect of HFCPSF4 against H₂O₂-induced cell death in Vero cells (B).

Fig. 41. The protective effect of HFCPSF4 against H₂O₂-induced apoptosis in Vero cells. (A) Nuclear morphology of non H₂O₂-treated cells. (B) Nuclear morphology of H₂O₂-treated cells. (C) Nuclear morphology of cells treated with 12.5 µg/mL of HFCPSF4 and H₂O₂. (D) Nuclear morphology of cells treated with 25 µg/mL of HFCPSF4 and H₂O₂. (E) Nuclear morphology of cells treated with 50 µg/mL of HFCPSF4 and H₂O₂. (F) Reactive apoptotic body formation.

Fig. 42. HFCPSF4 increases the expression of catalase and SOD-1 in H₂O₂-stimulated Vero cells.

Fig. 43. HFCPSF4 regulates Nrf/HO-1 pathway in H₂O₂-stimulated Vero cells.

Fig. 44. A schematic model of antioxidant activity of HFCPSF4 in Vero cells.

Fig. 45. The survival rate and heart-beating rate of zebrafish after treatment with HFCPSF4 and/or treatment with H₂O₂. (A) Survival rate; (B) heart-beating rate.

Fig. 46. The protective effect of HFCPSF4 against H₂O₂-induced ROS production in zebrafish embryos. (A) Zebrafish under fluorescence microscope; (B) the levels of ROS generation.

Fig. 47. The protective effect of HFCPSF4 against H₂O₂-induced cell death in zebrafish embryos. (A) Zebrafish embryo under fluorescence microscope; (B) the measured levels of cell death.

Fig. 48. The protective effect of HFCPSF4 against H₂O₂-induced lipid peroxidation in zebrafish embryos. (A) Zebrafish embryo under fluorescence microscope; (B) the measured levels of cell death.

Fig. 49. The effect of HFCPSF4 on LPS-induced NO generation and cytotoxicity in RAW 264.7 macrophages. (A) NO production in LPS-induced RAW 264.7 macrophages and (B) cell viability in LPS-induced RAW 264.7 macrophages.

Fig. 50. The effect of HFCPSF4 on the production of PGE₂, TNF- α , IL-1 β , and IL-6 in LPS-stimulated RAW 264.7 macrophages. (A) The production of PGE₂; (B) the production of TNF- α ; (C) the production of IL-1 β ; (D) the production of IL-6.

Fig. 51. The effect of HFCPSF4 on the expression of iNOS and COX-2 in RAW 264.7 macrophages stimulated with LPS. (A) The inhibitory effect of HFCPSF4 on iNOS and COX-2 expression; (B) the relative amount of iNOS and COX-2 levels.

Fig. 52. The effect of HFCPSF4 on NF- κ B activation in RAW 264.7 macrophages stimulated with LPS. (A) The cytosol I κ B α and p-I κ B α level; (B) the nuclear p50 and p65 NF- κ B level.

Fig. 53. A schematic model of anti-inflammation activity of HFCPSF4 in RAW 264.7 cells.

Fig. 54. The survival rate and heart-beating rate of zebrafish after treatment with HFCPSF4 and/or treatment with LPS. (A) Survival rate; (B) heart-beating rate.

Fig. 55. The protective effect of HFCPSF4 against LPS-induced ROS production in zebrafish embryos. (A) Zebrafish embryo under fluorescence microscope; (B) the levels of ROS generation.

Fig. 56. The protective effect of HFCPSF4 against LPS-induced cell death in zebrafish embryos. (A) Zebrafish embryo under fluorescence microscope; (B) the measured levels of cell death.

Fig. 57. The effect of HFCPSF4 on LPS-induced NO production in zebrafish embryos. (A) Zebrafish embryo under fluorescence microscope; (B) the measured levels of cell death.

Fig. 58. Cytotoxicity of HFCPSF4 on B16F10 cells.

Fig. 59. Melanin synthesis inhibitory effect of HFCPSF4 in α -MSH-stimulated B16F10 cells.

Fig. 60. Effect of HFCPSF4 on MITF, tyrosinase, TRP-1, and TRP-2 expression in α -MSH-stimulated B16F10 cells.

Fig. 61. Effect of HFCPSF4 on ERK-MAPK phosphorylation in α -MSH-stimulated B16F10 cells.

Fig. 62. A schematic model of whitening effect of HFCPSF4 in B16F10 cells.

Fig. 63. Protective effect of HFCPSF4 against UVB-induced HaCaT cells damage. (A) Intracellular ROS level of UVB-irradiated HaCaT cells; (B) the viability of UVB-irradiated HaCaT cells.

Fig. 64. The apoptotic body formation levels in UVB-irradiated HaCaT cells. (A) Nuclear morphology of non UVB-irradiated HaCaT cells; (B) nuclear morphology of UVB-irradiated HaCaT cells; (C) nuclear morphology of cells treated with 12.5 $\mu\text{g}/\text{mL}$ of HFCPSF4 and irradiated with UVB; (D) nuclear morphology of cells treated with 25 $\mu\text{g}/\text{mL}$ of HFCPSF4 and irradiated with UVB; (E) nuclear morphology of cells treated with 50 $\mu\text{g}/\text{mL}$ of HFCPSF4 and irradiated with UVB; (F) reactive apoptotic body formation.

Fig. 65. Effect of HFCPSF4 on Bax/Bcl-xL, PARP, and cleaved caspase-3 levels in UVB-irradiated HaCaT cells.

Fig. 66. A schematic model of UVB protective effect of HFCPSF4 in HaCaT cells.

Fig. 67. The protective effect of HFCPSF4 against UVB-induced ROS production in zebrafish. (A) Zebrafish under fluorescence microscope; (B) the levels of ROS generation.

Fig. 68. The protective effect of HFCPSF4 against UVB-induced cell death in zebrafish. (A) Zebrafish under fluorescence microscope; (B) the levels of cell death.

Fig. 69. The protective effect of HFCPSF4 against UVB-induced NO production in zebrafish. (A) Zebrafish under fluorescence microscope; (B) NO production levels.

Fig. 70. The protective effect of HFCPSF4 against UVB-induced lipid peroxidation in zebrafish. (A) Zebrafish under fluorescence microscope; (B) lipid peroxidation levels.

Fig. 71. Protective effects of HFCPSF4 against UVB-induced HDF cell damage. (A) Intracellular ROS scavenging effect of HFCPSF4 in UVB-induced HDF cells; (B) protective effects of HFCPSF4 against UVB-induced HDF cell death.

Fig. 72. HFCPSF4 inhibits cellular collagenase and elastase activities in UVB-irradiated HDF Cells.

Fig. 73. HFCPSF4 improves collagen synthesis and reduces MMPs expression in UVB-irradiated HDF cells. (A) Collagen synthesis level in UVB-irradiated HDF cells; (B) MMP-1 expression level in UVB-irradiated HDF cells; (C) MMP-2 expression level in UVB-irradiated HDF cells; (D) MMP-8 expression level in UVB-irradiated HDF cells; (E) MMP-9 expression level in UVB-irradiated HDF cells; (F) MMP-13 expression level in UVB-irradiated HDF cells.

Fig. 74. The effect of HFCPSF4 on the production of PGE₂, TNF- α , IL-1 β , and IL-6 in UVB-irradiated HDF cells. (A) The production of PGE₂; (B) the production of TNF- α ; (C) the production of IL-1 β ; (D) the production of IL-6.

Fig. 75. HFCPSF4 blocks UVB-induced NF- κ B activation and reduces AP-1 phosphorylation in UVB-induced HDF cells. (A) The cytosol I κ B α and p-I κ B α level; (B) the nuclear p50, p65 NF- κ B, and phosphorylated AP-1 levels.

Fig. 76. HFCPSF4 suppresses MAPKs activation in UVB-induced HDF cells.

Fig. 77. A schematic model of anti-wrinkle effect of HFCPSF4 in HDF cells.

Part I.

Extraction and bioactivity scavenging of seaweeds

Part I.

Extraction and bioactivity scavenging of seaweeds

ABSTRACT

Seaweeds are rich in various natural compounds, which possess a broad bioactivity. The edible seaweeds were consumed as a material for food processing or medicine has a long history. *Sargassum fulvellum*, *Codium fragile*, *Hizikia fusiforme* are the most popular edible seaweeds in Asian countries such as Korea, China, and Japan. *S. fulvellum*, *C. fragile*, and *H. fusiforme* are abundantly distributed in Jeju Island. It is a rich and potential natural resource could be used as an ingredient in functional food and medicine industries. Many reports support that *S. fulvellum*, *C. fragile*, and *H. fusiforme* contain various natural bioactive compounds and possess the potential to develop functional food and medicine. However, the cosmeceutical effects of these seaweeds had not been investigated so far. Therefore, in the present study, the cosmeceutical effects of these three edible seaweeds have been investigated. In this study, seaweeds had extracted by water, ethanol, and enzymes. The free radical scavenging activities of seaweed extracts were determined using Electron Spin Resonance (ESR) spectrometer. The results indicate that enzyme-assisted extraction could improve the extraction yield comparing to water and ethanol extraction, and all seaweed extracts possess strong free radical scavenging activity, especially on alkyl and hydroxyl radicals. In addition, *H. fusiforme* extracts possess relative stronger free radical scavenging activity than *S. fulvellum* and *C. fragile* extracts. In addition, the inhibitory effects on commercial tyrosinase, collagenase, and elastase of seaweed extracts were evaluated. The results demonstrate that *S. fulvellum* and *H. fusiforme* extracts possess stronger tyrosinase inhibitory effect than *C. fragile* extracts; *H.*

fusiforme extracts possess stronger collagenase and elastase inhibitory effects than *S. fulvellum* and *C. fragile* extracts. In addition, the Celluclast-assisted extract of *H. fusiforme* possesses strong free radical scavenging activity and tyrosinase, collagenase, and elastase inhibitory effect; it may possess the potential on cosmeceutical effects. Furthermore, the composition analysis results indicate that the main composition of Celluclast-assisted extract of *H. fusiforme* is polysaccharides. In a conclusion, the Celluclast-assisted extract of *H. fusiforme* is rich in polysaccharides and possesses strong free radical scavenging activity as well as cosmeceutical effects. It may use as a potential ingredient in pharmaceutical and cosmeceutical industries.

INTRODUCTION

The ocean is covering approximately 71% of the Earth's surface. The ocean contains 97% of Earth's water and 90% of the Earth's biosphere. The ocean is abundant with a complex diversity of marine organisms, which including marine plants such as algae and sea grasses, marine animals such as fish and shellfish, and marine microorganisms such as bacteria and fungi. The marine organisms offer a rich source of natural products, such as phenolic compounds, polysaccharides, proteins, lipids, minerals, and essential vitamins [1]. These natural compounds possess various bioactivities including antioxidant, anti-inflammation, anti-cancer, anti-microbial, anti-diabetes, anti-irradiation, anti-hypertension, and anti-obesity activity [2-9]. Kang et al. (2016) had investigated anti-obesity effects of seaweeds of Jeju Island 3T3-L1 preadipocytes and obese mice [9]. Ko et al. (2012) had isolation and characterization the angiotensin I-converting enzyme inhibitory peptide from *Styela clava* [10]. Sun et al. (2009) had isolated antioxidant polysaccharides from marine fungus *Penicillium* sp. F23-2 [11].

Algae can be classified into two subtypes. One of the subtype is microalgae, which are unicellular species and the sizes of microalgae can range from micrometers to hundred micrometers. Microalgae exist individually, or in groups or chains. Another subtype is macroalgae, which are macroscopic and multicellular. Marine macroalgae are referring as seaweed and it includes red, green, and brown seaweed. Seaweeds contain a large mass of nutrient contents such as carbohydrates, minerals, vitamins, proteins, fatty acids, and amino acids. It is also rich in natural compounds including polysaccharides, proteins, polyphenols, sterols, fatty acids, amino acids, alkaloids, and pigments, as well as possesses wide range a broad spectrum of bioactivity such as anti-microbial, antioxidant, anti-cancer, anti-coagulation, anti-aging, anti-inflammation, anti-irradiation, anti-hypertension, anti-obesity, and anti-diabetes properties [12-22].

Heo et al. had isolated a pigment, fucoxanthin from *Sargassum siliquastrum* and investigated the protective effect of fucoxanthin against ultraviolet B (UVB)-induced cell damage [23]. Wijesinghe et al. (2011) had purified a sulfated polysaccharide from *Ecklonia cava* and evaluated its anti-coagulative activity [24]. Kang et al. (2012) had isolated a polyphenol, dieckol from *Ecklonia cava* and investigated the hepatoprotective effect of dieckol [25]. Souza et al. (2009) had isolated and identified a bisindole alkaloid, caulerpin from *Genes gaulerpa* and evaluated the anti-inflammatory and antinociceptive effects of caulerpin in mice [22]. In addition, Fernando et al. (2018) had isolated alginic acid from *Sargassum horneri* and evaluated its anti-inflammatory effect [19].

Edible seaweed or sea vegetable is the seaweed can be directly eaten or used as a material for preparing food. Consumption of seaweeds as a food or medicine material has a long history, especially in Asian countries [12, 26]. Recent decade reports suggest that edible seaweeds are benefiting for human's health because they are rich in nutrients and various bioactive compounds, which could prevent, improve, or against above diseases [27-30]. Nowadays, there are many species of edible seaweeds had been cultured as large-scale such as *Saccharina japonica*, *Hizikia fusiforme*, *Undaria pinnatifida*, and *Porphyra yezoensis*, as well the edible seaweed had used for a wide range of food, pharmacy, and cosmetic industries [31-34].

Sargassum fulvellum (*S. fulvellum*) is an edible brown seaweed, which is popular low prices food ingredient in the Korean market. *S. fulvellum* is consumed as food and food additive, as well as consumed as herbal medicine to treat lump, dropsy, swollen, and painful scrotum, and urination problems [35]. *Codium fragile* (*C. fragile*) is an edible green seaweed. It is abundant in East Asian countries, especially in China, Korea, and Japan. In addition, it also distributes in Northern Europe and Oceania. *C.*

fragile has been used as a food ingredient and traditional medicine for a long history. In Korea, *C. fragile* is use as a food ingredient and use as a medicine for the treatment of dropsy, dysuria, and enterobiasis [36, 37]. *Hizikia fusiforme* (*H. fusiforme*) is an edible brown seaweed and mainly grows in the northwest Pacific. *H. fusiforme* is one of the most of popular seaweed consumed as food in Asian countries, especially in Korea, China, and Japan. In addition, *H. fusiforme* had used as herb medicine for a long history [38]. All of these three edible seaweeds that *S. fulvellum*, *C. fragile*, and *H. fusiforme* are abundant in Jeju Island. There are a rich and potential natural resource could be used as an ingredient in functional food, medicine, and cosmetic industries. Many reports support that *S. fulvellum*, *C. fragile*, and *H. fusiforme* contain various natural bioactive compounds and possess the potential to develop functional food and medicine. However, the cosmetic effects of these seaweeds had not been investigated so far. Therefore, in the present study, we investigated cosmetic effects these three edible seaweeds.

1. Materials and Methods

1.1. Reagents and chemicals

Commercial enzymes for extraction, 1-diphenyl-2-picrylhydrazyl (DPPH), 5,5-dimethyl-1-pyrrolin N-oxide (DMPO), 2,2-azobis(2-amidinopropane) hydrochloride (AAPH), and α -(4-Pyridyl-1-oxide)-N-ter-butyl nitron (POBN) were purchased from Sigma (St. Louis, MO, USA). $\text{FeSO}_4 \cdot 7\text{H}_2\text{O}$, and H_2O_2 were purchased from Fluka Co. (Buchs, Switzerland). Arbutin, (-)-epigallocatechin gallate (EGCG), gallic acid, glucose tyrosinase, L-tyrosin, collagenase from *clostridium histolyticum*, elastase from porcine pancreas, azo dye-impregnted collagen, and N-succinyl-Ala-Ala-Ala-p-nitroanilide were purchased from Sigma Co. (St. Louis, MO, USA). The Pierce™ BCA protein assay kit was purchased from Thermo Scientific (Thermo Scientific, Rockford, U.S.). All other chemicals and reagents were analytical grade.

1.2. Collection and process of seaweed samples

S. fulvellum, *C. fragile*, and *H. fusiforme* (Table 1 and Fig. 1) were collected in June 2016 from the coastal area of Jeju Island, South Korea. Samples were washed by the tap water to remove the salt, sand, and epiphytes and freeze-dried by a free dryer. The lyophilized seaweeds were kept in 4°C until use.



Sargassum fulvellum



Codium fragile



Hizikia fusiforme

Fig. 1. The photograph of *S. fulvellum*, *C. fragile*, and *H. fusiforme*.

Table 1. Korean name and abbreviation of *S. fulvellum*, *C. fragile*, and *H. fusiforme*

Scientific name	Korean name	Abbreviation
<i>Sargassum fulvellum</i>	참모자반	SF
<i>Codium fragile</i>	청각	CF
<i>Hizikia fusiforme</i>	툫	HF

1.3. Water and ethanol extraction

Each 1 g of lyophilized SF, CF, and HF was extracted by 100 mL distilled water (D.W) or 70% EtOH in the shaking condition (120 rpm) for 24 hours. The extract mixture was centrifuged and the supernatant was filtered through a Whatman No. 1 filter paper. Then, the EtOH extracts were dried in a vacuum dryer, and the water extracts were dried in a freeze dryer. Finally, the water extracts and EtOH extracts of SF, CF, and HF were obtained (Fig. 2). All extracts were kept at -20°C until use.

1.4. Enzyme-assisted extraction

For the enzyme extraction, ten commercial enzymes including 5 glycoenzymes (Viscozyme, Celluclast, AMG, Termamyl, and Ultraflo) and 5 proteases (Protantex, Kojizyme, Neutrase, Flavourzyme, and Alcalase) were used to hydrolyze seaweeds at their optimal conditions (Table 2). In brief, each 1 g lyophilized SF, CF, and HF powder was mixed with 100 mL distilled water, adjusted pH to the optimal pH, then 5% enzyme was added to the mixture and hydrolyzed at the optimal temperature under shaking condition (120 rpm). After hydrolysis, the enzyme was inactive by heating at 100°C for 10 minutes. Then the macerated mixture was centrifuged, filtered, and adjusted pH to 7 by 1 M HCl or 1 M NaOH. Finally, the extracts were dried in a freeze dryer, and the enzyme extracts of SF, CF, and HF were obtained (Fig. 3). All extracts were kept at -20°C until use.

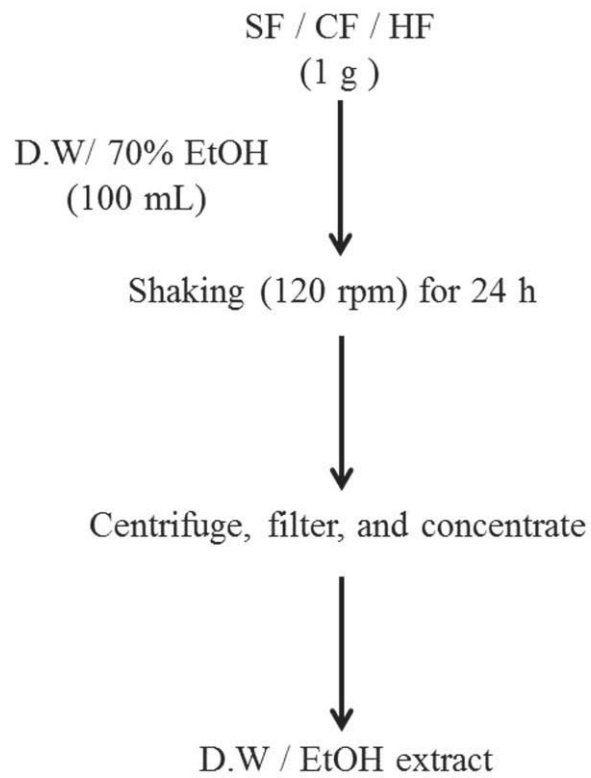


Fig. 2. The procedure of water and ethanol extraction of seaweeds.

Table 2. The optimal reaction condition of enzymes.

	Enzyme	pH	Temperature (°C)
	Viscozyme	4.5	50
	Celluclast	4.5	50
Glycoenzyme	AMG	4.5	60
	Termamyl	6.0	60
	Ultraflo	7.0	60
	Protamex	6.0	40
	Kojizyme	6.0	40
Protease	Neutrase	6.0	50
	Flavourzyme	7.0	50
	Alcalase	8.0	50

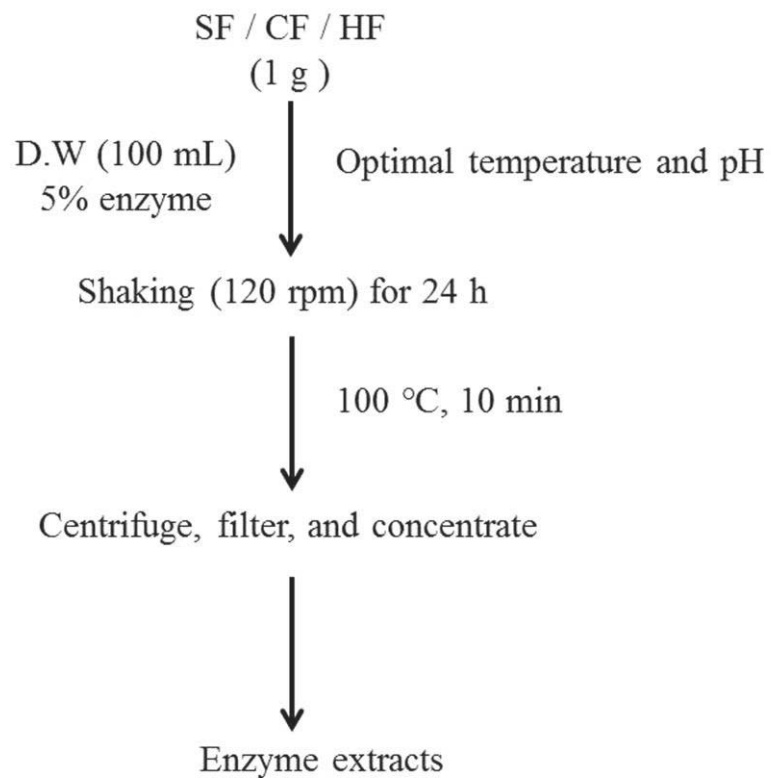


Fig. 3. The procedure of enzyme extraction of seaweeds.

1.5. Determination of chemical composition of seaweed extracts

1.5.1. Analysis of polysaccharide content of seaweed extracts

The total polysaccharide contents of seaweed extracts were determined based on the protocol of official methods for analysis of the Association of Official Analytical Chemists (AOAC) [39]. In brief, seaweed extracts were prepared to 0.1 mg/mL. A calibration standard composed of increasing concentrations of 0-0.1 mg/mL and sample solutions were prepared in triplicate in test tubes with a total volume of 1 mL. A volume of 25 μ L of 80% phenol was added into each test tube. Then, a volume of 2.5 mL of sulfuric acid was added in each test tube. The reaction mixture was mixed and reacted in the dark for 30 min. Finally, a volume of 200 μ L reaction mixture from each test tube was transferred to a 96-well plate, and the absorbance was measured at 480 nm using a microplate reader (BioTek, SYNERGY, HT, USA). The polysaccharide contents of seaweed extracts were evaluated according to the standard curve.

1.5.2. Analysis of total phenolic content of seaweed extracts

Total phenolic contents of seaweed extracts were determined by a Folin-Ciocalteu assay based on the method described by Chandler and Dodds with slight modifications [40]. In brief, each 1 mL of 0.1 mg/mL seaweed extracts or standard phenolic compound solution was mixed in a test tube containing 1 mL of 95% ethanol. A volume of 5 mL of D.W and 0.5 mL of 50% Folin–Ciocalteu reagent was introduced to each test tube sequentially and mixed thoroughly using. The resultant mixture was allowed to react for 5 min, following which 1 mL of 5% Na_2CO_3 was added to each test tube. After mixing thoroughly, the test tubes were incubated in the dark for 1 h. Finally, the absorbance was recorded at 700 nm using a microplate reader (BioTek, SYNERGY, HT, USA). Gallic acid was used as the reference compound to construct the standard

curve, and total phenolic contents of the seaweed extracts were calculated as gallic acid equivalents.

1.5.3. Analysis of protein content of seaweed extracts

The protein contents of seaweed extracts were measured by a Pierce™ BCA protein assay kit according to the specification. Bovine serum albumin (BSA) was used as the reference protein to construct the standard curve.

1.6. Evaluation of the free radical scavenging activity of seaweed extracts

The free radical scavenging activities of seaweed extracts were measured using an Electron Spin Resonance (ESR) spectrometer (JES-FA machine; JOEL, Tokyo, Japan). DPPH, alkyl, and hydroxyl radical scavenging activities were determined by the method described by Heo et al. [1].

1.7. Measurement of mushroom tyrosinase inhibitory effects of seaweed extracts

Tyrosinase inhibitory effects were measured by the method described by our previous study [41, 42]. In brief, a volume of 200 μ L assay mixture in 96-well microplate containing 40 μ L of 1.5 mM L-tyrosin, 140 μ L of 50 mM phosphate buffer (pH 6.5), 10 μ L of aqueous mushroom tyrosinase (1000 units/mL), and 10 μ L of sample solution. The assay mixture was reacted at 37°C for 12 min, and then the plate was kept on ice for 5 min to stop the reaction. The amount of dopachrome in the reaction mixture was measured at 490 nm using a microplate reader (BioTek, SYNERGY, HT, USA).

1.8. Measurement of collagenase inhibitory effects of seaweed extracts

In order to measure the collagenase inhibitory activity, a weight of 1 mg of azo dye-impregnated collagen was mixed with 800 μ L of 0.1 M Tris-HCl (pH 7.0), 100 μ L of 200 units/mL collagenase (stock solution), and 100 μ L sample and incubated at 43°C

for 1 h under shaking condition. Subsequently, the reaction mixture was centrifuged at 3000 rpm for 10 min and the absorbance of the supernatant was detected at 550 nm in a microplate reader (BioTek, SYNERGY, HT, USA).

1.9. Measurement of elastase inhibitory effects of seaweed extracts

The elastase inhibitory activity was evaluated base on a method reported by Kraunsoe et al. (1996) [43]. In brief, the reaction mixture contained 650 μL of 1.015 mM N-succinyl-Ala-Ala-Ala-p-nitroanilide (dissolved in Tris-HCl, pH 8.0) and 50 μL of sample. The reaction mixture was vortexed and incubated for 10 min at 25°C, after incubation, 50 μL of 0.0375 units/mL elastase was added to the reaction mixture and following vortexing, was incubated for 10 min at 25°C in a water bath. The amount of released p-nitroaniline was assessed by measuring absorbance at 410 nm using a microplate reader (BioTek, SYNERGY, HT, USA).

2. Results and Discussion

2.1. Extraction yield and proximate composition of seaweed extracts

The extraction yields of seaweeds were summarized in Table 3. The extraction yields of SF were range from $12.67\pm 1.53\%$ to $41.00\pm 1.00\%$; the yields of CF were range from $7.67\pm 2.31\%$ to $36.33\pm 4.16\%$, and the yields of HF were range from $6.67\pm 0.24\%$ to $44.00\pm 0.71\%$, respectively. These results indicate that EtOH extraction showed a relatively low yield compared to water extraction. In addition, the enzyme extraction can improve the yield compared to water extraction, especially glycoenzyme.

The polysaccharide contents of seaweed extracts were summarized in Table 4. As Table 4 shows, the polysaccharide contents of SF were range from $5.40\pm 0.11\%$ to $37.22\pm 2.63\%$, the water extract possesses the highest polysaccharide content in all of SF extracts. The polysaccharide contents of CF were range from $10.80\pm 1.70\%$ to $46.50\pm 2.60\%$, the AMG extract possesses the highest polysaccharide content in all of CF extracts. The polysaccharide contents of HF were range from $19.12\pm 3.30\%$ to $48.95\pm 0.71\%$, the Celluclast extract possesses the highest polysaccharide content in all of HF extracts. These results display that HF extracts contain a relatively higher polysaccharide content compared to SF and CF extracts, and the Celluclast extract of HF possess the highest polysaccharide in all of the seaweed extracts.

As Table 5 shows, the protein contents of SF were range from $3.66\pm 0.68\%$ to $16.06\pm 0.76\%$, the Neutrased extract possesses the highest protein content in all of SF extracts. The protein contents of CF were range from $5.20\pm 0.39\%$ to $22.53\pm 1.31\%$, the Neutrased extract possesses the highest protein content in all of CF extracts. The protein contents of HF were range from $7.91\pm 0.14\%$ to $10.84\pm 0.15\%$, the Alcalase extract showed the highest protein content in all of HF extracts. These results display that CF extracts contain a relatively higher protein content compared to SF and HF

extracts, and the Neutrase extract of CF possesses the highest protein in all of the seaweed extracts.

The total phenolic contents of seaweed extracts were summarized in Table 6. The phenolic contents of SF were range from $2.01\pm 0.32\%$ to $12.63\pm 0.23\%$, the EtOH extract possesses the highest phenolic content in all of SF extracts. The phenolic contents of CF were range from $1.88\pm 0.00\%$ to $3.96\pm 1.82\%$, the Viscozyme extract possesses the highest phenolic content in all of CF extracts. The phenolic contents of HF were range from $2.57\pm 0.09\%$ to $4.46\pm 0.14\%$, the EtOH extract possesses the highest phenolic content in all of HF extracts. These results display that EtOH extraction can get a higher phenolic content from seaweed, and SF extracts contain a relatively higher phenolic content compared to CF and HF extracts. In addition, the EtOH extract of SF possess the highest phenolic in all of the seaweed extracts.

Table 3. The yields of water, ethanol, and enzymes extraction of *S. fulvellum*, *C. fragile*, and *H. fusiforme*.

Extracts	Yield (%)		
	SF	CF	HF
D.W	21.33±4.51	11.67±1.63	36.67±0.62
EtOH	12.67±1.53	7.67±2.31	6.67±0.24
AMG	29.67±2.08	19.00±2.65	37.50±0.71
Cell	35.00±1.73	26.00±3.46	44.00±0.71
Ter	34.00±4.36	27.78±2.52	38.70±0.85
Ult	33.00±3.46	25.00±0.00	35.33±1.03
Vis	26.00±2.00	24.00±1.00	40.74±2.00
Alca	36.00±4.00	36.33±4.16	39.67±1.06
Koji	37.33±2.08	30.00±1.73	26.86±1.10
Nue	40.00±0.00	31.33±0.58	36.33±0.46
Pro	41.00±1.00	25.00±1.73	38.50±0.41
Fla	38.67±1.15	25.33±1.15	36.83±0.62

D.W: water extract; EtOH: water extract; AMG: AMG extract; Cell: Celluclast extract; Ter: Termamyl extracts; Ult: Ultraflo extract; Vis: Viscozyme extract; Alca: Alcalase extract; Koji: Kojizyme extract; Nue: Neutrased extract; Pro: Protamex extract; Fla: Flavourzyme extract. The experiments were conducted triplicate, and the data were expressed as the mean ± S.E (n=3).

Table 4. Polysaccharide contents of seaweed extracts.

Extracts	Polysaccharide content (%)		
	SF	CF	HF
D.W	37.22±2.63	22.40±4.80	27.18±0.93
EtOH	5.40±0.11	10.80±1.70	19.12±3.30
AMG	27.83±2.88	46.50±2.60	25.15±0.50
Cell	32.52±4.01	41.50±1.14	48.95±0.71
Ter	33.59±0.75	41.20±4.50	26.93±0.29
Ult	30.57±2.78	39.60±3.70	26.17±0.79
Vis	22.69±1.38	41.90±3.60	26.21±3.70
Alca	19.94±2.26	22.20±1.30	19.42±3.15
Koji	28.71±2.88	31.60±5.20	21.91±0.65
Nue	18.52±2.51	16.00±4.20	25.61±1.15
Pro	27.92±3.51	13.50±4.60	23.28±1.00
Fla	21.45±5.64	22.20±5.30	27.43±1.43

D.W: water extract; EtOH: water extract; AMG: AMG extract; Cell: Celluclast extract; Ter: Termamyl extracts; Ult: Ultraflo extract; Vis: Viscozyme extract; Alca: Alcalase extract; Koji: Kojizyme extract; Nue: Neutrased extract; Pro: Protamex extract; Fla: Flavourzyme extract. The experiments were conducted triplicate, and the data were expressed as the mean ± S.E (n=3).

Table 5. Protein contents of seaweed extracts.

Extracts	Protein content (%)		
	SF	CF	HF
D.W	6.32±0.16	7.03±0.13	8.69±0.14
EtOH	3.66±0.68	5.20±0.39	8.56±0.19
AMG	4.40±0.13	7.03±0.13	9.37±0.17
Cell	5.12±1.03	5.29±0.39	8.93±0.55
Ter	9.56±2.64	8.61±0.00	7.98±0.09
Ult	9.03±0.63	7.03±0.13	9.92±0.26
Vis	6.62±0.00	6.48±0.66	9.88±0.14
Alca	8.31±1.45	9.45±0.39	10.84±0.15
Koji	12.25±0.63	8.61±0.00	10.15±0.00
Nue	16.06±0.76	22.53±1.31	8.98±0.00
Pro	13.74±0.00	18.07±1.57	7.91±0.14
Fla	11.61±0.25	11.39±0.79	8.79±0.28

D.W: water extract; EtOH: water extract; AMG: AMG extract; Cell: Celluclast extract; Ter: Termamyl extracts; Ult: Ultraflo extract; Vis: Viscozyme extract; Alca: Alcalase extract; Koji: Kojizyme extract; Nue: Neutrase extract; Pro: Protamex extract; Fla: Flavourzyme extract. The experiments were conducted triplicate, and the data were expressed as the mean ± S.E (n=3).

Table 6. Phenolic contents of seaweed extracts.

Extracts	Phenolic content (%)		
	SF	CF	HF
D.W	2.01±0.32	2.08±0.56	3.97±0.00
EtOH	12.63±0.23	1.88±0.00	4.46±0.14
AMG	3.47±0.56	2.08±0.00	2.57±0.09
Cell	5.30±1.05	2.37±0.14	4.17±0.01
Ter	4.45±0.84	2.08±0.28	2.71±0.05
Ult	6.60±1.65	2.37±0.14	3.83±0.03
Vis	3.47±0.56	3.96±1.82	3.97±0.14
Alca	3.50±0.36	2.47±0.00	4.26±0.28
Koji	5.44±1.67	2.08±0.00	4.22±0.00
Nue	5.63±0.84	3.46±0.00	3.67±0.14
Pro	4.65±1.11	3.16±0.14	3.67±0.00
Fla	2.48±0.28	2.67±0.28	3.82±0.07

D.W: water extract; EtOH: water extract; AMG: AMG extract; Cell: Celluclast extract; Ter: Termamyl extracts; Ult: Ultraflo extract; Vis: Viscozyme extract; Alca: Alcalase extract; Koji: Kojizyme extract; Nue: Neutrase extract; Pro: Protamex extract; Fla: Flavourzyme extract. The experiments were conducted triplicate, and the data were expressed as the mean ± S.E (n=3).

2.2. Free radical scavenging activities of seaweed extracts

DPPH, alkyl, and hydroxyl radical scavenging activities of seaweed extracts were determined using ESR spectrum. The results of DPPH radical scavenging activities of seaweed extracts were summarized in Table 7. The IC_{50} values of DPPH radical scavenging activities of SF extracts were range from 1.16 ± 0.31 mg/mL to 5.07 ± 0.41 mg/mL, and the Protamex extract of SF shows the strongest DPPH radical scavenging activity in all of the SF extracts. The IC_{50} values of DPPH radical scavenging activities of the extracts from CF were range from 1.18 ± 0.37 mg/mL to 5.02 ± 1.20 mg/mL, and the Termamyl extract of CF shows the strongest DPPH radical scavenging activity in all of the CF extracts. In addition, the IC_{50} values of DPPH radical scavenging activities of the extracts from HF were range from 1.06 ± 0.08 mg/mL to 4.03 ± 0.11 mg/mL, and the Termamyl extract of HF shows the strongest DPPH radical scavenging activity in all of the HF extracts. These results demonstrate that all of the seaweed extracts possess strong DPPH radical scavenging activity, and HF extracts show relative strong DPPH radical scavenging activity that SF and CF extracts. In addition, the Celluclast extract from HF shows the strongest DPPH radical scavenging activity in all of the seaweed extracts.

The results of alkyl radical scavenging activities of seaweed extracts were summarized in Table 8. The IC_{50} values of alkyl radical scavenging activities of SF extracts were range from 0.23 ± 0.05 mg/mL to 0.97 ± 0.28 mg/mL, and the Kojizyme extract of SF shows the strongest alkyl radical scavenging activity in all of the SF extracts. The IC_{50} values of alkyl radical scavenging activities of the extracts from CF were range from 0.31 ± 0.01 mg/mL to 1.09 ± 0.24 mg/mL, and the Neutrased extract of CF shows the strongest alkyl radical scavenging activity in all of the CF extracts. In addition, the IC_{50} values of alkyl radical scavenging activities of the extracts from HF

were range from 0.21 ± 0.01 mg/mL to 1.06 ± 0.03 mg/mL, and the EtOH extract of HF shows the strongest alkyl radical scavenging activity in all of the HF extracts. These results indicate that all of the seaweed extracts possess strong alkyl radical scavenging activity, and HF extracts show relative strong alkyl radical scavenging activity that SF and CF extracts. In addition, the EtOH extract from HF shows the strongest alkyl radical scavenging activity in all of the seaweed extracts.

The results of hydroxyl radical scavenging activities of seaweed extracts were summarized in Table 9. The IC_{50} values of hydroxyl radical scavenging activities of SF extracts were range from 0.44 ± 0.09 mg/mL to 1.54 ± 0.15 mg/mL, and the water extract of SF shows the strongest hydroxyl radical scavenging activity in all of the SF extracts. The IC_{50} values of hydroxyl radical scavenging activities of the extracts from CF were range from 0.14 ± 0.06 mg/mL to 1.76 ± 0.42 mg/mL, and the water extract of CF shows the strongest hydroxyl radical scavenging activity in all of the CF extracts. In addition, the IC_{50} values of hydroxyl radical scavenging activities of the extracts from HF were range from 0.14 ± 0.03 mg/mL to 0.37 ± 0.00 mg/mL, and the Protamex extract of HF shows the strongest hydroxyl radical scavenging activity in all of the HF extracts. These results indicate that all of the seaweed extracts possess strong hydroxyl radical scavenging activity, and HF extracts show relative strong hydroxyl radical scavenging activity that SF and CF extracts. In addition, the water extract of CF and the Protamex extract from HF show the strongest hydroxyl radical scavenging activity in all of the seaweed extracts.

The above results indicate that the extracts from SF, CF, and HF possess strong free radical scavenging activity, especially in alkyl and hydroxyl radicals. In addition, HF extracts show relatively stronger free radical scavenging activity comparing to SF and CF, and the EtOH, Cellucalst, Alcalase, and Protamex extracts from HF possess

stronger free radical scavenging activities comparing to other HF extracts, and these extracts show the potential in cosmetic activities.

Table 7. DPPH radical scavenging activities of seaweed extracts.

Extracts	DPPH radical scavenging activity (IC ₅₀ , mg/mL)		
	SF	CF	HF
D.W	3.02±0.21	5.02±1.20	2.85±0.03
EtOH	2.19±0.63	3.91±0.60	3.07±0.01
AMG	5.07±0.41	3.83±0.48	4.03±0.11
Cell	1.88±0.38	2.65±0.35	1.06±0.08
Ter	2.41±0.52	1.18±0.37	3.99±0.10
Ult	3.07±0.56	2.23±0.62	3.24±0.01
Vis	3.10±0.45	3.48±0.17	2.93±0.09
Alca	1.46±0.51	2.52±0.20	2.44±0.12
Koji	3.55±0.65	4.48±0.35	3.46±0.05
Nue	1.46±0.40	1.75±0.66	2.93±0.11
Pro	1.16±0.31	1.93±0.31	2.93±0.06
Fla	1.88±0.10	2.34±0.43	3.06±0.03

D.W: water extract; EtOH: water extract; AMG: AMG extract; Cell: Celluclast extract;

Ter: Termamyl extracts; Ult: Ultraflo extract; Vis: Viscozyme extract; Alca: Alcalase

extract; Koji: Kojizyme extract; Nue: Neutrased extract; Pro: Protamex extract; Fla:

Flavourzyme extract. The experiments were conducted triplicate, and the data were expressed as the mean ± S.E (n=3).

Table 8. Alkyl radical scavenging activities of seaweed extracts.

Extracts	Alkyl radical scavenging activity (IC ₅₀ , mg/mL)		
	SF	CF	HF
D.W	0.73±0.21	0.82±0.13	0.23±0.03
EtOH	0.93±0.10	0.62±0.14	0.21±0.01
AMG	0.77±0.32	0.74±0.02	0.29±0.01
Cell	0.45±0.11	0.57±0.14	0.34±0.02
Ter	0.61±0.12	0.67±0.25	0.25±0.01
Ult	0.97±0.28	0.49±0.10	0.33±0.12
Vis	0.45±0.20	1.04±0.28	1.06±0.03
Alca	0.44±0.03	0.57±0.15	0.29±0.11
Koji	0.23±0.05	1.09±0.24	0.93±0.00
Nue	0.91±0.01	0.31±0.01	0.26±0.03
Pro	0.70±0.18	0.54±0.24	0.23±0.09
Fla	0.32±0.10	0.32±0.11	0.37±0.02

D.W: water extract; EtOH: water extract; AMG: AMG extract; Cell: Celluclast extract; Ter: Termamyl extracts; Ult: Ultraflo extract; Vis: Viscozyme extract; Alca: Alcalase extract; Koji: Kojizyme extract; Nue: Neutrased extract; Pro: Protamex extract; Fla: Flavourzyme extract. The experiments were conducted triplicate, and the data were expressed as the mean ± S.E (n=3).

Table 9. Hydroxyl radical scavenging activities of seaweed extracts.

Extracts	Hydroxyl radical scavenging activity (IC ₅₀ , mg/mL)		
	SF	CF	HF
D.W	0.44±0.09	0.14±0.06	0.19±0.23
EtOH	1.52±0.35	1.52±0.60	0.22±0.01
AMG	0.66±0.10	1.60±0.37	0.26±0.01
Cell	0.71±0.15	0.46±0.16	0.37±0.00
Ter	1.28±0.11	1.20±0.35	0.29±0.11
Ult	1.33±0.32	1.76±0.42	0.32±0.02
Vis	1.08±0.17	0.44±0.18	0.23±0.03
Alca	0.55±0.08	0.37±0.18	0.20±0.01
Koji	1.54±0.15	0.41±0.17	0.23±0.02
Nue	1.36±0.05	1.66±0.22	0.16±0.03
Pro	1.50±0.41	1.64±0.21	0.14±0.03
Fla	1.38±0.40	1.56±0.35	0.22±0.02

D.W: water extract; EtOH: water extract; AMG: AMG extract; Cell: Celluclast extract; Ter: Termamyl extracts; Ult: Ultraflo extract; Vis: Viscozyme extract; Alca: Alcalase extract; Koji: Kojizyme extract; Nue: Neutrased extract; Pro: Protamex extract; Fla: Flavourzyme extract. The experiments were conducted triplicate, and the data were expressed as the mean ± S.E (n=3).

2.3. Tyrosinase inhibitory effects of seaweed extracts

Tyrosinase is an oxidase that plays an important role in the process of melanin synthesis. It is the rate-limiting enzyme for controlling the production of melanin, which is the major factor for skin color. Therefore, a tyrosinase inhibitor that can inactive or inhibit the tyrosinase may stop or reducing melanin production. The inhibitor may show the potential in whitening effect.

In order to investigate the whitening effect of seaweed extracts, we measured tyrosinase inhibitory effects of seaweed extracts. As Fig. 4 shows, water, AMG, Kojizyme, and Protamex extract of SF, the EtOH and Celluclast extract of HF show strong tyrosinase inhibitory effect. Furthermore, SF and HF extracts possess stronger tyrosinase inhibitory effect than CF extracts, and the water extract of SF possess the strongest tyrosinase inhibitory effect in all of the seaweed extracts. These results indicate that SF and HF extracts possess the potential in skin whitening effect, and water, AMG, Kojizyme, and Protamex extract of SF, EtOH and Celluclast extract of HF possess strong tyrosinase inhibitory effect may be developed to a whitening ingredient use to cosmeceutical industry.

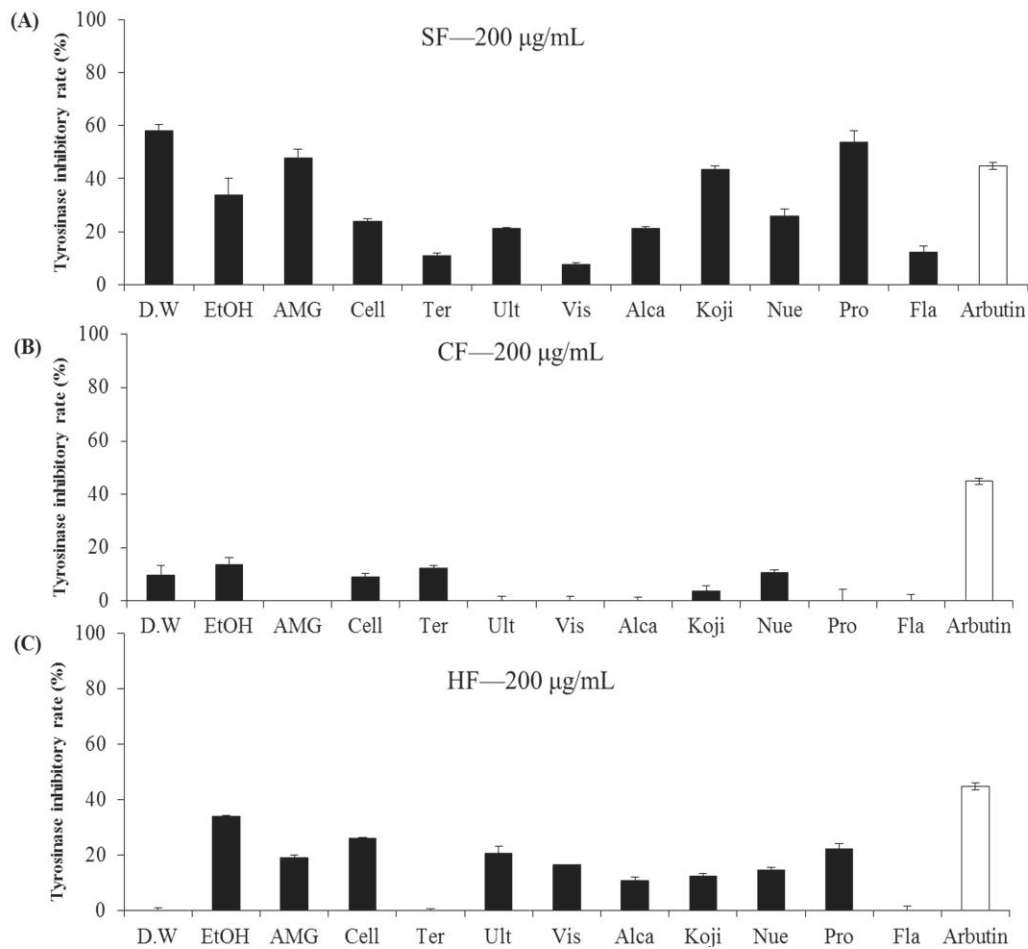


Fig. 4. Tyrosinase inhibitory effects of SF, CF, and HF extracts. (A) Tyrosinase inhibitory effects of SF extracts; (B) tyrosinase inhibitory effects of CF extracts; (C) tyrosinase inhibitory effects of HF extracts. D.W: water extract; EtOH: water extract; AMG: AMG extract; Cell: Celluclast extract; Ter: Termamyl extracts; Ult: Ultraflo extract; Vis: Viscozyme extract; Alca: Alcalase extract; Koji: Kojizyme extract; Nue: Neutrase extract; Pro: Protamex extract; Fla: Flavourzyme extract. Tyrosinase inhibitory effects were measured by colorimetric assay. The amount of dopachrome was measured at 490 nm using a microplate reader. The experiments were conducted triplicate, and the data were expressed as the mean \pm S.E (n=3).

2.4. Collagenase inhibitory effects of seaweed extracts

Collagenases are the enzymes, which break the peptide bonds in collagen. Collagen is the key component of the animal extracellular matrix (ECM), is produced via cleavage of pro-collagen by collagenase once it has been secreted from the cell. The degradation of collagen is the major factor that leads to skin wrinkling and decreased skin thickness. Thus, a chemical or compound, which can inhibit or inactive collagenase may protect or against skin wrinkling through reducing the collagen degradation.

In order to investigate the anti-wrinkle effects of seaweed extracts, we measured collagenase inhibitory effects of seaweed extracts. As Fig. 5 shows, EtOH and Kojizyme extract of SF, EtOH, Celluclast, and Protamex extract of HF show strong collagenase inhibitory effects. In addition, HF extracts possess stronger collagenase inhibitory effect than SF and CF extracts, and the Celluclast extract of HF possess strongest collagenase inhibitory effect in all of the seaweed extracts. These results indicate that HF extracts possess the potential in anti-wrinkle effect, and EtOH and Kojizyme extract of SF, EtOH, Celluclast, and Protamex extract of HF possess strong collagenase inhibitory effect may be developed to an anti-wrinkle ingredient use to cosmeceutical industry.

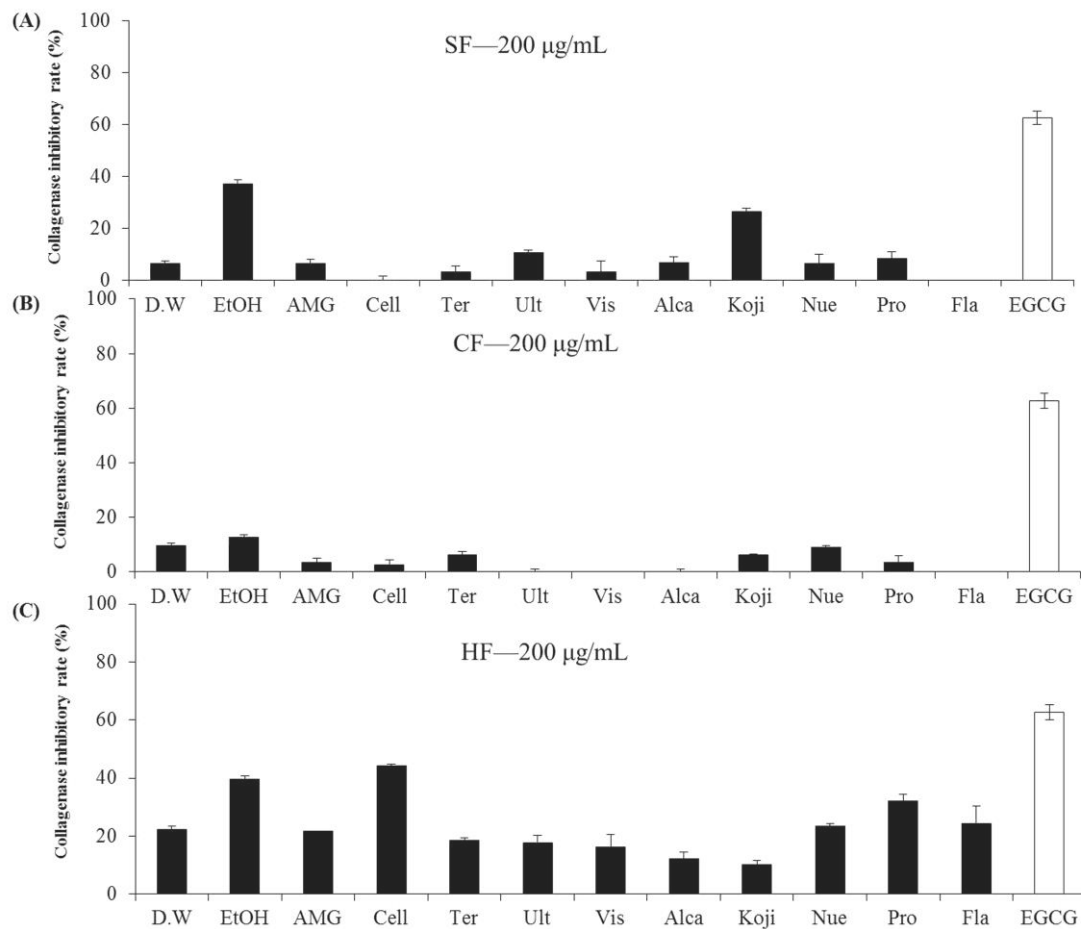


Fig. 5. Collagenase inhibitory effects of SF, CF, and HF extracts. (A) Collagenase inhibitory effects of SF extracts; (B) collagenase inhibitory effects of CF extracts; (C) collagenase inhibitory effects of HF extracts. D.W: water extract; EtOH: water extract; AMG: AMG extract; Cell: Celluclast extract; Ter: Termamyl extracts; Ult: Ultraflo extract; Vis: Viscozyme extract; Alca: Alcalase extract; Koji: Kojizyme extract; Nue: Neutrase extract; Pro: Protamex extract; Fla: Flavourzyme extract. Collagenase inhibitory effects were measured by colorimetric assay. The experiments were conducted triplicate, and the data were expressed as the mean \pm S.E (n=3).

2.5. Elastase inhibitory effects of seaweed extracts

Elastase is an enzyme related to skin wrinkle formation. Elastase is the enzyme that breaks down elastin, which is an elastic fiber. In human skin, the degradation of elastin results in losing skin elasticity. Therefore, an elastase inhibitor, which can inhibit or inactivate elastase may protect or against skin wrinkling through reducing the elastin degradation.

In this study, we investigate elastase inhibitory effects of seaweed extracts. As Fig. 6 shows, EtOH and Celluclast extract of HF shows strong elastase inhibitory effects. In addition, HF extracts possess stronger elastase inhibitory effect than SF and CF extracts, and the Celluclast extract of HF possess the strongest elastase inhibitory effect in all of the seaweed extracts. These results display that HF extracts possess the potential in anti-wrinkle effect; and the Celluclast extract of HF possess strong elastase inhibitory effect may be developed to an anti-wrinkle ingredient use to cosmeceutical industry.

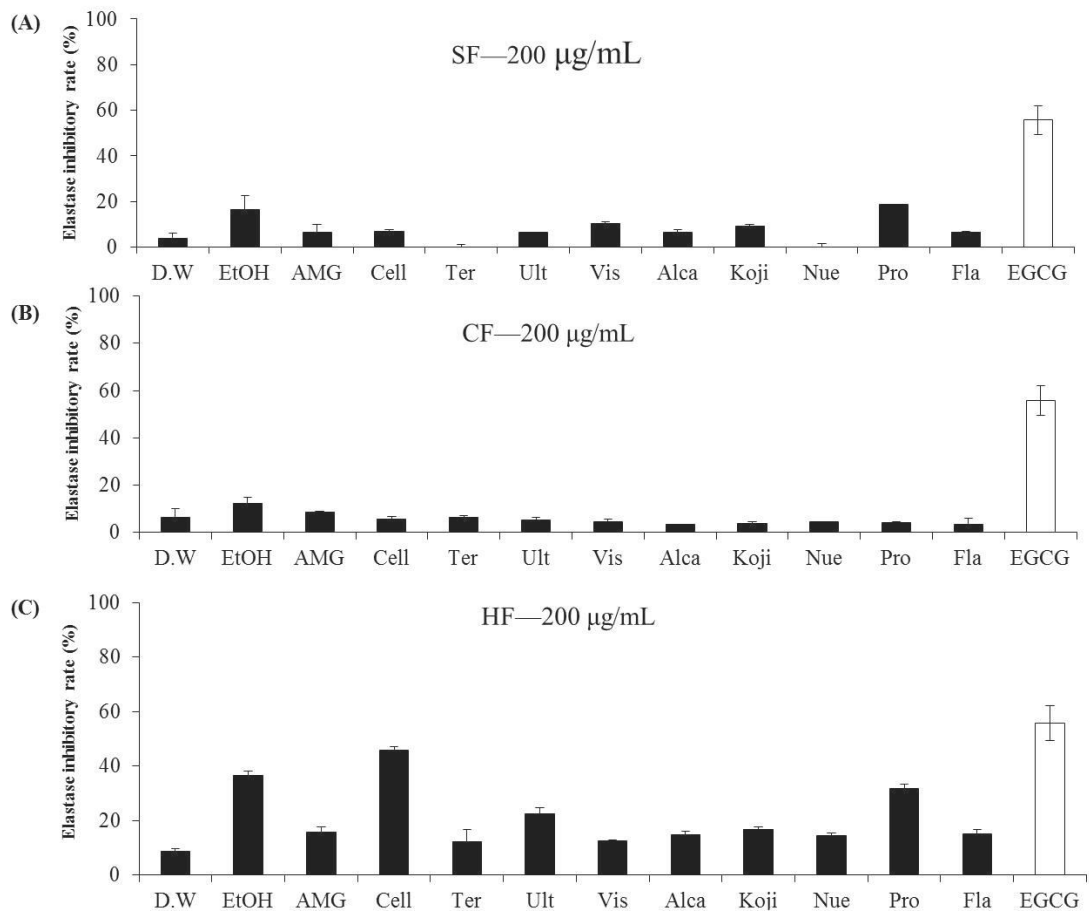


Fig. 6. Elastase inhibitory effects of SF, CF, and HF extracts. (A) Elastase inhibitory effects of SF extracts; (B) elastase inhibitory effects of CF extracts; (C) elastase inhibitory effects of HF extracts. D.W: water extract; EtOH: water extract; AMG: AMG extract; Cell: Celluclast extract; Ter: Termamyl extracts; Ult: Ultraflo extract; Vis: Viscozyme extract; Alca: Alcalase extract; Koji: Kojizyme extract; Nue: Neutrase extract; Pro: Protamex extract; Fla: Flavourzyme extract. Elastase inhibitory effects were measured by colorimetric assay. The experiments were conducted triplicate, and the data were expressed as the mean \pm S.E (n=3).

CONCLUSION

Marine algae are rich in various natural compounds and possess broad bioactivities.

S. fulvellum, *C. fragile*, and *H. fusiforme* are three edible seaweeds, which had consumed as food and medicine ingredient for a long history. The above data demonstrate that: 1) enzyme-assisted extraction can improve the extraction yield; 2) all three algae possess strong free radical scavenging activity; 3) HF extracts possess the best free radical scavenging activity in all three seaweeds; 4) Celluclast-assisted extract and EtOH of HF possess the potential to developing the cosmeceutical; 5) the main composition of the Celluclast-assisted extract of HF is polysaccharides.

According to the above results, HF contains a high amount of polysaccharide and shows the cosmetic potential. The polysaccharides from Celluclast-assisted extract need to be separated and the cosmeceutical effects of the polysaccharides need to be investigated.

Part II.

Preparation of crude polysaccharides of *Hizikia fusiforme* (HFCPS) and evaluation of its bioactivities

Part II.

Preparation of crude polysaccharides of *Hizikia fusiforme* (HFCPS) and evaluation of its bioactivities

ABSTRACT

Polysaccharides were extracted by Celluclast-assisted hydrolysis and ethanol precipitation from *Hizikia fusiforme* (HFCPS). HFCPS contains $63.56 \pm 0.32\%$ sulfated polysaccharides, which comprise fucose (53.53%), galactose (23.15%), glucose (5.95%), and xylose (17.37%). The cosmeceutical effects of HFCPS were measured including antioxidant activity, anti-inflammatory activity, whitening effect, ultraviolet (UV) protective effect, and anti-wrinkle effect. The results indicate that HFCPS significantly reduces hydrogen peroxide (H_2O_2)-induced oxidative stress in monkey kidney fibroblast cells (Vero cells) and in zebrafish; remarkably attenuates lipopolysaccharide (LPS)-induced inflammation in RAW 264.7 macrophages; inhibits alpha-melanocyte stimulating hormone (α -MSH)-stimulated melanogenesis in B16F10 melanoma cells; against UVB-induced photo-damage in keratinocytes (HaCaT cells) and in zebrafish; protects UVB-induced skin wrinkling in human dermal fibroblasts (HDF cells). These results demonstrate that HFCPS possesses potent cosmeceutical effect, and can be a potential ingredient in the cosmetic industry.

INTRODUCTION

Oxidative stress occurs when there is an imbalance between the systemic manifestation of reactive oxygen species (ROS) and the ability of the biological system to detoxify the reactive intermediates or to repair the damage induced by ROS. An abnormal cellular redox state can cause toxicity through the production and accumulation of ROS, including free radicals and peroxides, which damage cellular components including DNA, proteins, and lipids. ROS are naturally generated during aerobic metabolism, but environmental stresses, such as chemicals and ultraviolet irradiation, can induce an imbalance between the antioxidant defense system and the accumulation of ROS, which include HO• (hydroxyl radical), O₂^{•-} (superoxide anion radical), and H₂O₂ (hydrogen peroxide) [44].

ROS play an important role in human health, and ROS imbalances are associated with various diseases. Normally, cells have an endogenous antioxidant system that protects them against damage induced by ROS through producing antioxidant enzymes such as catalase (CAT), glutathione peroxidase (GSH-Px), and superoxide dismutase (SOD). In some cases, the endogenous antioxidants cannot scavenge all the ROS generated by the intracellular metabolism. Excess ROS accumulated in the cells will damage bio-macromolecules, and induce diseases such as inflammation, cancer, liver injury, diabetes, and abnormal aging [45, 46]. The use of supplementary antioxidants, with strong antioxidant activity and low toxicity, is potentially beneficial for humans. Compared with synthetic compounds, naturally occurring compounds are safe, and have few side effects. Increasing attention has therefore been focused on the discovery of natural antioxidants.

Seaweeds contain various bioactive compounds, especially polysaccharides. Algal polysaccharides generally comprise carrageenan, fucoidan, and alginate. Normally,

algal polysaccharides have unique physicochemical properties, and possess potent antioxidant, anti-inflammatory, anticancer, anti-aging, anti-coagulant, radio-protective, and immune activating activities [47-49]. Lee et al. have previously studied the anti-inflammatory effect of fucoidan extracted from *Ecklonia cava* [50]. Ahn et al. have previously studied immune system activation and modulation, as well as the anticancer activity, of a sulfated polysaccharide extracted from *Ecklonia cava* [51, 52]. Lee et al. measured the antioxidant activity of polysaccharides extracted from *Pyropia yezoensis* [53].

H. fusiforme is an edible brown seaweed that mainly grows in the northwest Pacific, including Korea, China, and Japan. It contains various bioactive compounds, especially polysaccharides. Polysaccharides from *H. fusiforme* possess extensive and potent anti-coagulant, immune-modulating, and anti-toxicity bioactive effects [54-56]. The previous results indicate that Cellucalst-assisted extract of *H. fusiforme* possesses strong free radical scavenging activity as well as cosmetic effects and the main composition of the Cellucalst-assisted extract of *H. fusiforme* is polysaccharides. Therefore, we separate polysaccharides from the Cellucalst-assisted extract of *H. fusiforme* and evaluate the cosmetic effects including antioxidant, anti-inflammatory, anti-melanogenesis, UV protection, and anti-wrinkle effects.

Section 1: Celluclast-assisted extraction of *Hizikia fusiforme* and separation of polysaccharides from Celluclast-assisted extract of *Hizikia fusiforme*

Abstract

The above results indicate that Celluclast-assisted extract of *H. fusiforme* is rich in polysaccharide and possess strong free radical scavenging activity as well as cosmetic effects. In order to investigate the cosmetic effects of polysaccharides (HFCPS) from Celluclast-assisted extract (HFC) of *H. fusiforme*, we prepare HFCPS by ethanol precipitation and analysis its proximate composition. The results demonstrate that HFCPS contains $63.56\pm 0.32\%$ sulfated polysaccharides and constitutes by glucose (5.95%), xylose (17.37%), galactose (23.15%), and fucose (53.53%). HFCPS contains high amount of sulfated polysaccharides, which may possess a broad bioactivity.

1. Materials and Methods

1.1. Reagents and chemicals

H. fusiforme was collected in June 2016 from the coastal area of Jeju Island, South Korea. The Celluclast was purchased from Sigma (Sigma, St. Louis, MO, USA, ≥ 700 units/g). Trifluoroacetic acid, arabinose, fucose, galactose, glucose, rhamnose, and xylose were purchased from Sigma (Sigma, St. Louis, MO, USA). All other chemicals and reagents were analytical grade.

1.2. Preparation of polysaccharides from *H. fusiforme*

The lyophilized *H. fusiforme* powder was hydrolyzed by Celluclast (Sigma, St. Louis, MO, USA, ≥ 700 units/g) in the shaking incubator at the optimal condition (pH 4.5, 50°C) for 24 hours and the polysaccharides were obtained by ethanol precipitation. In briefly, a weight of 50 g lyophilized seaweed powder was mixed with 5 L distilled water, and adjusted pH by 1 M HCl, then, 2.5 mL of Celluclast was added to make 5% enzyme ratio to the seaweed. Finally, the enzyme-assisted extract was performed under shaking condition. After hydrolysis, the enzyme was inactive by heating at 100°C for 10 minutes. The macerated mixture was centrifuged, filtered, and adjusted pH to 7 by 1 M NaOH, then got the Celluclast-assisted extract of *H. fusiforme* and named as HFC. HFC mixed with two times volume of 95% ethanol and keep at 4°C for 24 hours, the precipitates were collected and named as HFCPS. HFCPS was thought as the crude polysaccharides of *H. fusiforme*.

1.3. Chemical analysis of HFC and HFCPS

The total carbohydrate content of HFC and HFCPS were determined based on the protocol of official methods for analysis of the Association of Official Analytical Chemists (AOAC) [57]. Glucose was used as a standard to evaluate the total

carbohydrate content of HFC and HFCPS. To determine the sulfate content, HFC and HFCPS were hydrolyzed by 4 M trifluoroacetic acid at 100°C for 5 hours. The sulfate content was measured by the method described by Wang et al. [33].

In order to analyze the neutral sugars components of HCF and HFCPS, HCF and HFCPS were hydrolyzed by 4 M of trifluoroacetic acid in sealed glass vials for 4 h at 100°C. Then, the neutral sugar components and contents of samples were determined by HPLC. Arabinose, fucose, galactose, glucose, rhamnose, and xylose had used as the standard, the procedure described by Kang et al. [58].

2. Results and Discussion

2.1. Yield, total carbohydrate, phenolic, and sulfate content of HFC and HFCPS

H. fusiforme was hydrolyzed by Celluclast and then precipitated using ethanol (Fig. 7), and the component contents of HFC and HFCPS were analyzed. The yields of HFC and HFCPS were $44.00\pm 1.10\%$ and $29.35\pm 1.41\%$, and the phenolic content of HFC and HFCPS were $1.78\pm 0.05\%$ and $1.56\pm 0.08\%$, respectively (Table 10). The carbohydrate content of HFC and HFCPS were $48.05\pm 1.10\%$ and $55.05\pm 0.09\%$, and the sulfate content of HFC and HFCPS were $4.97\pm 0.04\%$ and $7.78\pm 0.23\%$, respectively. Altogether, HFC and HFCPS contain $53.02\pm 1.14\%$ and $63.56\pm 0.32\%$ sulfated polysaccharides, respectively.

2.2. Natural sugar composition of HFC and HFCPS

The monosaccharide content of HFC and HFCPS were determined using HPLC. Six monosaccharides had used as standards: fucose, rhamnose, arabinose, galactose, glucose, and xylose. The polysaccharides of HFC and HFCPS comprise four monosaccharides: fucose, galactose, glucose, and xylose (Table 11). The proportions of these monosaccharides in HFC were 24.04%, 14.24%, 56.75%, and 4.97%, and in HFCPS were 53.53%, 23.15%, 5.95%, and 17.37%, respectively. The major monosaccharide in HFC is glucose, while the major monosaccharide in HFCPS is fucose.

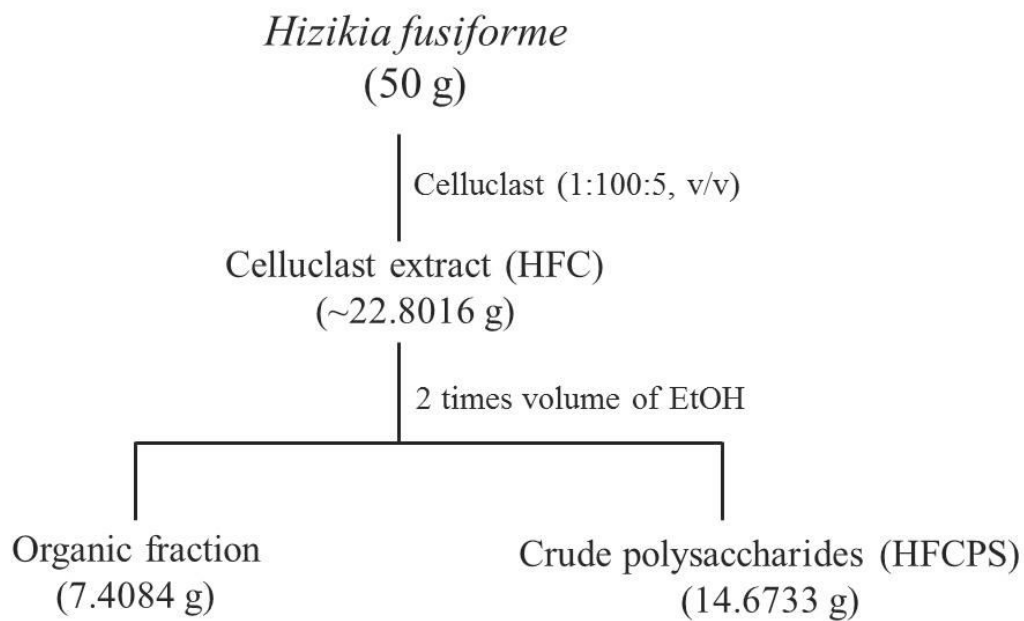


Fig. 7. The procedure of large-scale extraction and separation polysaccharides from *Hizikia fusiforme*.

Table 10. The yields, total carbohydrate contents, total phenolic contents, and sulfate contents of HFC and HFCPS obtained from *H. fusiforme*.

Sample	HFC	HFCPS
Yield (%)	44.00±1.10	29.35±1.41
Phenolic content (%)	1.78±0.05	1.56±0.08
Carbohydrate content (%)	48.05±1.10	55.05±0.09
Sulfate content (%)	4.97±0.04	7.78±0.23
Sulfated polysaccharide	53.02±1.14	63.56±0.32

HFC: Celluclast-assisted extract of *H. fusiforme*; HFCPS: polysaccharides from Celluclast-assisted extract of *H. fusiforme*. The experiments were conducted triplicate, and the data were expressed as the mean ± S.E (n=3).

Table 11. The proportion of monosaccharide of HFC and HFCPS obtained from *H. fusiforme*.

Proportion of monosaccharide (%)	HFC	HFCPS
Fucose	24.04	53.53
Galactose	14.24	23.15
Glucose	56.75	5.95
Xylose	4.97	17.37

HFC: Celluclast-assisted extract of *H. fusiforme*; HFCPS: polysaccharides from Celluclast-assisted extract of *H. fusiforme*. The experiments were conducted triplicate, and the data were expressed as the mean \pm S.E (n=3).

3. Conclusion

A large-scale Celluclast-assisted extraction of *H. fusiforme* was performed and the crude polysaccharide from the Celluclast-assisted extract of *H. fusiforme* (HFCPS) was obtained. HFCPS contains $63.56 \pm 0.32\%$ sulfated polysaccharide and constitutes by glucose (5.95%), xylose (17.37%), galactose (23.15%), and fucose (53.53%). The bioactivities of HFCPS need to be examined.

Section 2: Antioxidant activity of polysaccharides from Celluclast-assisted extract of *Hizikia fusiforme* *in vitro* in Vero cells and *in vivo* in zebrafish

Abstract

The polysaccharides of *Hizikia fusiforme* (HFCPS) were obtained by Celluclast-assisted hydrolysis and ethanol precipitation, and the *in vitro* antioxidant effects of HFCPS were evaluated by investigation of free radical scavenging activities and protective effects against hydrogen peroxide (H₂O₂)-induced oxidative stress in Vero cells. HFCPS scavenged DPPH, alkyl, and hydroxyl radicals at the IC₅₀ values of 0.81±0.02 mg/mL, 0.25±0.02 mg/mL, and 0.21±0.03 mg/mL, respectively. HFCPS significantly reduced cytotoxicity induced by H₂O₂ on Vero cells. Furthermore, HFCPS reduced cellular ROS level and apoptosis body formation induced by H₂O₂. In addition, HFCPS has shown strongly protective effects against H₂O₂-stimulated oxidative stress *in vivo* zebrafish that demonstrated by improving survival rate, decreasing heart beating rate, and reducing ROS generation and cell death. These results suggest that HFCPS may be useful as a beneficial antioxidant ingredient in medical and cosmetic industries.

1. Materials and methods

1.1. Reagents and Chemicals

3-(4,5-dimethylthiazol-2-yl)-2,5-Diphenyltetrazolium bromide (MTT), dimethyl sulfoxide (DMSO), 1-diphenyl-2-picrylhydrazyl (DPPH), 5,5-dimethyl-1-pyrroline N-oxide (DMPO), 2,2-azobis (2-amidinopropane) hydrochloride (AAPH), α -(4-Pyridyl-1-oxide)-N-ter-butyl nitron (POBN), acridine orange, and 2,7-dichlorofluorescein diacetate (DCFH-DA) were purchased from Sigma (St. Louis, MO, USA). $\text{FeSO}_4 \cdot 7\text{H}_2\text{O}$, and H_2O_2 were purchased from Fluka Co. (Buchs, Switzerland). The monkey kidney fibroblast (Vero) cell line was purchased from the Korea Cell Line Bank (KCLB, Seoul, Korea). Roswell Park Memorial Institute-1640 (RPMI-1640) medium, fetal bovine serum (FBS), penicillin-streptomycin, and trypsin-EDTA were purchased from Gibco-BRL (Grand Island, NY, USA). All other chemicals and reagents were analytical grade.

1.2. Evaluation of free radical scavenging activities of HFC and HFCPS

The free radical scavenging activities of HFC and HFCPS were determined using an electron spin resonance (ESR) spectrometer (JES-FA machine; JOEL, Tokyo, Japan) according to the methods described by Wang et al. [59].

1.3. Cell culture

Vero cells were maintained in RPMI-1640 medium containing 10% heat-inactivated FBS, penicillin (100 unit/mL), and streptomycin (100 $\mu\text{g}/\text{mL}$) at 37°C in an incubator under the humidified atmosphere containing 5% CO_2 . Vero cells were sub-cultured for 3 days and seeded at a concentration of 1×10^5 cells/mL in 96-well plates.

1.4. Determination of the cytotoxicity of HFCPS on Vero cells

To evaluate the cytotoxicity of HFCPS, Vero cells were seeded and incubated for 24 h. Cells were treated with 10 μ L of samples to final concentrations of 25, 50, and 100 μ g/mL, and incubated for 24 h at 37°C. Cell viability was estimated using an MTT assay as described by Fernando et al. [5].

1.5. Determination of the protective effect of HFCPS against H₂O₂-induced intracellular ROS generation in Vero cells

Vero cells were seeded as described above, and cultured for 24 h. Different concentrations of HFCPS were added to cells prior to incubation for 1 h. After incubation, H₂O₂ (1 mM) was added to the cells, followed by incubation for 1 h. Finally, DCFH-DA (500 μ g/mL) was introduced to the cells, and the fluorescence emission of DCF-DA was detected using a fluorescence a microplate reader (Olympus, Japan).

1.6. Measurement of the protective effect of HFCPS against H₂O₂-induced cytotoxicity in Vero cells

Vero cells were seeded in a 96-well plate as described above. After 24 h incubation, cells were treated with different concentrations of HFCPS and incubated for 1 h. After incubation, H₂O₂ (1 mM) was added to the cells prior to incubation for 24 h. Cell viability was measured by MTT assay, according to Fernando et al. [5].

1.7. Nuclear staining with Hoechst 33342

To assess the protective effects of HFCPS against H₂O₂-induced cell apoptosis, the nuclear morphology of cells was analyzed by Hoechst 33342 staining. Nuclear staining was performed base on the method described by Wijesinghe et al. [60]. The

degree of nuclear condensation of cells was examined under a fluorescence microscope equipped with a Cool SNAP-Pro color digital camera (Olympus, Japan).

1.8. Maintenance of zebrafish

Adult zebrafish were purchased from a commercial market (Seoul Aquarium, Korea). Each 10 fish were kept in a 3 L acrylic tank at 28.5°C, under a 14/10 h light/dark cycle. The fish were fed with Tetramin flake feed supplemented with live brine shrimp (*Artemia salina*) three times per day, 6 days a week. Embryos were collected after natural spawning that was induced by light, and embryo collection was completed within 30 min.

1.9. Application of HFCPS and H₂O₂ to zebrafish embryos

Approximately 3~4 hours post-fertilization (hpf), the embryos were transferred to individual wells in a 12-well plate (15 embryos per group) and maintained in embryo medium containing HFCPS (25, 50, and 100 µg/mL). After 1 hour incubation, 5 mM H₂O₂ was added to the medium, and the embryos were incubated until 24 hpf. The survival rate was measured at 3 days post-fertilization (dpf) after treatment with H₂O₂ by counting live embryos, and the surviving fish were then used for further analysis.

1.10. Determination of heart-beating rate, ROS generation, and cell death in zebrafish

The zebrafish heart-beating rate was measured according to Kim et al. [61]. The zebrafish heart-beating rate in both the atrium and ventricle was recorded for 1 min at 2 dpf under a microscope. The intracellular ROS and cell death levels were measured in live embryos using DCFH-DA and acridine orange staining, respectively, followed the procedure described by Kim et al. [46]. The zebrafish were observed and photographed under a fluorescence microscope equipped with a Cool SNAP-Pro color

digital camera (Olympus, Japan). The fluorescence intensity of individual zebrafish larva was quantified using the image J program.

1.11. Statistical analysis

All experiments were conducted in triplicate. The data are expressed as the mean \pm standard error (S.E), and one-way ANOVA was used to compare the mean values of each treatment in SPSS 12.0. Significant differences between the means were identified by the Turkey test. Significance was established if $*p < 0.05$, $** p < 0.01$ as compared to the H₂O₂-treated group, and $^{##}p < 0.01$ as compared to control group.

2. Results and Discussion

2.1. Free radical scavenging activities of HFC and HFCPS

The DPPH, alkyl, and hydroxyl radical scavenging activities of HFC and HFCPS were determined. Both samples show strong radical scavenging activity (Table 12) and HFCPS showing stronger radical scavenging activities than HFC, and both samples showing the strongest activity against the hydroxyl radical. Therefore, H₂O₂ was selected as a stimulator to induce oxidative stress *in vitro* in Vero cells and *in vivo* in zebrafish for evaluation of the protective effects of HFCPS against oxidative stress.

2.2. Cytotoxicity of HFCPS on Vero cells

The cytotoxicity of HFCPS on Vero cells was determined. As Fig. 8 shows, HFCPS has not shown toxicity on Vero cells at the concentration from 25 µg/mL to 100 µg/mL, but shown toxicity on Vero cells at 200 µg/mL. Thus, the highest concentration of HFCPS has performed as 100 µg/mL in the further studies.

Table 12. Free radical scavenging activities of HFC and HFCPS obtained from *H. fusiforme*.

Sample	Free radical scavenging activity (IC ₅₀ , mg/mL)		
	DPPH	Alkyl	Hydroxyl
HFC	0.91±0.02	0.43±0.02	0.37±0.00
HFCPS	0.81±0.02	0.25±0.02	0.21±0.03

HFC: Celluclast-assisted extract of *H. fusiforme*; HFCPS: polysaccharides of *H. fusiforme*; DPPH: DPPH radical scavenging activity; Alkyl: alkyl scavenging activity; Hydroxyl: hydroxyl scavenging activity. The experiments were conducted triplicate in this study. The data were expressed as the mean ± standard error (S.E).

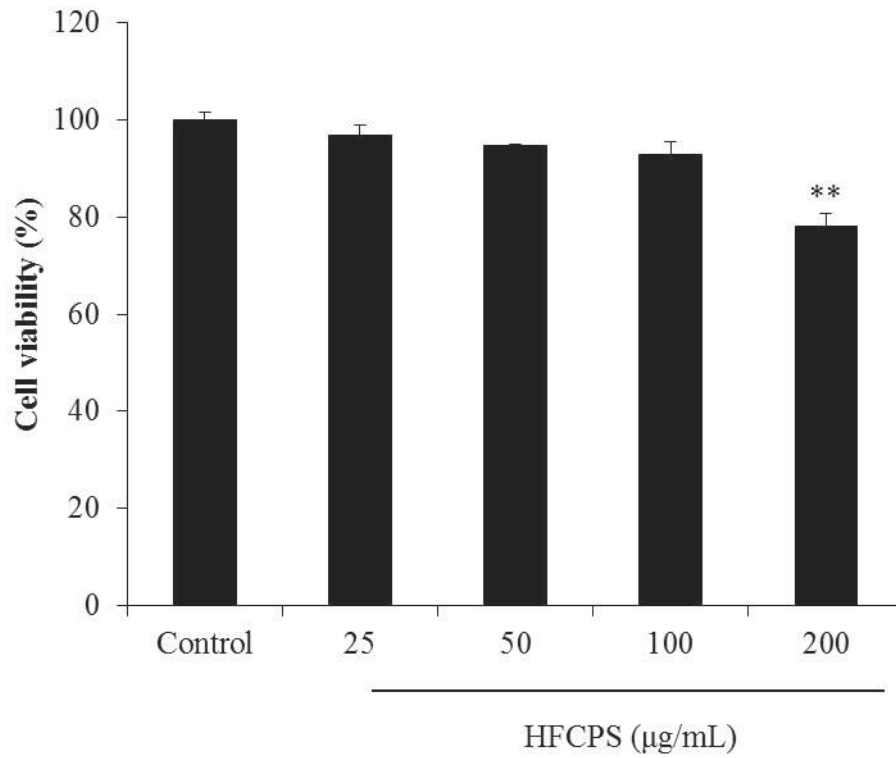


Fig. 8. Cytotoxicity of HFCPS on Vero cells. Cell viability was measured by MTT assay. The experiments were conducted in triplicate, and the data are expressed as the mean \pm standard error (S.E). ** $p < 0.01$ as compared to the control group.

2.3. Protective effect of HFCPS against H₂O₂-induced oxidative stress in Vero cells

As Fig. 9 shows, the intracellular ROS level increased significantly, and cell viability decreased, following treatment with H₂O₂. However, the intracellular ROS levels decreased, and cell viability increased, following treatment at all measured concentrations of HFCPS. Both effects occurred in a dose-dependent manner.

2.4. Protective effect of HFCPS against H₂O₂-induced apoptosis

In order to measure the apoptotic body formation stimulated by H₂O₂, Vero cells were stained with Hoechst 33342 and visualized by a fluorescent microscopy. There were significant apoptotic bodies formed in the cells treated with H₂O₂ (Fig. 10). The amount of apoptotic bodies formed in cells pretreated with different concentrations of HFCPS significantly decreased in a dose-dependent manner.

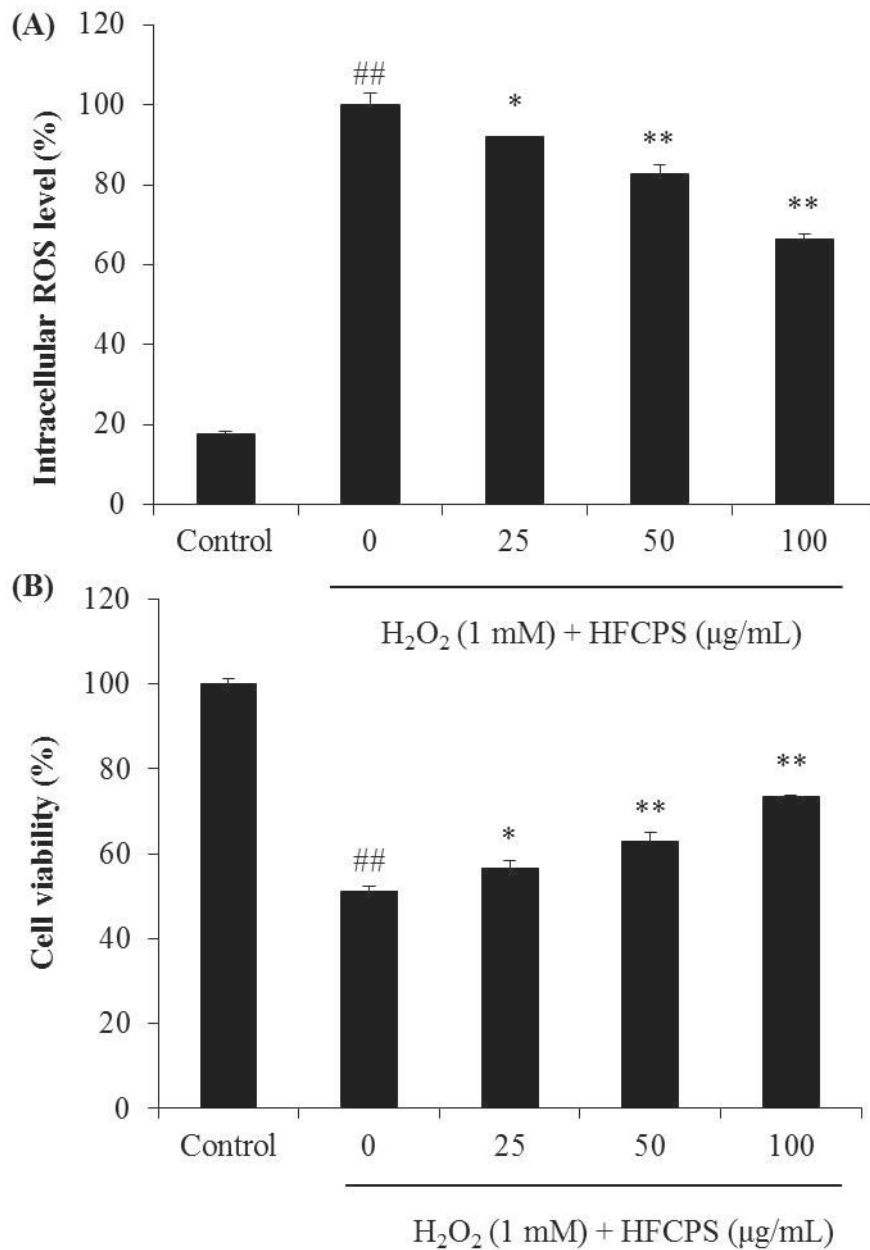


Fig. 9. The intracellular ROS scavenging effect of HFCPS during H₂O₂-induced oxidative stress in Vero cells (A) and the protective effects of HFCPS against H₂O₂-induced cell death in Vero cells (B). The experiments were conducted in triplicate, and the data are expressed as the mean \pm standard error (S.E). * $p < 0.05$, ** $p < 0.01$ as compared to the H₂O₂-treated group and ## $p < 0.01$ as compared to the control group.

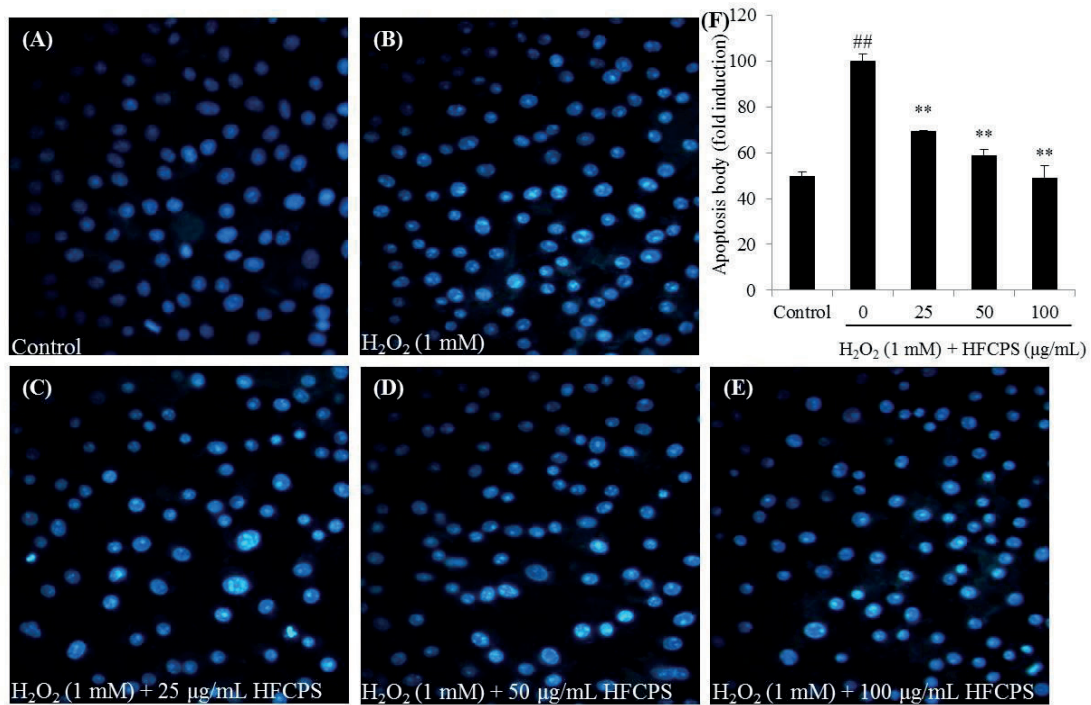


Fig. 10. The protective effect of HFCPS against H₂O₂-induced apoptosis in Vero cells. (A) Nuclear morphology of non H₂O₂-treated cells. (B) Nuclear morphology of H₂O₂-treated cells. (C) Nuclear morphology of cells treated with 25 µg/mL of HFCPS and H₂O₂. (D) Nuclear morphology of cells treated with 50 µg/mL of HFCPS and H₂O₂. (E) Nuclear morphology of cells treated with 100 µg/mL of HFCPS and H₂O₂. (F) Reactive apoptotic body formation. The apoptotic body formation was observed under a fluorescence microscope after Hoechst 33342 staining. Apoptosis levels were measured using Image J software. ** $p < 0.01$ as compared to the H₂O₂-treated group and ^{##} $p < 0.01$ as compared to the control group.

2.5. HFCPS improve survival rate and reduce heart-beating rate in H₂O₂-induced zebrafish

The survival rates and heart-beating rates of zebrafish were determined. The survival rate and heart-beating rate of zebrafish that did not receive H₂O₂ treatment were considered to be 100% (Fig. 11). The survival rate of zebrafish treated with H₂O₂ significantly decreased to 66.67% (Fig. 11A). However, the survival rates of zebrafish pretreated with HFCPS at 50 and 100 µg/mL prior to H₂O₂ treatment significantly increased. The heart rate of the zebrafish treated with H₂O₂ was 113.52% (Fig. 11B) of that of the control, but significantly decreased with high concentrations of HFCPS treatment.

2.6. Protective effect of HFCPS against H₂O₂-induced ROS generation and cell death in zebrafish

The antioxidant effect of HFCPS on ROS generation in H₂O₂-treated zebrafish embryos was measured by detection of DCF-DA. The ROS level in zebrafish that did not receive H₂O₂ treatment was considered to be 100%, and the ROS level in H₂O₂ treated zebrafish was 129.22%. However, pretreatment with HFCPS resulted in decreased ROS levels in a dose-dependent manner (Fig. 12). In addition, the protective effect of HFCPS against H₂O₂-induced cell death in zebrafish was evaluated by measuring the acridine orange fluorescence intensity. HFCPS treatment at 50 and 100 µg/mL significantly reduced the H₂O₂-induced cell death in zebrafish (Fig. 13).

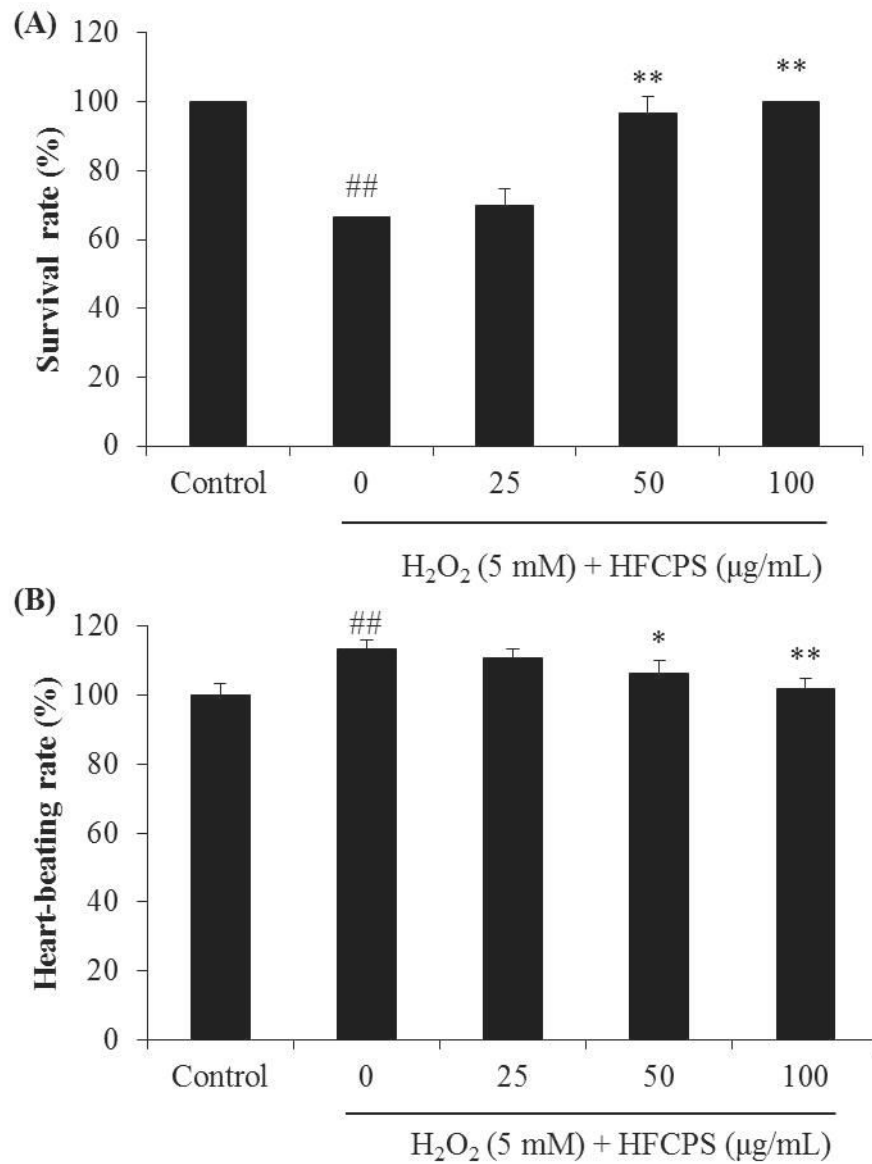


Fig. 11. The survival rate and heart-beating rate of zebrafish after pretreatment with HFCPS and/or treatment with H₂O₂. (A) Survival rate; (B) heart-beating rate. The experiments were conducted in triplicate, and the data are expressed as the mean ± standard error (S.E). **p* < 0.05, ** *p* < 0.01 as compared to the H₂O₂-treated group and ^{##}*p* < 0.01 as compared to the control group.

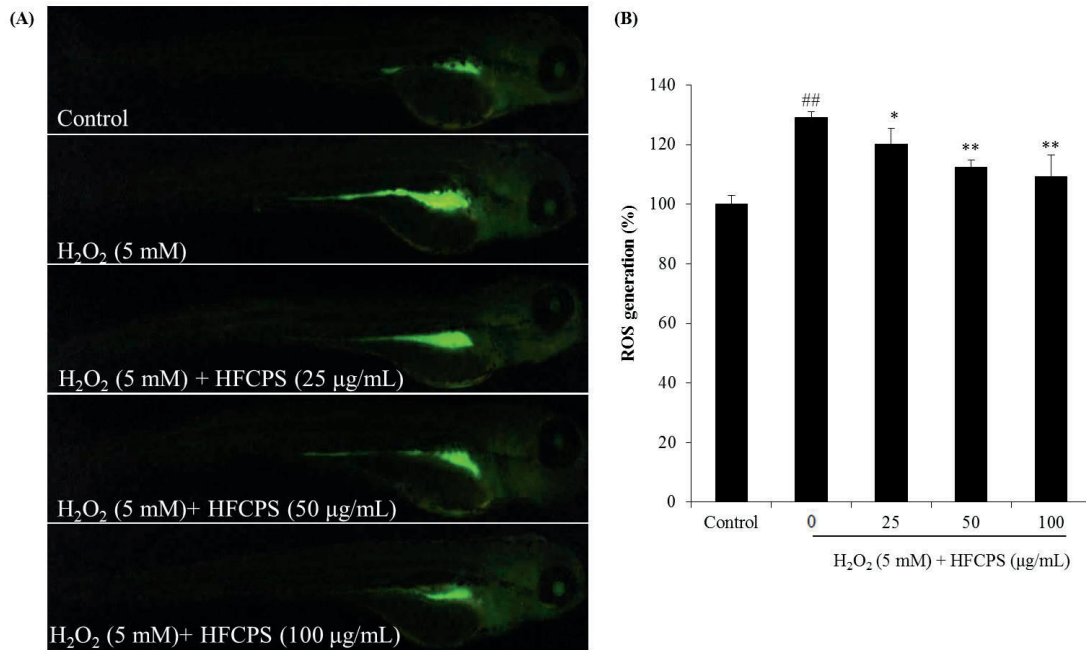


Fig. 12. The protective effect of HFCPS during H₂O₂-induced ROS production in zebrafish embryos. (A) Zebrafish embryo under fluorescence microscope; (B) the levels of ROS generation. ROS levels were measured using Image J software. The experiments were conducted in triplicate, and the data are expressed as the mean \pm standard error (S.E). * $p < 0.05$, ** $p < 0.01$ as compared to the H₂O₂-treated group and ^{##} $p < 0.01$ as compared to the control group.

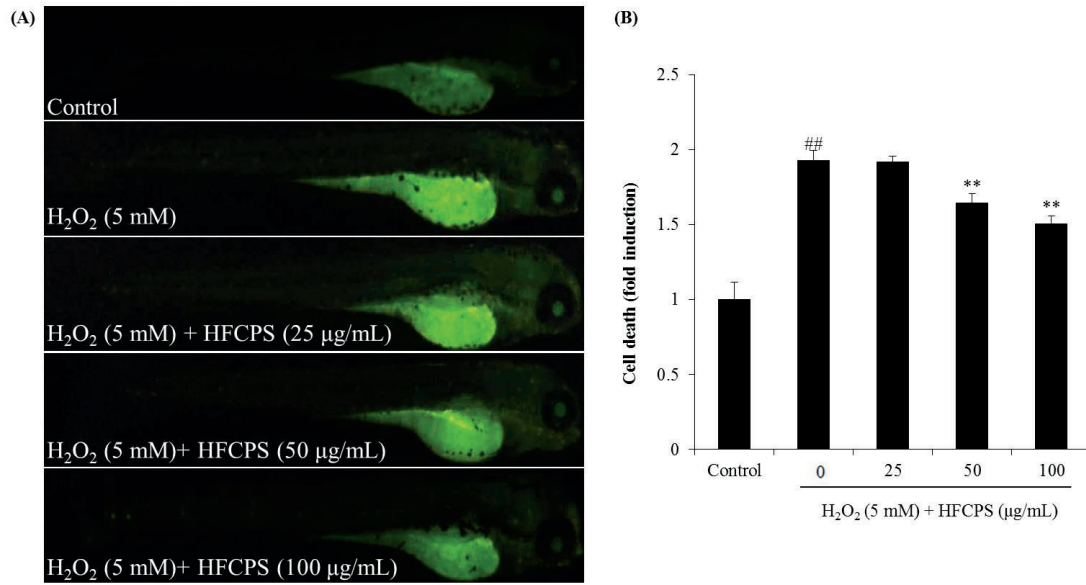


Fig. 13. The protective effect of HFCPS during H₂O₂-induced cell death in zebrafish embryos. (A) Zebrafish embryo under fluorescence microscope; (B) the measured levels of cell death. Cell death levels were measured using Image J software. The experiments were conducted in triplicate, and the data are expressed as the mean \pm standard error (S.E). * $p < 0.05$, ** $p < 0.01$ as compared to the H₂O₂-treated group and ### $p < 0.01$ as compared to the control group.

3. Conclusion

The antioxidant effects of HFCPS have been investigated. HFCPS possesses strong *in vitro* and *in vivo* antioxidant activities demonstrate in scavenging free radicals, reducing intracellular ROS and improving cell viability in H₂O₂-stimulated Vero cells as well as in improving the survival rate, decreasing heart-beating rate, and reducing ROS generation and cell death in H₂O₂-stimulated zebrafish. These results suggest that HFCPS may be considered for use in the medical and cosmetic industries.

Section 3: Anti-inflammatory effect of polysaccharides from Celluclast-assisted extract of *Hizikia fusiforme*

Abstract

In the present study, the anti-inflammatory effect of polysaccharides from Celluclast-assisted extract of *Hizikia fusiforme* (HFCPS) was investigated in lipopolysaccharide (LPS)-stimulated RAW 264.7 macrophages. The results indicate that HFCPS significantly inhibits nitric oxide (NO) generation stimulated by LPS in RAW 264.7 cells. In addition, HFCPS dose-dependently improves the cell viability in LPS-stimulated RAW 264.7 cells. Moreover, HFCPS significantly decreases the expression of tumor necrosis factor alpha (TNF- α), prostaglandin E₂ (PGE₂), interleukin-1 beta (IL-1 β), and interleukin-6 (IL-6). Furthermore, HFCPS suppresses the expression of inducible nitric oxide synthase (iNOS) and cyclooxygenase-2 (COX-2). These results demonstrate that HFCPS possesses strong *in vitro* anti-inflammatory activity and could potentially use as an ingredient to developing anti-inflammatory agent or cosmetic.

1. Materials and methods

1.1. Reagents and Chemicals

Dulbecco's modified Eagle's medium (DMEM), fetal bovine serum (FBS), penicillin–streptomycin, and trypsin-EDTA were purchased from Gibco-BRL (Grand Island, NY, USA). The LPS and DMSO were purchased from Sigma (St. Louis, MO, USA). The ELISA kits used for the analysis of TNF- α , PGE₂, IL-1 β , and IL-6 production levels were purchased from R&D Systems Inc. (Minneapolis, MN, USA). Protein assay kit (BCA kit) was purchased from Bio-Rad (Richmond, CA, USA). COX-2, iNOS, β -actin, anti-rabbit antibody, and anti-mouse antibody were purchased from Thermo Scientific (Waltham, MA, USA). All other chemicals used in this study were of analytical grade.

1.2. Cell culture

RAW 264.7 macrophages were purchased from ATCC (TIB-71™). RAW 264.7 cells were grown in DMEM supplemented with 10% FBS, penicillin (100 unit/mL), and streptomycin (100 μ g/mL). Cells were maintained at 37°C in an incubator containing 5% CO₂.

1.3. Measurement of NO production and cell viability

The experiments were performed following the methods described by Heo et al. [62]. RAW 264.7 cells were seeded in a 24-well plate for 24 h. HFCPS was added into each well, achieving final concentrations of 25, 50, and 100 μ g/mL. After 1 h, LPS (1 μ g/mL) was introduced into all wells, except control. After 24 h, 100 μ L of the culture medium from each well was transferred to a 96-well plate and mixed with 100 μ L Griess reagent (1% sulfanilamide and 0.1% naphthylethylenediamine dihydrochloride in 2.5% phosphoric acid). The absorbance was read on a microplate reader after 10 minutes, at a

wavelength of 540 nm. In addition, 100 μ L of MTT solution (2 mg/mL) was added to the remaining cells in the 24-well plate, and incubated for 3 h. The resulting formazan crystals of MTT were then dissolved in DMSO and absorbance was determined using a microplate reader at a wavelength of 540 nm [58].

1.4. Measurement of PGE₂ and pro-inflammatory cytokines (TNF- α , IL-1 β , and IL-6) production

RAW 264.7 cells were pre-treated with HFCPS and eventually exposed to LPS for 24 h. Then, the culture media was collected and used for measuring the respective cytokines and PGE₂ expression levels. These experiments were performed using commercial enzyme immunoassay kits following the manufacturer's instructions.

1.5. Western blot analysis

RAW 264.7 cells were seeded (1×10^5 cells/mL) in 6-well plates. After 24 h, cells were treated with HFCPS and exposed to LPS (1 μ g/mL) 1 h later. Following a second incubation period of 24 h, the cells were washed twice with PBS buffer, harvested and lysed using lysis buffer (1% Nonidet P-40, 50 mM Tris-HCl (pH 7.5), 150 mM NaCl, 1 mM EGTA, 2 mM EDTA, 1 mM dithiothreitol, 1 mM NaVO₃, 1 mM phenylmethylsulfonyl fluoride, 15 μ g/mL aprotinin, 0 mM NaF, and 25 μ g/mL leupeptin). The resulting lysates were centrifuged at 4°C (10000 g, 15 min) to remove cell debris, and the protein concentration of each lysate was determined using a BCA™ kit. Each 50 μ g of protein were separated on a 12% SDS-polyacrylamide gel, and the protein bands were transferred onto a polyvinylidene fluoride membrane. The membranes were blocked with blocking buffer (5% blotting-grade blocker), and the membrane was then incubated with specific primary antibodies overnight at 4°C. After incubation, the membranes were washed with TBS-T buffer (3 mM KCl, 25 mM Tric,

150 mM NaCl, and 0.2% Tween 20) and incubated with secondary antibodies at room temperature for 3 h. Finally, the signals were developed by an ECL western blotting detection kit, and exposed on X-ray films.

1.6. Statistical analysis

All experiments were conducted in triplicate. The data are expressed as the mean \pm standard error (S.E), and one-way ANOVA was used to compare the mean values of each treatment in SPSS 12.0. Significant differences between the means were identified by the Turkey test. Significance was established if $*p < 0.05$, $** p < 0.01$ as compared to the LPS-treated group, and $^{##} p < 0.01$ as compared to control group.

2. Results and Discussion

2.1. The effect of HFCPS on LPS-induced NO generation and cytotoxicity in RAW 264.7 macrophages

LPS is a component of the cell wall in gram-negative bacteria, which stimulates inflammatory responses in macrophages. Therefore, LPS-stimulated RAW 264.7 cells are an excellent choice for investigating the anti-inflammatory activity of HFCPS. The effect of HFCPS on NO generation and cytotoxicity were measured in LPS-induced RAW 264.7 macrophages. As Fig. 14 shows, HFCPS significantly inhibits NO generation in LPS-induced RAW 264.7 cells (Fig. 14A). In addition, HFCPS remarkably improves cell viability. Both effects were dose-dependent.

2.2. HFCPS decreased PGE₂ and pro-inflammatory cytokines release in LPS-induced RAW 264.7 macrophages

Macrophages play an important role in inflammatory responses via producing various inflammatory mediators such as NO, TNF- α , IL-1 β , IL-6, and PGE₂. The abnormal production of these inflammatory mediators is pivotal to the progression of inflammatory responses [63-65]. Therefore, we measured these inflammatory mediators' levels in the present study. The results were shown as Fig. 15. As the results show, LPS significantly increases the production of TNF- α , IL-1 β , IL-6, and PGE₂ compared with the control. However, the TNF- α , IL-1 β , IL-6, and PGE₂ levels in HFCPS treated RAW 264.7 cells were significantly decreasing, which was dose-dependent with increasing sample concentrations.

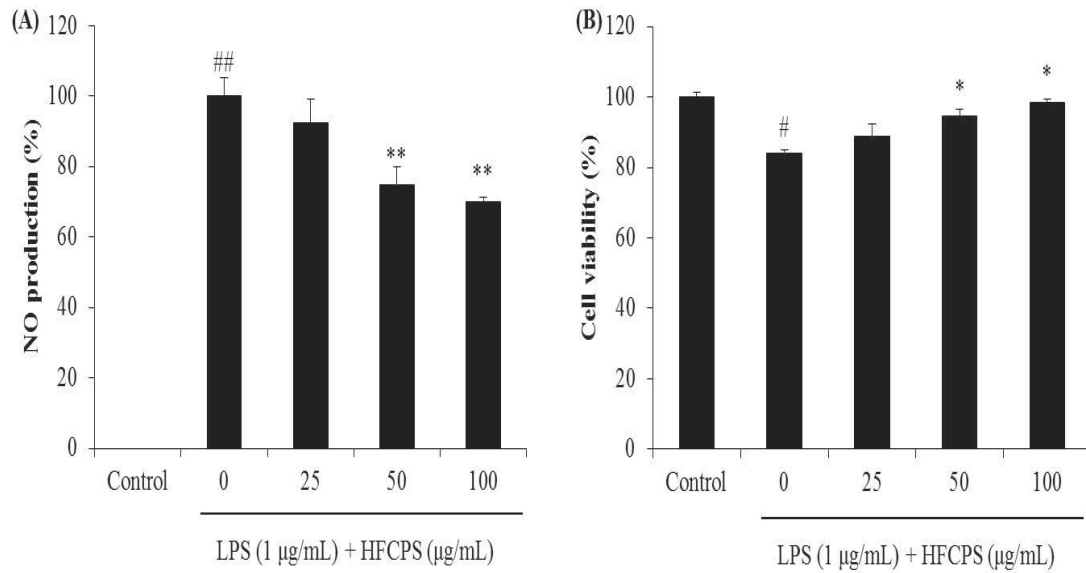


Fig. 14. The effect of HFCPS on LPS-induced NO generation and cytotoxicity in RAW 264.7 macrophages. (A) NO production in LPS-induced RAW 264.7 macrophages and (B) Cell viability in LPS-induced RAW 264.7 macrophages. The experiments were conducted in triplicate, and the data are expressed as the mean \pm standard error (S.E). * $p < 0.05$, ** $p < 0.01$ as compared to the LPS-treated group and ## $p < 0.01$ as compared to the control group.

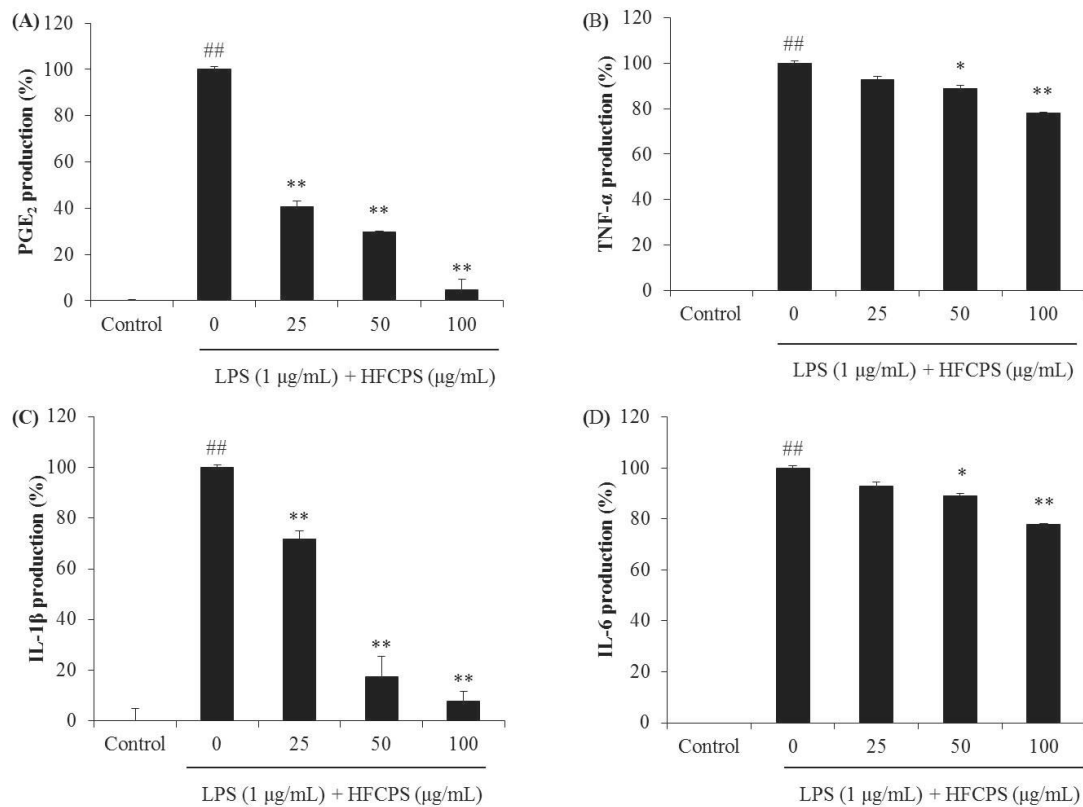


Fig. 15. The effect of HFCPS on the production of PGE₂, TNF- α , IL-1 β , and IL-6 in LPS-stimulated RAW 264.7 macrophages. (A) The production of PGE₂; (B) the production of TNF- α ; (C) the production of IL-1 β ; (D) the production of IL-6. The levels of PGE₂, TNF- α , IL-1 β , and IL-6 expression were examined using ELISA kit. The experiments were conducted in triplicate, and the data are expressed as the mean \pm standard error (S.E). * p < 0.05, ** p < 0.01 as compared to the LPS-treated group and ## p < 0.01 as compared to the control group.

2.3. HFCPS inhibited the expression of iNOS and COX-2 in LPS-induced RAW 264.7 macrophages

The expression levels of iNOS and COX-2 are shown in Fig. 16. According to the results, the expression levels of iNOS and COX-2 were significantly increasing in the cells treated with LPS only. However, HFCPS effectively suppressed iNOS and COX-2 expression in a dose-dependent manner.

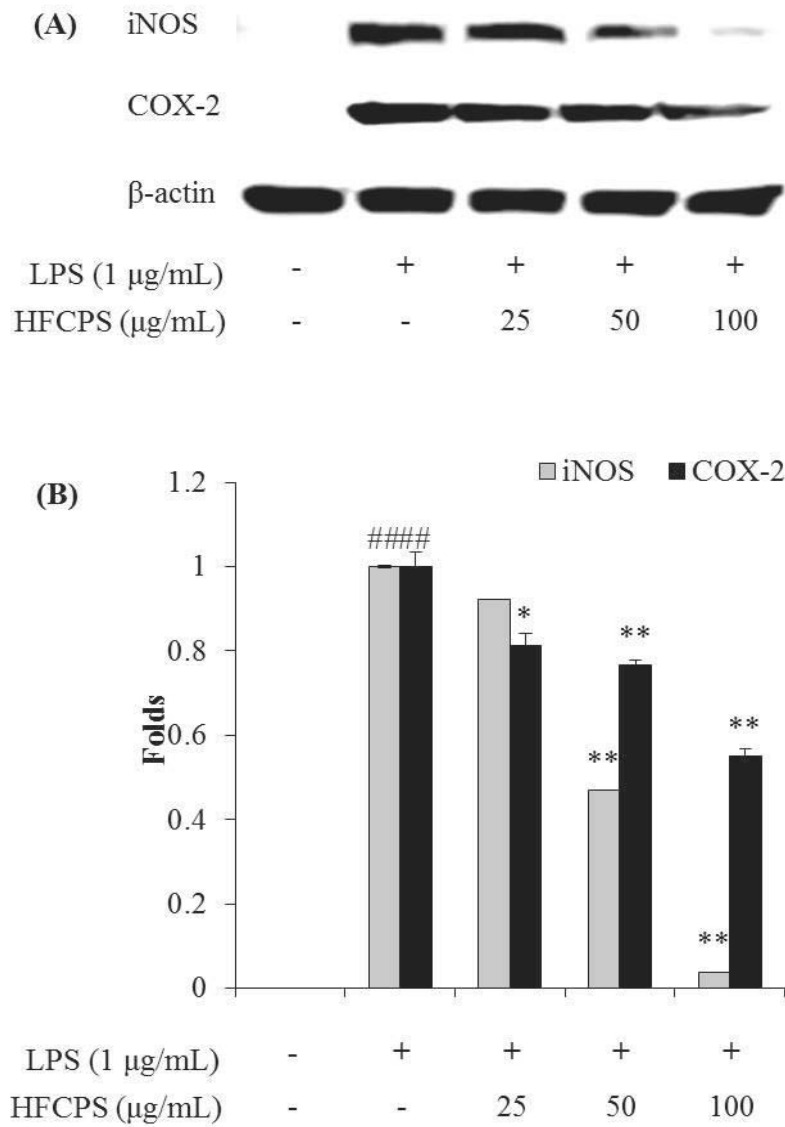


Fig. 16. The effect of HFCPS on the expression of iNOS and COX-2 in RAW 264.7 macrophages stimulated with LPS. (A) The inhibitory effect of HFCPS on iNOS and COX-2 expression; (B) the relative amount of iNOS and COX-2 levels. The relative amounts of iNOS and COX-2 levels were compared with β -actin. The experiments were conducted in triplicate, and the data are expressed as the mean \pm standard error (S.E). * $p < 0.05$, ** $p < 0.01$ as compared to the LPS-treated group and $^{###}p < 0.01$ as compared to the control group.

3. Conclusion

In this study, we investigated the anti-inflammatory activity of HFCPS. The results indicate that HFCPS significantly inhibits NO generation and improves cell viability in LPS-stimulated RAW 264.7 cells. In addition, HFCPS significantly decreases the expression of TNF- α , PGE₂, IL-1 β , and IL-6, as well as suppresses the expression of iNOS and COX-2. In a conclusion, HFCPS possess strong *in vitro* anti-inflammatory activity and be used for developing novel anti-inflammatory drugs or ingredients in cosmetic products.

Section 4: Whitening effect of polysaccharides from Celluclast-assisted extract of

Hizikia fusiforme

Abstract

In the present study, the whitening effect of HFCPS was investigated. The whitening effect was evaluated by measuring its mushroom tyrosinase inhibitory effect and melanin synthesis inhibitory effect in alpha-melanocyte stimulating hormone (α -MSH)-stimulated B16F10 melanoma cells. The results show that HFCPS inhibited tyrosinase in a dose-dependent manner as well as inhibited melanin synthesis and intracellular tyrosinase activity in α -MSH-stimulated B16F10 cells. Further study suggests that HFCPS inhibits α -MSH-stimulated melanogenesis through down-regulation tyrosinase, TRP-1, and TRP-2 levels via inhibiting MITF expression in α -MSH-stimulated B16F10 cells. These results demonstrate that HFCPS possesses whitening effect and may be used as a melanogenesis inhibitor to develop a cosmetic in the cosmetic industry.

1. Materials and methods

1.1. Reagents and Chemicals

Tyrosinase from mushroom, MTT, DMSO, and alpha-melanocyte stimulating hormone (α -MSH) were purchased from Sigma Co. (St. Louis, MO, USA). The Dulbecco's modified Eagle medium (DMEM), fetal bovine serum (FBS), and penicillin/streptomycin were purchased from Gibco BRL (Life Technologies, Burlington, ON, Canada). Antibodies against microphthalmia-associated transcription factor (MITF), tyrosinase, and tyrosinase-related protein-1 and -2 (TRP-1 and 2) were purchased from Thermo Scientific (Waltham, MA, USA). Anti-mouse and anti-rabbit IgG antibodies were purchased from Cell Signaling Technology (Beverly, MA, USA). All other chemicals used in this study were of analytical grade.

1.2. Measurement of the mushroom tyrosinase inhibitory effect of HFCPS

The tyrosinase inhibitory activity of HFCPS was determined using the protocol described by Kang et al. [42]. In brief, a 200 μ L reaction mixture in containing 40 μ L of 1.5 mM L-tyrosin, 10 μ L of sample solution, 140 μ L of 50 mM phosphate buffer (pH 6.5), and 10 μ L of aqueous mushroom tyrosinase (1000 units/mL) in a 96-well plate. The assay mixture was reacted at 37°C for 12 min, and kept on ice for 5 min to stop the reaction. Finally, the amount of dopachrome in the reaction mixture was measured at 490 nm using a microplate reader (BioTek, SYNERGY, HT, USA).

1.3. Cell culture

B16F10 mouse melanoma cells (ATCC[®] CRL-6475[™]) were purchased from ATCC (American Type Culture Collection, Manassas, VA, USA). The cells were grown in DMEM supplemented with 10% heat-inactivated FBS, 100 μ g/mL of streptomycin,

and 100 U/mL of penicillin. The cells were sub-cultured every 4 days and seeded at a concentration of 5×10^4 cells/mL for experiments.

1.4. Cytotoxicity assay

Cytotoxicity of HFCPS on B16F10 cells was performed by MTT assay [66]. Cells were seeded in a 96-well plated and incubated for 24 h. Cells were treated with different concentrations of HFCPS and incubated for 72 h. A volume of 50 μ L MTT stock solution (2 mg/mL) was added to each well. After 3 h incubation, the supernatant was aspirated and 150 μ L of DMSO was added to each well. Finally, the resulting formazan crystals of MTT were dissolved in DMSO and the absorbance was measured at 540 nm using a microplate reader.

1.5. Determination of cellular melanin content

In order to measure the cellular melanin contents of α -MSH stimulated B16F10 cells. B16F10 cells were seeded in a 6-well plate and incubated for 24 h. Then, cells were treated with various concentrations of HFCPS and stimulated with α -MSH (50 nM). After 72 h incubation, the cells were harvested. The harvested cells were incubated in 1 mL of 1N NaOH containing 10% DMSO at 80°C for 1 h. After incubation, the solution was centrifuged at 13,000 g for 10 min and the absorbance of the supernatant was measured at 490 nm using a microplate reader.

1.6. Measurement of intracellular tyrosinase activity

B16F10 cells were treated with HFCPS and stimulated with α -MSH (50 nM). The cells were harvested after 72 h incubation. Cells were lysed in PBS containing 1% Triton X-100 and centrifuged at 13,000 g for 10 min. After centrifuge and quantification of the protein of supernatant, 90 μ L of each supernatant was incubated in duplicate with

10 μ L of 10 mM L-DOPA at 37 °C for 1 h. After incubation, dopachrome was monitored by measuring the absorbance at 490 nm using an ELISA reader.

1.7. Western blot analysis

The effect of HFCPS on the expression of melanogenesis-related proteins including MITF, tyrosinase, TRP-1, and TRP-2 were assessed by Western blot assay performed according to the procedure as described by Kim [66]. In brief, B16F10 treated with HFCPS and stimulated with α -MSH (50 nM). After 72 h incubation, cells were harvested and lysed. The protein level of each sample was measured by a BCATM kit. The proteins (30 μ g) were separated on 12% SDS-PAGE and transferred onto nitrocellulose transfer membranes. The membranes were blocked with blocking buffer (5% skim milk) and incubated with primary antibodies for 16 h at 4°C. Then, the membranes were further incubated with secondary antibody at room temperature for 3 h. Finally, the protein bands were visualized using an ECL Western blotting detection kit and exposed on X-ray films.

1.8. Statistical analysis

All experiments were performed in triplicate. The data were expressed as the mean \pm standard error (S.E). The mean values of each experiment were compared using one-way ANOVA test. Significant differences between the means of parameters were determined by the Turkey test. The p -value ($p < 0.05$) was considered to be statistically significant. A value of * $p < 0.05$, ** $p < 0.01$, and ## $p < 0.01$ were considered as significantly different.

2. Results and Discussion

2.1. Tyrosinase inhibitory activity of HFCPS

The tyrosinase inhibitory effect of HFCPS was examined and arbutin was used as a positive compound. As Fig. 17 shows, the tyrosinase inhibitory rates of HFCPS were 4.36%, 11.97%, and 36.66% at the concentration of 25, 50, and 100 $\mu\text{g/mL}$. This result displays that HFCPS inhibits tyrosinase in a dose-dependent manner.

2.2. Cytotoxicity of HFCPS

Cytotoxicity of HFCPS on B16F10 cells was examined by MTT assay, and the results were summarized in Fig. 18. As the result shows, HFCPS showed significant cytotoxicity on B16F10 cells at the 100 $\mu\text{g/mL}$. Therefore, the concentration of HFCPS on B16F10 cells for further study was determined not beyond 50 $\mu\text{g/mL}$.

2.3. Effect of HFCPS on melanin synthesis in α -MSH-stimulated B16F10 cells

The melanin contents of α -MSH-stimulated B16F10 cells were measured and the melanin content of the cells non-stimulated with α -MSH was referred as 100%. As Fig. 19A indicates, the melanin content of the cells stimulated with α -MSH was over than 200%. However, the melanin contents of cells treated with HFCPS were dose-dependently decreasing. These results indicate that HFCPS possesses melanogenesis inhibitory effect in α -MSH-stimulated B16F10 cells.

2.4. Effect of HFCPS on intracellular tyrosinase activity in α -MSH-stimulated B16F10 cells

As Fig. 19B indicates, the relative tyrosinase activity of the cells non-stimulated with α -MSH was referred as 100% and the relative tyrosinase activity of the cells stimulated with α -MSH was 157.29%. However, the relative tyrosinase activities of cells treated with HFCPS were 120.18%, 113.69%, and 108.29% at the concentration of 12.5, 25, and 50 μ g/mL.

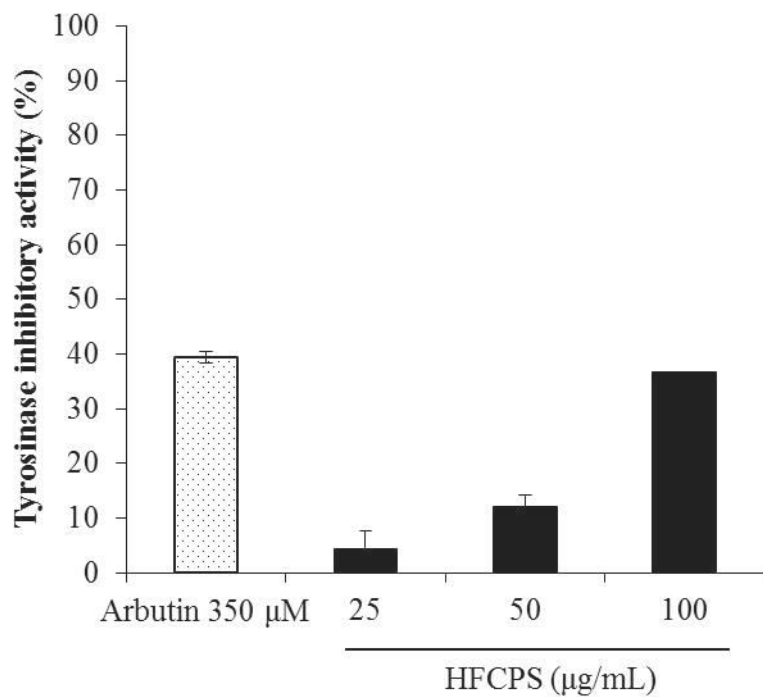


Fig. 17. Tyrosinase inhibitory effects of HFCPS. Tyrosinase inhibitory effects were measured by colorimetric assay. The amount of dopachrome was measured at 490 nm using a microplate reader. The data were expressed as the mean \pm S.E (n=3).

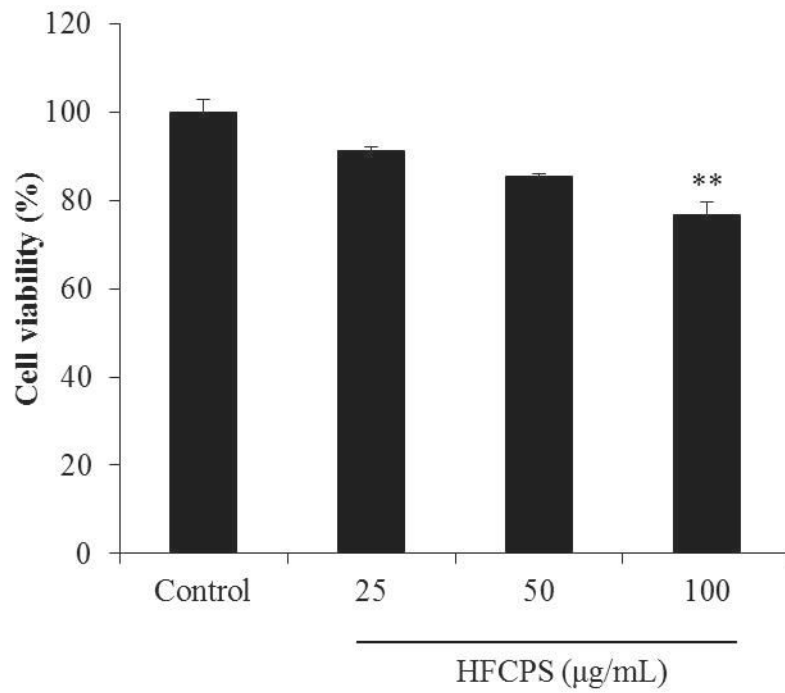


Fig. 18. Cytotoxicity of HFCPS on B16F10 cells. Cell viability was measured by MTT assay. The data were expressed as the mean \pm S.E (n=3). ** $p < 0.01$ as compared to control group.

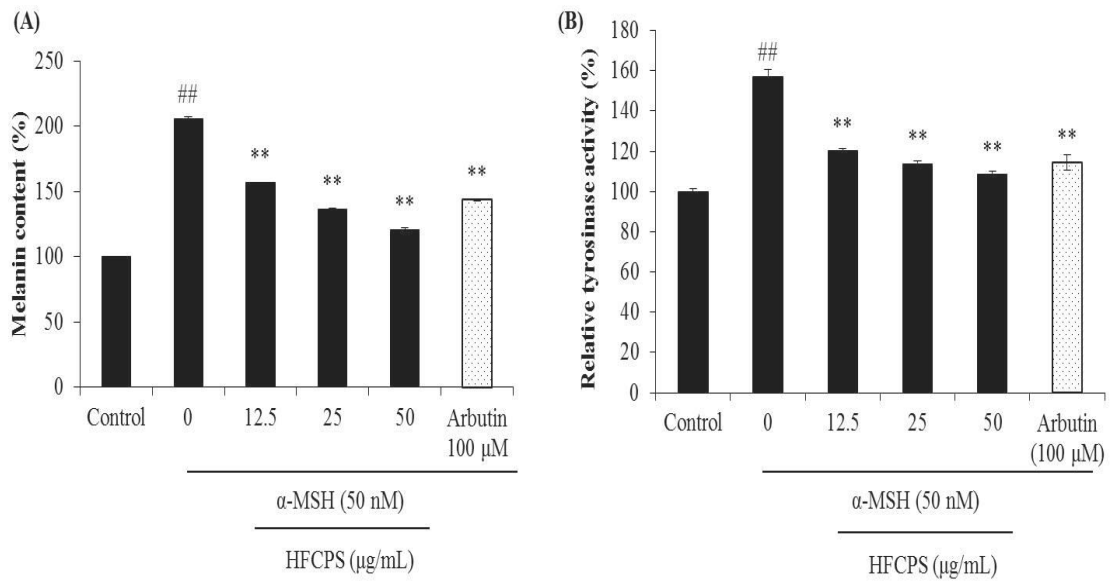


Fig. 19. Melanin synthesis and intracellular tyrosinase inhibitory effect of HFCPS in α -MSH-stimulated B16F10 cells. (A) Melanin synthesis levels in α -MSH-stimulated B16F10 cells; relative intracellular tyrosinase activity of α -MSH-stimulated B16F10 cells. The data were expressed as the mean \pm S.E (n=3). ** $p < 0.01$ as compared to α -MSH-treated group and ## $p < 0.01$ as compared to control group.

2.5. Effect of HFCPS on tyrosinase, TRP-1, TRP-2, and MITF expression in α -MSH-stimulated B16F10 cells

In order to elucidate the mechanism of HFCPS against α -MSH-stimulated melanogenesis in B16F10 cells, the effect of HFCPS on the expression of MITF, tyrosinase, TRP-1, and TRP-2 were examined by Western blot assay. As Fig. 20 shows, the expression levels of MITF, tyrosinase, TRP-1, and TRP-2 were improved by α -MSH stimulation. However, the expression levels of these proteins were reduced in the cells treated with different concentrations of HFCPS. These results demonstrate that HFCPS against α -MSH-stimulated melanogenesis by inhibiting the expression of MITF, tyrosinase, TRP-1, and TRP-2 in B16F10 cells.

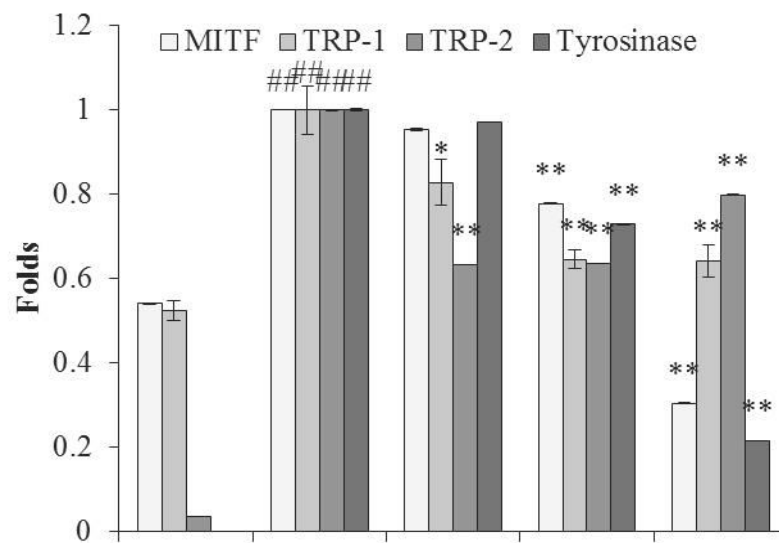
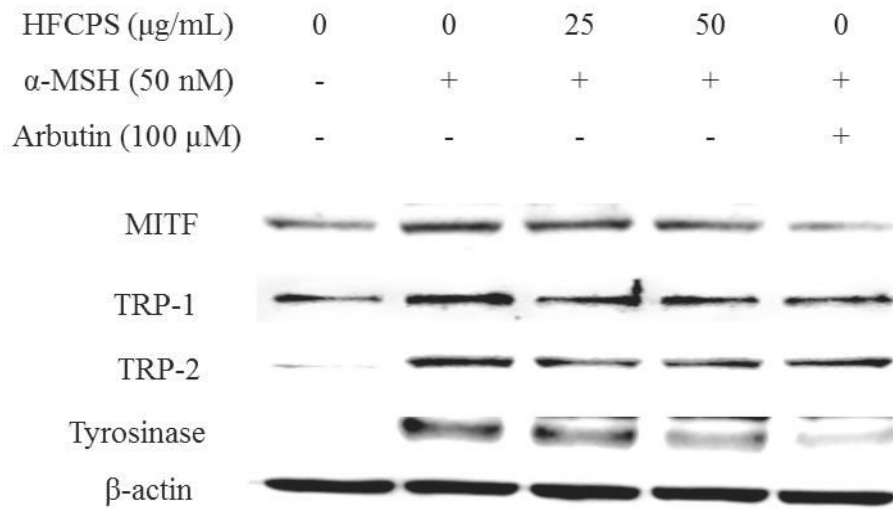


Fig. 20. Effect of HFCPS on MITF, tyrosinase, TRP-1, and TRP-2 expression in α -MSH-stimulated B16F10 cells. The relative amounts of on MITF, tyrosinase, TRP-1, and TRP-2 levels were compared with β -actin. The data were expressed as the mean \pm S.E (n=3). * p < 0.05 and ** p < 0.01 as compared to α -MSH-treated group and ### p < 0.01 as compared to control group.

3. Conclusion

The present study investigated the melanogenesis inhibitory effects of HFCPS in α -MSH-stimulated B16F10 melanoma cells. The results indicate that HFCPS possesses tyrosinase inhibitory effect, as well as melanin synthesis and intracellular tyrosinase inhibitory effect in α -MSH-stimulated B16F10 cells. In addition, Western bolt results suggest that HFCPS inhibit α -MSH-stimulated melanogenesis through down-regulation tyrosinase, TRP-1, and TRP-2 levels via inhibiting MITF expression in B16F10 cells. These results demonstrate that HFCPS possesses whitening effect and may be used as a melanogenesis inhibitor to develop a cosmetic in the cosmetic industry.

Section 5: UV protective effect of polysaccharides from Celluclast-assisted extract of *Hizikia fusiforme*

Abstract

In the present study, the ultraviolet (UV) protective effect of HFCPS was investigated *in vitro* in keratinocytes (HaCaT cells) and *in vivo* in zebrafish. The intracellular ROS levels and the viabilities of UVB-irradiated HaCaT cells were measured. The results indicate that HFCPS significant reduce intracellular ROS level and improve the viability of UVB-irradiated HaCaT cells. Furthermore, HFCPS remarkable decrease the apoptosis formation in UVB-irradiated HaCaT cells in a dose-dependent manner. In addition, the *in vivo* UV protective of HFCPS was investigated using a zebrafish model. The results demonstrate that HFCPS significant reduce intracellular ROS level, cell death, NO production, and lipid peroxidation in UVB-irradiated zebrafish in a dose-dependent manner. These results suggest that HFCPS possesses potent *in vitro* and *in vivo* UV protective effect and it may be considered for use as an ingredient in the cosmetic industry.

1. Materials and methods

1.1. Reagents and Chemicals

The fluorescent probe 2', 7'-dichlorodihydrofluorescein diacetate (DCFH-DA), acridine orange, diaminofluorophore 4-amino-5-methylamino-2',7'-difluorofluorescein diacetate (DAF-FM DA), 1,3-Bis (diphenylphosphino) propane (DPPP), 3-(4,5-dimethyl-2yl)-2,5-diphenyltetrasolium bromide (MTT), and dimethyl sulfoxide (DMSO) were purchased from Sigma Co. (St. Louis, MO, USA). The Dulbecco's modified Eagle medium (DMEM), fetal bovine serum (FBS), and penicillin/streptomycin were purchased from Gibco BRL (Life Technologies, Burlington, ON, Canada). All other chemicals used in this study were of analytical grade.

1.2. Cell culture and UVB irradiation

Human keratinocytes (HaCaT) cell line was purchased from Korean Cell Line Bank. The HaCaT cells were maintained in DMEM supplemented with 10% heat-inactivated FBS, streptomycin (100 µg/mL), and penicillin (100 unit/mL) at 37°C in an incubator under humidified atmosphere containing 5% CO₂. Cells were sub-cultured at 3 days intervals and seeded at a density of 1.0×10^5 cells / mL. Ultraviolet (UV) B irradiation was imposed using a UVB meter (UV Lamp, VL-6LM, Vilber Lourmat, France) with a fluorescent bulb emitting 280~320 nm wavelengths with a peak at 313 nm. HaCaT cells were irradiated at a dose of 30 mJ/cm² of UVB in PBS [44, 67]. Cells were subsequently incubated until analysis.

1.3. Determination of cytotoxicity of HFCPS on HaCaT cells

The cytotoxicity of HFCPS on HaCaT cells was evaluated by MTT assay. HaCaT cells were seeded in 24-well plate and incubated for 24 h. The cells were treated with 25 µL

of HFCPS carried a final concentration of 6.25, 12.5, 25, 50, and 100 $\mu\text{g/mL}$ and the control groups were treated with the same volume of 1X PBS. After sample treatment, cells were incubated for 24 h at 37°C. Then, a volume of 100 μL of MTT stock solution (2 mg/mL) was applied to each well. After 3 h incubation, the supernatant was aspirated. The formazan crystal in each well was dissolved in DMSO, and the absorbance was measured by a microplate reader at 540 nm.

1.4. Measurement of intracellular ROS generation in UVB-irradiated HaCaT cells

HaCaT cells were seeded and incubated for 24 h. Cells were treated with HFCPS for 30 min, then DCFH-DA (500 $\mu\text{g/mL}$) was added into each well. After 30 min incubation, cells were exposed to UVB (30 mJ/cm^2) and the fluorescent intensities of cells were determined at an excitation wavelength of 485 nm and an emission wavelength of 535 nm, using a fluorescent microplate reader.

1.5. Determination of cell viability

For measuring the protective effect of HFCPS against UVB-induced cell damage, HaCaT cells were treated with HFCPS for 2 h. Cells were then exposed to UVB (30 mJ/cm^2) and incubated for 24 h. Subsequently, cell viability was assessed by MTT assay described previously [59, 68].

1.6. Measurement of apoptosis body formation

The apoptosis body formation of UVB-irradiated HaCaT cells was determined by nuclear staining. HaCaT cells were seeded in a 24-well plate and incubated for 24 h. After incubation, cells were treated with HFCPS and incubated for 2 h and exposed to UVB (30 mJ/cm^2). Then, cells were incubated with serum-free DMEM medium for 6 h. After incubation, cells were treated with 25 μL of Hoechst 33342 (stock, 10 mg/mL)

and incubated for 10 min. The stained cells were observed using a fluorescence microscope equipped with a Cool SNAP-Pro color digital camera (Olympus, Japan).

1.7. Maintenance of zebrafish

Adult zebrafish were purchased from a commercial market (Seoul Aquarium, Korea). Each 10 fish were kept in a 3 L acrylic tank at 28.5°C, under a 14/10 h light/dark cycle. The fish were fed with Tetramin flake feed supplemented with live brine shrimp (*Artemia salina*) three times per day, 6 days a week. Embryos were collected after natural spawning that was induced by light, and embryo collection was completed within 30 min.

1.8. Application of HFCPS and UVB to zebrafish

At 2 dpf, the zebrafish larvae were transferred to a 24-well plate and treated with HFCPS as the final concentration of 25, 50 and 100 µg/mL. After 1 h, the zebrafish larvae were washed with embryo media and exposed to UVB (50 mJ/cm²) individual [23, 69]. After 6 h incubation, the zebrafish larvae were washed with embryo media and stained with DCFH-DA (20 µg/mL, 1 h), acridine orange (10 µg/mL, 30 min), DAF-FM-DA (10 µM, 3 h), and DPPP (3 µM, 1 h) for measuring ROS level, cell death, NO production, and lipid peroxidation, respectively. After incubation, the zebrafish larvae were washed two times with embryo media and anesthetized by phenoxyethanol before visualization. After anesthetized, the zebrafish larvae were photographed under the microscope Cool SNAP-Pro color digital camera (Olympus, Japan). And the individual zebrafish larvae fluorescence intensity was quantified using an image J program.

1.9. Statistical Analysis

All experiments were conducted in triplicate. The data are expressed as the mean \pm standard error (S.E), and one-way ANOVA was used to compare the mean values of each treatment in SPSS 12.0. Significant differences between the means were identified by the Turkey test. Significance was established if $*p < 0.05$, $** p < 0.01$ as compared to the UVB-treated group, and $^{##} p < 0.01$ as compared to control group.

2. Results and Discussion

2.1. Cytotoxicity of HFCPS on HaCaT cells

Cytotoxicity of HFCPS on HaCaT cells was measured by MTT assay. As the result shows (Fig. 21), the viabilities of cells treated with different concentrations of HFCPS were no significantly decreasing. This result suggests that HFCPS is no toxicity on HaCaT cells at the concentration range from 6.25 to 100 $\mu\text{g/mL}$. Thus, 100 $\mu\text{g/mL}$ was considered as the safety concentration used in the further study.

2.2. Effect of HFCPS on intracellular ROS generation and cell death in UVB-irradiated HaCaT cells

The HaCaT cell damage level induced by UVB irradiation was detected by measuring the intracellular ROS generation and cell death. The intracellular ROS level was determined by DCF-DA assay and the result was summarized in Fig. 22A. As Fig. 22A shows, the ROS level of UVB-irradiated cells was significantly increased compared with non-irradiated cells. However, the ROS levels of the cells treated with different concentration of HFCPS were significantly decreasing in a dose-dependent manner. In addition, the viability of UVB-irradiated HaCaT cells was measured by MTT assay. As shown in Fig. 22B, the viability of cells irradiated by UVB was significantly decreased and dose-dependently increased in HFCPS treated cells. These results indicate that HFCPS possesses potent protective effect against UVB-induced HaCaT cell damage.

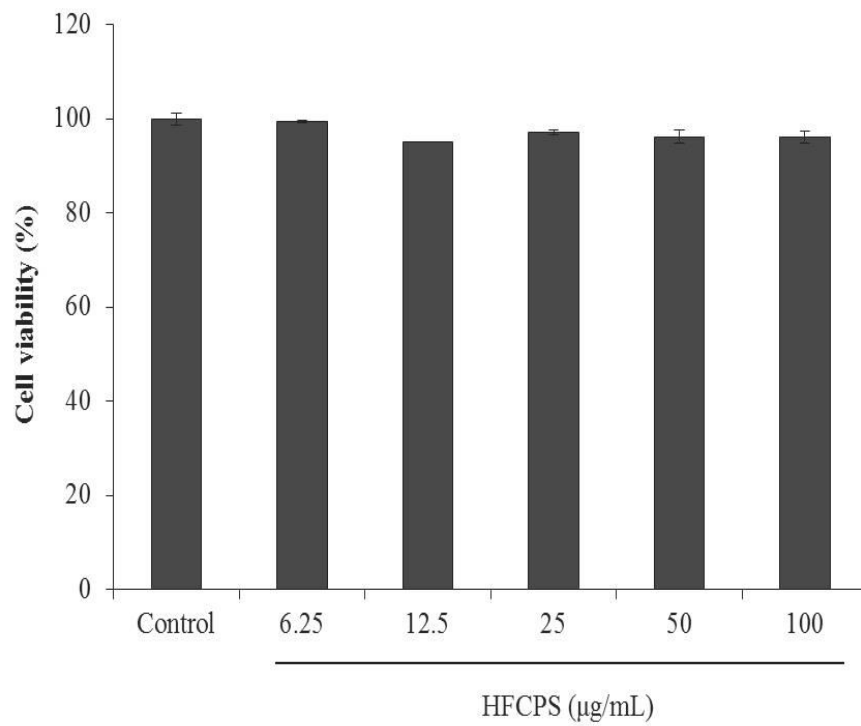


Fig. 21. Cytotoxicity of HFCPS on HaCaT cells. Cell viability was measured by MTT assay. The data were expressed as the mean \pm S.E (n=3).

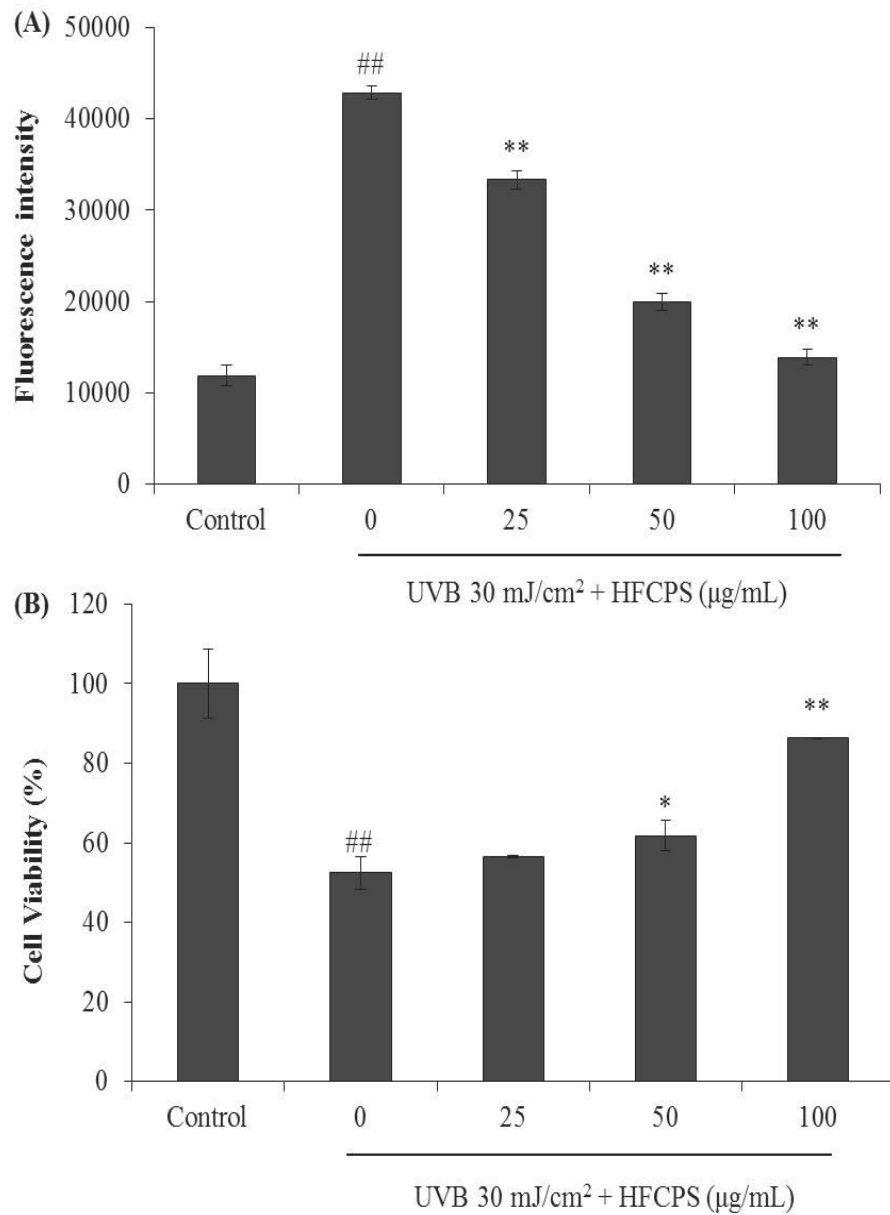


Fig. 22. Protective effect of HFCPS against UVB-induced HaCaT cells damage. (A) Intracellular ROS level of UVB-irradiated HaCaT cells; (B) the viability of UVB-irradiated HaCaT cells. The experiments were conducted in triplicate, and the data are expressed as the mean \pm standard error (S.E). * $p < 0.05$, ** $p < 0.01$ as compared to the UVB-treated group and ## $p < 0.01$ as compared to the control group.

2.3. Effect of HFCPS on apoptosis formation in UVB-irradiated HaCaT cells

In order to measure the apoptosis body formation, the cells were stained with a cell permeable DNA dye Hoechst 33342. Then the nuclear morphology of cells was examined using a fluorescence microscopy. The cell images were shown in Fig. 23. According to the results, the amount of apoptotic bodies of HFCPS-treated HaCaT cells were significantly decreased in a dose-dependent manner. It means HFCPS possesses the effect against UVB-induced HaCaT cell apoptotic.

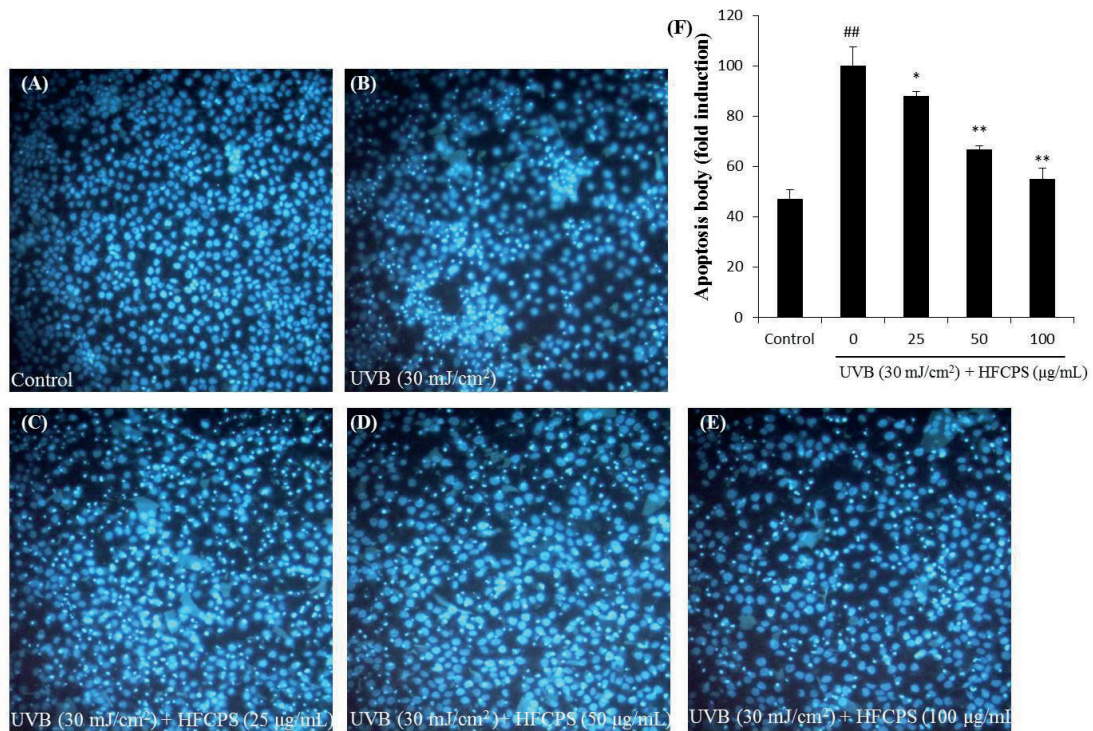


Fig. 23. The apoptotic body formation levels in UVB-irradiated HaCaT cells. (A) Nuclear morphology of non UVB-irradiated HaCaT cells; (B) nuclear morphology of UVB-irradiated HaCaT cells; (C) nuclear morphology of cells treated with 25 µg/mL of HFCPS and irradiated with UVB; (D) nuclear morphology of cells treated with 50 µg/mL of HFCPS and irradiated with UVB; (E) nuclear morphology of cells treated with 100 µg/mL of HFCPS and irradiated with UVB; (F) reactive apoptotic body formation. The apoptotic body formation was observed under a fluorescence microscope after Hoechst 33342 staining. Apoptosis levels were measured using Image J software. * $p < 0.05$, ** $p < 0.01$ as compared to the UVB-treated group and ### $p < 0.01$ as compared to the control group.

2.4. Effect of HFCPS on ROS generation, cell death, NO production, and lipid peroxidation in UVB-irradiated zebrafish

The *in vivo* UV protective effect of HFCPS was investigated in a zebrafish model. The ROS generation, cell death, NO production, and lipid peroxidation level were measured using different fluorescence probes. The results were summarized in Fig. 24, 25, 26, and 27. As Fig. 24 shows, the ROS level in the zebrafish irradiated with UVB was significantly increased compared with non-irradiated zebrafish. However, the ROS levels in the zebrafish treated with different concentrations of HFCPS were dose-dependently decreased. The results of HFCPS against UVB induced cell death were summarized in Fig. 25. As the results show, HFCPS remarkably attenuated cell death level in a dose-dependent manner. As Fig. 26 shows, the NO generation in the zebrafish irradiated with UVB was significantly increased compared with non-irradiated zebrafish. However, the NO generation in HFCPS-treated zebrafish significantly decreased in a dose-dependent manner. Furthermore, HFCPS remarkable and significant reduces lipid peroxidation in UVB-irradiated zebrafish (Fig. 27). These results demonstrate that HFCPS possesses strong *in vivo* UV protective effect.

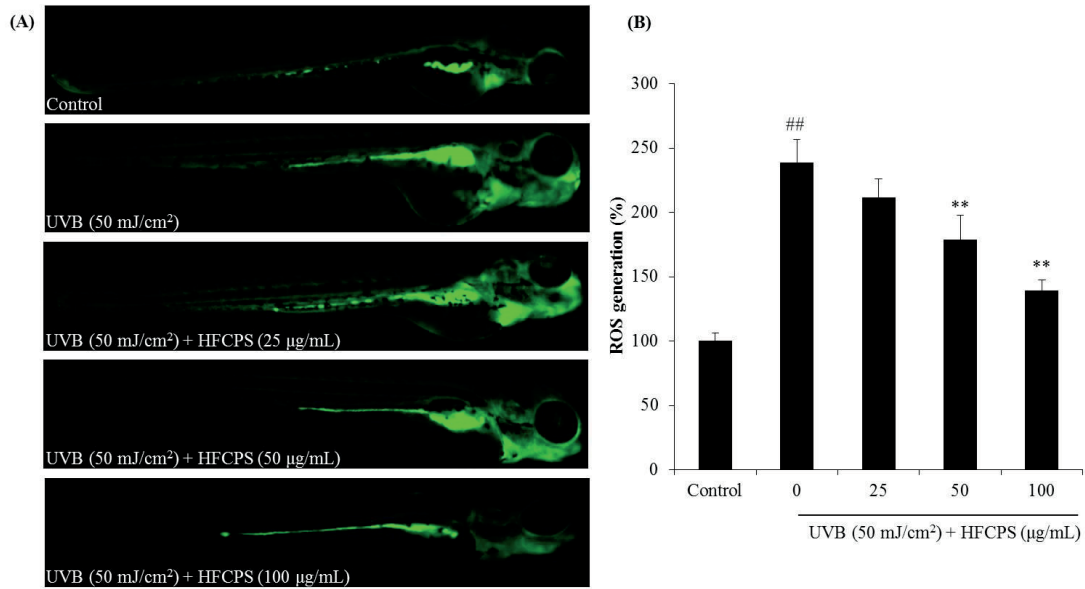


Fig. 24. The protective effect of HFCPS against UVB-induced ROS production in zebrafish. (A) Zebrafish under fluorescence microscope; (B) the levels of ROS generation. ROS levels were measured using Image J software. The experiments were conducted in triplicate, and the data are expressed as the mean \pm standard error (S.E). ** $p < 0.01$ as compared to the UVB-treated group and ## $p < 0.01$ as compared to the control group.

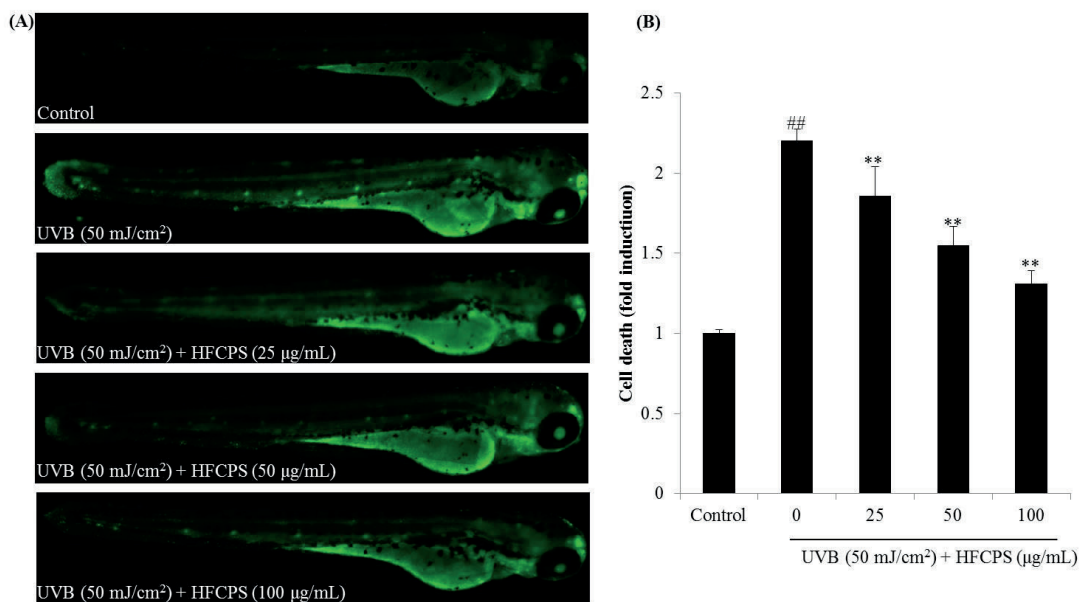


Fig. 25. The protective effect of HFCPS against UVB-induced cell death in zebrafish. (A) Zebrafish under fluorescence microscope; (B) the levels of cell death. Cell death was measured using Image J software. The experiments were conducted in triplicate, and the data are expressed as the mean \pm standard error (S.E). ** $p < 0.01$ as compared to the UVB-treated group and ## $p < 0.01$ as compared to the control group.

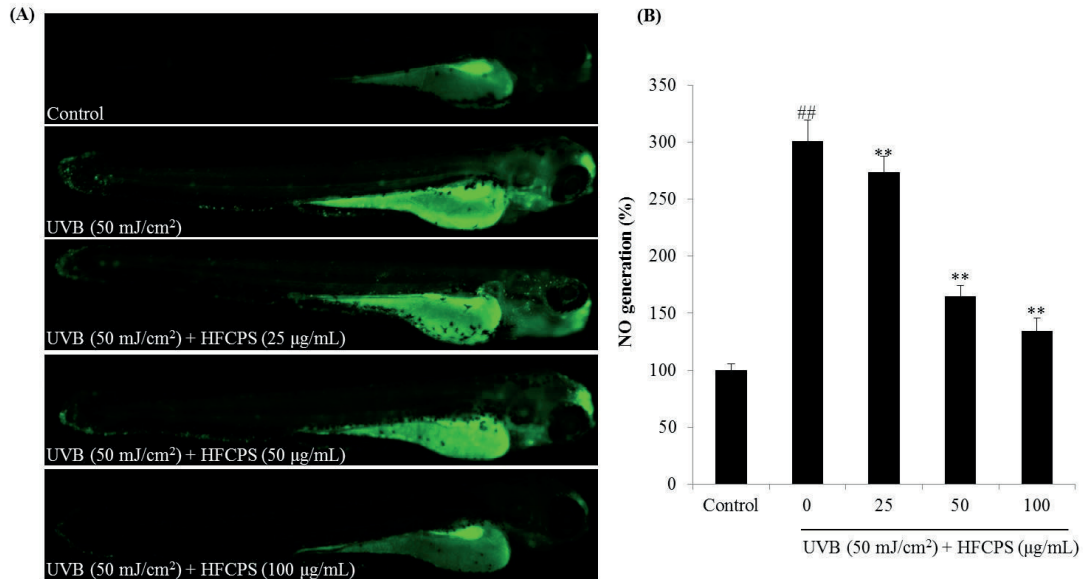


Fig. 26. The protective effect of HFCPS against UVB-induced NO production in zebrafish. (A) Zebrafish under fluorescence microscope; (B) NO production levels. NO production was measured using Image J software. The experiments were conducted in triplicate, and the data are expressed as the mean \pm standard error (S.E). ** $p < 0.01$ as compared to the UVB-treated group and ^{##} $p < 0.01$ as compared to the control group.

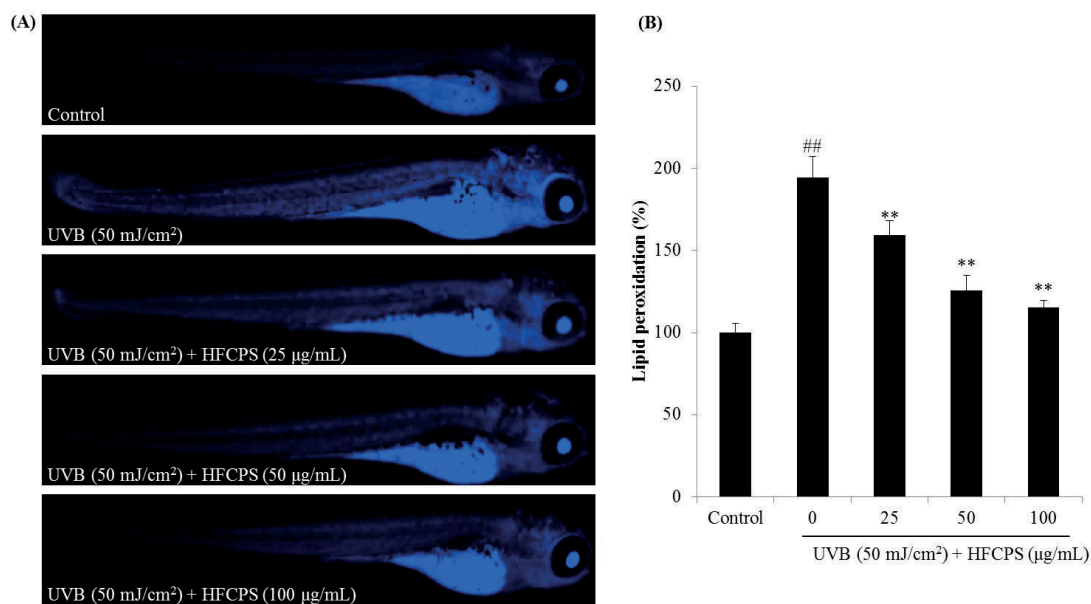


Fig. 27. The protective effect of HFCPS against UVB-induced lipid peroxidation in zebrafish. (A) Zebrafish under fluorescence microscope; (B) lipid peroxidation levels. Lipid peroxidation was measured using Image J software. The experiments were conducted in triplicate, and the data are expressed as the mean \pm standard error (S.E). ** $p < 0.01$ as compared to the UVB-treated group and ^{##} $p < 0.01$ as compared to the control group.

3. Conclusion

In the present study, the UV protective effect of HFCPS was investigated *in vitro* in keratinocytes (HaCaT cells) and *in vivo* in zebrafish. The results indicate that HFCPS significant reduce intracellular ROS level and improve the viability of UVB-irradiated HaCaT cells, as well as decrease the apoptosis formation. Furthermore, the *in vivo* test results demonstrate that HFCPS significant reduce intracellular ROS level, cell death, NO production, and lipid peroxidation in UVB-irradiated zebrafish in a dose-dependent manner. These results suggest HFCPS possesses potent *in vitro* and *in vivo* UV protective effect and it may be considered for use as an ingredient in the cosmetic industry.

**Section 6: Anti-wrinkle effect of polysaccharides from Celluclast-assisted extract
of *Hizikia fusiforme***

Abstract

In the present study, we investigated the protective effect of HFCPS against ultraviolet (UV) B-induced skin wrinkling *in vitro* in human dermal fibroblasts (HDF cells). The results indicated that HFCPS significantly decreased intracellular reactive oxygen species (ROS) level and increased the viability of UVB-irradiated HDF cells in a dose-dependent manner. In addition, HFCPS significantly inhibited intracellular collagenase and elastase activities, remarkably improved collagen synthesis, and reduced matrix metalloproteinases (MMPs) expression by regulating nuclear factor kappa B (NF- κ B), activator protein 1 (AP-1), and mitogen-activated protein kinases (MAPKs) signaling pathways in UVB-irradiated HDF cells. These results suggest that HFCPS possesses strong UV protective effect, and can be a potential anti-wrinkle ingredient in the cosmetic industry.

1. Materials and methods

1.1. Reagents and Chemicals

The 3-(4,5-dimethyl-2-yl)-2,5-diphenyltetrazolium bromide (MTT), fluorescent probe 2', 7'-dichlorodihydrofluorescein diacetate (DCFH-DA), dimethyl sulfoxide (DMSO), collagenase from *clostridium histolyticum*, elastase from porcine pancreas, azo dye-impregnated collagen, and N-succinyl-Ala-Ala-Ala-p-nitroanilide were purchased from Sigma Co. (St. Louis, MO, USA). The Dulbecco's modified Eagle medium (DMEM), Ham's Nutrient Mixtures medium (F-12), 1X phosphate buffered saline (PBS), penicillin/streptomycin, and fetal bovine serum (FBS) were purchased from Gibco BRL (Life Technologies, Burlington, ON, Canada). Antibodies against GAPDH, C23, p-c-Jun, ERK and phospho-ERK, JNK and phospho-JNK, p38 and phospho-p38, and NF- κ B p65 and NF- κ B p50 were purchased from Santa Cruz Biotechnology (Santa Cruz, CA, USA). Anti-rabbit IgG antibody was purchased from Cell Signaling Technology (Beverly, MA, USA). PIP ELISA kit was purchased from TaKaRa Bio Inc. (Japan) and Human MMP-1, 2, 8, 9, and 13 ELISA kits were purchased from Sigma Co. (St. Louis, MO, USA). All other chemicals used in this study were of analytical grade.

1.2. Measurement of collagenase inhibitory effect of HFCPS

In order to measure the collagenase inhibitory activity, a weight of 1 mg of azo dye-impregnated collagen was mixed with 800 μ L of 0.1 M Tris-HCl (pH 7.0), 100 μ L of 200 units/mL collagenase (stock solution), and 100 μ L of HFCPS solution; the reaction mixture was incubated at 43°C for 1 h under shaking condition. Subsequently, the reaction mixture was centrifuged at 3000 rpm for 10 min and the absorbance of the supernatant was detected at 550 nm in a microplate reader (BioTek, SYNERGY, HT, USA).

1.3. Measurement of elastase inhibitory effect of HFCPS

The elastase inhibitory activity was evaluated based on a method reported by Kraunsoe et al. (1996) [43]. In brief, the reaction mixture contains 650 μL of 1.015 mM N-succinyl-Ala-Ala-Ala-p-nitroanilide (dissolved in Tris-HCl, pH 8.0) and 50 μL of sample. The reaction mixture was incubated for 10 min at 25°C, and then 50 μL of elastase (0.0375 units/mL) was added to the reaction mixture and following vortexing, was incubated for 10 min at 25°C in a water bath. The amount of released p-nitroaniline was assessed by measuring absorbance at 410 nm using a microplate reader (BioTek, SYNERGY, HT, USA).

1.4. Cell culture and UVB-irradiation

Human dermal fibroblasts (HDF cells, ATCC[®] PCS201012[™]) were purchased from ATCC (American Type Culture Collection, Manassas, VA, USA). HDF cells were cultured in DMEM and F-12 mixed with a ratio of three to one supplemented with 10% heat-inactivated FBS, 100 unit/mL of penicillin, and 100 $\mu\text{g}/\text{mL}$ of streptomycin. Cells were sub-cultured every 5 days. Cells were incubated at 37°C under a humidified atmosphere containing 5% CO_2 in an incubator (Sanyo MCO-18AIC CO_2 Incubator, Moriguchi, Japan). UVB irradiation was carried out using a UVB meter (UV Lamp, VL-6LM, Vilber Lourmat, France), equipped with a fluorescent bulb emitting 280~320 nm wavelength with a peak at 313 nm. HDF cells were irradiated in 1X PBS. Cell medium was subsequently replaced with serum-free medium and incubated until analysis.

1.5. Determination of cytotoxicity of HFCPS and UVB irradiation on HDF cells

HDF cells were seeded (5.0×10^4 cells/well in 24-well plate) and incubated for 24 h. After incubation, cells were treated with different concentrations of HFCPS (25, 50,

and 100 $\mu\text{g}/\text{mL}$) or irradiated with the different dose of UVB (10, 30, 50, 80, and 100 mJ/cm^2). After sample treatment or UVB irradiation, cells were further incubated for 48 h. After incubation, the cell viabilities were measured by MTT assay [70, 71].

1.6. Determination of the effect of HFCPS against UVB-induced HDF cell damage

The protective effect of HFCPS against UVB-induced HDF cell damage was determined by measuring intracellular ROS level and viability of UVB-irradiated HDF cells. For intracellular ROS analysis, HDF cells were seeded (5.0×10^4 cells/well in 24-well plate) and incubated for 24 h, then, cells were treated with HFCPS and incubated for 30 min. Subsequently, cells were treated with DCFH-DA (stock, 500 $\mu\text{g}/\text{mL}$) and incubated for 30 min. After incubation, cells were exposed to UVB (50 mJ/cm^2) and the fluorescence intensity of cells was determined according to the method described previously [72-74]. For measuring the viabilities of UVB-irradiated HDF cells, HDF cells were treated with HFCPS and incubated for 2 h at 37°C. Cells were then exposed to 50 mJ/cm^2 of UVB and incubated for 48 h. Cell viability was assessed by MTT assay.

1.7. Determination of relative intracellular elastase and collagenase activities on UVB-irradiated HDF cells

HDF cells were seeded in 100 mm culture dishes at a density of 2.0×10^6 cells per dish and incubated for 24 h. Cells were treated with HFCPS and incubated for 2 h. Following incubation, cells were irradiated with UVB. After 48 h incubation, cells were harvested and lysed with 0.1 M Tris-HCl (pH 7.6) buffer containing 1 mM PMSF and 0.1% Triton-X 100, followed by sonication for 5 min on ice. The lysates were centrifuged (4000 rpm, 20 min) at 4°C. Supernatants were quantified the protein levels

and used as the fibroblastic enzyme solutions. The relative elastase and collagenase activities were measured by the method described by Suganuma et al. [75].

1.8. Determination of collagen synthesis level and MMPs expression levels on UVB-irradiated HDF cells

HDF cells were incubated with HFCPS for 2 h, and exposed to UVB (50 mJ/cm²). After 48 h incubation, the culture media were collected and used for assessment of matrix metalloproteinases (MMPs) expression levels and PIP level that reflect the level of collagen synthesis. The amounts of PIP and MMPs were measured by commercial ELISA kits based on the manufacturer's instructions.

1.9. Western blot analysis

The effect of HFCPS on the expressions of nuclear factor kappa B (NF-κB), activator protein 1 (AP-1), and mitogen-activated protein kinases (MAPKs) was assessed by Western blot analysis performed as described previously [43, 47]. In brief, cells were pretreated with HFCPS and irradiated with UVB. After 1 h (for MAPKs assay) or 6 h (for NF-κB and p-c-Jun assay) incubation, cells were harvested. Proteins were extracted with the PROPREP protein extraction kit (iNtRON Biotechnology, Sungnam, Korea). The protein level of each sample was measured by a BCA™ kit. Total proteins (50 μg) were separated on 10% SDS-polyacrylamide gels and transferred to pure nitrocellulose membranes. Membranes were blocked with 5% skim milk for 3 h at room temperature and incubated with primary antibodies overnight at 4°C. After washing with TBS-T buffer, membranes were incubated with secondary antibodies for 3 h at room temperature. Finally, the protein bands were visualized using an ECL western blotting detection kit and exposed on X-ray films.

1.10. Statistical Analysis

The experiments were performed in triplicate. The data are expressed as the mean \pm standard error (S.E), and one-way ANOVA was used to compare the mean values of each treatment in SPSS 12.0. Significant differences between the means were identified by the Turkey test. A value of $*p < 0.05$, $**p < 0.01$, and $^{##}p < 0.01$ were considered as significantly different.

2. Results and Discussion

2.1. HFCPS inhibits collagenase from *Clostridium Histolyticum* and elastase from porcine pancreas

In this study, the inhibitory effects of HFCPS against commercial collagenase and elastase were measured. As shown in Fig. 28, HFCPS inhibits collagenase and elastase in a dose-dependent manner. The collagenase inhibitory rates of HFCPS were 13.46, 22.58, and 49.77% at the concentrations of 50, 100, and 200 $\mu\text{g}/\text{mL}$, respectively (Fig. 28A), and the elastase inhibitory rates of HFCPS were 18.78, 38.14, and 56.53% at the concentrations of 50, 100, and 200 $\mu\text{g}/\text{mL}$, respectively (Fig. 28B). These results indicate that HFCPS may possess the activity against skin aging through inhibition of collagenase and elastase.

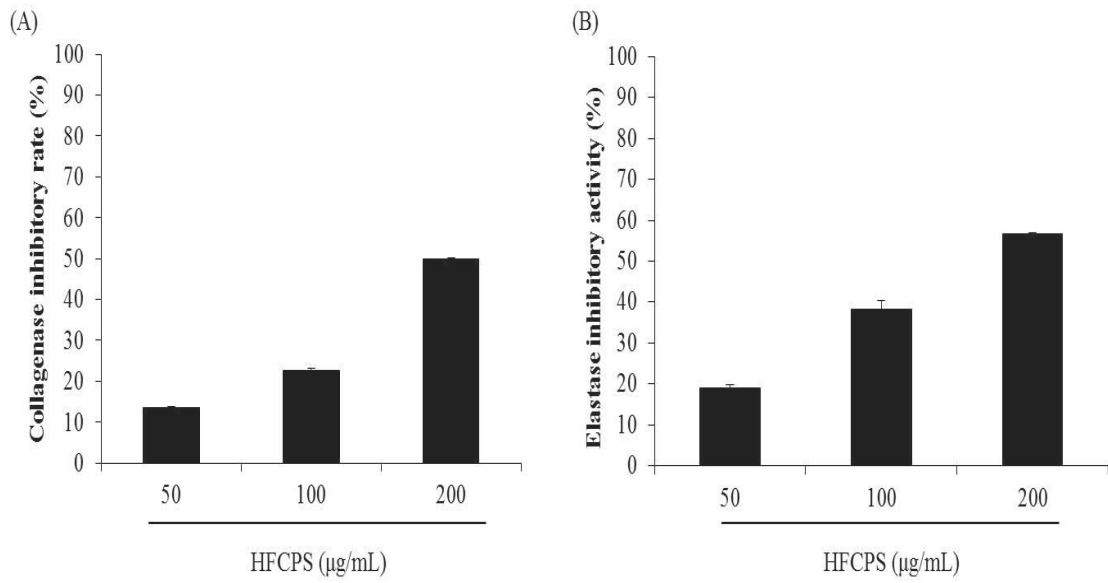


Fig. 28. HFCPS inhibits commercial collagenase and elastase. (A) Collagenase inhibitory activity of HFCPS; (B) elastase inhibitory activity of HFCPS. The experiments were conducted triplicate, and the data were expressed as the mean \pm standard error (S.E).

2.2. HFCPS promotes HDF cell proliferation and UVB irradiation damages HDF cells

As the first step to evaluate protective effect and mechanisms of HFCPS against UVB-induced skin photoaging in HDF cells, we employed various levels of UVB irradiation to induce cell damage in HDF cells, and determined the protective effect of HFCPS at different concentrations on HDF cells. As Fig. 29 shows, UVB irradiation significantly decreased the viability of HDF cells in a dose-dependent manner (Fig. 29A). Furthermore, the optimal UVB dose applied to HDF cells based on the 50% growth inhibitory dose was determined to be 50 mJ/cm². We then assessed the cytotoxicity of HFCPS on HDF cells. The cytotoxicity results (Fig. 29B) suggest that HFCPS is non-toxic on HDF cells and promotes HDF cells proliferation in a dose-dependent manner. From these results, 50 mJ/cm² was determined as the optimal UVB dose applied to HDF cells and 100 µg/mL was selected as the maximum concentration of HFCPS for further study.

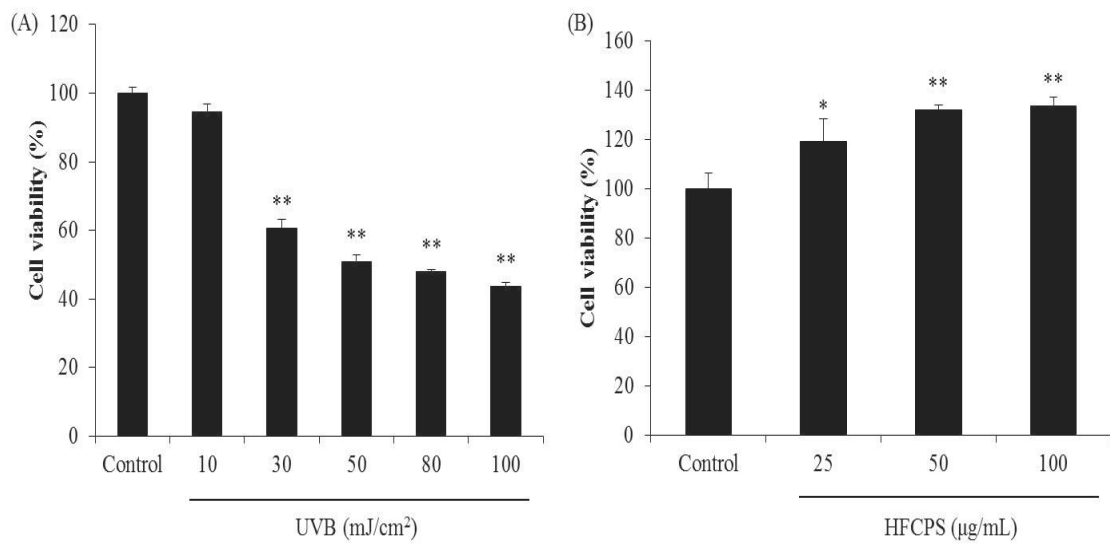


Fig. 29. HFCPS promotes HDF cell proliferation and UVB irradiation damages HDF cells. (A) Cytotoxicity of UVB irradiation on HDF cells; (B) proliferation effect of HFCPS on HDF cells. Cell viability was measured by MTT assay. The experiments were conducted triplicate, and the data were expressed as the mean \pm standard error (S.E), * $p < 0.05$, ** $p < 0.01$ as compared to control group.

2.3. HFCPS improves cell viability and reduces intracellular ROS in UVB-irradiated HDF cells

In the present study, HDF cells were treated with HFCPS and irradiated with UVB at a dose of 50 mJ/cm². Cell viability was subsequently measured by MTT assay and intracellular ROS level was analyzed by DCF-DA assay. As Fig. 30 shows, cell viability was decreased while intracellular ROS level was increased after UVB irradiation. Therefore, treatment with increasing concentrations of HFCPS (25, 50, and 100 µg/mL) improved cell viability by 11.78, 14.97, and 19.21% (Fig. 30A) and reduced intracellular ROS by 21.95, 36.44, and 48.14% (Fig. 30B). These results indicate that HFCPS possesses a potent protective effect against UVB-induced cell damage via ROS clearance in HDF cells.

2.4. HFCPS inhibits intracellular collagenase and elastase activities in UVB-irradiated HDF cells

As Fig. 31 shows, the relative collagenase and elastase activities of UVB-irradiated HDF cells were significantly increased compared with non-irradiated cells. However, the relative activities of both enzymes were decreased in the cells treated with HFCPS in a dose-dependent manner. These results suggest that HFCPS may act as an inhibitor of fibroblast collagenase and elastase and may prevent wrinkle formation induced by UVB irradiation.

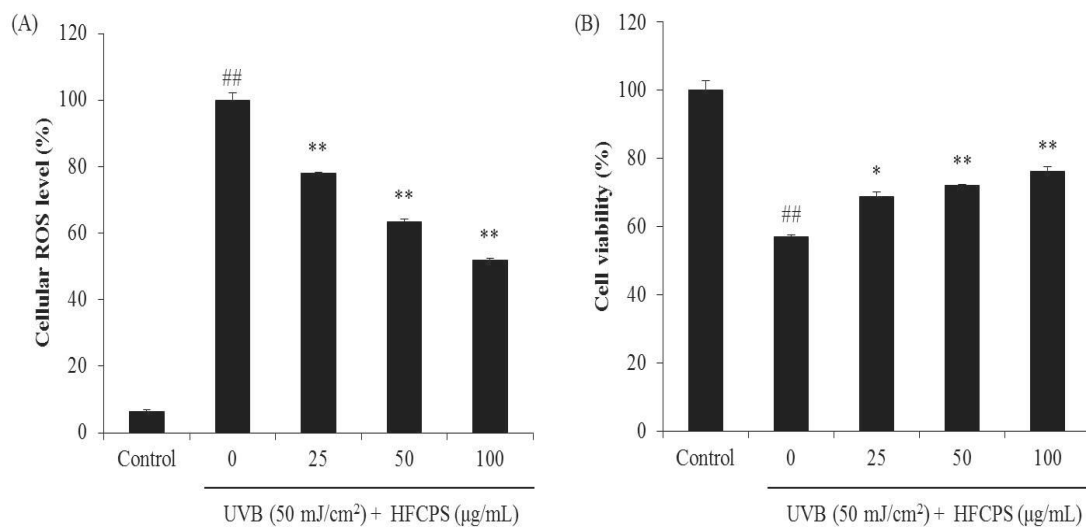


Fig. 30. Protective effects of HFCPS against UVB-induced HDF cell damage. (A) Intracellular ROS scavenging effect of HFCPS in UVB-induced HDF cells; (B) protective effect of HFCPS against UVB-induced HDF cell death. Cell viability was measured by MTT assay and intracellular ROS level was measured by DCF-DA assay. The experiments were conducted triplicate, and the data were expressed as the mean \pm standard error (S.E). * $p < 0.05$, ** $p < 0.01$ as compared to UVB-treated group and ^{##} $p < 0.01$ as compared to control group.

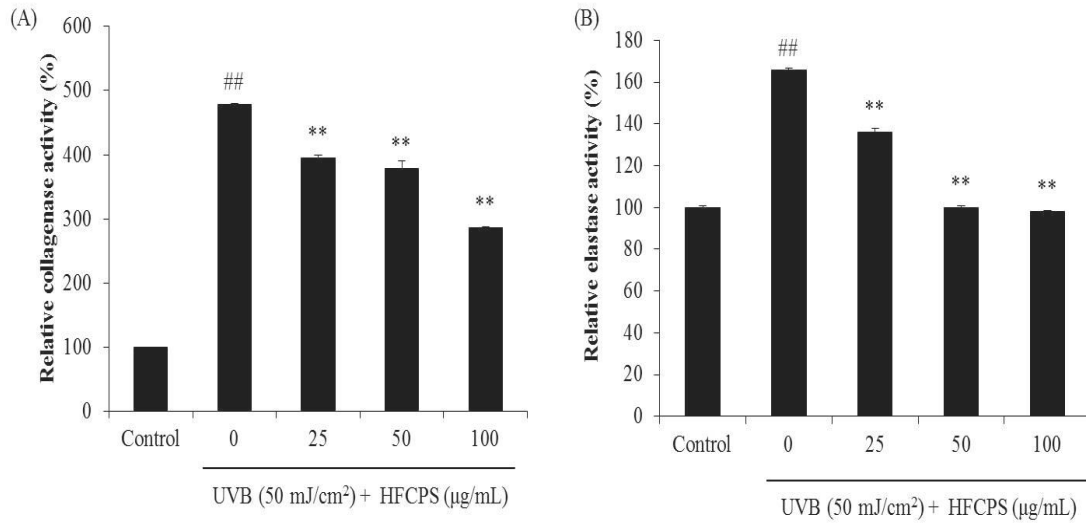


Fig. 31. HFCPS inhibits cellular collagenase and elastase activities in UVB-irradiated HDF Cells. (A) Relative collagenase activity; (B) relative elastase activity. The experiments were conducted triplicate, and the data were expressed as the mean \pm standard error (S.E). * $p < 0.05$, ** $p < 0.01$ as compared to UVB-treated group and ## $p < 0.01$ as compared to control group.

2.5. HFCPS protects collagen synthesis and reduces MMPs expression levels in UVB-irradiated HDF cells

As Fig. 32 shows, UVB irradiation significantly decreased collagen synthesis in HDF cells and HFCPS dose-dependently protects collagen synthesis (Fig. 32A). Furthermore, MMPs expression levels were significant increase in UVB-irradiated HDF cells but decreased in HFCPS treated cells (Fig. 32B-F). These results indicate that HFCPS effectively protects collagen synthesis and reduces the expression of MMPs.

2.6. HFCPS inhibits NF- κ B activation, reduces AP-1 phosphorylation, and suppresses MAPKs activation in UVB-induced HDF cells

In order to investigate the mechanism of HFCPS against UVB-induced skin wrinkling in HDF cells, we measured the activated AP-1 and MAPKs levels by Western blot analysis. The results indicate that UVB irradiation significantly phosphorylates AP-1 and HFCPS remarkably reduces the phosphorylated AP-1 (p-c-Jun) levels (Fig. 33). In addition, UVB irradiation significantly increases nuclear levels of NF- κ B (p65 and p50); however, HFCPS treatment remarkably reduces nuclear NF- κ B levels in UVB-irradiated HDF cells (Fig. 33). Furthermore, HFCPS treatment effectively suppresses UVB-induced p38, JNK, and ERK phosphorylation in UVB-irradiated HDF cells (Fig. 34). All effects are dose-dependently. These results demonstrate that HFCPS blocks NF- κ B activation, and reduces AP-1 phosphorylation through suppression of MAPKs activation in UVB-induced HDF cells.

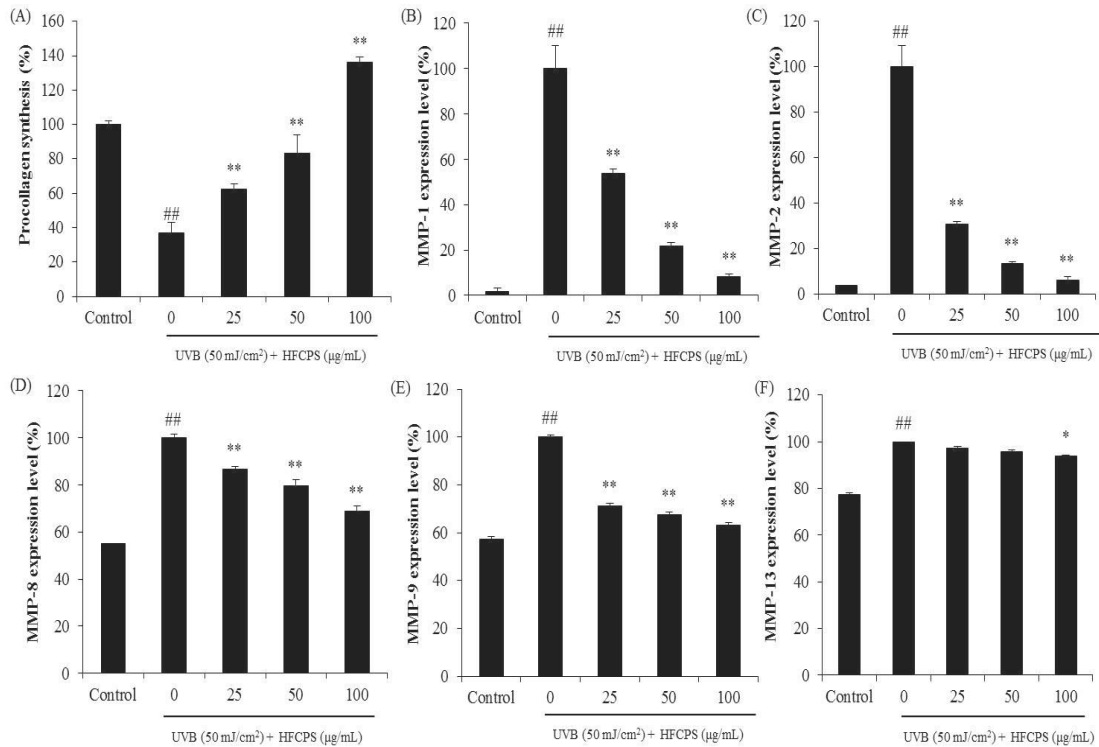


Fig. 32. HFCPS improves collagen synthesis and reduces MMPs expression in UVB-irradiated HDF cells. (A) Collagen synthesis level in UVB-irradiated HDF cells; (B) MMP-1 expression level in UVB-irradiated HDF cells; (C) MMP-2 expression level in UVB-irradiated HDF cells; (D) MMP-8 expression level in UVB-irradiated HDF cells; (E) MMP-9 expression level in UVB-irradiated HDF cells; (F) MMP-13 expression level in UVB-irradiated HDF cells. Collagen synthesis level was reflected by the amounts of PIP, and the amounts of PIP and MMPs were measured by the commercially ELISA kits, based on the manufacturer's instructions. The experiments were conducted triplicate, and the data were expressed as the mean \pm standard error (S.E). * $p < 0.05$, ** $p < 0.01$ as compared to UVB-treated group and ^{##} $p < 0.01$ as compared to control group.

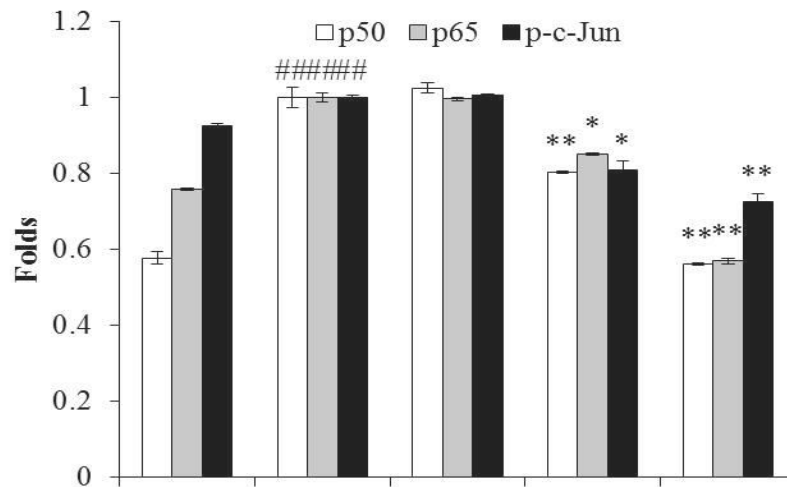
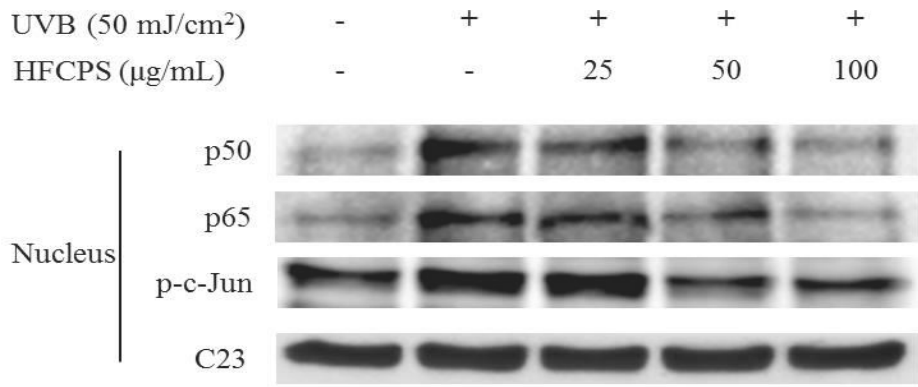


Fig. 33. HFCPS blocks UVB-induced NF- κ B activation and reduces AP-1 phosphorylation in UVB-induced HDF cells. There relative NF- κ B and phosphorylated AP-1 levels were compared with C23. The experiments were conducted triplicate, and the data were expressed as the mean \pm standard error (S.E). ** $p < 0.01$ as compared to UVB-treated group and ^{##} $p < 0.01$ as compared to control group.

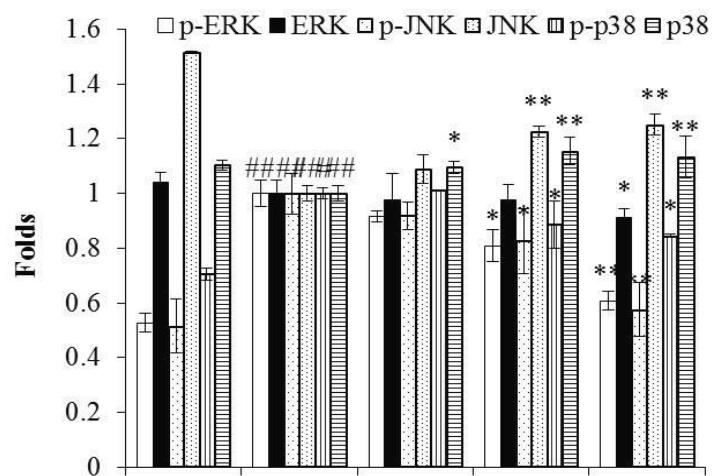
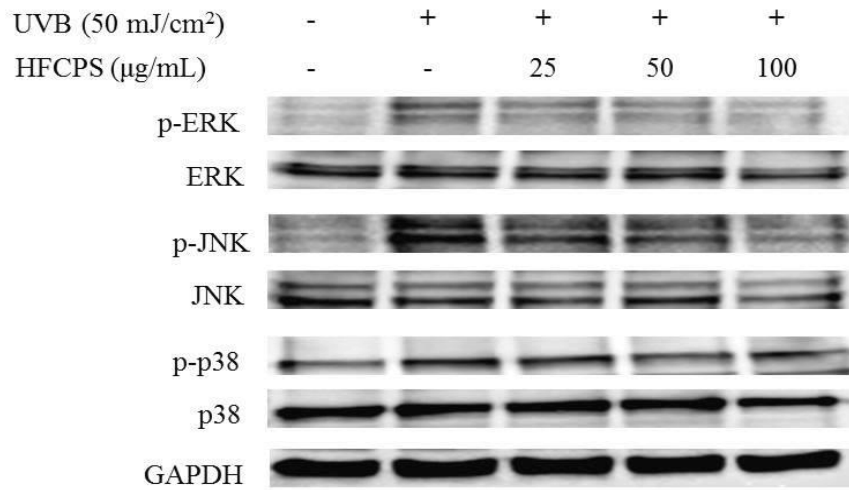


Fig. 34. HFCPS suppresses MAPKs activation in UVB-induced HDF cells. The relative amounts of activated MAPKs levels were compared with GAPDH. The experiments were conducted triplicate, and the data were expressed as the mean \pm standard error (S.E). ** $p < 0.01$ as compared to UVB-treated group and $^{###}p < 0.01$ as compared to control group.

3. Conclusion

In the present study, the protective effect of HFCPS against UVB-induced skin damage *in vitro* in HDF cells was investigated. The results indicates that HFCPS significantly protected collagen synthesis and reduced MMPs expression in UVB-irradiated HDF cells by regulating NF- κ B, AP-1, and MAPKs signaling pathways. These results suggest that HFCPS possesses strong UV protective effect and has the potential to be used as an ingredient in the pharmaceutical and cosmetic industries.

CONCLUSION

The above results suggest that the sulfated polysaccharides from Celluclast-assisted extract from *Hizikia fusiforme* (HFCPS) possesses strong cosmeceutical effects including antioxidant, anti-inflammation, whitening, UV protection, and anti-wrinkle activity, and can use as a potential ingredient in the cosmetic industry. The individual sulfated polysaccharides of HFCPS need to separate and the mechanisms of its cosmeceutical effects need to be further investigated.

Part III.

**Isolation of fucoidan from crude polysaccharides of *Hizikia fusiforme* and
evaluation of its bioactivities**

Part III.

Isolation of fucoidan from crude polysaccharides of *Hizikia fusiforme* and evaluation of its bioactivities

ABSTRACT

Fucoidan (HFCPSF4) was separated from polysaccharides from Celluclast-assisted extract from *Hizikia fusiforme* (HFCPS). HFCPSF4 contains $99.01 \pm 0.61\%$ sulfated polysaccharides, which comprise fucose (97.20%), rhamnose (2.09%), mannose (18.32%), and arabinose (0.38%). The cosmeceutical effects of HFCPSF4 were measured including antioxidant activity, anti-inflammatory activity, whitening effect, UV protective effect, and anti-wrinkle effect. The results indicate that HFCPSF4 significant reduces hydrogen peroxide (H_2O_2)-induced oxidative stress in monkey kidney fibroblast cells (Vero cells) and in zebrafish; remarkable attenuates lipopolysaccharide (LPS)-induced inflammation in RAW 264.7 macrophages; inhibits alpha-melanocyte stimulating hormone (α -MSH)-stimulated melanogenesis in B16F10 melanoma cells; against UVB-induced photo-damage in keratinocytes (HaCaT cells) and in zebrafish; protects UVB-induced skin wrinkling in human dermal fibroblasts (HDF cells). These results demonstrate that HFCPSF4 possesses potent cosmeceutical effects and can be a potential ingredient in the cosmetic industry.

INTRODUCTION

In human, skin is the largest organ of the integumentary system. It undergoes chronological aging like other organs. Skin is in direct exposure to the outside environment, therefore it undergoes aging as a consequence of environmental damage [76]. Ultraviolet (UV) irradiation from sunlight is the primary environmental factor that induces human skin aging, and results in pigment accumulation and wrinkle formation. Human skin is frequently affected by oxidative stress caused by continuous exposure to UV irradiation from sunlight. Skin exposed to UV and environmental oxidizing pollutants is associated with diverse abnormal reactions including inflammatory responses, epidermal hyperplasia, breakdown of collagen, and melanin accumulation [77, 78].

UV can be classified into three subtypes including UVA, UVB, and UVC, based on the wavelength. UVB has a medium wavelength and is thought to bring more cellular stress to humans compared to the other two subtypes [79-81]. UVB is known to be associated with human health through stimulating reactive oxygen species (ROS) generation [82, 83]. This excessive ROS subsequently activate cell signaling pathways including nuclear factor kappa B (NF- κ B), activator protein 1 (AP-1), and mitogen-activated protein kinases (MAPKs), which stimulate pro-inflammatory cytokines and matrix metalloproteinases (MMPs) expression [84]. MMPs are a class of structurally similar enzymes, and play a major role in physiological and pathological tissue remodeling. The imbalance of MMPs expression could lead to cartilage, cardiac, and cancer-related diseases [85]. MMPs degrade the collagenous extracellular matrix (ECM) in connective tissues, which is the main factor of wrinkling. Therefore, an ideal MMPs inhibitor or an agent that reduces the expression of MMPs may be effective against

wrinkle formation, and could be thought as a promising candidate to be used as an ingredient in the cosmetic industry.

The above research displayed that the sulfated polysaccharides from Celluclast-assisted extract of *Hizikia fusiforme* (HFCPS) possesses strong antioxidant, anti-inflammation, whitening, UV protection, and anti-wrinkle activity. However, the sulfated polysaccharide of HFCPS had not been purified and the mechanisms of its cosmeceutical effects had not been investigated so far. Therefore, in this study, we separated pure fucoidan and evaluated its cosmeceutical effects.

Section 1: Isolation fucoidan from crude polysaccharides from Celluclast-assisted extract of *Hizikia fusiforme*

Abstract

The above results indicate that HFCPS (the sulfated polysaccharides from Celluclast-assisted extract of *H. fusiforme*) possesses strong cosmetic effects. In order to investigating the cosmetic effects of pure fucoidan, HFCPS were separated by DEAE-cellulose column. After separation, four fractions (HFCPSF1, HFCPSF2, HFCPSF3, and HFCPSF4,) were obtained. HFCPSF4 contains $99.01 \pm 0.61\%$ sulfated polysaccharides, which comprise fucose (97.20%), rhamnase (2.09%), mannose (18.32%), and arabinose (0.38%); it was thought as the pure fucoidan. In addition, the cosmeceutical effects of all 4 fractions were evaluated. HFCPSF4 possesses the strongest free radical scavenging activity, tyrosinase inhibitory activity, elastase inhibitory activity, and collagenase inhibitory activity comparing to other fractions. These results demonstrate that the fucoidan from HFCPS possesses strong cosmeceutical effect, and can be a potential ingredient in the cosmetic industry.

1. Materials and Methods

1.1. Reagents and chemicals

HFCPS were prepared in the previous study. Trifluoroacetic acid, arabinose, fucose, galactose, glucose, rhamnose, and xylose were purchased from Sigma (Sigma, St. Louis, MO, USA). 1-diphenyl-2-picrylhydrazyl (DPPH), 5,5-dimethyl-1-pyrroline N-oxide (DMPO), 2,2-azobis(2-amidinopropane) hydrochloride (AAPH), and α -(4-Pyridyl-1-oxide)-N-ter-butyl nitron (POBN) were purchased from Sigma (St. Louis, MO, USA). Arbutin, (-)-epigallocatechin gallate (EGCG), gallic acid, glucose tyrosinase, L-tyrosin, collagenase from clostridium histolyticum, elastase from porcine pancreas, azo dye-impregnated collagen, and N-succinyl-Ala-Ala-Ala-p-nitroanilide were purchased from Sigma Co. (St. Louis, MO, USA). $\text{FeSO}_4 \cdot 7\text{H}_2\text{O}$ and H_2O_2 were purchased from Fluka Co. (Buchs, Switzerland). All other chemicals and reagents were analytical grade.

1.2. Separation of fucoidan from HFCPS

HFCPS was applied to a DEAE-cellulose column (17 cm \times 2.5 cm) equilibrated in 50 mM sodium acetate (pH 5.0) and washed with the same buffer. Elution was carried out at a flow rate of 15 mL/h with a linear gradient of 0–2 M NaCl containing 50 mM sodium acetate (pH 5.0). Fractions of 10 mL were collected and measured for polysaccharide content by phenol– H_2SO_4 assay. The fractions were pooled, dialyzed and freeze-dried.

1.3. Chemical analysis of fractions separated from HFCPS

The total carbohydrate contents of fractions separated from HFCPS were determined based on the protocol of official methods for analysis of the Association of Official Analytical Chemists (AOAC) [57]. Glucose was used as a standard to evaluate the total

carbohydrate content of fractions separated from HFCPS. To determine the total sulfate content, fractions separated from HFCPS were hydrolyzed by 4 M trifluoroacetic acid at 100°C for 5 hours. The sulfate content was measured by the method described by Wang et al. [33].

In order to analyze the neutral sugars components of fractions separated from HFCPS, fractions separated from HFCPS were hydrolyzed by 4 M of trifluoroacetic acid in sealed glass vials for 4 h at 100°C. Then, the neutral sugar components and contents of samples were determined by HPLC and arabinose, fucose, galactose, glucose, rhamnose, and xylose had used as the standard, the procedure described by Kang et al. [58].

1.4. Evaluation of the free radical scavenging activity of seaweed extracts

The free radical scavenging activities of the fractions separated from HFCPS were measured using an Electron Spin Resonance (ESR) spectrometer (JES-FA machine; JOEL, Tokyo, Japan). DPPH, alkyl, and hydroxyl radical scavenging activities were determined by the method described by Heo et al. [1, 86].

1.5. Measurement of mushroom tyrosinase inhibitory effects of seaweed extracts

In brief, a volume of 200 μ L assay mixture in 96-well microplate containing 40 μ L of 1.5 mM L-tyrosin, 140 μ L of 50 mM phosphate buffer (pH 6.5), 10 μ L of aqueous mushroom tyrosinase (1000 units/mL), and 10 μ L of sample solution. The assay mixture was reacted at 37°C for 12 min, and then the plate was kept on ice for 5 min to stop the reaction. The amount of dopachrome in the reaction mixture was measured at 490 nm using microplate reader (BioTek, SYNERGY, HT, USA).

1.6. Measurement of collagenase inhibitory effects of seaweed extracts

In order to measure the collagenase inhibitory activity, a weight of 1 mg of azo dye-impregnated collagen was mixed with 800 μL of 0.1 M Tris-HCl (pH 7.0), 100 μL of 200 units/mL collagenase (stock solution), and 100 μL sample and incubated at 43°C for 1 h under shaking condition. Subsequently, the reaction mixture was centrifuged at 3000 rpm for 10 min and the absorbance of the supernatant was detected at 550 nm in a microplate reader (BioTek, SYNERGY, HT, USA).

1.7. Measurement of elastase inhibitory effects of seaweed extracts

The elastase inhibitory activity was evaluated base on a method reported by Kraunsoe et al. (1996) [43]. In brief, the reaction mixture contained 650 μL of 1.015 mM N-succinyl-Ala-Ala-Ala-p-nitroanilide (dissolved in Tris-HCl, pH 8.0) and 50 μL of sample. The reaction mixture were vortexed and incubated for 10 min at 25°C, after which 50 μL of 0.0375 units/mL elastase was added to the reaction mixture and following vortexing, was incubated for 10 min at 25°C in a water bath. The amount of released p-nitroaniline was assessed by measuring absorbance at 410 nm using a microplate reader (BioTek, SYNERGY, HT, USA).

1.8. Characterization of the purified fucoidan from HFCPS by Fourier transform infrared (FT-IR) spectroscopy

The IR spectrum of the purified fucoidan (target fraction) from HFCPS was recorded using a FT-IR spectrometer (Nicolet™ 6700 FT-IR spectrometer; Madison, WI, USA). The polysaccharides were homogenized with KBr powder and then pressed into pellets for FT-IR measurement in the frequency range of 500–4000 cm^{-1} .

2. Results and Discussion

2.1. Total carbohydrate, phenolic, and sulfate content of fractions separated from HFCPS

The component contents of fractions from HFCPS (Fig. 35) were investigated. The phenolic content of fractions from HFCPS is range from $0.00\pm 0.12\%$ to and $0.28\pm 0.08\%$, respectively (Table 13). The carbohydrate content of fractions from HFCPS is range from $50.38\pm 1.25\%$ and $71.79\pm 0.56\%$, and the sulfate content of fractions from HFCPS is range from $0.00\pm 0.04\%$ and $27.22\pm 0.05\%$, respectively. Altogether, HFCPSF4 contains $99.01\pm 0.61\%$ sulfate polysaccharide and thought as purified fucoidan.

2.2. Natural sugar composition of fractions separated from HFCPS

The monosaccharide content of fractions from HFCPS was determined, using six monosaccharides as standards: fucose, rhamnose, arabinose, galactose, glucose, and xylose. The results (Table 13) indicate that HFCPSF4 comprised by fucose (97.20%), rhamnose (2.09%), Mannose (18.32%), and arabinose (0.38%).

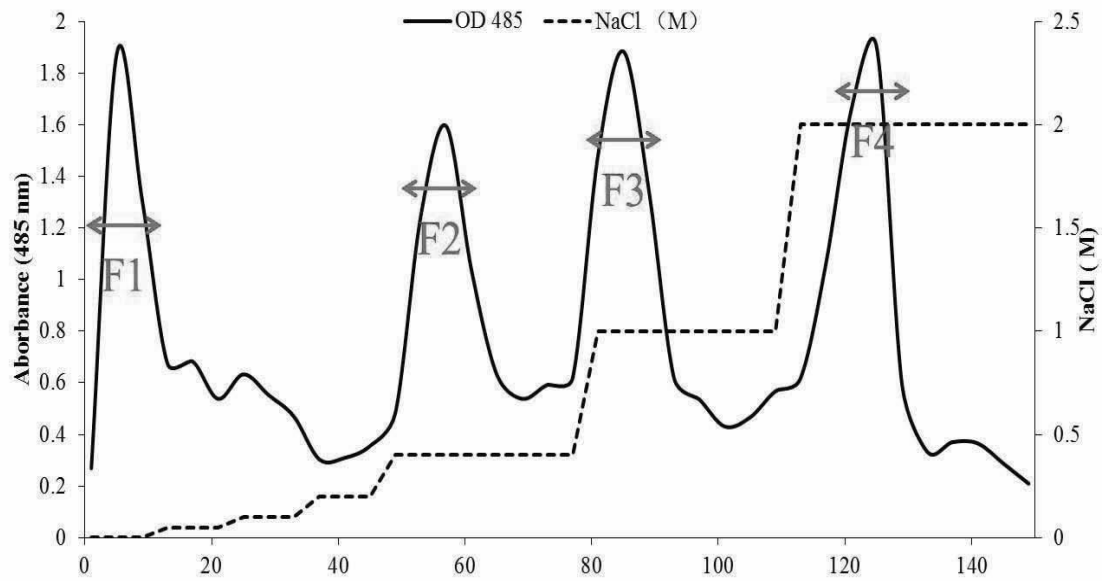


Fig. 35. DEAE-cellulose chromatogram of the polysaccharides separated from HFCPS.

Table 13. Total carbohydrate contents, phenolic contents, sulfate contents, and natural sugar components of polysaccharides separated from HFCPS.

Sample	HFCPS	F1	F2	F3	F4
Phenolic content (%)	1.56±0.08	0.28±0.08	0.00±0.19	0.00±0.19	0.00±0.12
Carbohydrate content (%)	55.05±0.09	57.06±2.77	52.33±1.46	50.38±1.25	71.79±0.56
Sulfate content (%)	7.78±0.23	0.00±0.04	0.00±0.07	11.86±0.52	27.22±0.05
Sulfate polysaccharide content (%)	62.83±0.32	-	-	62.24±1.77	99.01±0.61
Sugar components (%)					
Fucose	53.53	51.790356	34.36	54.32	79.20
Rhamnose	-	0.7596208	5.55	1.02	2.09
Galactose	23.15	8.5673269	23.21	26.24	-
Glucose	5.95	-	34.18	4.15	-
Mannose	-	38.737638	-	14.27	18.32
Xylose	17.37				
Arabinose	-	0.145058	2.70	-	0.38

HFCPS: polysaccharides of Celluclast-assisted extract of *H. fusiforme*; HFCPSF1: fraction 1 from HFCPS; HFCPSF2: fraction 3 from HFCPS; HFCPSF3: fraction 3 from HFCPS; HFCPSF4: fraction 4 from HFCPS. The experiments were conducted triplicate in this study. The data were expressed as the mean ± standard error (S.E).

2.3. Free radical scavenging activities of fractions separated from HFCPS

The results of free radical scavenging activities of fractions from HFCPS summarized in Table 14. The IC_{50} values of DPPH radical scavenging activities of fractions from HFCPS were range from 0.55 ± 0.06 mg/mL to 1.06 ± 0.08 mg/mL, and HFCPSF4 shows the strongest DPPH radical scavenging activity in all of the fractions. The IC_{50} values of alkyl radical scavenging activities of the fractions from HFCPS were range from 0.12 ± 0.02 mg/mL to 0.83 ± 0.03 mg/mL, and the HFCPSF4 shows the strongest alkyl radical scavenging activity in all of the fractions. In addition, the IC_{50} values of hydroxyl radical scavenging activities of the fractions from HFCPS were range from 0.09 ± 0.00 mg/mL to 0.52 ± 0.03 mg/mL, and HFCPSF4 shows the strongest hydroxyl radical scavenging activity in all of the fractions. These results indicate that all of the fractions from HFCPS possess strong free radical scavenging activity, and HFCPSF4 shows relative strong hydroxyl radical scavenging activity than other fractions.

Table 14. Free radical scavenging activities of polysaccharides of HFCPS.

Sample	IC ₅₀ (mg/mL)		
	DPPH	Alkyl	Hydroxyl
HFCPS	0.81±0.02	0.25±0.01	0.21±0.03
HFCPSF1	0.93±0.04	0.66±0.08	0.48±0.06
HFCPSF2	1.06±0.08	0.83±0.03	0.52±0.03
HFCPSF3	0.65±0.12	0.21±0.06	0.18±0.05
HFCPSF4	0.55±0.06	0.12±0.02	0.09±0.00

HFCPS: polysaccharides of *H. fusiforme*; HFCPSF1: fraction 1 from HFCPS; HFCPSF2: fraction 3 from HFCPS; HFCPSF3: fraction 3 from HFCPS; HFCPSF4: fraction 4 from HFCPS; DPPH: DPPH radical scavenging activity; Alkyl: alkyl scavenging activity; Hydroxyl: hydroxyl scavenging activity. The experiments were conducted triplicate in this study. The data were expressed as the mean ± standard error (S.E).

2.4. Tyrosinase inhibitory effects of fractions from HFCPS

Tyrosinase is the rate-limiting enzyme for controlling the production of melanin, which is the major factor for skin color. Therefore, a tyrosinase inhibitor that can inactive or inhibit the tyrosinase may stopping or reducing melanin production. The inhibitor may show the potential in whitening effect. In order to investigate the whitening effect of the fractions from HFCPS, we measured tyrosinase inhibitory effects of fractions from HFCPS. As Fig. 36 shows, all fractions have shown tyrosinase inhibitory effect. Furthermore, HFCPSF4 possesses stronger tyrosinase inhibitory effect than other fractions. These results indicate that the fractions from HFCPS possess the potential in skin whitening effect, and HFCPSF4 possesses strong tyrosinase inhibitory effect may be developing to a whitening ingredient use to cosmeceutical industry.

2.5. Collagenase inhibitory effects of fractions from HFCPS

In order to investigate the anti-wrinkle effects of the fractions from HFCPS, we measured collagenase inhibitory effects of the fractions from HFCPS. As Fig. 37 shows, the fractions of HFCPS show strong collagenase inhibitory effects. In addition, HFCPSF3 and HFCPSF4 possess stronger collagenase inhibitory effect than other fractions, and HFCPSF4 possesses the strongest collagenase inhibitory effect in all of fractions. These results indicate that the fractions from HFCPS possess the potential in anti-wrinkle effect, and HFCPSF4 possess strong collagenase inhibitory effect may be developing to an anti-wrinkle ingredient use to cosmeceutical industry.

2.6. Elastase inhibitory effects of fractions from HFCPS

In this study, we investigate elastase inhibitory effects of the fractions from HFCPS. As Fig. 38 shows, the fractions from HFCPS show strong elastase inhibitory effects. In addition, HFCPSF4 possesses the strongest elastase inhibitory effect in all of fractions.

These results display that the fractions from HFCPS possess the potential in anti-wrinkle effect and the HFCPSF4 possess strong elastase inhibitory effect may develop to an anti-wrinkle ingredient use to cosmeceutical industry.

2.7. FT-IR analysis of purified fucoïdan

The FT-IR spectra of purified fucoïdan (HFCPSF4) and commercial fucoïdan are shown in Fig. 39 with its major absorbance peaks. Base on the previous studies, the peaks between 1120 and 1270 cm^{-1} indicate the sulfate groups (S=O stretching) branching off from fucoïdan backbone; the absorption at 845 cm^{-1} indicate a sulfate group at axial C-4; the shoulder absorption at 820 cm^{-1} indicate a sulfate group at C-2 [87]. These data demonstrate the presences of fucoïdan.

According to the polysaccharide content, sulfate content, FT-IR spectrum, and mono-sugar components of HFCPSF4, HFCPSF4 showed the similarities to the well-known commercial fucoïdan from brown algal. Therefore, HFCPSF4 was thought as *Hizikia* fucoïdan for further study.

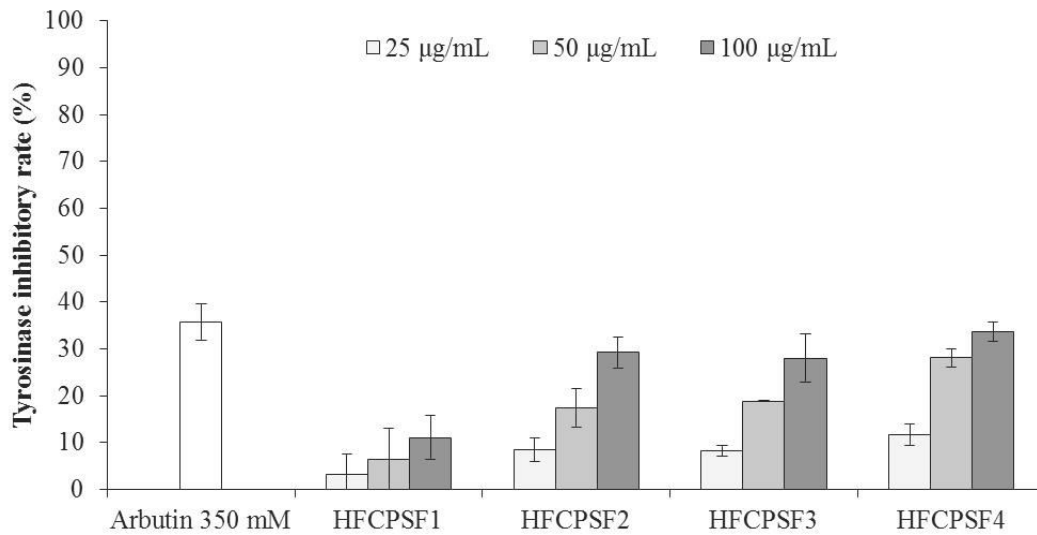


Fig. 36. Tyrosinase inhibitory effects of fractions from HFCPS. The amount of dopachrome was measured at 490 nm using a microplate reader. The experiments were conducted triplicate, and the data were expressed as the mean \pm S.E (n=3).

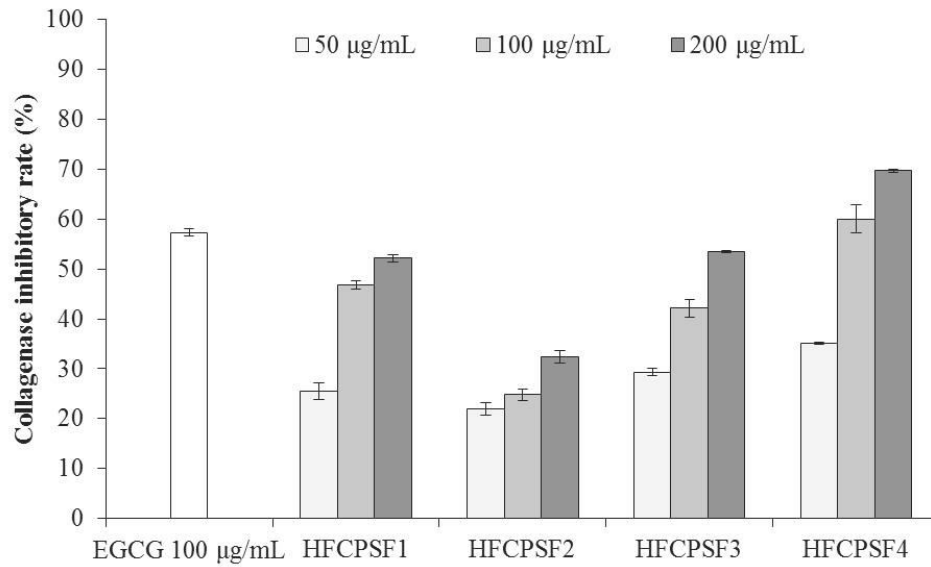


Fig. 37. Collagenase inhibitory effects of the fractions form HFCPS. Collagenase inhibitory effects were measured by colorimetric assay. The experiments were conducted triplicate, and the data were expressed as the mean \pm S.E (n=3).

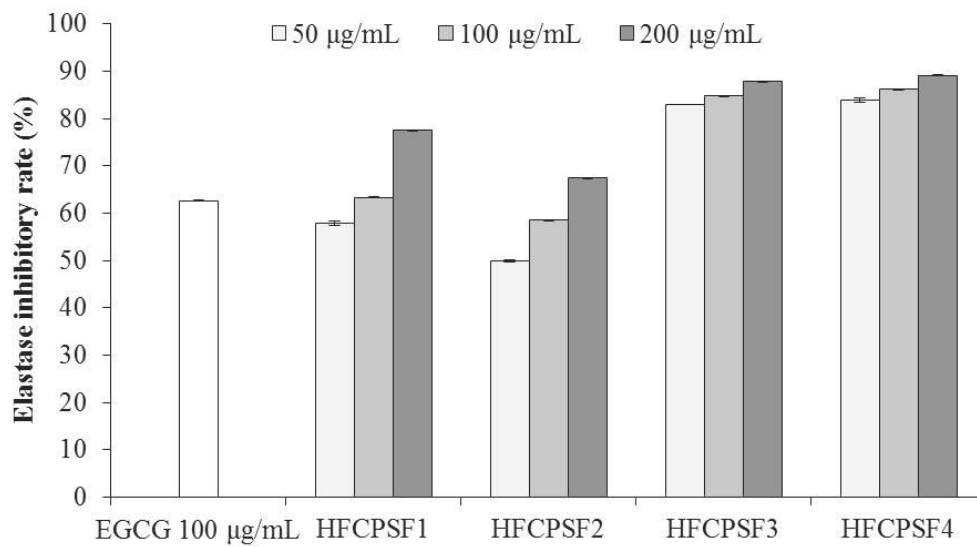


Fig. 38. Elastase inhibitory effects of the fractions form HFCPS. Elastase inhibitory effects were measured by colorimetric assay. The experiments were conducted triplicate, and the data were expressed as the mean \pm S.E (n=3).

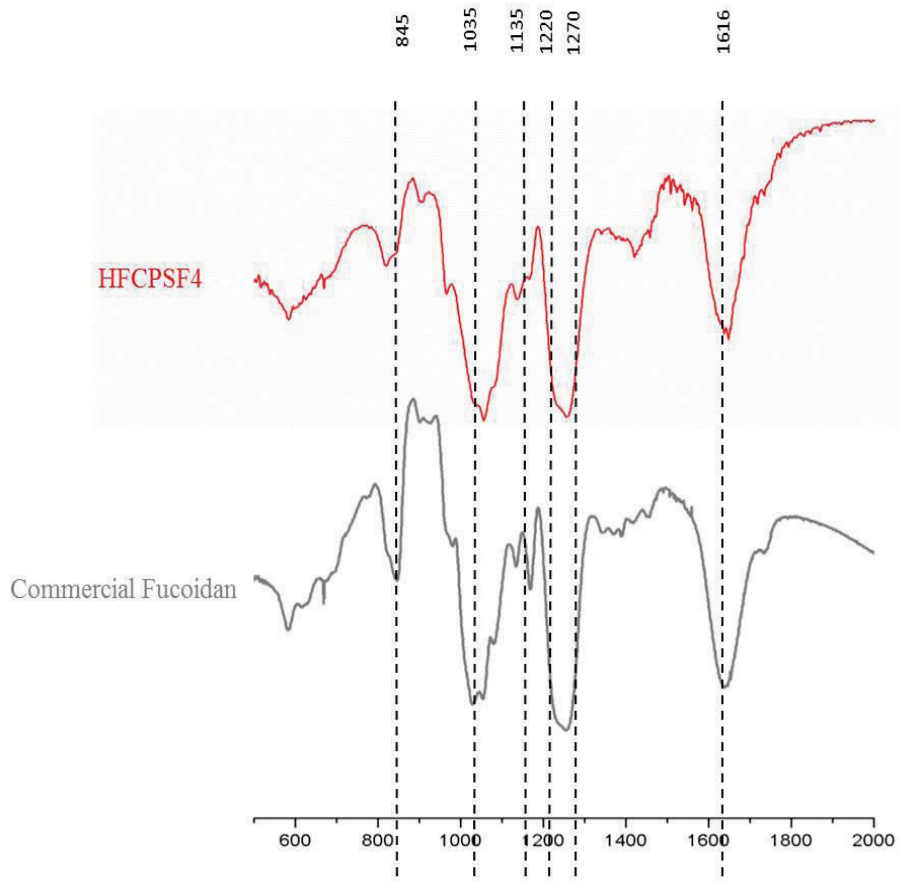


Fig. 39. Spectroscopic analysis of the purified fucoïdan from HFCPS.

3. Conclusion

Four polysaccharides (HFCPSF1, HFCPSF2, HFCPSF3, and HFCPSF4) from crude polysaccharides from Celluclast-assisted extract of *H. fusiforme* were separated by DEAE-cellulose column and the cosmetic effects of the polysaccharides had been investigated. HFCPSF4 contains $99.01 \pm 0.61\%$ sulfated polysaccharides, which comprise fucose (97.20%), rhamnose (2.09%), mannose (18.32%), and arabinose (0.38%). HFCPSF4 was thought as *Hizikia* fucoidan from Celluclast-assisted extract of *H. fusiforme*. HFCPSF4 possess strongest free radical scavenging activity, tyrosinase inhibitory activity, elastase inhibitory activity, and collagenase inhibitory activity comparing to other fractions. These results demonstrate that the *Hizikia* fucoidan (HFCPSF4) from HFCPS possesses strong cosmeceutical effects, and can be a potential ingredient in the cosmetic industry.

Section 2: Antioxidant activity of *Hizikia* fucoidan *in vitro* in Vero cells and *in vivo* in zebrafish

Abstract

Protective effect of *Hizikia* fucoidan (HFCPSF4) isolated from HFCPS against hydrogen peroxide (H₂O₂)-induced oxidative stress *in vitro* in Vero cells and *in vivo* in zebrafish had been investigated. HFCPSF4 significantly reduced cytotoxicity induced by H₂O₂ on Vero cells. In addition, HFCPSF4 reduced cellular ROS level and apoptosis body formation induced by H₂O₂. The Western blot results demonstrate that HFCPSF4 against oxidative stress by improving the expression of endogenous antioxidant enzymes including catalase and superoxidase dismutase (SOD) via regulating Nrf2/HO-1 pathways. In addition, HFCPSF4 has shown strongly protective effects against H₂O₂-stimulated oxidative stress *in vivo* zebrafish that demonstrated by improving survival rate, decreasing heart beating rate, and reducing ROS generation and cell death. These results suggest that HFCPSF4 may use as a beneficial antioxidant ingredient in medical and cosmetic industries.

1. Materials and methods

1.1. Reagents and Chemicals

MTT, DMSO, acridine orange, and DCFH-DA were purchased from Sigma (St. Louis, MO, USA). H₂O₂ were purchased from Fluka Co. (Buchs, Switzerland). Vero cells were purchased from the Korea Cell Line Bank (KCLB, Seoul, Korea). RPMI-1640 medium, FBS, penicillin-streptomycin, and trypsin-EDTA were purchased from Gibco-BRL (Grand Island, NY, USA). Catalase, superoxidase dismutase-1 (SOD-1), β -actin, nuclear factor (erythroid-derived 2)-like 2 (Nrf2), and heme oxygenase (HO-1) antibodies, anti-mouse and anti-rabbit IgG antibodies were purchased from Cell Signaling Technology (Beverly, MA, USA). All other chemicals and reagents were analytical grade.

1.2. Cell culture

Vero cells were maintained in RPMI-1640 medium containing 10% heat-inactivated FBS, penicillin (100 unit/mL) and streptomycin (100 μ g/mL) at 37°C in an incubator under humidified atmosphere containing 5% CO₂. Vero cells were sub-cultured every 3 days, and seeded at a concentration of 1×10^5 cells/mL in 96-well plates.

1.3. Determination of the protective effect of HFCPSF4 against H₂O₂-induced intracellular ROS generation in Vero cells

Vero cells were seeded and cultured for 24 h. Different concentrations of HFCPSF4 were added to cells prior to incubation for 1 h. After incubation, H₂O₂ (1 mM) was added to the cells and cells were incubated for 1 h. Finally, DCFH-DA (500 μ g/mL) was introduced to the cells, and the fluorescence emission of DCF-DA was detected using a fluorescence microplate reader (Olympus, Japan).

1.4. Measurement of the protective effect of HFCPSF4 against H₂O₂-induced cytotoxicity in Vero cells

Vero cells were treated with different concentrations of HFCPSF4 and incubated for 1 h. After incubation, H₂O₂ (1 mM) was added to the cells prior to incubation for 24 h. Cell viability was measured by MTT assay, according to Fernando et al. [5].

1.5. Nuclear staining with Hoechst 33342

To assess the apoptosis body's formation in H₂O₂-induced Vero cells, the nuclear morphology of cells was analyzed by Hoechst 33342 staining. Nuclear staining was performed base on the method described by Wijesinghe et al. [60]. The degree of nuclear condensation of cells was examined under a fluorescence microscope equipped with a Cool SNAP-Pro color digital camera (Olympus, Japan).

1.6. Western blot analysis

The effect of HFCPSF4 on the expressions of catalase, SOD, Nrf2, HO-1 was assessed by Western blot analysis performed as described previously. In brief, cells were treated with HFCPSF4 and stimulated with H₂O₂. After 24 h incubation, cells were harvested. Proteins were extracted with the PROPREP protein extraction kit (iNtRON Biotechnology, Sungnam, Korea). The protein level of each sample was measured by a BCATM kit. Total proteins (50 µg) were separated on 12% SDS-polyacrylamide gels and transferred to pure nitrocellulose membranes. Membranes were blocked with 5% skim milk for 3 h at room temperature and incubated with primary antibodies overnight at 4°C. After washing with TBS-T buffer, membranes were incubated with secondary antibodies for 3 h at room temperature. Finally, the protein bands were visualized using an ECL western blotting detection kit and exposed on X-ray films.

1.7. Application of HFCPSF4 and H₂O₂ to zebrafish embryos

Approximately 3~4 hours post-fertilization (hpf), the embryos were transferred to individual wells in a 12-well plate (15 embryos per group) and maintained in embryo medium containing HFCPSF4 (12.5, 25, and 50 µg/mL). After 1 hour incubation, 5 mM H₂O₂ was added to the medium, and the embryos were incubated until 24 hpf. The survival rate was measured at 3 days post-fertilization (dpf) after treatment with H₂O₂ by counting live embryos, and the surviving fish were then used for further analysis.

1.8. Determination of heart-beating rate, ROS generation, cell death, and lipid peroxidation in zebrafish

The zebrafish heart-beating rate was measured according to Kim et al. [61]. The zebrafish heart-beating rate in both the atrium and ventricle was recorded for 1 min at 2 dpf under a microscope. Intracellular ROS level, cell death, and lipid peroxidation were measured in live zebrafish using DCFH-DA, acridine orange, and DPPP staining, respectively, followed the previous procedure [46, 88, 89]. The zebrafish were observed and photographed under a fluorescence microscope equipped with a Cool SNAP-Pro color digital camera (Olympus, Japan). The fluorescence intensity of individual zebrafish larva was quantified using the image J program.

1.9. Statistical analysis

All experiments were conducted in triplicate. The data are expressed as the mean ± standard error (S.E), and one-way ANOVA was used to compare the mean values of each treatment in SPSS 12.0. Significant differences between the means were identified by the Turkey test. Significance was established if * $p < 0.05$, ** $p < 0.01$ as compared to the H₂O₂-treated group, and ^{##} $p < 0.01$ as compared to control group.

2. Results and Discussion

2.1. Protective effect of HFCPSF4 against H₂O₂-induced oxidative stress in Vero cells

As Fig. 40 shows, the intracellular ROS level significantly increased and cell viability decreased following treatment with H₂O₂. However, the intracellular ROS levels decreased and cell viability increased following treatment at all measured concentrations of HFCPSF4. Both effects occurred in a dose-dependent manner.

2.2. Protective effect of HFCPSF4 against H₂O₂-induced apoptosis

In order to measure the apoptotic body formation stimulated by H₂O₂, Vero cells were stained with Hoechst 33342 and visualized by fluorescent microscopy. There were significantly apoptotic bodies formed in the cells treated with H₂O₂ (Fig. 41). The amount of apoptotic bodies formed in cells pretreated with different concentrations of HFCPSF4 significantly decreased in a dose-dependent manner.

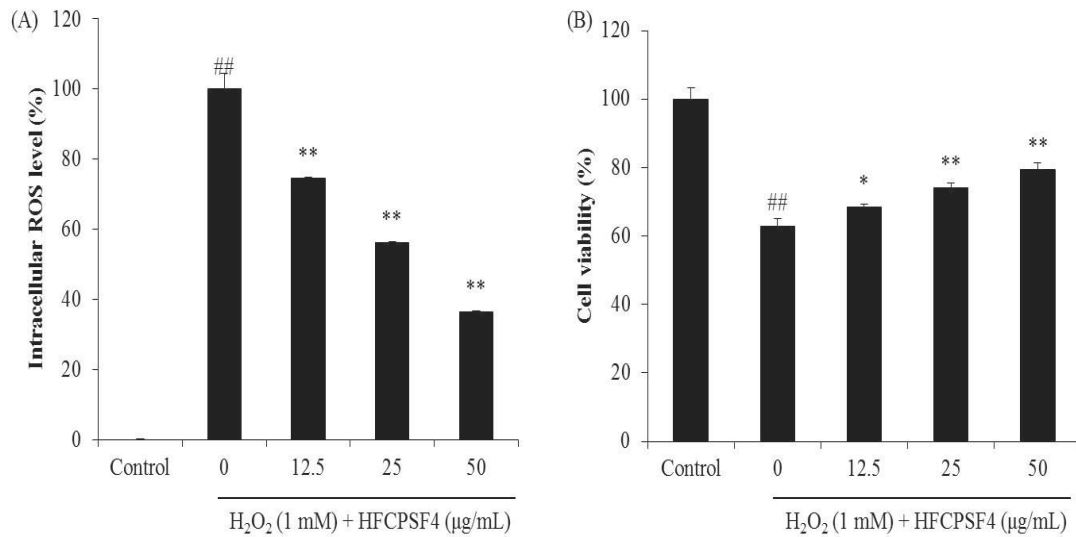


Fig. 40. The intracellular ROS scavenging effect of HFCPSF4 during H₂O₂-induced oxidative stress in Vero cells (A) and the protective effect of HFCPSF4 against H₂O₂-induced cell death in Vero cells (B). The experiments were conducted in triplicate, and the data are expressed as the mean \pm standard error (S.E). * $p < 0.05$, ** $p < 0.01$ as compared to the H₂O₂-treated group and ## $p < 0.01$ as compared to the control group.

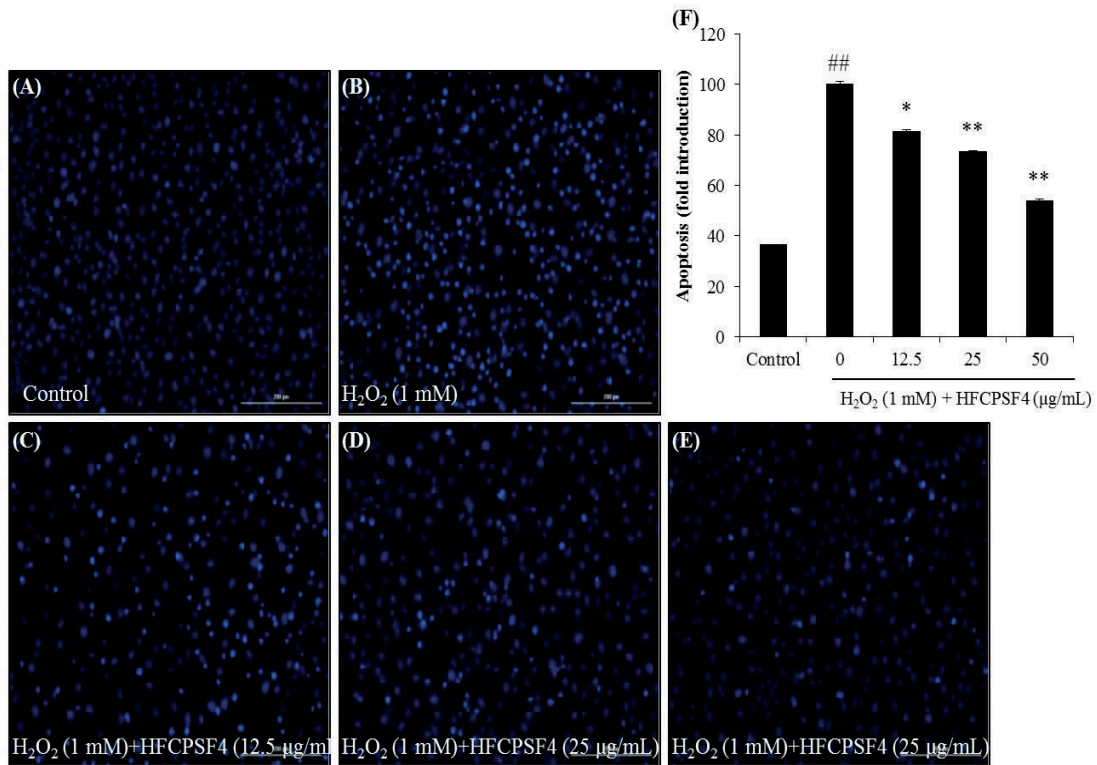


Fig. 41. The protective effect of HFCPSF4 against H₂O₂-induced apoptosis in Vero cells. (A) Nuclear morphology of non H₂O₂-treated cells. (B) Nuclear morphology of H₂O₂-treated cells. (C) Nuclear morphology of cells treated with 12.5 µg/mL of HFCPSF4 and H₂O₂. (D) Nuclear morphology of cells treated with 25 µg/mL of HFCPSF4 and H₂O₂. (E) Nuclear morphology of cells treated with 50 µg/mL of HFCPSF4 and H₂O₂. (F) Reactive apoptotic body formation. The apoptotic body formation was observed under a fluorescence microscope after Hoechst 33342 staining. Apoptosis levels were measured using Image J software. ** $p < 0.01$ as compared to the H₂O₂-treated group and ### $p < 0.01$ as compared to the control group.

2.3. HFCPSF4 improves the expression of catalase and SOD-1 via regulating Nrf2/HO-1 pathway in H₂O₂-induced Vero cells

Normally, Nrf2 located in the cytosol and bound to a control protein that Kelch-like ECH-associated protein 1 (Keap1). In the oxidative stress condition, Nrf2 is parted from Keap1, initiates translocation to the nucleus, and active the antioxidant genes to expression antioxidant enzymes such as catalase and SOD-1 [90, 91]. As Fig. 42 shows, H₂O₂ significant reduce catalase and SOD-1 levels. However, HFCPSF4 remarkably increase the catalase and SOD-1 levels in H₂O₂-stimulated Vero cells. Further results indicate that HFCPSF4 stimulated total Nrf2 and HO-1 levels in H₂O₂-stimulated Vero cells (Fig. 43). These results demonstrate that HFCPSF4 possesses the effect against oxidative stress induced by H₂O₂ through production of antioxidant enzymes including catalase and SOD-1 via regulating the Nrf2/HO-1 pathway (Fig. 44).

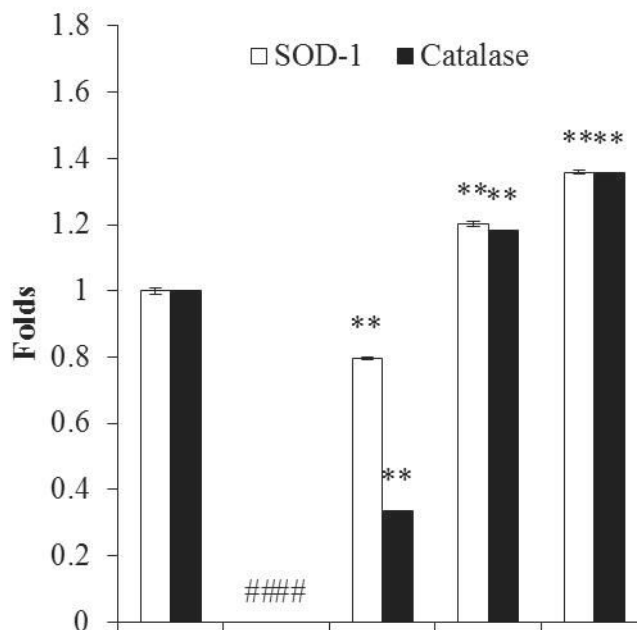
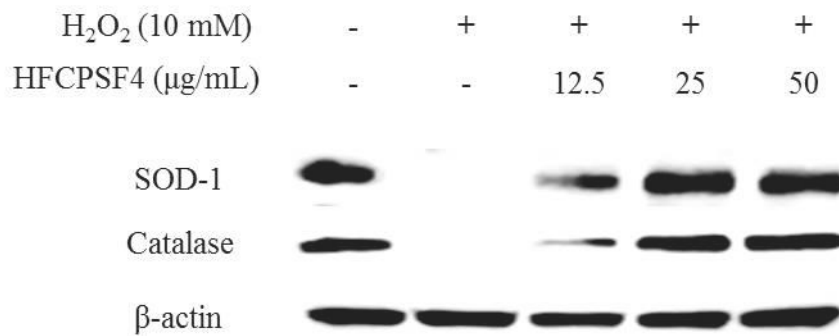


Fig. 42. HFCPSF4 increases the expression of catalase and SOD-1 in H₂O₂-stimulated Vero cells. The relative amounts of catalase and SOD-1 levels were compared with β-actin. The experiments were conducted in triplicate, and the data are expressed as the mean ± standard error (S.E). **p* < 0.05, ** *p* < 0.01 as compared to the H₂O₂-treated group and ^{##}*p* < 0.01 as compared to the control group.

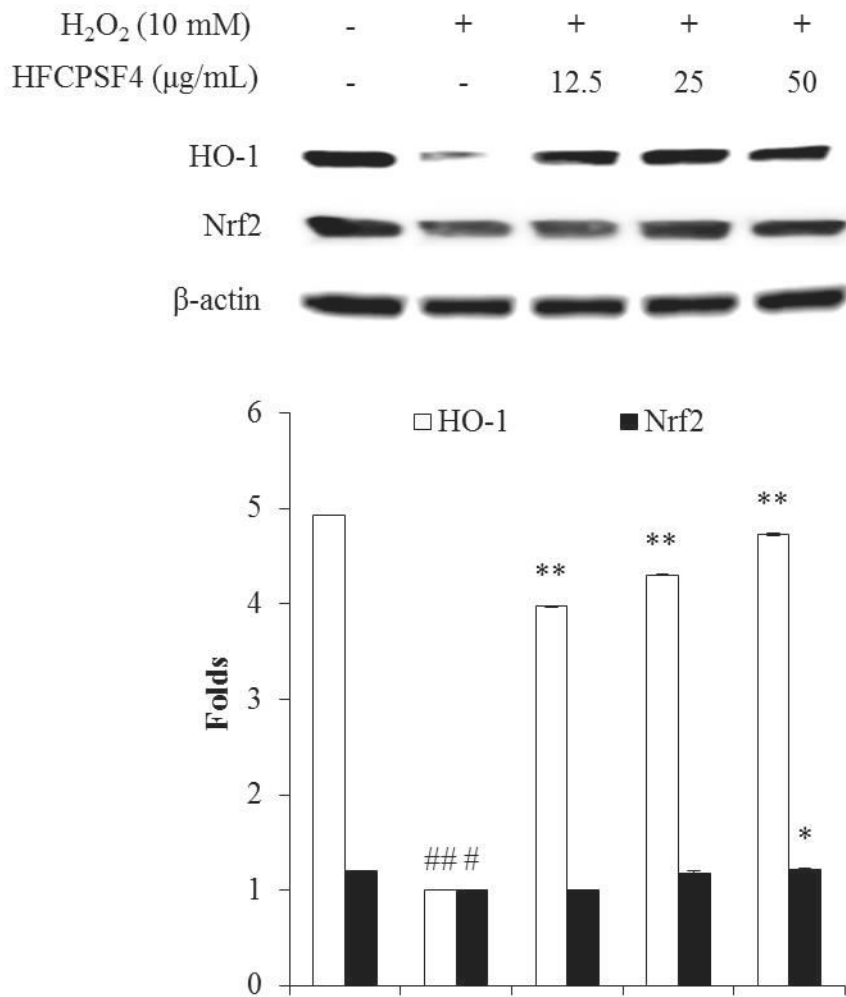


Fig. 43. HFCPSF4 regulates Nrf/HO-1 pathway in H₂O₂-stimulated Vero cells. The relative amounts of Nrf and HO-1 levels were compared with β-actin. The experiments were conducted in triplicate, and the data are expressed as the mean ± standard error (S.E). **p* < 0.05, ** *p* < 0.01 as compared to the H₂O₂-treated group and ^{###}*p* < 0.01 as compared to the control group.

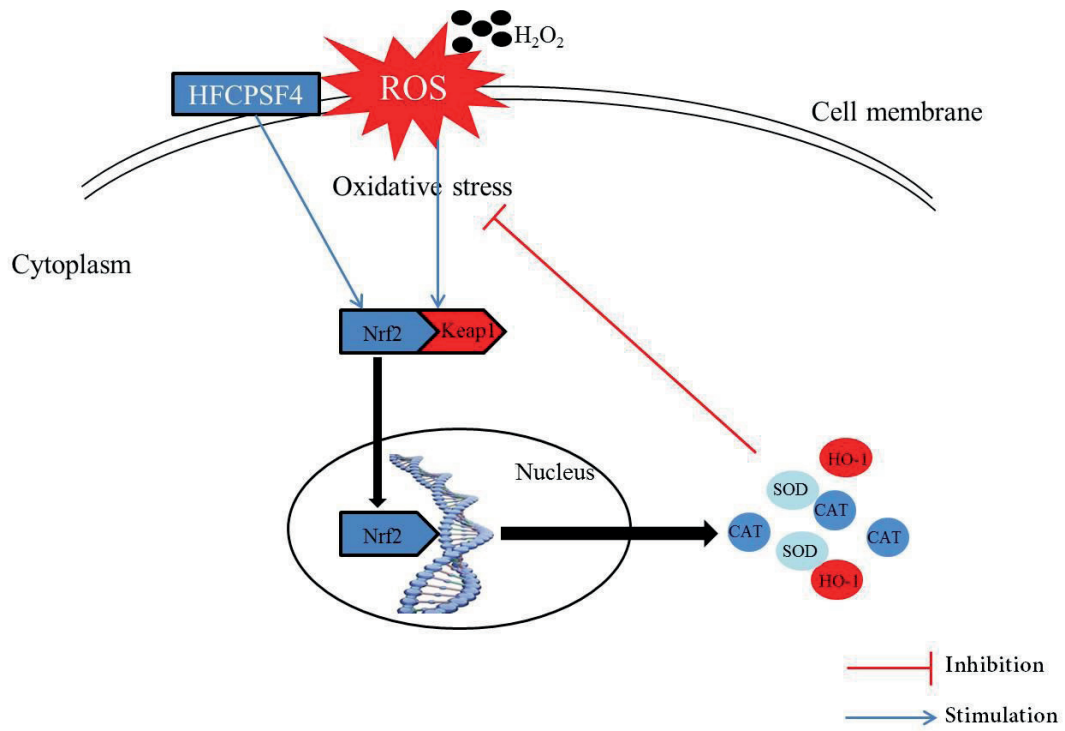


Fig. 44. A schematic model of antioxidant activity of HFCPSF4 in Vero cells.

2.4. HFCPSF4 improves survival rate and reduces heart-beating rate in H₂O₂-induced zebrafish

The survival rates and heart-beating rates of H₂O₂-treated zebrafish were measured. The survival rate and heart-beating rate of zebrafish that did not treat with H₂O₂ were considered to be 100% (Fig. 45). The survival rate of zebrafish treated with H₂O₂ was significantly decreased (Fig. 45A). However, the survival rates of HFCPSF4-treated zebrafish were significantly increased. The heart-beating rate of the zebrafish treated with H₂O₂ was 121.81% (Fig. 45B), but significantly decreased with HFCPSF4 treatment.

2.5. Protective effect of HFCPSF4 against H₂O₂-induced ROS generation, cell death, and lipid peroxidation in zebrafish

The effect of HFCPSF4 on ROS generation in H₂O₂-treated zebrafish was measured by detection of DCF-DA. As Fig. 46 shows, HFCPSF4 significantly decreased ROS levels in a dose-dependent manner. In addition, HFCPSF4 effective against H₂O₂-induced cell death and lipid peroxidation in zebrafish (Fig. 47 and Fig. 48).

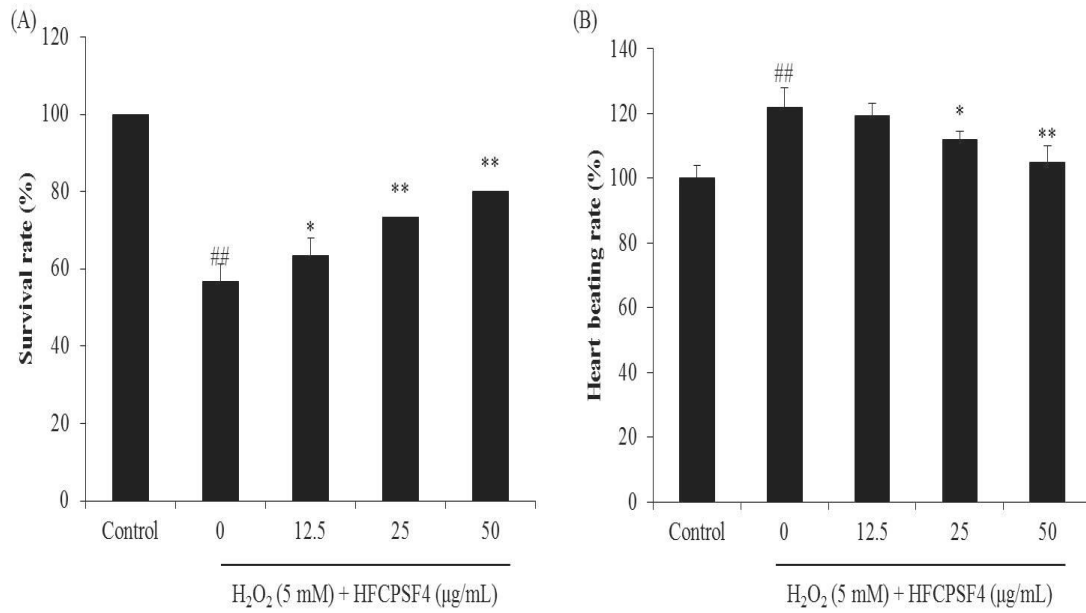


Fig. 45. The survival rate and heart-beating rate of zebrafish after pretreatment with HFCPSF4 and/or treatment with H₂O₂. (A) Survival rate; (B) heart-beating rate. The experiments were conducted in triplicate, and the data are expressed as the mean ± standard error (S.E). * $p < 0.05$, ** $p < 0.01$ as compared to the H₂O₂-treated group and ^{##} $p < 0.01$ as compared to the control group.

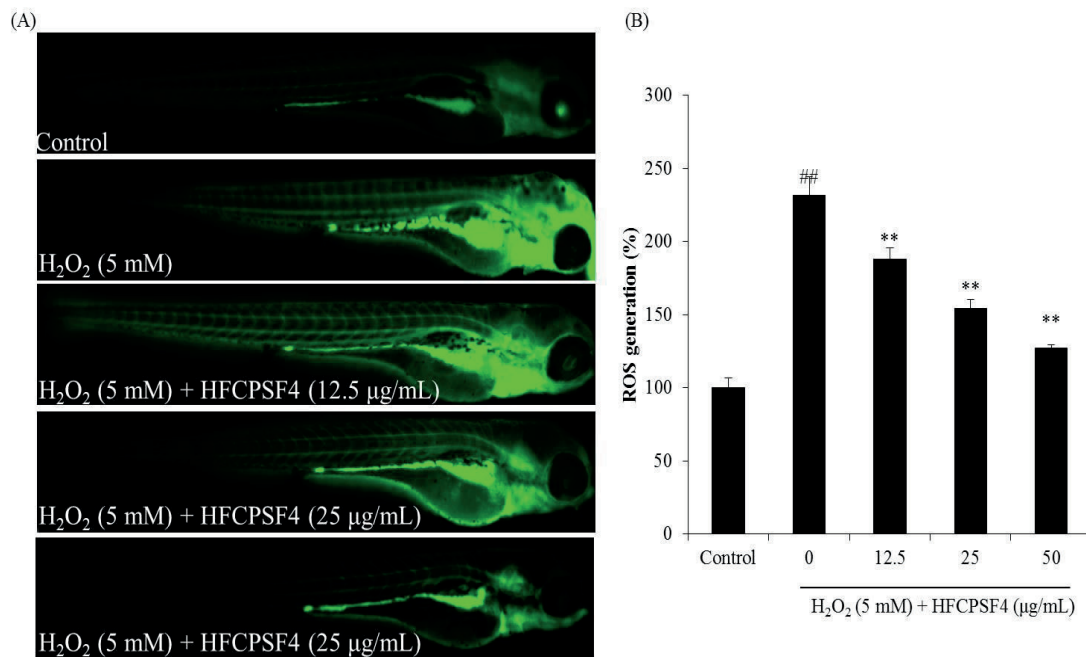


Fig. 46. The protective effect of HFCPSF4 against H₂O₂-induced ROS production in zebrafish embryos. (A) Zebrafish under fluorescence microscope; (B) the levels of ROS generation. ROS levels were measured using Image J software. The experiments were conducted in triplicate, and the data are expressed as the mean \pm standard error (S.E). * $p < 0.05$, ** $p < 0.01$ as compared to the H₂O₂-treated group and ## $p < 0.01$ as compared to the control group.

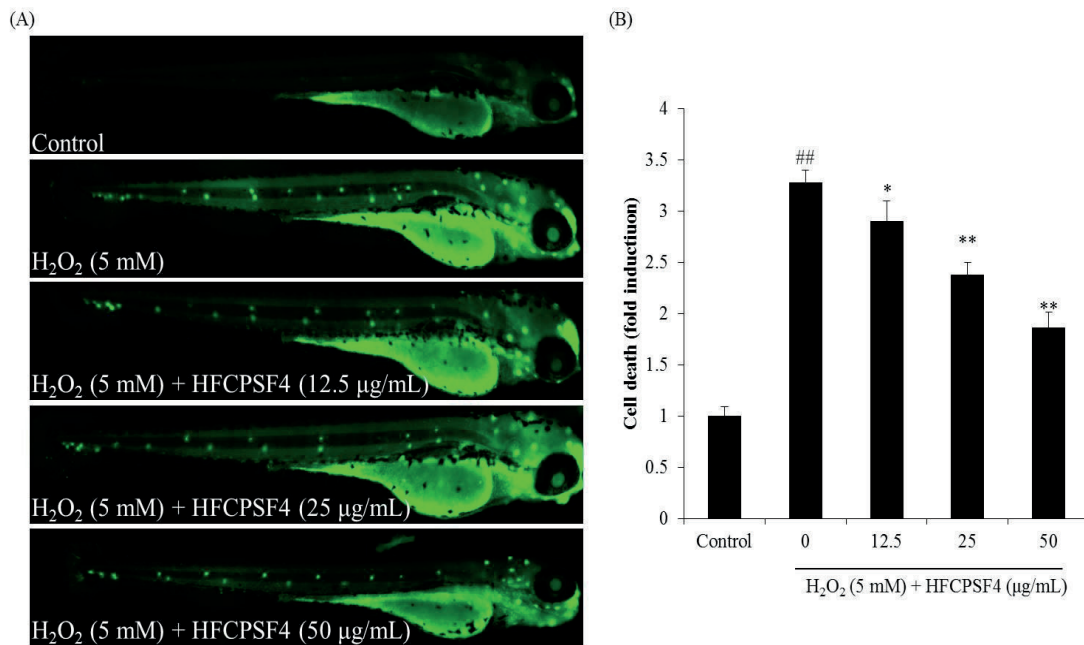


Fig. 47. The protective effect of HFCPSF4 against H₂O₂-induced cell death in zebrafish. (A) Zebrafish under fluorescence microscope; (B) the measured levels of cell death. Cell death levels were measured using Image J software. The experiments were conducted in triplicate, and the data are expressed as the mean \pm standard error (S.E). * $p < 0.05$, ** $p < 0.01$ as compared to the H₂O₂-treated group and ### $p < 0.01$ as compared to the control group.

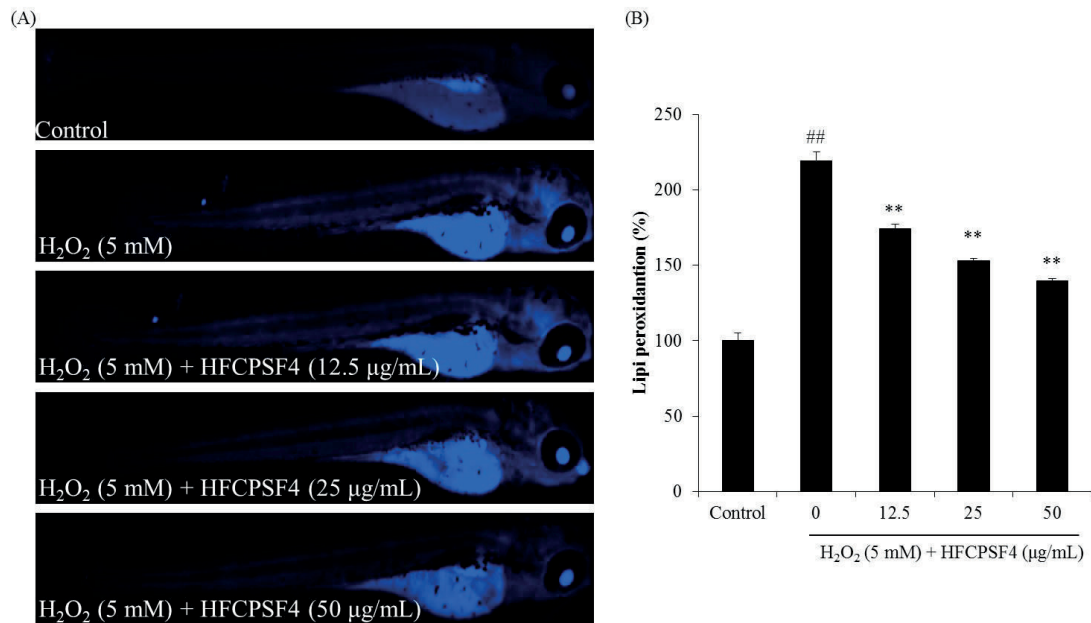


Fig. 48. The protective effect of HFCPSF4 against H₂O₂-induced lipid peroxidation in zebrafish. (A) Zebrafish under fluorescence microscope; (B) the measured levels of cell death. Cell death levels were measured using Image J software. The experiments were conducted in triplicate, and the data are expressed as the mean \pm standard error (S.E). * $p < 0.05$, ** $p < 0.01$ as compared to the H₂O₂-treated group and ^{##} $p < 0.01$ as compared to the control group.

3. Conclusion

In a conclusion, HFCPSF4 possesses strong *in vitro* and *in vivo* antioxidant activities demonstrate in reducing intracellular ROS and improving cell viability in H₂O₂-stimulated Vero cells as well as in improving the survival rate, decreasing heart-beating rate, and reducing ROS generation and cell death in H₂O₂-stimulated zebrafish. These results suggest that HFCPSF4 may consider for use in the medical and cosmetic industries.

Section 3: Anti-inflammatory effect of *Hizikia* fucoïdan *in vitro* in RAW 264.7 macrophages and *in vivo* in zebrafish

Abstract

In the present study, the anti-inflammatory effect of *Hizikia* fucoïdan (HFCPSF4) isolated from HFCPS was investigated in LPS-stimulated RAW 264.7 macrophages and zebrafish. The results indicate that HFCPSF4 significantly inhibits NO generation stimulated by LPS in RAW 264.7 cells. In addition, HFCPSF4 dose-dependently improves the cell viability in LPS-stimulated RAW 264.7 cells. Moreover, HFCPSF4 significantly decreases the expression of tumor necrosis factor alpha (TNF- α), prostaglandin E₂ (PGE₂), interleukin-1 beta (IL-1 β), and interleukin-6 (IL-6). Furthermore, HFCPS suppresses the expression of inducible nitric oxide synthase (iNOS) and cyclooxygenase-2 (COX-2) by regulating the nuclear factor kappa-B (NF- κ B) pathway. The *in vivo* test results suggest HFCPSF4 significantly reduced ROS, cell death, and NO levels in LPS-stimulated zebrafish. These results demonstrate that HFCPSF4 possesses strong *in vitro* and *in vivo* anti-inflammatory activities and could potentially use as an ingredient to developing anti-inflammatory agent or cosmetic.

1. Materials and methods

1.1. Reagents and Chemicals

DMEM, FBS, penicillin–streptomycin, and trypsin-EDTA were purchased from Gibco-BRL (Grand Island, NY, USA). The LPS and DMSO were purchased from purchased from Sigma (St. Louis, MO, USA). The ELISA kits used for the analysis of TNF- α , PGE₂, IL-1 β , and IL-6 levels were purchased from R&D Systems Inc. (Minneapolis, MN, USA). Protein assay kit (BCA™ kit) was purchased from Bio-Rad (Richmond, CA, USA). COX-2, iNOS, I κ B α , p-I κ B α , p50 NF- κ B, p65 NF- κ B nucleolin, β -actin, and anti-rabbit antibody antibodies were purchased from Thermo Scientific (Waltham, MA, USA). All other chemicals used in this study were of analytical grade.

1.2. Cell culture

RAW 264.7 macrophages were purchased from ATCC (TIB-71™). RAW 264.7 cells were grown in DMEM supplemented with 10% FBS, penicillin (100 unit/mL) and streptomycin (100 μ g/mL). Cells were maintained at 37°C in an incubator containing 5% CO₂ and seeded at a concentration of 1×10^5 cells/mL for the experiment.

1.3. Measurement of NO production and cell viability

The experiments were performed following the methods described by Heo et al. [62]. RAW 264.7 cells were seeded in 24-well plates for 24 h. HFCPSF4 were added into each well, achieving final concentrations of 12.5, 25, and 50 μ g/mL. After 1 h, LPS (1 μ g/mL) was introduced into all wells, except control. After 24 h, the NO production was measured by Griess assay and cell viability was measured by MTT assay according to the protocol described in the previous study [50, 58, 92].

1.4. Measurement of PGE₂ and pro-inflammatory cytokine (TNF- α , IL-1 β , and IL-6) production

RAW 264.7 cells were pre-treated with HFCPSF4 and eventually exposed to LPS for 24 h. Then, the culture media was collected and used for measuring the respective cytokine and PGE₂ expression levels. These experiments were performed using commercial enzyme immunoassay kits following the manufacturer's instructions.

1.5. Western blot analysis

RAW 264.7 cells were seeded in 6-well plates. After 24 h, cells were treated with HFCPSF4 and exposed to LPS (1 μ g/mL) 1 h later. Following a second incubation period of 1 h (for NF- κ B analysis) or 24 h (for COX-2 and iNOS analysis), the cells were harvested and the proteins were extracted with the PROPREP protein extraction kit (iNtRON Biotechnology, Sungnam, Korea). The protein concentration of each lysate was determined using a BCATM kit. Each 50 μ g of protein were separated on a 12% SDS-polyacrylamide gel, and the protein bands were transferred onto a polyvinylidene fluoride membrane. The membranes were blocked with blocking buffer (5% blotting-grade blocker), and the membrane was then incubated with specific primary antibodies overnight, at 4°C. After incubation, the membranes were washed with TBS-T buffer (3 mM KCl, 25 mM Tris, 150 mM NaCl, and 0.2% Tween 20) and incubated with secondary antibodies at room temperature for 3 h. Finally, the signals were developed by an ECL western blotting detection kit, and exposed on X-ray films.

1.6. Application of HFCPSF4 and LPS to zebrafish embryos

Approximately 3~4 hours post-fertilization (hpf), the embryos were transferred to individual wells in a 12-well plate (15 embryos per group) and maintained in embryo

medium containing HFCPSF4 (12.5, 25, and 50 $\mu\text{g}/\text{mL}$). After 1 hour incubation, 10 $\mu\text{g}/\text{mL}$ LPS was added to the medium, and the embryos were incubated until 24 hpf. The survival rate was measured at 3 days post-fertilization (dpf) after treatment with LPS by counting live embryos, and the surviving fish were then used for further analysis.

1.7. Determination of heart-beating rate, ROS generation, cell death, and NO generation in zebrafish

The zebrafish heart-beating rate was measured according to Sanjeeva et al. [87]. The zebrafish heart-beating rate in both the atrium and ventricle was recorded for 1 min at 2 dpf under a microscope. Intracellular ROS level, cell death, and NO generation were measured in live embryos using DCFH-DA, acridine orange, and DAF-FM-DA staining, respectively, followed the previous procedure [21, 93, 94]. The zebrafish were observed and photographed under a fluorescence microscope equipped with a Cool SNAP-Pro color digital camera (Olympus, Japan). The fluorescence intensity of individual zebrafish larva was quantified using the image J program.

1.8. Statistical analysis

All experiments were conducted in triplicate. The data are expressed as the mean \pm standard error (S.E), and one-way ANOVA was used to compare the mean values of each treatment in SPSS 12.0. Significant differences between the means were identified by the Turkey test. Significance was established if $*p < 0.05$, $**p < 0.01$ as compared to the LPS-treated group, and $^{##}p < 0.01$ as compared to control group.

2. Results and Discussion

2.1. The effect of HFCPSF4 on LPS-induced NO generation and cytotoxicity in RAW 264.7 macrophages

The effect of HFCPSF4 on NO generation and cytotoxicity were measured in LPS-induced RAW 264.7 macrophages. As Fig. 49 shows, HFCPSF4 significant inhibits NO generation in LPS-induced RAW 264.7 cells. In addition, HFCPSF4 remarkable improves cell viability. Both effects were dose-dependent.

2.2. HFCPSF4 decreased PGE₂ and pro-inflammatory cytokines release in LPS-induced RAW 264.7 macrophages

As Fig. 50 shows, LPS significant increase in the production of TNF- α , IL-1 β , IL-6, and PGE₂ compared with the control. However, the TNF- α , IL-1 β , IL-6, and PGE₂ levels in HFCPSF4 treated RAW 264.7 cells were significantly decreasing, which was dose-dependent with increasing sample concentrations.

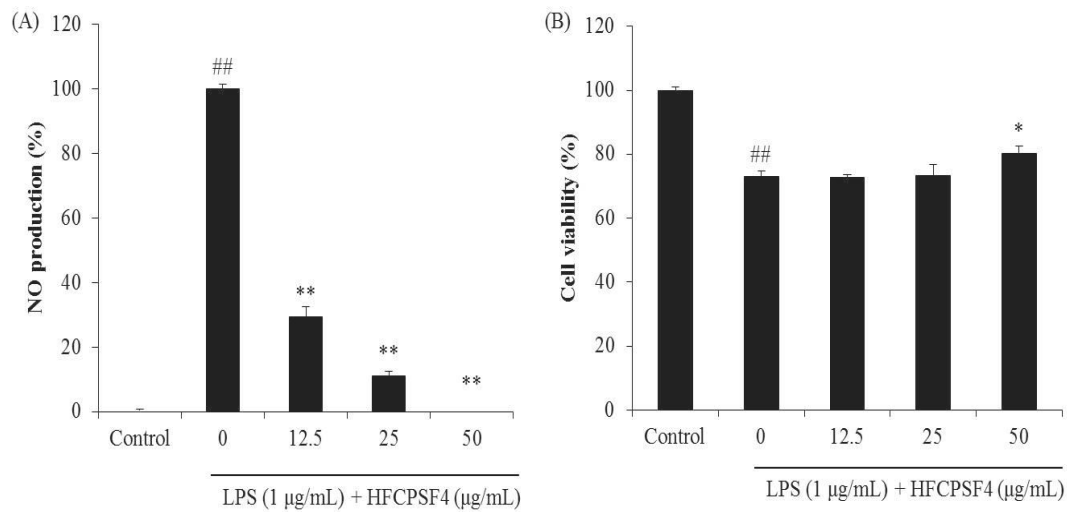


Fig. 49. The effect of HFCPSF4 on LPS-induced NO generation and cytotoxicity in RAW 264.7 macrophages. (A) NO production in LPS-induced RAW 264.7 macrophages and (B) cell viability in LPS-induced RAW 264.7 macrophages. The experiments were conducted in triplicate, and the data are expressed as the mean \pm standard error (S.E). * $p < 0.05$, ** $p < 0.01$ as compared to the LPS-treated group and ## $p < 0.01$ as compared to the control group.

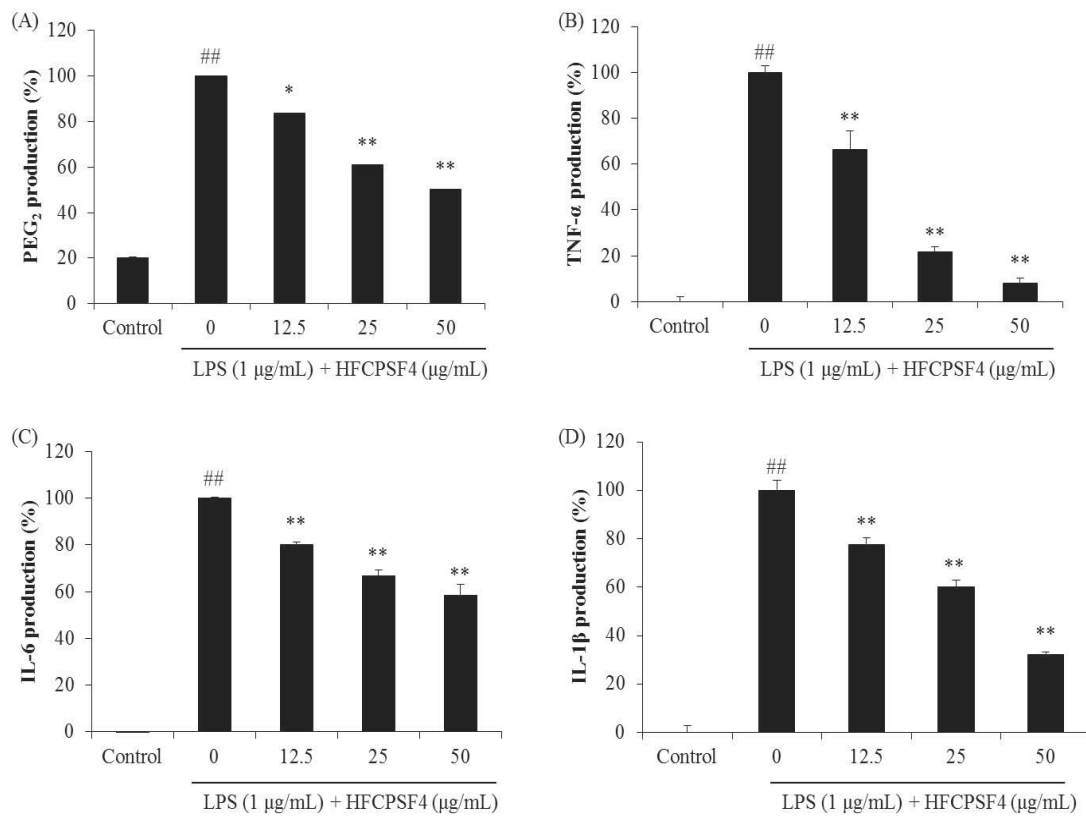


Fig. 50. The effect of HFCPSF4 on the production of PGE₂, TNF-α, IL-1β, and IL-6 in LPS-stimulated RAW 264.7 macrophages. (A) The production of PGE₂; (B) the production of TNF-α; (C) the production of IL-1β; (D) the production of IL-6. The levels of PGE₂, TNF-α, IL-1β, and IL-6 expression were examined using ELISA kit. The experiments were conducted in triplicate, and the data are expressed as the mean ± standard error (S.E). * $p < 0.05$, ** $p < 0.01$ as compared to the LPS-treated group and ## $p < 0.01$ as compared to the control group.

2.3. HFCPSF4 inhibited the expression of iNOS and COX-2 in LPS-induced RAW 264.7 macrophages

The expression levels of iNOS and COX-2 are shown in Fig. 51. According to the results, the expression levels of iNOS and COX-2 were significantly increased in the cells treated with LPS only. However, HFCPSF4 effectively suppressed iNOS and COX-2 expression in a dose-dependent manner.

2.4. HFCPSF4 inhibited NF- κ B in LPS-induced RAW 264.7 macrophages

The cytosol and nuclear NF- κ B levels of LPS-induced RAW 264.7 are shown in Fig. 52. According to the results, LPS significantly active NF- κ B, however, HFCPSF4 effectively suppressed NF- κ B activation in a dose-dependent manner. These results suggest that HFCPSF4 suppresses LPS-induced inflammatory in RAW 264.7 cells by inhibiting the expression of pro-inflammatory cytokines and inflammatory proteins via regulating NF- κ B pathway.

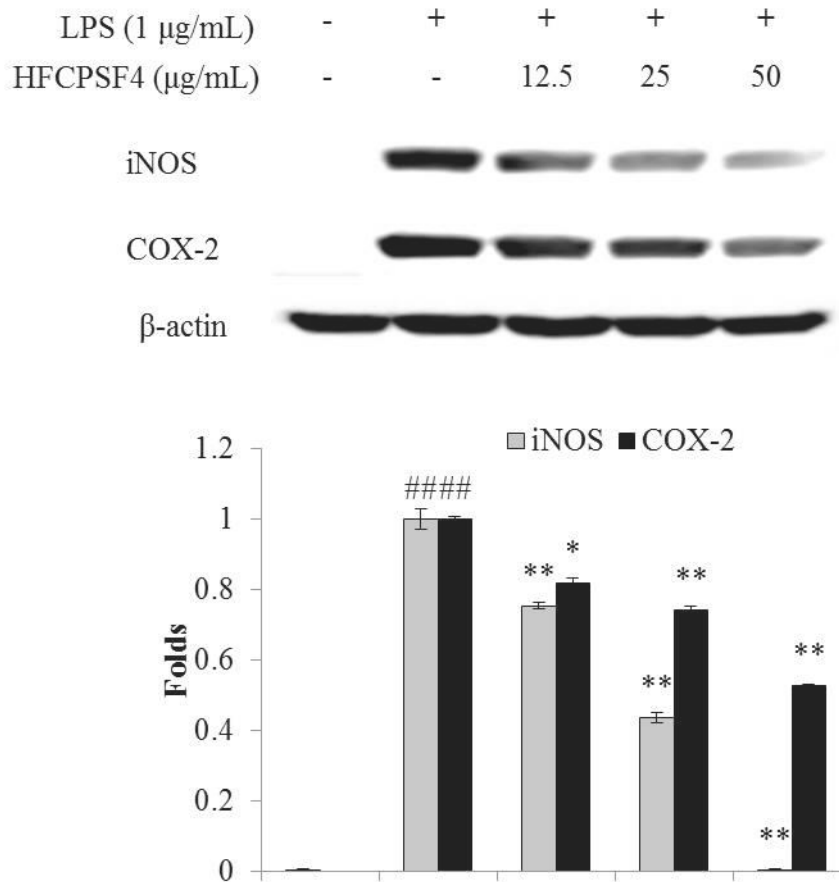


Fig. 51. The effect of HFCPSF4 on the expression of iNOS and COX-2 in RAW 264.7 macrophages stimulated with LPS. (A) The inhibitory effect of HFCPSF4 on iNOS and COX-2 expression; (B) the relative amount of iNOS and COX-2. The relative amounts of iNOS and COX-2 were compared with β -actin. The experiments were conducted in triplicate, and the data are expressed as the mean \pm standard error (S.E). * $p < 0.05$, ** $p < 0.01$ as compared to the LPS-treated group and $^{##}p < 0.01$ as compared to the control group.

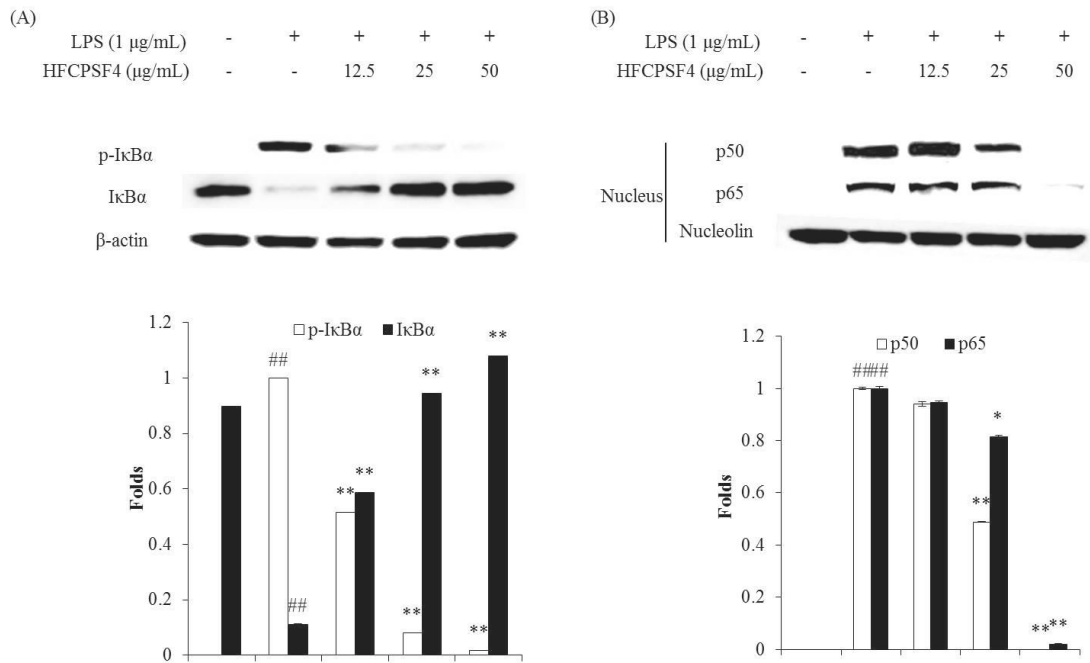


Fig. 52. The effect of HFCPSF4 on NF-κB activation in RAW 264.7 macrophages stimulated with LPS. (A) The cytosol IκBα and p-IκBα level; (B) the nuclear p50 and p65 NF-κB level. The relative amounts of IκBα and p-IκBα levels were compared with β-actin, and the relative amounts of p50 and p65 NF-κB levels were compared with nucleolin. The experiments were conducted in triplicate, and the data are expressed as the mean ± standard error (S.E). * $p < 0.05$, ** $p < 0.01$ as compared to the LPS-treated group and ^{##} $p < 0.01$ as compared to the control group.

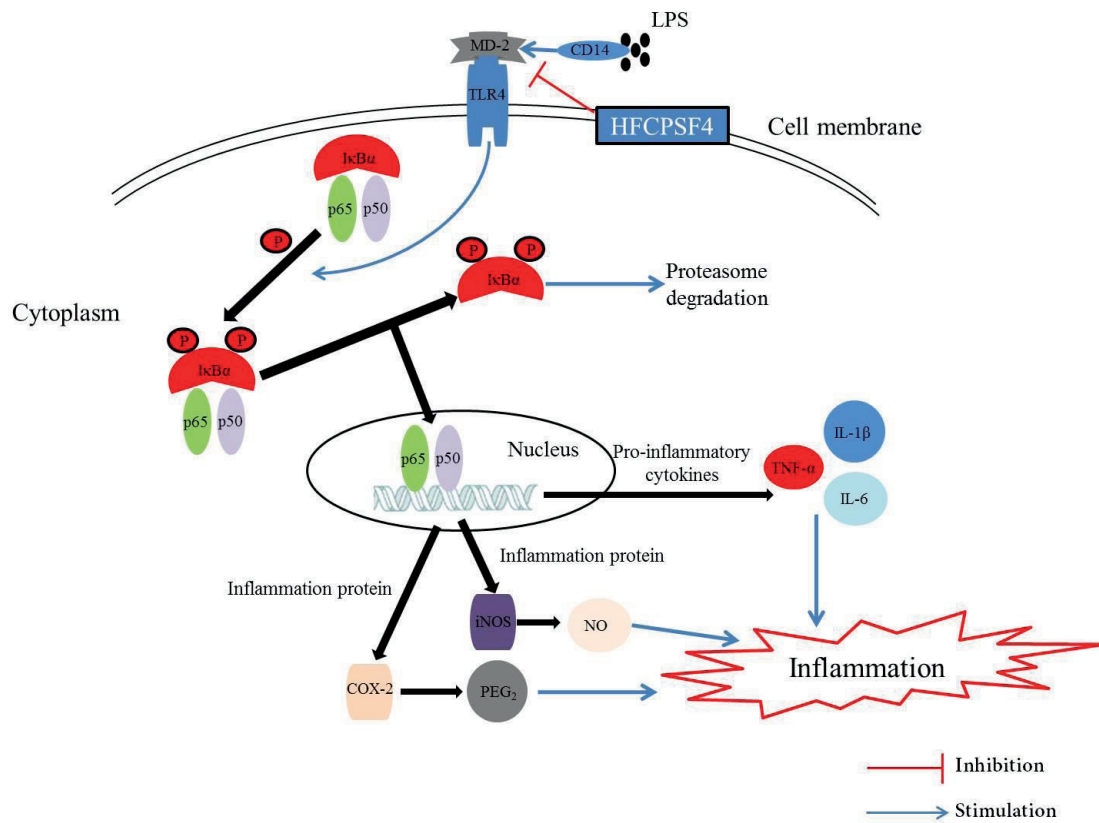


Fig. 53. A schematic model of anti-inflammation activity of HFCPSF4 in RAW 264.7 cells.

2.5. HFCPSF4 improved survival rate and reduced heart-beating rate in LPS-induced zebrafish

The survival rates and heart-beating rates of zebrafish were determined. The survival rate and heart-beating rate of zebrafish that did not receive LPS treatment were considered to be 100% (Fig. 54). The survival rate of LPS-treated zebrafish was significantly decreased (Fig. 54A). However, the survival rates of zebrafish pretreated with HFCPSF4 prior to LPS treatment significantly increased. The heart-beating rate of the zebrafish treated with LPS was significantly increased compared to control, but significantly decreased with HFCPSF4 treatment.

2.6. Protective effect of HFCPSF4 against LPS-induced ROS generation, cell death, and NO production in zebrafish

The effect of HFCPSF4 on ROS generation, cell death, and NO production in LPS-treated zebrafish was measured. As Fig. 55 shows, HFCPSF4 significantly decreased ROS levels in a dose-dependent manner. In addition, HFCPSF4 effectively against LPS-induced cell death and NO production in zebrafish (Fig. 56 and Fig. 57).

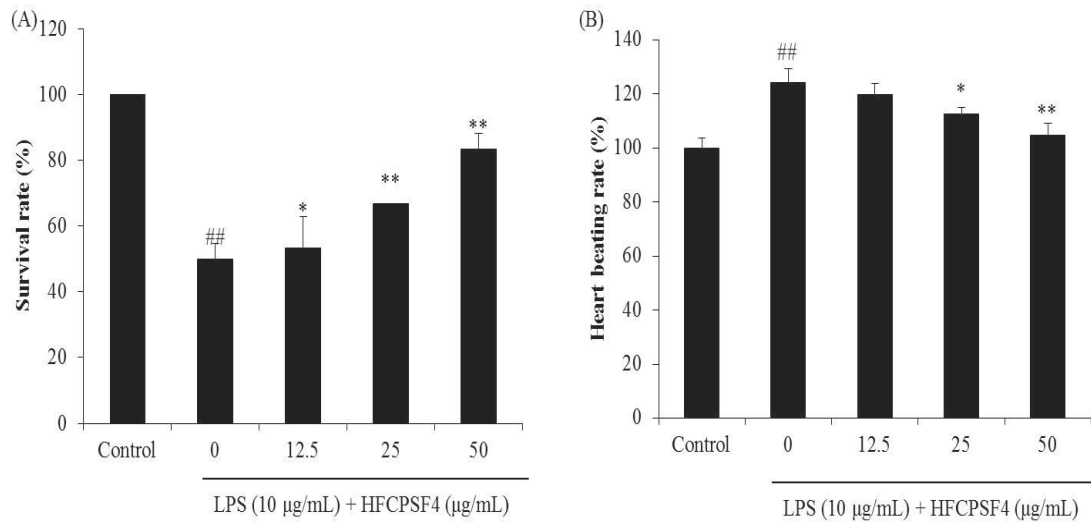


Fig. 54. The survival rate and heart-beating rate of zebrafish after treatment with HFCPSF4 and/or treatment with LPS. (A) Survival rate; (B) heart-beating rate. The experiments were conducted in triplicate, and the data are expressed as the mean \pm standard error (S.E). * $p < 0.05$, ** $p < 0.01$ as compared to the LPS-treated group and ^{##} $p < 0.01$ as compared to the control group.

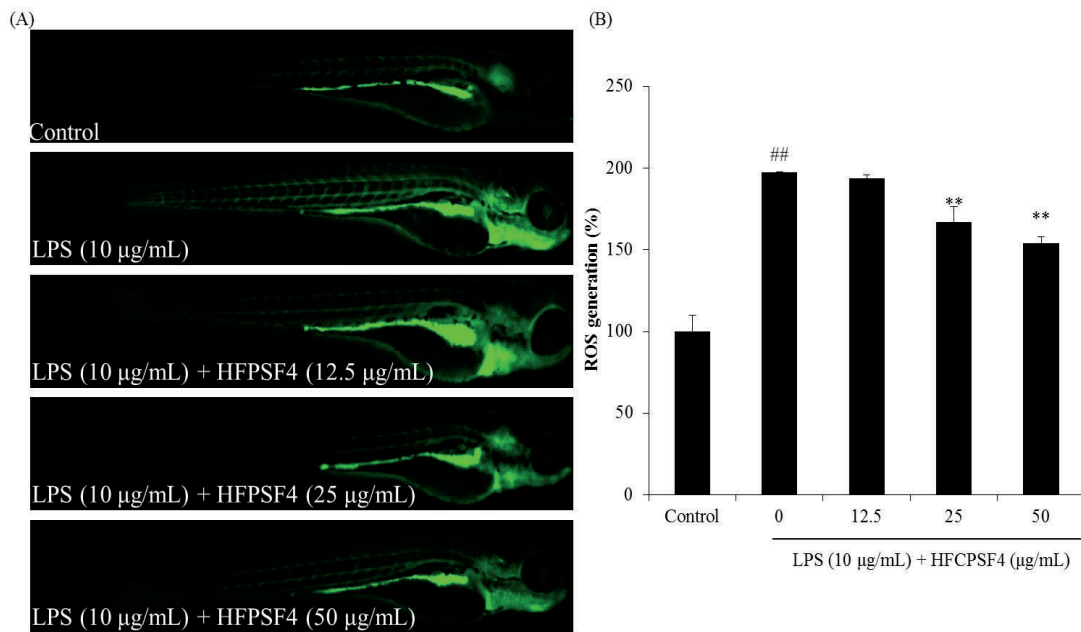


Fig. 55. The protective effect of HFCPSF4 against LPS-induced ROS production in zebrafish. (A) Zebrafish under fluorescence microscope; (B) the measured levels of ROS. ROS levels were measured using Image J software. The experiments were conducted in triplicate, and the data are expressed as the mean \pm standard error (S.E). * $p < 0.05$, ** $p < 0.01$ as compared to the LPS-treated group and $^{##}p < 0.01$ as compared to the control group.

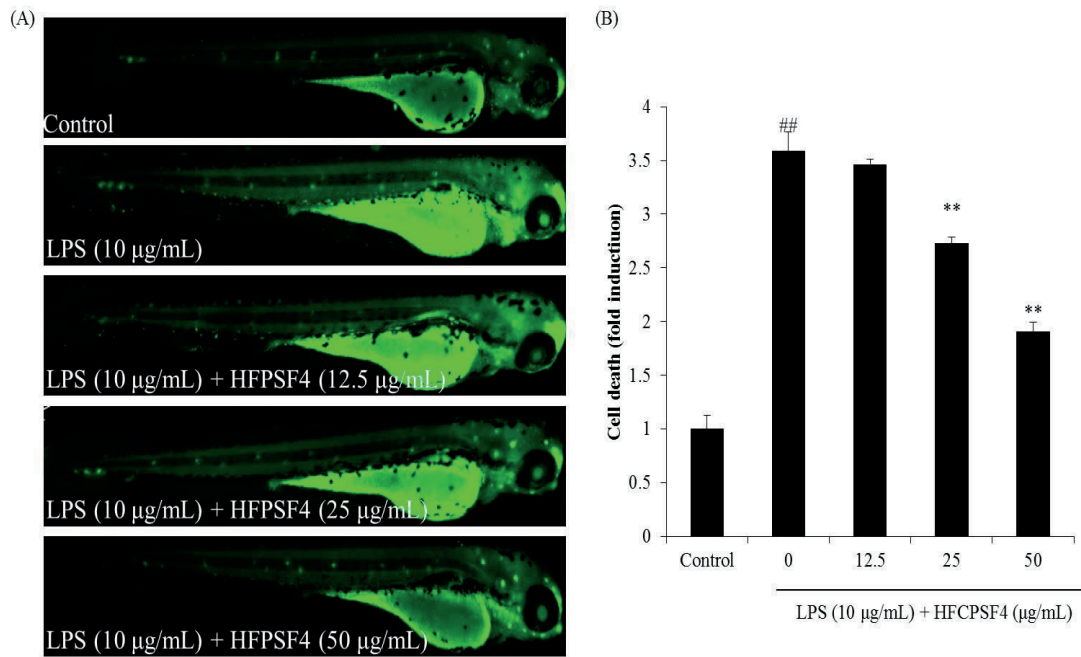


Fig. 56. The protective effect of HFCPSF4 against LPS-induced cell death in zebrafish. (A) Zebrafish under fluorescence microscope; (B) the measured levels of cell death. Cell death levels were measured using Image J software. The experiments were conducted in triplicate, and the data are expressed as the mean \pm standard error (S.E). * $p < 0.05$, ** $p < 0.01$ as compared to the LPS-treated group and ### $p < 0.01$ as compared to the control group.

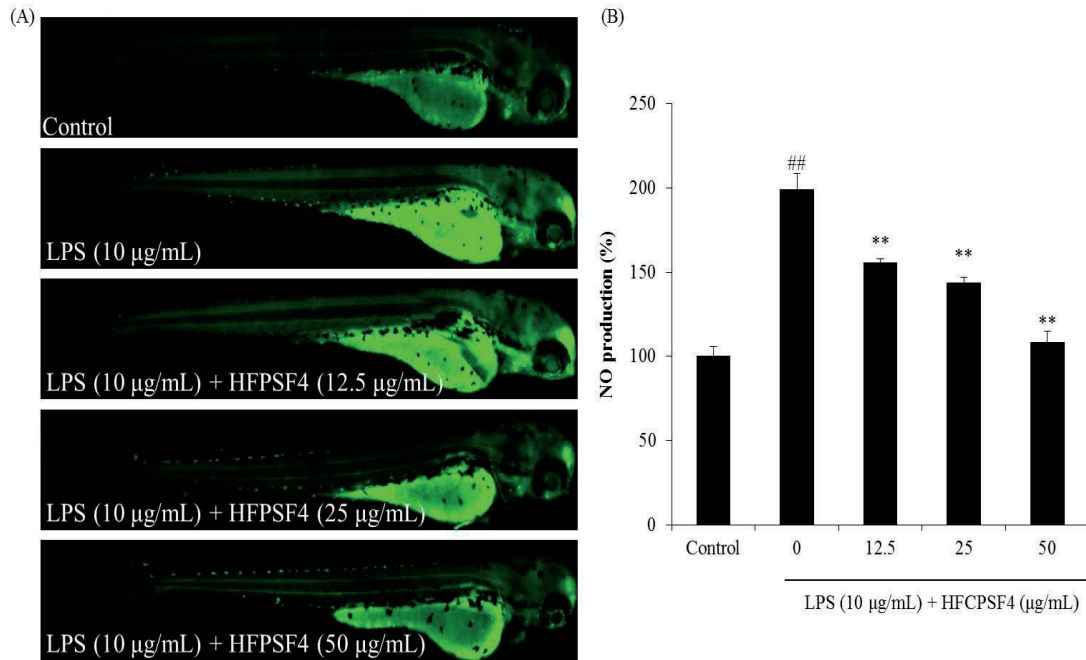


Fig. 57. The effect of HFCPSF4 on LPS-induced NO production in zebrafish. (A) Zebrafish under fluorescence microscope; (B) the measured levels of cell death. NO production levels were measured using Image J software. The experiments were conducted in triplicate, and the data are expressed as the mean \pm standard error (S.E). * $p < 0.05$, ** $p < 0.01$ as compared to the LPS-treated group and $^{##}p < 0.01$ as compared to the control group.

3. Conclusion

In this study, we investigated anti-inflammatory activity of HFCPSF4 *in vitro* in RAW 264.7 cells and *in vivo* in zebrafish. The results indicate that HFCPSF4 possesses strong *in vitro* and *in vivo* anti-inflammatory activities and could use for developing novel anti-inflammatory drugs or ingredients in cosmetic products.

**Section 4: Whitening effect *Hizikia* fucoidan isolated from HFCPS *in vitro* in
B16F10 melanoma cells**

Abstract

In the present study, the whitening effect of *Hizikia* fucoidan (HFCPSF4) was investigated. The whitening effect was evaluated in alpha-melanocyte stimulating hormone (α -MSH)-stimulated B16F10 melanoma cells. The result shows that HFCPSF4 inhibited melanin synthesis through down-regulation tyrosinase, TRP-1, and TRP-2, and MITF expressions by regulating the ERK-MAPK pathway in B16F10 cells. These results demonstrate that HFCPSF4 possesses whitening effect and may use as a melanogenesis inhibitor to develop a cosmetic in the cosmetic industry.

1. Materials and methods

1.1. Reagents and Chemicals

MTT, DMSO, and alpha-melanocyte stimulating hormone (α -MSH) were purchased from Sigma Co. (St. Louis, MO, USA). The DMEM, FBS, and penicillin/streptomycin were purchased from Gibco BRL (Life Technologies, Burlington, ON, Canada). Antibodies against microphthalmia-associated transcription factor (MITF), tyrosinase, tyrosinase-related protein-1 and -2 (TRP-1 and 2), and ERK-MAPK were purchased from Thermo Scientific (Waltham, MA, USA). Anti-mouse and anti-rabbit IgG antibodies were purchased from Cell Signaling Technology (Beverly, MA, USA). All other chemicals used in this study were of analytical grade.

1.2. Cell culture

B16F10 mouse melanoma cells (ATCC[®] CRL-6475[™]) were purchased from ATCC (American Type Culture Collection, Manassas, VA, USA). The cells were grown in DMEM supplemented with 10% heat-inactivated FBS, 100 μ g/mL of streptomycin, and 100 U/mL of penicillin. The cells were sub-cultured every 4 days and seeded at a concentration of 5×10^4 cells/mL for experiments.

1.3. Cytotoxicity assay

Cytotoxicity of HFCPSF4 on B16F10 cells was performed by MTT assay [95]. Cells were seeded in a 96-well plated and incubated for 24 h. Cells were treated with different concentrations of HFCPSF4 and incubated for 72 h. A volume of 50 μ L MTT stock solution (2 mg/mL) was added to each well. After 3 h incubation, the supernatant was aspirated and 150 μ L of DMSO was added to each well. Finally, the resulting formazan crystals of MTT were dissolved in DMSO and the absorbance was measured at 540 nm using a microplate reader.

1.4. Determination of cellular melanin contents

In order to measure the cellular melanin contents of α -MSH stimulated B16F10 cells. B16F10 cells were seeded in a 6-well plate and incubated for 24 h. Then, cells were treated with various concentrations of HFCPSF4 and stimulated with α -MSH (50 nM). After 72 h incubation, the cells were harvested. The harvested cells were incubated in 1 mL of 1N NaOH containing 10% DMSO at 80°C for 1 h. After incubation, the solution was centrifuged at 13,000g for 10 min and the absorbance of the supernatant was measured at 490 nm using a microplate reader.

1.5. Western blot analysis

The effect of HFCPSF4 on the levels of melanogenesis-related proteins including MITF, tyrosinase, TRP-1, TRP-2, ERK, and p-ERK was assessed by Western blot assay performed according to the procedure as described by Kim et al. [66]. In brief, B16F10 treated with HFCPSF4 and stimulated with α -MSH (50 nM). After 72 h incubation, cells were harvested and lysed. The protein level of each sample was measured by a BCATM kit. The proteins (30 μ g) were separated on 12% SDS-PAGE and transferred onto nitrocellulose transfer membranes. The membranes were blocked with blocking buffer (5% skim milk) and incubated with primary antibodies for 16 h at 4°C. Then, the membranes were further incubated with secondary antibody at room temperature for 3 h. Finally, the protein bands were visualized using an ECL western blotting detection kit and exposed on X-ray films.

1.6. Statistical analysis

All experiments were performed in triplicate. The data are expressed as the mean \pm standard error (S.E), and one-way ANOVA was used to compare the mean values of each treatment in SPSS 12.0. Significant differences between the means were

identified by the Turkey test. The p -value ($p < 0.05$) was considered to be statistically significant. A value of $*p < 0.05$, $**p < 0.01$, and $##p < 0.01$ were considered as significantly different.

2. Results and Discussion

2.1. Cytotoxicity of HFCPSF4

Cytotoxicity of HFCPSF4 on B16F10 cells was examined by MTT assay, and the results were summarized in Fig. 58A. As the result shows, HFCPSF4 shows significant cytotoxicity on B16F10 cells at the 100 $\mu\text{g}/\text{mL}$. Therefore, the concentration of HFCPSF4 on B16F10 cells for further study was determined not beyond 50 $\mu\text{g}/\text{mL}$.

2.2. Effect of HFCPSF4 on melanin synthesis in α -MSH-stimulated B16F10 cells

The melanin contents of α -MSH-stimulated B16F10 cells were measured. The melanin content of the cells non-stimulated with α -MSH was referred as 100%. As Fig. 58B indicates, the melanin content of the cells stimulated with α -MSH was over than 180%. However, the melanin contents of cells treated with HFCPSF4 were dose-dependently decreasing. These results indicate that HFCPSF4 possesses melanogenesis inhibitory effect in α -MSH-stimulated B16F10 cells.

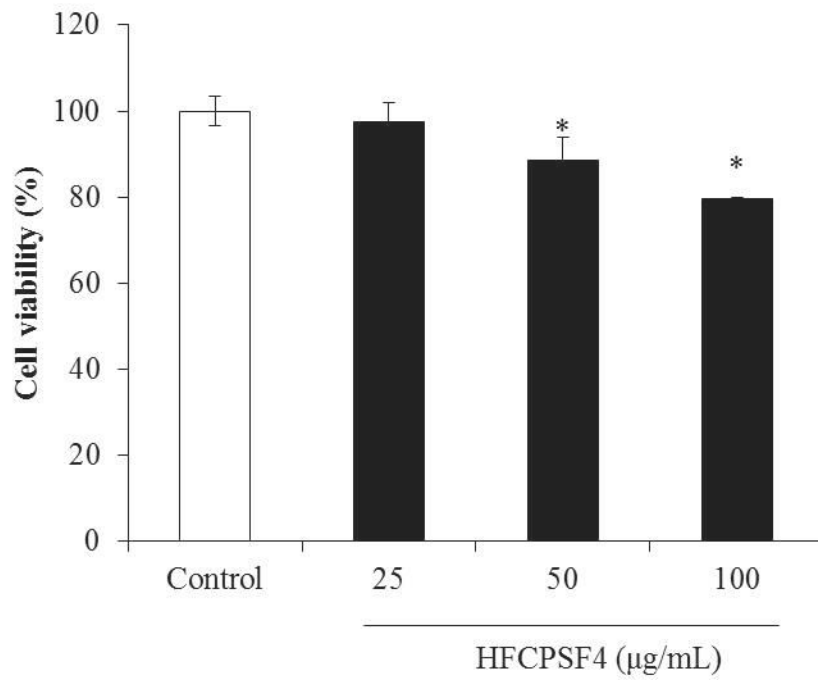


Fig. 58. Cytotoxicity of HFCPSF4 on B16F10 cells. Cell viability was measured by MTT assay. The data were expressed as the mean \pm S.E (n=3). * $p < 0.05$ as compared to control group.

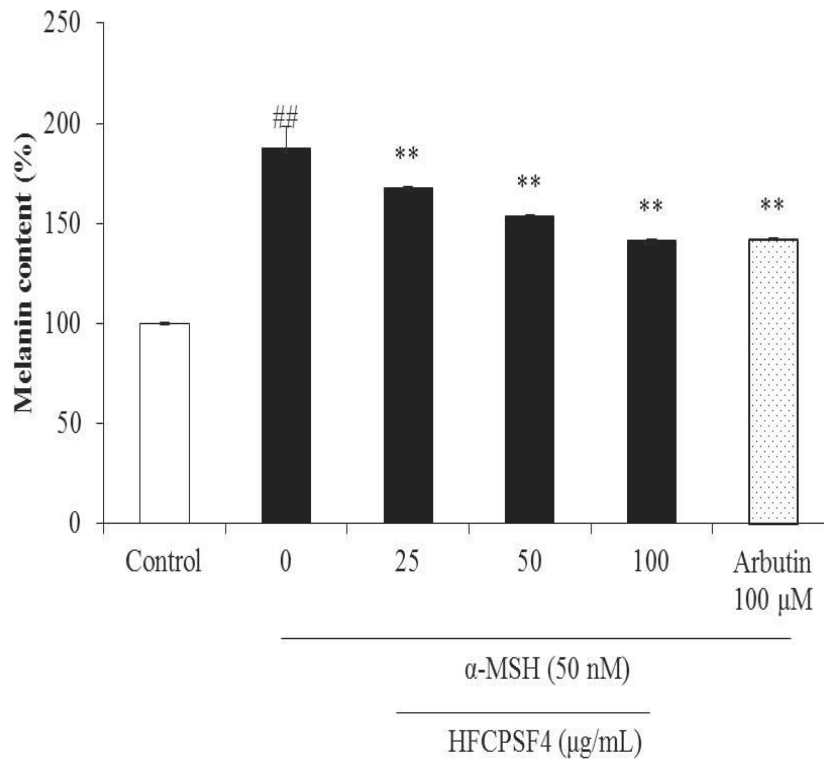


Fig. 59. Melanin synthesis inhibitory effect of HFCPSF4 in α -MSH-stimulated B16F10 cells. The data were expressed as the mean \pm S.E (n=3). ** $p < 0.01$ as compared to α -MSH-treated group and ### $p < 0.01$ as compared to control group.

2.3. Effect of HFCPSF4 on tyrosinase, TRP-1, TRP-2, and MITF levels and ERK-MAPK phosphorylation in α -MSH-stimulated B16F10 cells

As Fig. 60 shows, the expression levels of MITF, tyrosinase, TRP-1, and TRP-2 were improved by α -MSH stimulation. However, the expression levels of these proteins were reduced in the cells treated with HFCPSF4. These results demonstrate that HFCPSF4 against α -MSH-stimulated melanogenesis by inhibiting the expression of MITF, tyrosinase, TRP-1, and TRP-2 in B16F10 cells. In addition, Fig. 61 shows that HFCPSF4 significantly phosphorylated ERK-MAPK. The phosphorylated ERK-MAPK subsequently leads to the degradation of MITF. These results demonstrate that HFCPSF4 inhibited melanin synthesis through down-regulation tyrosinase, TRP-1, and TRP-2 levels via inhibiting MITF by regulating the ERK-MAPK pathway in B16F10 cells.

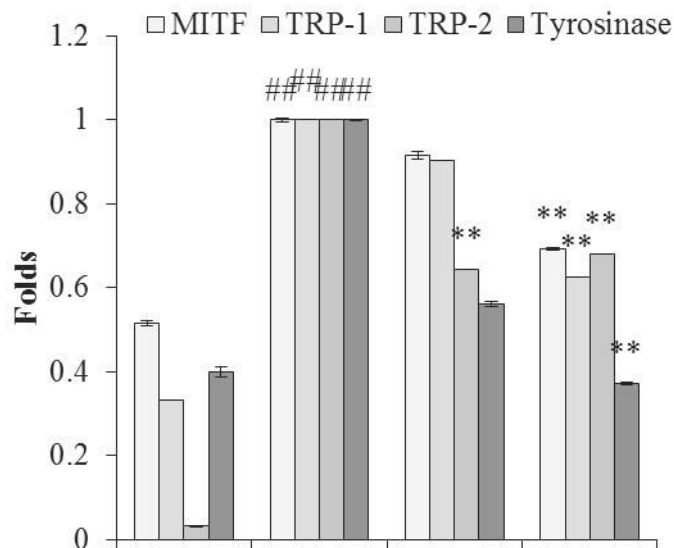
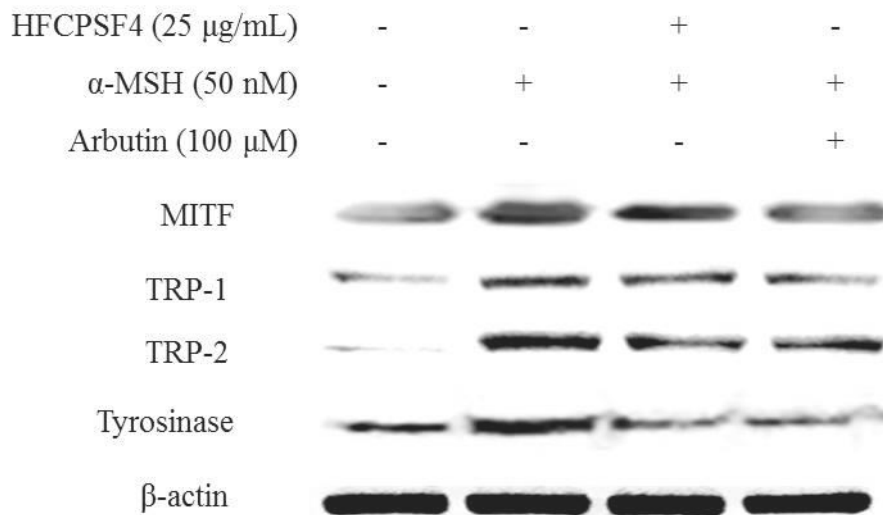


Fig. 60. Effect of HFCPSF4 on MITF, tyrosinase, TRP-1, and TRP-2 expression in α -MSH-stimulated B16F10 cells. The relative amounts of MITF, tyrosinase, TRP-1, and TRP-2 levels were compared with β -actin. The data were expressed as the mean \pm S.E (n=3). * p < 0.05 and ** p < 0.01 as compared to α -MSH-treated group and ### p < 0.01 as compared to control group.

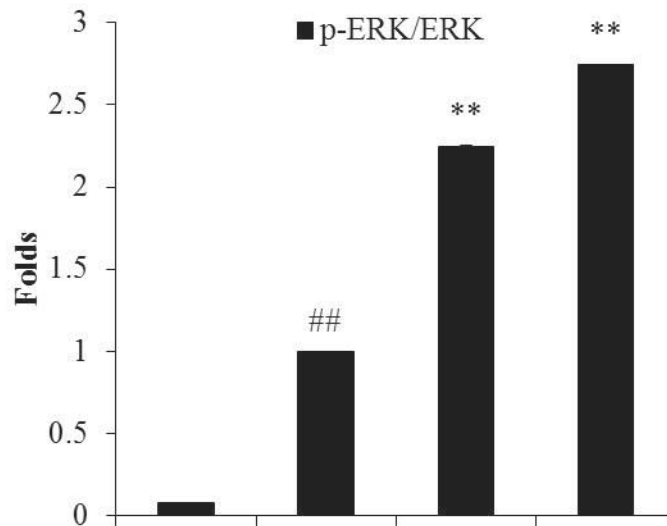
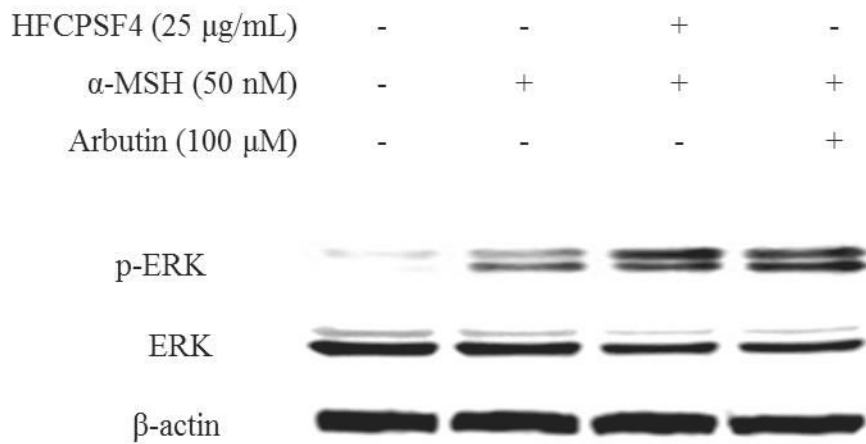


Fig. 61. Effect of HFCPSF4 on ERK-MAPK phosphorylation in α -MSH-stimulated B16F10 cells. The relative amounts of ERK and p-ERK levels were compared with β -actin. The data were expressed as the mean \pm S.E (n=3). * p < 0.05 and ** p < 0.01 as compared to α -MSH-treated group and ## p < 0.01 as compared to control group.

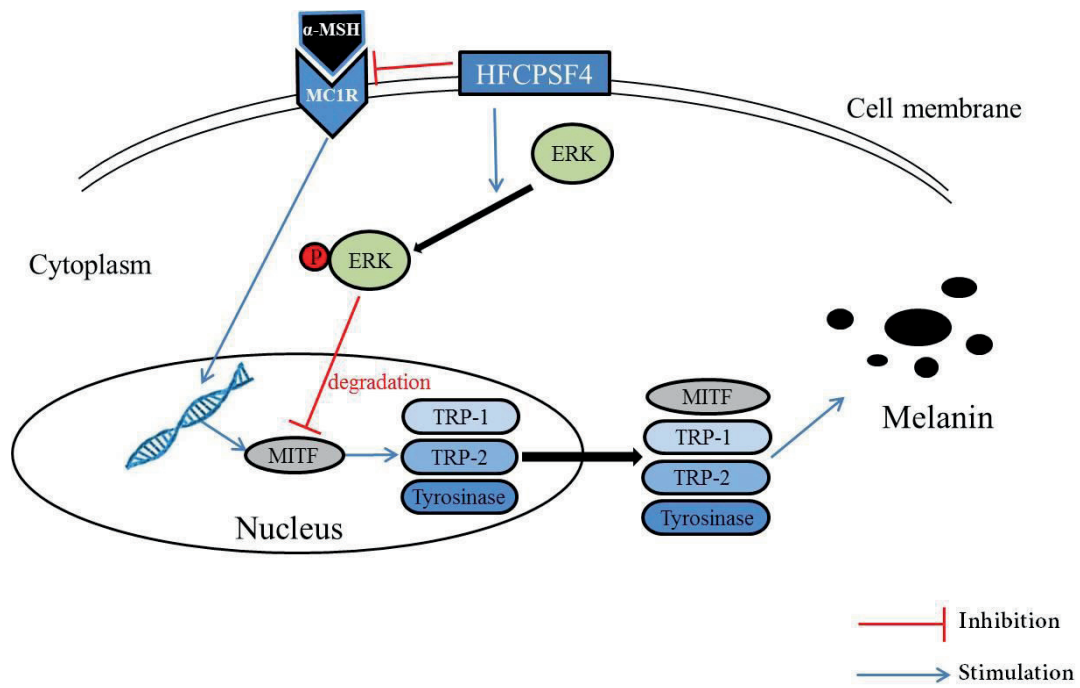


Fig. 62. A schematic model of whitening effect of HFCPSF4 in B16F10 cells.

3. Conclusion

The present study investigated the melanogenesis inhibitory effect of HFCPSF4 in α -MSH-stimulated B16F10 melanoma cells. The results indicate that HFCPSF4 inhibited melanin synthesis through down-regulation tyrosinase, TRP-1, and TRP-2 levels via inhibiting MITF by regulating the ERK-MAPK pathway in B16F10 cells. These results demonstrate that HFCPSF4 possesses whitening effect and may use as a melanogenesis inhibitor to develop a cosmetic in the cosmetic industry.

**Section 5: UV protective effect of *Hizikia* fucoidan isolated from HFCPS *in vitro*
in HaCaT cells and *in vivo* in zebrafish**

Abstract

In the present study, the ultraviolet (UV) protective effect of HFCPSF4 was investigated *in vitro* in keratinocytes (HaCaT cells) and *in vivo* in zebrafish. The intracellular ROS levels and the viabilities of UVB-irradiated HaCaT cells were measured. The results indicate that HFCPSF4 significantly reduce intracellular ROS level and improve viability of UVB-irradiated HaCaT cells. Furthermore, HFCPSF4 remarkably decrease the apoptosis by regulating the expression of Bax/Bcl-xL, PARP, and caspase-3 in UVB-irradiated HaCaT cells in a dose-dependent manner. In addition, the *in vivo* UV protective of HFCPSF4 was investigated using a zebrafish model. The results demonstrate that HFCPSF4 significantly reduce intracellular ROS level, cell death, NO production, and lipid peroxidation in UVB-irradiated zebrafish in a dose-dependent manner. These results suggest HFCPSF4 possesses potent *in vitro* and *in vivo* UV protective effect and it may be considered for use as an ingredient in the cosmetic industry.

1. Materials and methods

1.1. Reagents and Chemicals

The DCFH-DA, acridine orange, 1,3-Bis (diphenylphosphino) propane (DPPP), diaminofluorophore 4-amino-5-methylamino-2',7'-difluorofluorescein diacetate (DAF-FM DA), MTT, and DMSO were purchased from Sigma Co. (St. Louis, MO, USA). The DMEM, FBS, and penicillin/streptomycin were purchased from Gibco BRL (Life Technologies, Burlington, ON, Canada). Bax, Bcl-xL, PARP, cleaved caspase-3, and β -actin antibodies were purchased from Thermo Scientific (Waltham, MA, USA). Anti-mouse and anti-rabbit IgG antibodies were purchased from Cell Signaling Technology (Beverly, MA, USA). All other chemicals used in this study were of analytical grade.

1.2. Cell culture and UVB irradiation

Human Keratinocytes (HaCaT) cell line was purchased from Korean Cell Line Bank. The HaCaT cells were maintained in DMEM supplemented with 10% heat-inactivated FBS, streptomycin (100 μ g/mL), and penicillin (100 unit/mL) at 37°C. Cells were sub-cultured at every 3 days and seeded at a density of 1.0×10^5 cells / mL. Ultraviolet (UV) B irradiation was imposed using a UVB meter (UV Lamp, VL-6LM, Vilber Lourmat, France) with a fluorescent bulb emitting 280~320 nm wavelengths with a peak at 313 nm. HaCaT cells were irradiated at a dose of 30 mJ/cm² of UVB in PBS [44, 67, 96]. Cells were subsequently incubated until analysis.

1.3. Measurement of intracellular ROS generation in UVB-irradiated HaCaT cells

HaCaT cells were seeded and incubated for 24 h. Cells were treated with HFCPSF4 for 30 min, then DCFH-DA (500 μ g/mL) was added into each wells. After 30 min

incubation, cells were exposed to UVB (30 mJ/cm²) and the fluorescent intensities of cells were determined at an excitation wavelength of 485 nm and an emission wavelength of 535 nm, using a fluorescent microplate reader.

1.4. Determination of cell viability

For measuring the protective effect of HFCPSF4 against UVB-induced cell damage, HaCaT cells were treated with HFCPSF4 for 2 h. Cells were then exposed to UVB (30 mJ/cm²) and incubated for another 24 h. Subsequently, cell viability was assessed by MTT assay described previously [59, 68, 97].

1.5. Measurement of apoptosis body formation

The apoptosis body formation of UVB-irradiated HaCaT cells was determined by nuclear staining. HaCaT cells were seeded and incubated for 24 h. After incubation, cells were treated with HFCPSF4 and incubated for 2 h. After incubation, cells were exposed to UVB (30 mJ/cm²) and incubated with serum-free DMEM medium for 6 h. After incubation, cells were treated with 25 µL of Hoechst 33342 (stock, 10 mg/mL) and incubated for 10 min. The stained cells were observed using a fluorescence microscope equipped with a Cool SNAP-Pro color digital camera (Olympus, Japan).

1.6. Western blot analysis

The effect of HFCPSF4 on the expression of apoptosis-related proteins including in Bax, Bcl-xL, PARP, and cleaved caspase-3 were assessed by Western blot assay performed according to the procedure as described by Wijesinghe et al. [3, 5, 60]. In brief, HaCaT cells treated with HFCPSF4 and irradiated with UVB. After 24 h incubation, cells were harvested and lysed. The protein level of each sample was measured by a BCA™ kit. The proteins (50 µg) were separated on 12% SDS-PAGE and transferred onto nitrocellulose transfer membranes. The membranes were blocked

with blocking buffer (5% skim milk) and incubated with primary antibodies for 16 h at 4°C. Then, the membranes were further incubated with secondary antibody at room temperature for 3 h. Finally, the protein bands were visualized using an ECL western blotting detection kit and exposed on X-ray films.

1.7. Application of HFCPSF4 and UVB to zebrafish

At 2 dpf, the zebrafish were transferred to a 24-well plate and treated with HFCPSF4 as the final concentration of 12.5, 25, and 50 µg/mL. After 1 hour, the zebrafish were washed with embryo media and exposed to UVB (50 mJ/cm²) individual [23, 69]. After 6 h incubation, the zebrafish were washed with embryo media and stained with DCFH-DA (20 µg/mL, 1 h), acridine orange (10 µg/mL, 30 min), DAF-FM-DA (10 µM, 3 h), and DPPP (3 µM, 1 h) for measuring ROS level, cell death, NO production, and lipid peroxidation, respectively. After incubation, the zebrafish were washed two times with embryo media and anesthetized by phenoxyethanol before visualization. After anesthetized, the zebrafish larvae were photographed under the microscope Cool SNAP-Procolor digital camera (Olympus, Japan). And the individual zebrafish larvae fluorescence intensity was quantified using an image J program.

1.8. Statistical Analysis

All experiments were conducted in triplicate. The data are expressed as the mean ± standard error (S.E), and one-way ANOVA was used to compare the mean values of each treatment in SPSS 12.0. Significant differences between the means were identified by the Turkey test. Significance was established if * $p < 0.05$, ** $p < 0.01$ as compared to the UVB-treated group, and ^{##} $p < 0.01$ as compared to control group.

2. Results and Discussion

2.1. Effect of HFCPSF4 on intracellular ROS generation and cell death in UVB-irradiated HaCaT cells

The HaCaT cell damage level induced by UVB irradiation was detected by measuring the intracellular ROS generation and cell death. As Fig. 63A shows, the ROS level of UVB-irradiated cells was significantly increased compared with non-irradiated cells. However, the ROS levels of the cells treated with different concentration of HFCPSF4 were significantly decreasing in a dose-dependent manner. In addition, the viability of cells irradiated by UVB was significantly decreased, and dose-dependently increased in HFCPSF4 treated cells (Fig. 63B). These results indicate that HFCPSF4 possesses potent protective effect against UVB-induced HaCaT cell damage.

2.2. Effect of HFCPSF4 on apoptosis formation in UVB-irradiated HaCaT cells

In order to measure the apoptosis body formation, the cells were stained with a cell permeable DNA dye Hoechst 33342. Then the nuclear morphology of cells was examined by a fluorescence microscopy. The cell images were shown in Fig. 64. According to the results, the amount of apoptotic bodies of HFCPSF4-treated HaCaT cells were significantly decreased in a dose-dependent manner. It means HFCPSF4 possesses effect against UVB-induced HaCaT cell apoptotic.

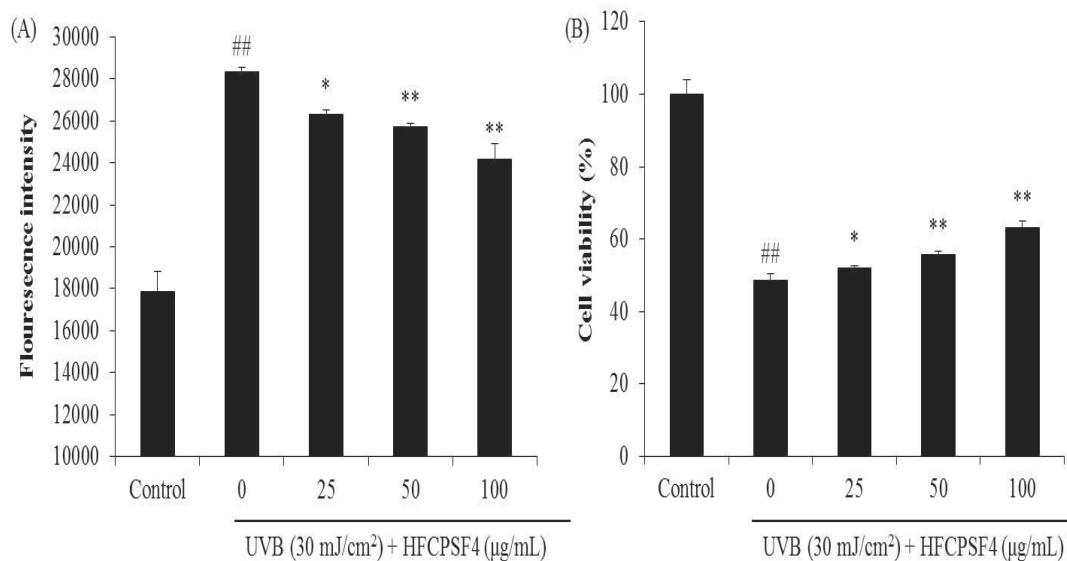


Fig. 63. Protective effect of HFCPSF4 against UVB-induced HaCaT cells damage. (A) Intracellular ROS level of UVB-irradiated HaCaT cells; (B) the viability of UVB-irradiated HaCaT cells. The experiments were conducted in triplicate, and the data are expressed as the mean \pm standard error (S.E). * $p < 0.05$, ** $p < 0.01$ as compared to the UVB-treated group and ^{##} $p < 0.01$ as compared to the control group.

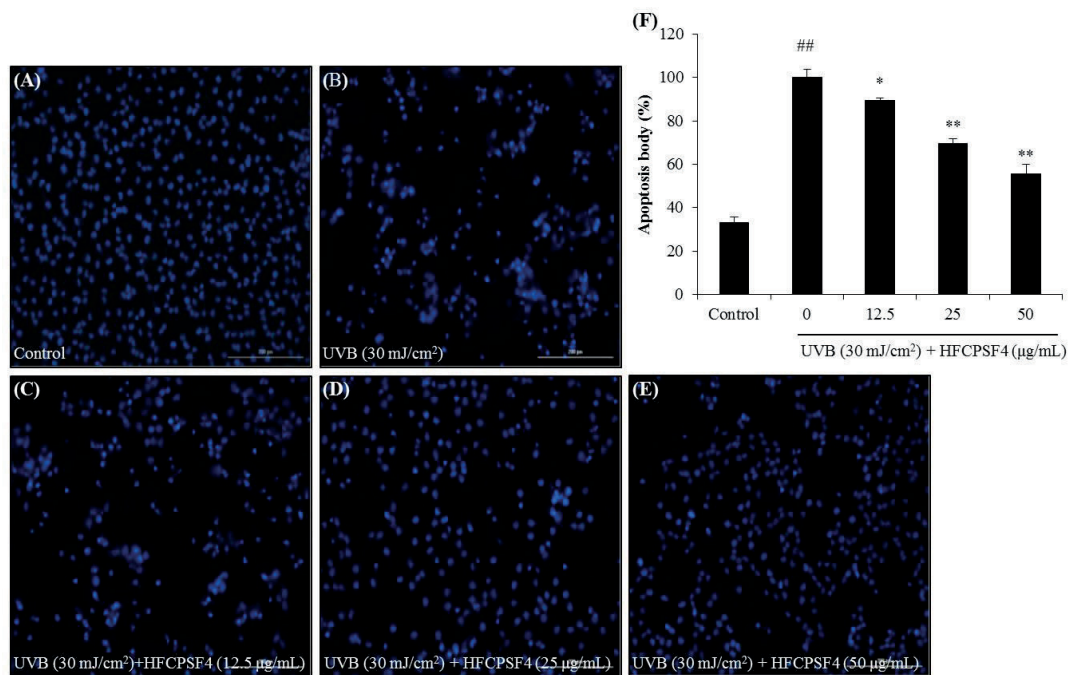


Fig. 64. The apoptotic body formation levels in UVB-irradiated HaCaT cells. (A) Nuclear morphology of non UVB-irradiated HaCaT cells; (B) nuclear morphology of UVB-irradiated HaCaT cells; (C) nuclear morphology of cells treated with 12.5 of $\mu\text{g/mL}$ HFCPSF4 and irradiated with UVB; (D) nuclear morphology of cells treated with 25 of $\mu\text{g/mL}$ HFCPSF4 and irradiated with UVB; (E) nuclear morphology of cells treated with 50 of $\mu\text{g/mL}$ HFCPSF4 and irradiated with UVB; (F) reactive apoptotic body formation. The apoptotic body formation was observed under a fluorescence microscope after Hoechst 33342 staining. Apoptosis levels were measured using Image J software. * $p < 0.05$, ** $p < 0.01$ as compared to the UVB-treated group and ## $p < 0.01$ as compared to the control group.

2.3. Effect of HFCPSF4 on Bax/Bcl-xL, PARP, and cleaved caspass-3 levels in UVB-irradiated HaCaT cells

The Bax/Bcl-xL, PARP, and cleaved caspass-3 levels of UVB-irradiated HaCaT cells were measured by Western blot analysis, the results summarized in Fig. 65. As the results shows, the UVB irradiation increase Bax level and decrease Bcl-xL level, however, HFCPSF4 significantly increase Bcl-xL level and decrease Bax level in a dose-dependent manner. In addition, HFCPSF4 reduce UVB-induced caspass-3 activation as well as improve PARP level in UVB-irradiated HaCaT cells. These results indicated that HFCPSF4 inhibits UVB-induced apoptosis by regulation of Bax, Bcl-xL, PARP, and cleaved caspass-3 levels.

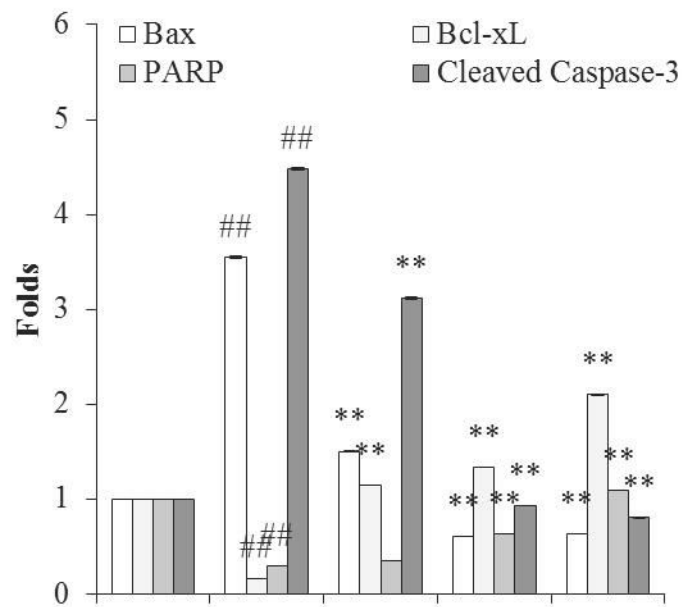
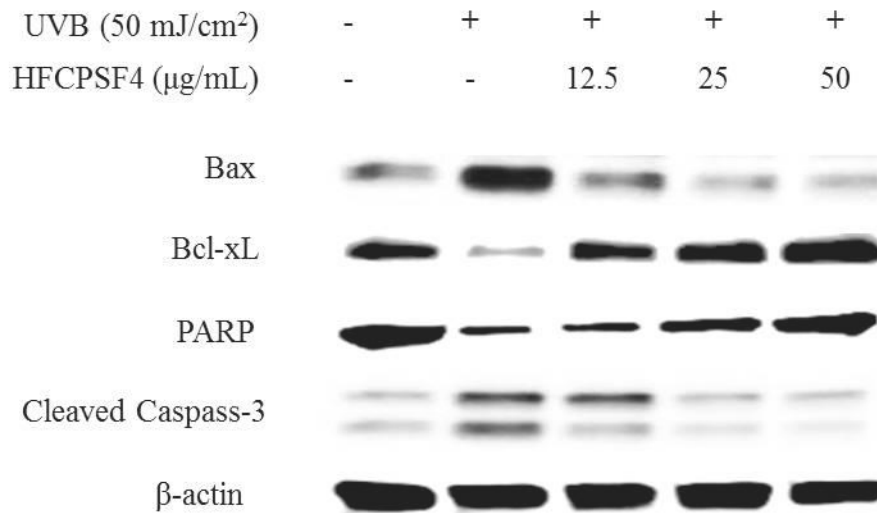


Fig. 65. Effect of HFCPSF4 on Bax/Bcl-xL, PARP, and cleaved caspase-3 levels in UVB-irradiated HaCaT cells. The relative amounts of Bax/Bcl-xL, PARP, and cleaved caspase-3 levels were compared with β -actin. The data were expressed as the mean \pm S.E (n=3). * p < 0.05 and ** p < 0.01 as compared to UVB-treated group and ## p < 0.01 as compared to control group.

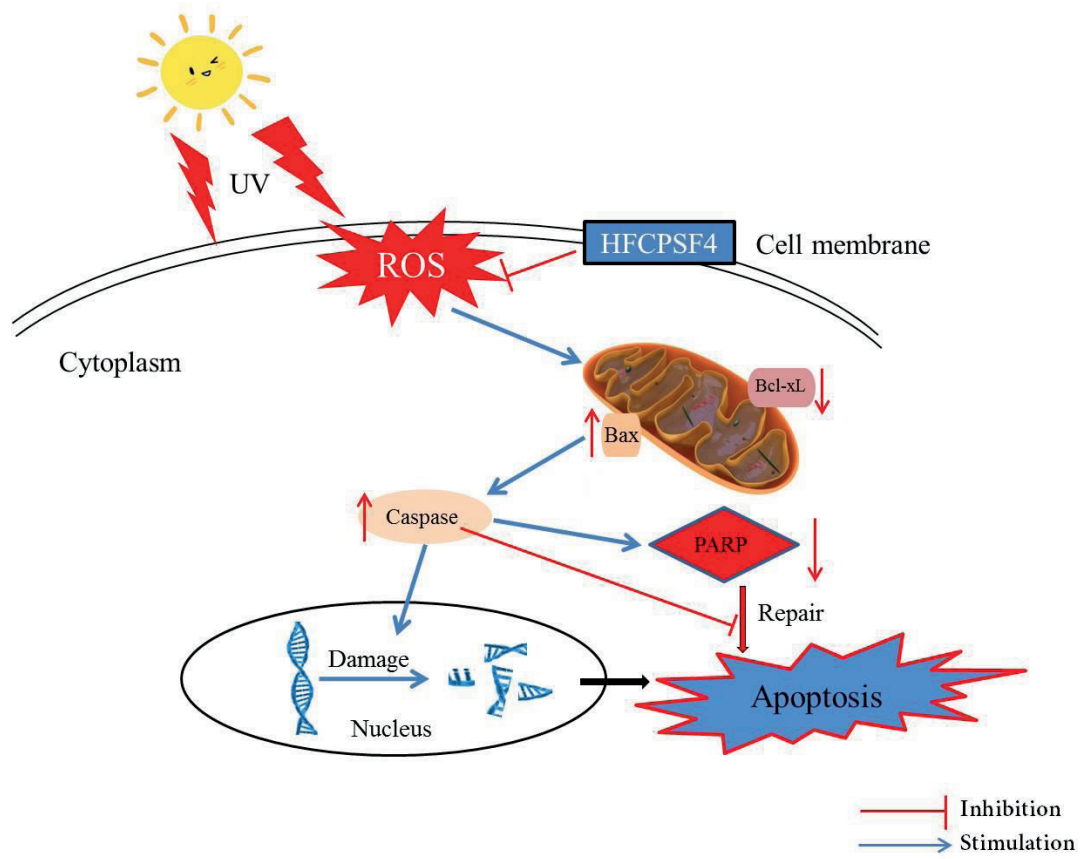


Fig. 66. A schematic model of UVB protective effect of HFCPSF4 in HaCaT cells.

2.4. Effect of HFCPSF4 on ROS generation, cell death, NO production, and lipid peroxidation in UVB-irradiated zebrafish

As Fig. 67 shows, the ROS level in the zebrafish irradiated with UVB was significantly increased comparing with non-irradiated zebrafish. However, the ROS level in the zebrafish treated with different concentration of HFCPSF4 was dose-dependently decreased. As Fig. 68 shows, HFCPSF4 remarkably attenuated cell death level in a dose-dependent manner. In addition, Fig. 69 shows, the NO generation in the UVB-irradiated zebrafish was significantly increased comparing with non-irradiated zebrafish. However, the NO generation in HFCPSF4-treated zebrafish significantly decreased in a dose-dependent manner. Furthermore, HFCPSF4 remarkable and significant reduce lipid peroxidation in UVB-irradiated zebrafish (Fig. 70). These results demonstrate that HFCPSF4 possesses strong *in vivo* UV protective effect.

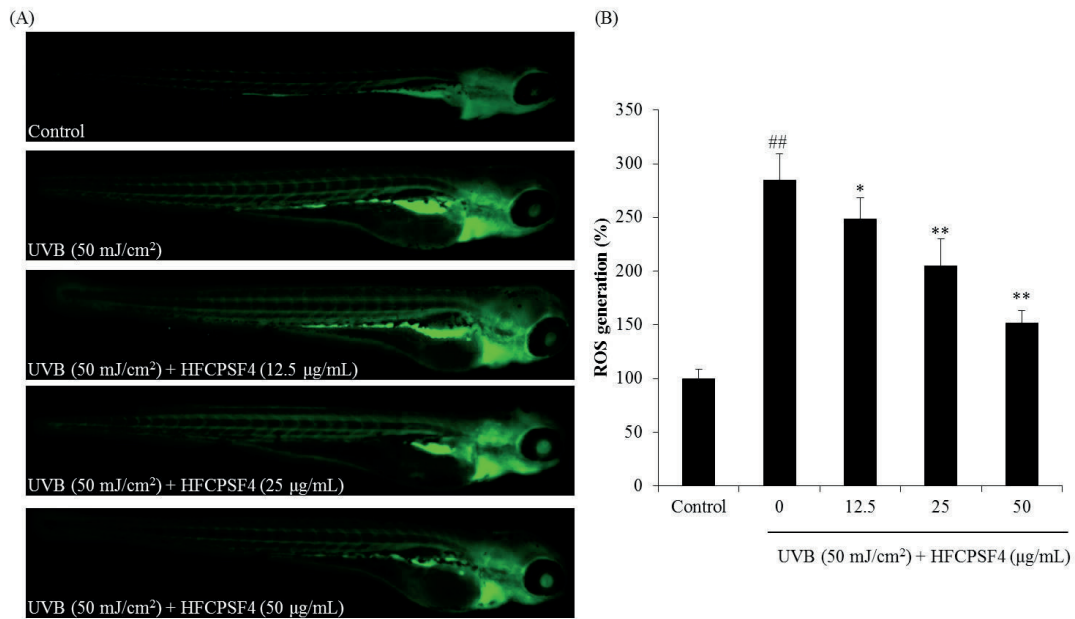


Fig. 67. The protective effect of HFCPSF4 against UVB-induced ROS production in zebrafish. (A) Zebrafish under fluorescence microscope; (B) the levels of ROS. ROS levels were measured using Image J software. The experiments were conducted in triplicate, and the data are expressed as the mean \pm standard error (S.E). ** $p < 0.01$ as compared to the UVB-treated group and ## $p < 0.01$ as compared to the control group.

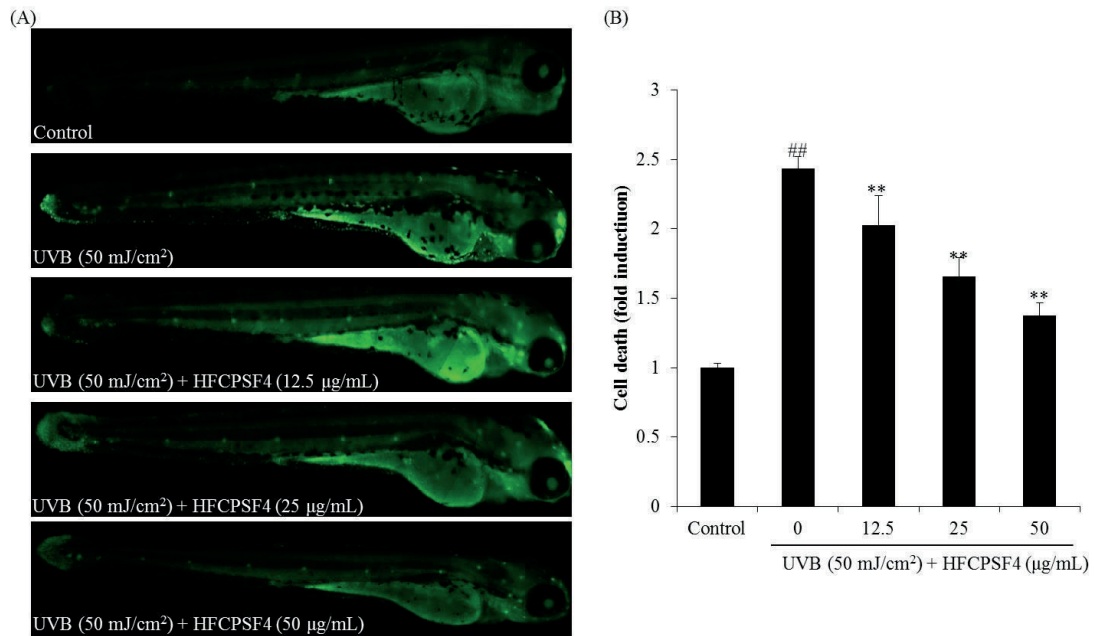


Fig. 68. The protective effect of HFCPSF4 against UVB-induced cell death in zebrafish. (A) Zebrafish under fluorescence microscope; (B) the levels of cell death. Cell death was measured using Image J software. The experiments were conducted in triplicate, and the data are expressed as the mean \pm standard error (S.E). ** $p < 0.01$ as compared to the UVB-treated group and ^{##} $p < 0.01$ as compared to the control group.

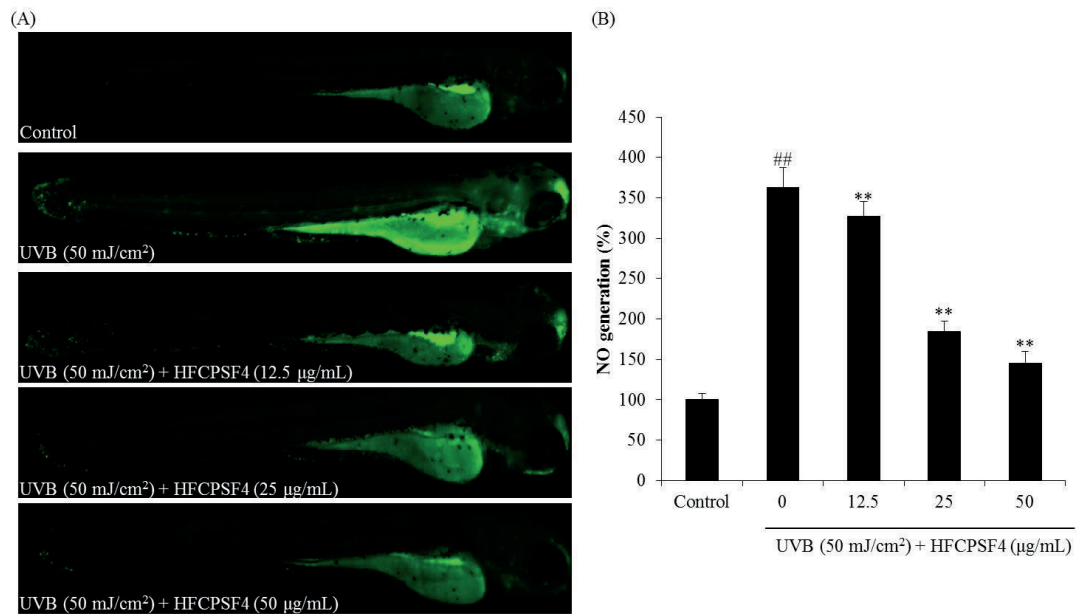


Fig. 69. The protective effect of HFCPSF4 against UVB-induced NO production in zebrafish. (A) Zebrafish under fluorescence microscope; (B) NO production levels. NO production level was measured using Image J software. The experiments were conducted in triplicate, and the data are expressed as the mean \pm standard error (S.E). ** $p < 0.01$ as compared to the UVB-treated group and ^{##} $p < 0.01$ as compared to the control group.

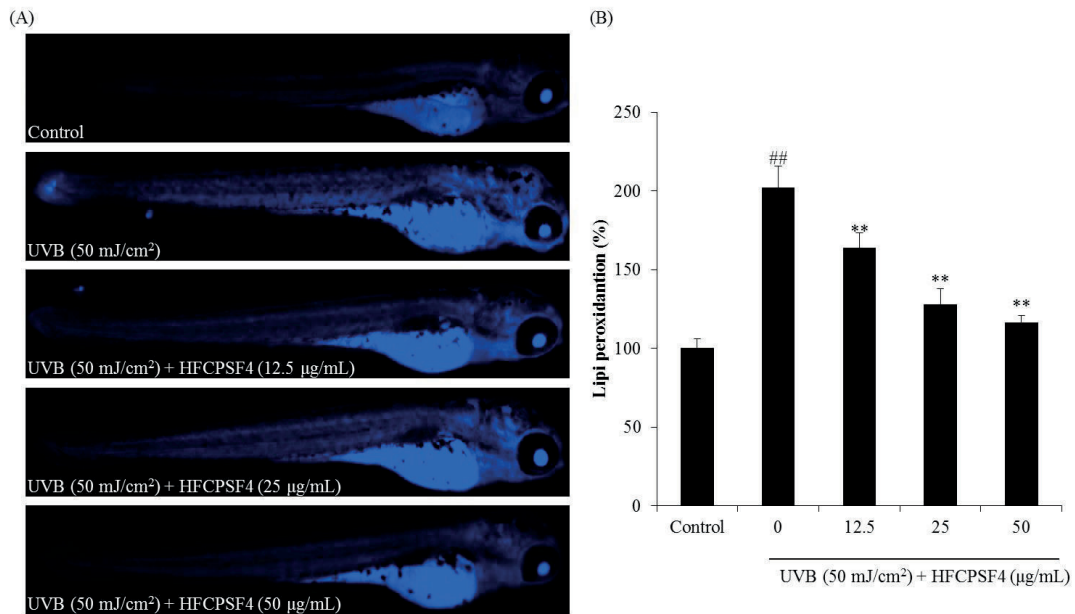


Fig. 70. The protective effect of HFCPSF4 against UVB-induced lipid peroxidation in zebrafish. (A) Zebrafish under fluorescence microscope; (B) lipid peroxidation levels. Lipid peroxidation was measured using Image J software. The experiments were conducted in triplicate, and the data are expressed as the mean \pm standard error (S.E). ** $p < 0.01$ as compared to the UVB-treated group and $^{##}p < 0.01$ as compared to the control group.

3. Conclusion

In the present study, the UV protective effect of HFCPSF4 was investigated *in vitro* in HaCaT cells and *in vivo* in zebrafish. The results indicate that HFCPSF4 significantly reduce intracellular ROS level, improve cell viability, reduce apoptosis body formation, and regulate the expression of Bax/Bcl-xL, PARP, and caspase-3 in UVB-irradiated HaCaT cells. In addition, HFCPSF4 significantly reduce intracellular ROS level, cell death, NO production, and lipid peroxidation in UVB-irradiated zebrafish in a dose-dependent manner. These results suggest HFCPSF4 possesses potent *in vitro* and *in vivo* UV protective effect and it may be considered for use as an ingredient in the cosmetic industry.

Section 6: Anti-wrinkle effect of *Hizikia* fucoidan isolated from HFCPS *in vitro* in human dermal fibroblasts

Abstract

In the present study, we investigated the protective effect of HFCPSF4 against ultraviolet (UV) B-induced skin wrinkling *in vitro* in human dermal fibroblasts (HDF cells). The results indicate that HFCPSF4 significantly decreased intracellular reactive oxygen species (ROS) level and increased the viability of UVB-irradiated HDF cells in a dose-dependent manner. In addition, HFCPS significantly inhibited intracellular collagenase and elastase activities, remarkably improved collagen synthesis, and reduced matrix metalloproteinases (MMPs) and pro-inflammatory cytokines expression by regulating nuclear factor kappa B (NF- κ B), activator protein 1 (AP-1), and mitogen-activated protein kinases (MAPKs) signaling pathways in UVB-irradiated HDF cells. These results suggest that HFCPSF4 possesses strong UV protective effect, and can be a potential anti-wrinkle ingredient in the cosmetic industry.

1. Materials and methods

1.1. Reagents and Chemicals

The MTT, DCFH-DA, DMSO, azo dye-impregnated collagen, and N-succinyl-Ala-Ala-Ala-p-nitroanilide were purchased from Sigma Co. (St. Louis, MO, USA). The DMEM, Ham's Nutrient Mixtures medium (F-12), 1X PBS, penicillin/streptomycin, and FBS were purchased from Gibco BRL (Life Technologies, Burlington, ON, Canada). Antibodies against β -actin, nucleolin, p-c-Jun, ERK and phospho-ERK, JNK and phospho-JNK, p38 and phospho-p38, and NF- κ B p65 and NF- κ B p50 were purchased from Santa Cruz Biotechnology (Santa Cruz, CA, USA). Anti-rabbit IgG antibodies was purchased from Cell Signaling Technology (Beverly, MA, USA). The ELISA kits used for the analysis of TNF- α , PGE₂, IL-1 β , and IL-6, and production were purchased from Sigma Co. (St. Louis, MO, USA). PIP ELISA kit was purchased from TaKaRa Bio Inc. (Japan) and Human MMP-1, 2, 8, 9, and 13 ELISA kits were purchased from GE Healthcare Life Sciences (UK). All other chemicals used in this study were of analytical grade.

1.2. Cell culture and UVB-irradiation

Human dermal fibroblasts (HDF cells, ATCC[®] PCS201012[™]) were purchased from ATCC (American Type Culture Collection, Manassas, VA, USA). HDF cells were cultured in DMEM and F-12 mixed with a ratio of three to one supplemented with 10% heat-inactivated FBS, 100 unit/mL of penicillin and 100 μ g/mL of streptomycin. Cells were sub-cultured every 5 days. Cells were incubated at 37°C under humidified atmosphere containing 5% CO₂ in an incubator (Sanyo MCO-18AIC CO₂ Incubator, Moriguchi, Japan). UVB irradiation was carried out using a UVB meter (UV Lamp, VL-6LM, Vilber Lourmat, France), equipped with a fluorescent bulb emitting 280~320

nm wavelength with a peak at 313 nm. HDF cells were irradiated in 1X PBS. Cell medium was subsequently replaced with serum-free medium and incubated until analysis.

1.3. Determination of the effect of HFCPSF4 against UVB-induced HDF cell damage

The protective effect of HFCPSF4 against UVB-induced HDF cell damage was determined by measuring intracellular ROS level and viability of UVB-irradiated HDF cells. For intracellular ROS analysis, HDF cells were seeded and incubated for 24 h, then, cells were treated with HFCPSF4 and incubated for 30 min. Subsequently, cells were treated with DCFH-DA (stock, 500 $\mu\text{g}/\text{mL}$) and incubated for 30 min. After incubation, cells were exposed to UVB (50 mJ/cm^2) and the fluorescence intensity of cells was determined according to the method described previously [72-74]. For measuring the viabilities of UVB-irradiated HDF cells, HDF cells were treated with HFCPSF4 and incubated for 2 h at 37°C. Cells were then exposed to 50 mJ/cm^2 of UVB and incubated for 48 h. Cell viability was assessed by MTT assay.

1.4. Determination of relative intracellular elastase and collagenase activities on UVB-irradiated HDF cells

HDF cells were seeded in 100 mm culture dishes at a density of 2.0×10^6 cells per dish and incubated for 24 h. Cells were treated with HFCPSF4 and incubated for 2 h. Following incubation, cells were irradiated with UVB. After 48 h incubation, cells were harvested and lysed with 0.1 M Tris-HCl (pH 7.6) buffer containing 1 mM PMSF and 0.1% Triton-X 100, followed by sonication for 5 min on ice. The lysates were centrifuged (4000 rpm, 20 min) at 4°C. Supernatants were quantified for their protein

content and were used as the fibroblastic enzyme solution. The relative elastase and collagenase activities were measured by the method described by Suganuma et al. [75].

1.5. Determination of collagen synthesis level, MMPs expression levels, pro-inflammatory cytokines levels on UVB-irradiated HDF cells

HDF cells were incubated with HFCPSF4 for 2 h, and exposed to UVB (50 mJ/cm²). After 48 h incubation, the culture media were collected and used for assessment of matrix metalloproteinases (MMPs) expression levels, pro-inflammatory cytokines levels, and PIP level that reflect the level of collagen synthesis. The amounts of PIP, pro-inflammatory cytokines, and MMPs were measured by commercial ELISA kits based on the manufacturer's instructions.

1.6. Western blot analysis

The effect of HFCPSF4 on the expressions of nuclear factor kappa B (NF- κ B), activator protein 1 (AP-1), and mitogen-activated protein kinases (MAPKs) were assessed by Western blot analysis performed as described previously [98]. In brief, cells were treated with HFCPSF4 and irradiated with UVB. Cells were harvested after 1 h (for MAPKs assay) or 6 h (for NF- κ B and AP-1 assay) incubation. Proteins were extracted with the PROPREP protein extraction kit (iNtRON Biotechnology, Sungnam, Korea). The protein level of each sample was measured by a BCATM kit. The proteins (50 μ g) were separated on 12% SDS-polyacrylamide gels and transferred to pure nitrocellulose membranes. Membranes were blocked with 5% skim milk for 3 h at room temperature and incubated with primary antibodies overnight at 4°C. After washing with TBS-T buffer, membranes were incubated with secondary antibodies for 3 h at room temperature. Finally, the protein bands were visualized using an ECL western blotting detection kit and exposed on X-ray films.

1.7. Statistical Analysis

The experiments were performed in triplicate. The data are expressed as the mean \pm standard error (S.E), and one-way ANOVA was used to compare the mean values of each treatment in SPSS 12.0. Significant differences between the means were identified by the Turkey test. A value of $*p < 0.05$, $**p < 0.01$, and $^{##}p < 0.01$ were considered as significantly different.

2. Results and Discussion

2.1. HFCPSF4 improves cell viability and reduces intracellular ROS in UVB-irradiated HDF cells

As Fig. 71 shows, cell viability was decreased while intracellular ROS level was increased after UVB irradiation. However, the viabilities of cells treated with HFCPSF4 were improved as well as the intracellular ROS level was reduced in a dose-dependent manner. These results indicate that HFCPSF4 possesses a potent protective effect against UVB-induced cell damage via ROS clearance in HDF cells.

2.2. HFCPSF4 inhibits intracellular collagenase and elastase activities in UVB-irradiated HDF cells

As Fig. 72 shows, the relative collagenase and elastase activities of UVB-irradiated HDF cells were significantly increased comparing to non-irradiated cells. However, relative activities of both two enzymes were dose-dependently decreased in HFCPSF4-treated cells. These results suggest that HFCPSF4 may act as an inhibitor of fibroblast collagenase and elastase and may prevent wrinkle formation induced by UVB irradiation.

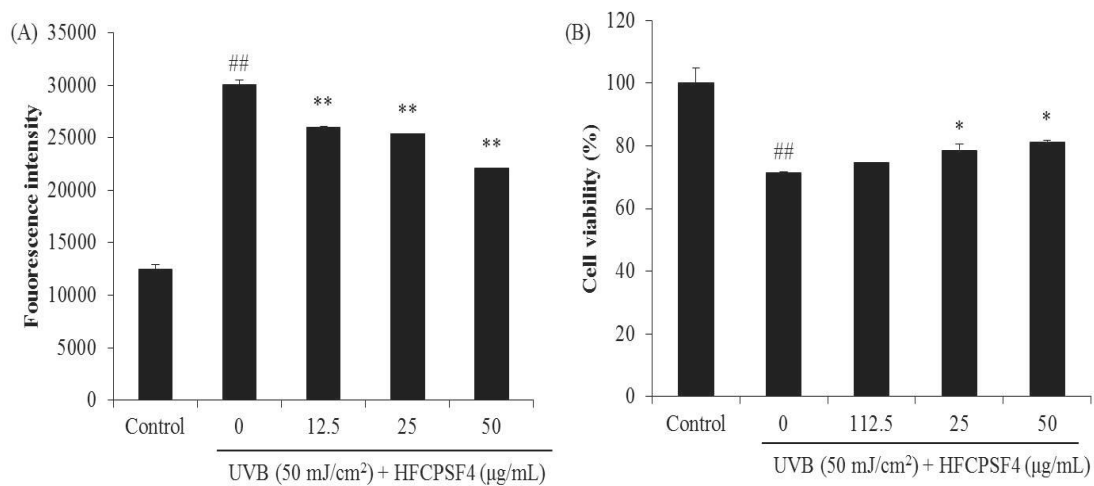


Fig. 71. Protective effect of HFCPSF4 against UVB-induced HDF cell damage. (A) Intracellular ROS scavenging effect of HFCPSF4 in UVB-irradiated HDF cells; (B) protective effect of HFCPSF4 against UVB-induced HDF cell death. Cell viability was measured by MTT assay and intracellular ROS level was measured by DCF-DA assay. The experiments were conducted triplicate, and the data were expressed as the mean \pm standard error (S.E). * $p < 0.05$, ** $p < 0.01$ as compared to UVB-irradiated group and ## $p < 0.01$ as compared to control group.

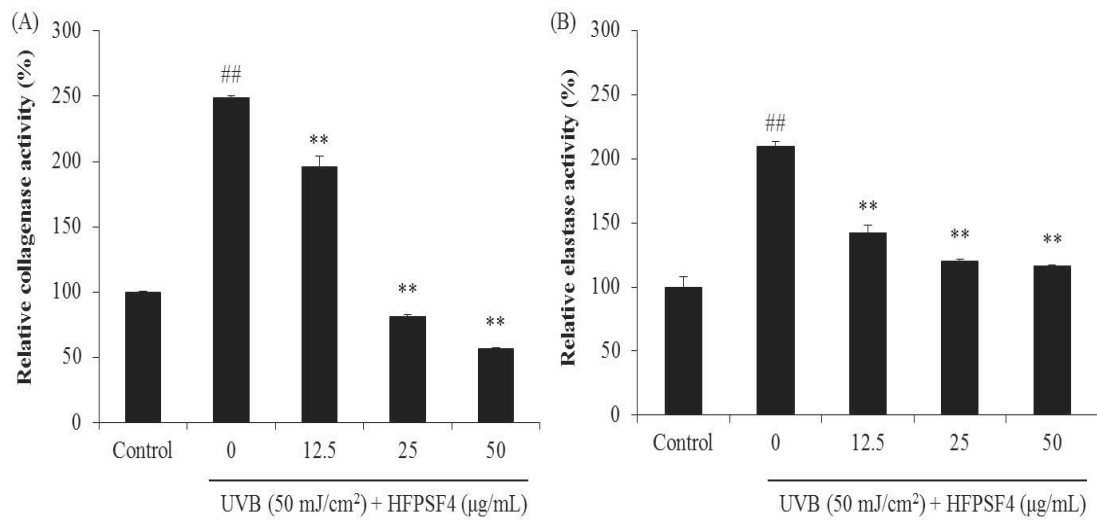


Fig. 72. HFCPSF4 inhibits cellular collagenase and elastase activities in UVB-irradiated HDF Cells. (A) Relative collagenase activity; (B) relative elastase activity. The experiments were conducted triplicate, and the data were expressed as the mean \pm standard error (S.E). * $p < 0.05$, ** $p < 0.01$ as compared to UVB-irradiated group and ^{##} $p < 0.01$ as compared to control group.

2.3. HFCPSF4 protects collagen synthesis and reduces MMPs and pro-inflammatory cytokines expression levels in UVB-irradiated HDF cells

As Fig. 73 shows, UVB irradiation significantly decreased collagen synthesis in HDF cells and HFCPSF4 dose-dependently protects collagen synthesis (Fig. 73A). Furthermore, MMPs and pro-inflammatory cytokines expression levels were significant increase in UVB-irradiated HDF cells but decrease in HFCPSF4-treated cells (Fig. 73B-F and Fig. 74). These results indicate that HFCPSF4 effectively protects collagen synthesis and reduces the expressions of MMPs and pro-inflammatory cytokines.

2.4. HFCPSF4 inhibits NF- κ B activation, reduces AP-1 phosphorylation, and suppresses MAPKs activation in UVB-irradiated HDF cells

The activated NF- κ B, AP-1, and MAPKs levels by Western blot analysis. The results indicate that UVB irradiation significant phosphorylates AP-1, however, HFCPSF4 remarkable reduces the phosphorylated AP-1 levels (Fig. 75 B). In addition, UVB irradiation significant increases nuclear levels of NF- κ B (p65 and p50); however, HFCPSF4 treatment remarkably reduces nuclear NF- κ B levels in UVB-irradiated HDF cells (Fig. 75B). Furthermore, HFCPSF4 treatment effective suppresses UVB-induced p38, JNK, and ERK phosphorylation in UVB-irradiated HDF cells (Fig. 76). All effects are dose-dependently. These results demonstrate that HFCPSF4 blocks NF- κ B activation, and reduces AP-1 phosphorylation through suppression of MAPKs activation in UVB-induced HDF cells.

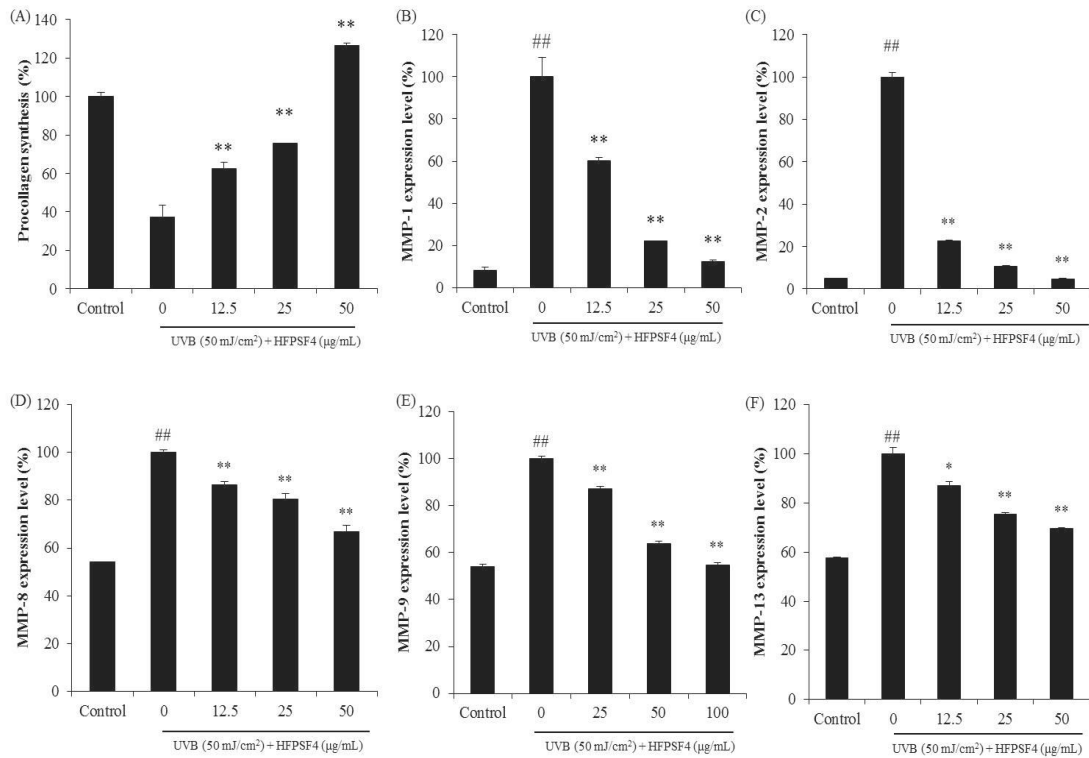


Fig. 73. HFCPSF4 improves collagen synthesis and reduces MMPs expression in UVB-irradiated HDF cells. (A) Collagen synthesis level in UVB-irradiated HDF cells; (B) MMP-1 expression level in UVB-irradiated HDF cells; (C) MMP-2 expression level in UVB-irradiated HDF cells; (D) MMP-8 expression level in UVB-irradiated HDF cells; (E) MMP-9 expression level in UVB-irradiated HDF cells; (F) MMP-13 expression level in UVB-irradiated HDF cells. Collagen synthesis level was reflected by the amounts of PIP, and the amounts of PIP and MMPs were measured by the commercially ELISA kits, based on the manufacturer's instructions. The experiments were conducted triplicate, and the data were expressed as the mean \pm standard error (S.E). * $p < 0.05$, ** $p < 0.01$ as compared to UVB-irradiated group and ## $p < 0.01$ as compared to control group.

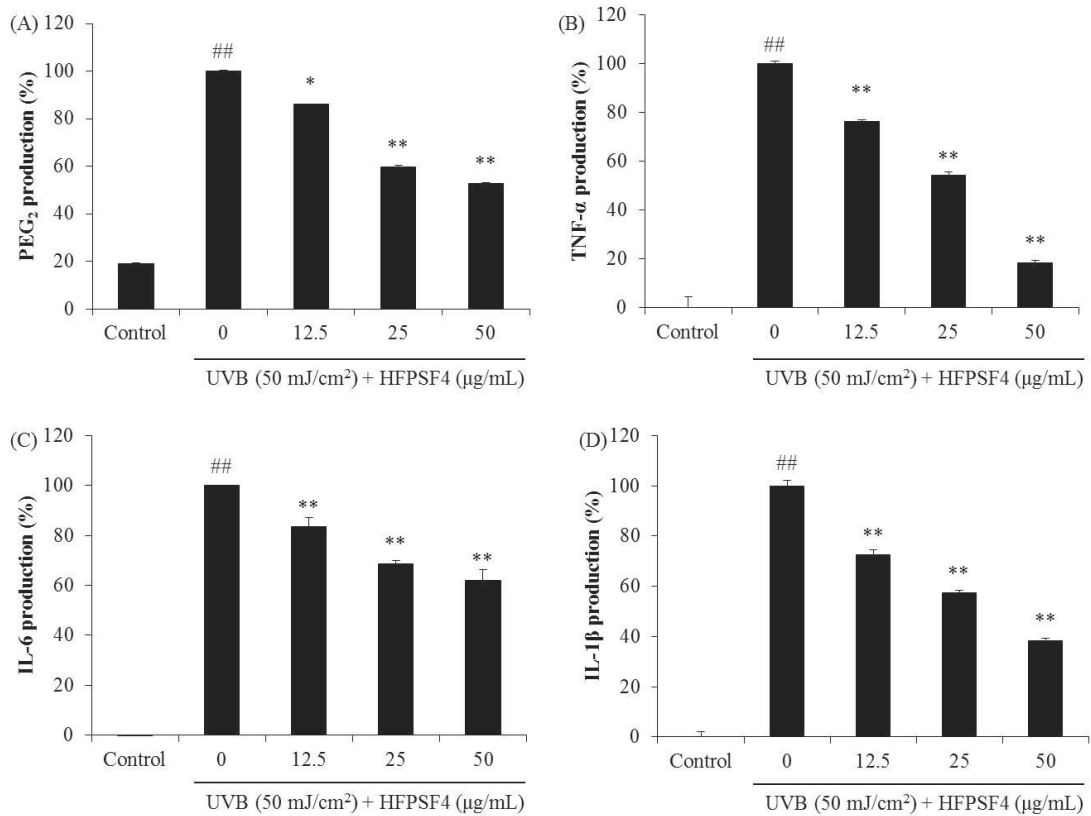


Fig. 74. The effect of HFCPSF4 on the production of PGE₂, TNF- α , IL-1 β , and IL-6 in UVB-irradiated HDF cells. (A) The production of PGE₂; (B) the production of TNF- α ; (C) the production of IL-1 β ; (D) the production of IL-6. The levels of PGE₂, TNF- α , IL-1 β , and IL-6 production were examined using ELISA kit. The experiments were conducted in triplicate, and the data are expressed as the mean \pm standard error (S.E). * $p < 0.05$, ** $p < 0.01$ as compared to the UVB-irradiated group and ^{##} $p < 0.01$ as compared to the control group.

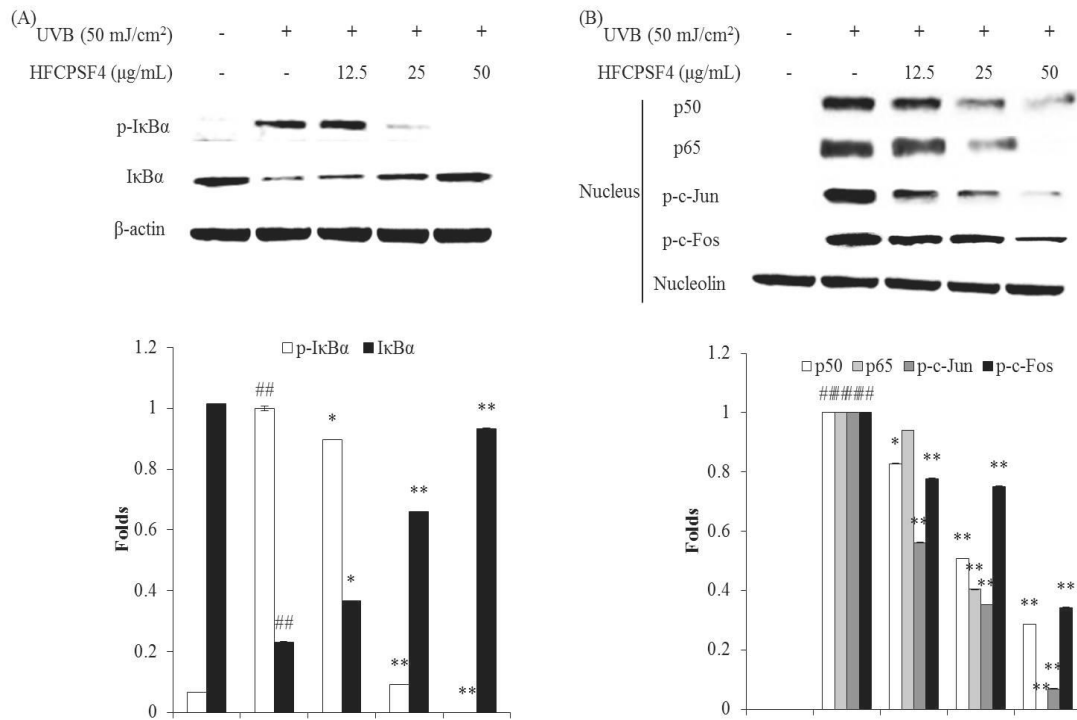


Fig. 75. HFCPSF4 blocks UVB-induced NF- κ B activation and reduces AP-1 phosphorylation in UVB-induced HDF cells. (A) The cytosol I κ B α and p-I κ B α level; (B) the nuclear p50, p65 NF- κ B, and phosphorylated AP-1 levels. The relative amounts of I κ B α and p-I κ B α levels were compared with β -actin, and the relative amounts of p50, p65 NF- κ B, and phosphorylated AP-1 levels were compared with nucleolin. The experiments were conducted triplicate, and the data were expressed as the mean \pm standard error (S.E). ** $p < 0.01$ as compared to UVB-irradiated group and ^{##} $p < 0.01$ as compared to control group.

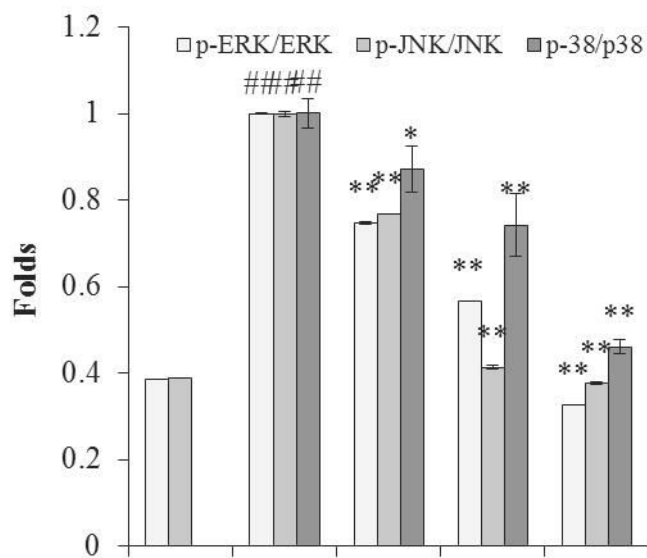
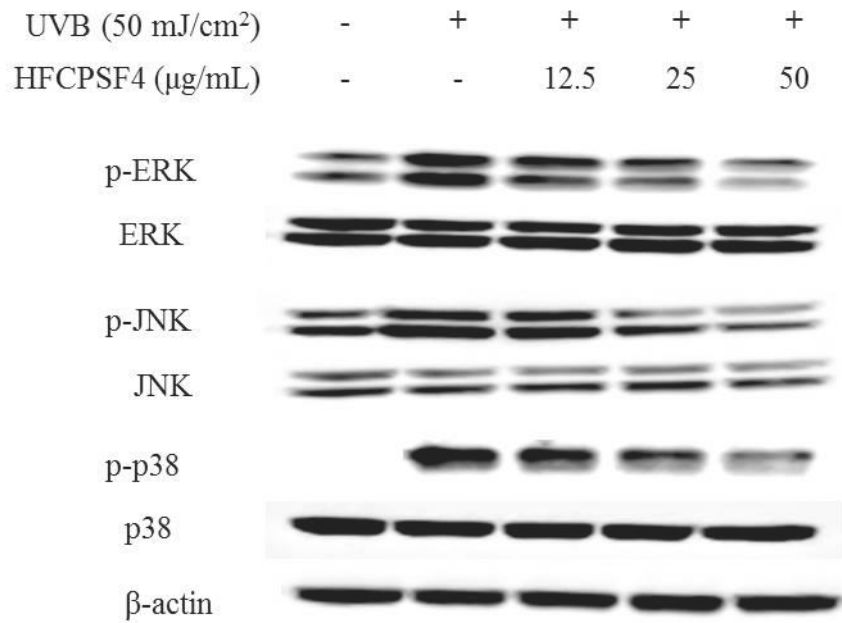


Fig. 76. HFCPSF4 suppresses MAPKs activation in UVB-irradiated HDF cells. The relative amounts of activated MAPKs levels were compared with β-actin. The experiments were conducted triplicate, and the data were expressed as the mean ± standard error (S.E). ** $p < 0.01$ as compared to UVB-irradiated group and ### $p < 0.01$ as compared to control group.

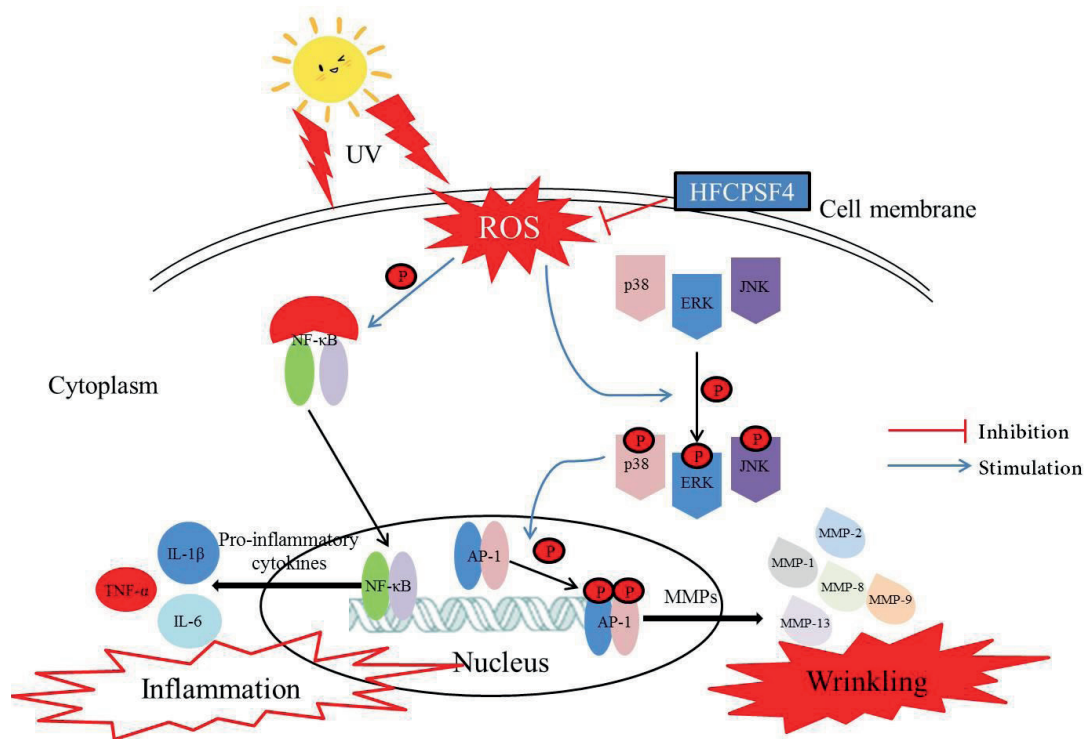


Fig. 77. A schematic model of anti-wrinkle effect of HFCPSF4 in HDF cells.

3. Conclusion

In conclusion, in the present study, the effect of *Hizikia* fucoidan isolated from HFCPS against UVB-induced skin damage *in vitro* in HDF cells was investigated. The results indicate that HFCPSF4 significantly protected collagen synthesis, reduced MMPs and pro-inflammatory expressions in UVB-irradiated HDF cells by regulating NF- κ B, AP-1, and MAPKs signaling pathways. These results suggest that HFCPSF4 possesses strong UV protective effect and has the potential to be used as an ingredient in pharmaceutical and cosmetic industries.

CONCLUSION

The above results suggest *Hizikia* fucoidan possesses strong cosmeceutical effects including antioxidant, anti-inflammatory, whitening, UV protective, and anti-wrinkle activity, and can use as a potential ingredient in pharmaceutical and cosmetic industries.

REFERENCES

1. Heo, S.-J., E.-J. Park, K.-W. Lee and Y.-J. Jeon, *Antioxidant activities of enzymatic extracts from brown seaweeds*. Bioresource Technology, 2005. **96**(14): p. 1613-1623.
2. Nguyen, V.-T., S.-C. Ko, S.-J. Heo, D.-H. Kang, C. Oh, K.-N. Kim, Y.-J. Jeon, Y.-M. Kim, W.S. Park, I.-W. Choi, N.G. Park and W.-K. Jung, *Ciona intestinalis calcitonin-like peptide promotes osteoblast differentiation and mineralization through MAPK pathway in MC3T3-E1 cells*. Process Biochemistry, 2018. **67**: p. 127-138.
3. Fernando, I.P.S., K.K.A. Sanjeeva, Y.-S. Ann, C.-i. Ko, S.-H. Lee, W.W. Lee and Y.-J. Jeon, *Apoptotic and antiproliferative effects of Stigmast-5-en-3-ol from Dendronephthya gigantea on human leukemia HL-60 and human breast cancer MCF-7 cells*. Toxicology in Vitro, 2018. **52**: p. 297-305.
4. Park, C., J.-W. Jeong, D.-S. Lee, M.-J. Yim, J. Lee, M. Han, S. Kim, H.-S. Kim, G.-Y. Kim, E. Park, Y.-J. Jeon, H.-J. Cha and Y. Choi, *Sargassum serratifolium Extract Attenuates Interleukin-1 β -Induced Oxidative Stress and Inflammatory Response in Chondrocytes by Suppressing the Activation of NF- κ B, p38 MAPK, and PI3K/Akt*. International Journal of Molecular Sciences, 2018. **19**(8): p. 2308.
5. Fernando, I.P.S., K.K.A. Sanjeeva, H.-S. Kim, L. Wang, W.W. Lee and Y.-J. Jeon, *Apoptotic and antiproliferative properties of 3 β -hydroxy- Δ 5-steroidal congeners from a partially purified column fraction of Dendronephthya gigantea against HL-60 and MCF-7 cancer cells*. Journal of Applied Toxicology, 2018. **38**(4): p. 527-536.

6. Kumaresan, M., K. Vijai Anand, K. Govindaraju, S. Tamilselvan and V. Ganesh Kumar, *Seaweed Sargassum wightii mediated preparation of zirconia (ZrO₂) nanoparticles and their antibacterial activity against gram positive and gram negative bacteria*. Microbial Pathogenesis, 2018. **124**: p. 311-315.
7. Praiboon, J., S. Palakas, T. Noiraksa and K. Miyashita, *Seasonal variation in nutritional composition and anti-proliferative activity of brown seaweed, Sargassum oligocystum*. J Appl Physiol, 2018. **30**(1): p. 101-111.
8. Ahn, C.-B., Y.-J. Jeon, Y.-T. Kim and J.-Y. Je, *Angiotensin I converting enzyme (ACE) inhibitory peptides from salmon byproduct protein hydrolysate by Alcalase hydrolysis*. Process Biochemistry, 2012. **47**(12): p. 2240-2245.
9. Kang, M.-C., N. Kang, S.-C. Ko, Y.-B. Kim and Y.-J. Jeon, *Anti-obesity effects of seaweeds of Jeju Island on the differentiation of 3T3-L1 preadipocytes and obese mice fed a high-fat diet*. Food Chem Toxicol, 2016. **90**: p. 36-44.
10. Ko, S.-C., J.-K. Lee, H.-G. Byun, S.-C. Lee and Y.-J. Jeon, *Purification and characterization of angiotensin I-converting enzyme inhibitory peptide from enzymatic hydrolysates of Styela clava flesh tissue*. Process Biochemistry, 2012. **47**(1): p. 34-40.
11. Sun, H.-H., W.-J. Mao, Y. Chen, S.-D. Guo, H.-Y. Li, X.-H. Qi, Y.-L. Chen and J. Xu, *Isolation, chemical characteristics and antioxidant properties of the polysaccharides from marine fungus Penicillium sp. F23-2*. Carbohydr Polym, 2009. **78**(1): p. 117-124.
12. Wang, L., Y.-J. Park, Y.-J. Jeon and B. Ryu, *Bioactivities of the edible brown seaweed, Undaria pinnatifida: A review*. Aquaculture, 2018. **495**: p. 873-880.
13. Sun, Z., Z. Dai, W. Zhang, S. Fan, H. Liu, R. Liu and T. Zhao, *12 - Antiobesity, Antidiabetic, Antioxidative, and Antihyperlipidemic Activities of Bioactive*

- Seaweed Substances*, in *Bioactive Seaweeds for Food Applications*, Y. Qin, Editor. 2018, Academic Press. p. 239-253.
14. Ferreira, J., A.A. Ramos, T. Almeida, A. Azqueta and E. Rocha, *Drug resistance in glioblastoma and cytotoxicity of seaweed compounds, alone and in combination with anticancer drugs: A mini review*. *Phytomedicine*, 2018. **48**: p. 84-93.
 15. Sanjeewa, K.K.A., N. Kang, G. Ahn, Y. Jee, Y.-T. Kim and Y.-J. Jeon, *Bioactive potentials of sulfated polysaccharides isolated from brown seaweed *Sargassum spp* in related to human health applications: A review*. *Food Hydrocolloids*, 2018. **81**: p. 200-208.
 16. Fernando, I.P.S., D. Kim, J.-W. Nah and Y.-J. Jeon, *Advances in functionalizing fucoidans and alginates (bio)polymers by structural modifications: A review*. *Chemical Engineering Journal*, 2019. **355**: p. 33-48.
 17. Shanura Fernando, I.P., K.K. Asanka Sanjeewa, K.W. Samarakoon, H.-S. Kim, U.K.D.S.S. Gunasekara, Y.-J. Park, D.T.U. Abeytunga, W.W. Lee and Y.-J. Jeon, *The potential of fucoidans from *Chnoospora minima* and *Sargassum polycystum* in cosmetics: antioxidant, anti-inflammatory, skin-whitening, and antiwrinkle activities*. *J Appl Physiol*, 2018.
 18. Fernando, I.P.S., K.K.A. Sanjeewa, S.-Y. Kim, J.-S. Lee and Y.-J. Jeon, *Reduction of heavy metal (Pb²⁺) biosorption in zebrafish model using alginic acid purified from *Ecklonia cava* and two of its synthetic derivatives*. *International Journal of Biological Macromolecules*, 2018. **106**: p. 330-337.
 19. Fernando, I.P.S., T.U. Jayawardena, K.K.A. Sanjeewa, L. Wang, Y.-J. Jeon and W.W. Lee, *Anti-inflammatory potential of alginic acid from *Sargassum horneri**

- against urban aerosol-induced inflammatory responses in keratinocytes and macrophages. Ecotoxicology and Environmental Safety, 2018. 160: p. 24-31.*
20. Asanka Sanjeeva, K.K., W.W. Lee, J.-I. Kim and Y.-J. Jeon, *Exploiting biological activities of brown seaweed Ishige okamurae Yendo for potential industrial applications: a review. J Appl Physiol, 2017. 29(6): p. 3109-3119.*
 21. Lee, J.-H., J.-Y. Ko, E.-A. Kim, E.-K. Hwang, C.S. Park, J.-S. Lee, C.-Y. Kim, H.-S. Lee, H.-K. Kang, S.-H. Cha and Y.-J. Jeon, *Identification and large isolation of an anti-inflammatory compound from an edible brown seaweed, Undariopsis peterseniana, and evaluation on its anti-inflammatory effect in in vitro and in vivo zebrafish. J Appl Physiol, 2017. 29(3): p. 1587-1596.*
 22. De Souza, É.T., D. Pereira de Lira, A. Cavalcanti de Queiroz, D.J. Costa da Silva, A. Bezerra de Aquino, E. Campessato Mella, V. Prates Lorenzo, G.E. De Miranda, J.X. De Araújo-Júnior, M.C. De Oliveira Chaves, J.M. Barbosa-Filho, P. Filgueiras de Athayde-Filho, B.V. De Oliveira Santos and M.S. Alexandre-Moreira, *The Antinociceptive and Anti-Inflammatory Activities of Caulerpin, a Bisindole Alkaloid Isolated from Seaweeds of the Genus Caulerpa. Marine Drugs, 2009. 7(4): p. 689.*
 23. Heo, S.-J. and Y.-J. Jeon, *Protective effect of fucoxanthin isolated from Sargassum siliquastrum on UV-B induced cell damage. Journal of Photochemistry and Photobiology B: Biology, 2009. 95(2): p. 101-107.*
 24. Wijesinghe, W.A.J.P., Y. Athukorala and Y.-J. Jeon, *Effect of anticoagulative sulfated polysaccharide purified from enzyme-assistant extract of a brown seaweed Ecklonia cava on Wistar rats. Carbohydr Polym, 2011. 86(2): p. 917-921.*

25. Kang, M.-C., G. Ahn, X. Yang, K.-N. Kim, S.-M. Kang, S.-H. Lee, S.-C. Ko, J.-Y. Ko, D. Kim, Y.-T. Kim, Y. Jee, S.-J. Park and Y.-J. Jeon, *Hepatoprotective effects of dieckol-rich phlorotannins from Ecklonia cava, a brown seaweed, against ethanol induced liver damage in BALB/c mice*. Food Chem Toxicol, 2012. **50**(6): p. 1986-1991.
26. Hou, X. and X. Yan, *Study on the concentration and seasonal variation of inorganic elements in 35 species of marine algae*. Science of The Total Environment, 1998. **222**(3): p. 141-156.
27. Romarís-Hortas, V., A. Moreda-Piñeiro and P. Bermejo-Barrera, *Microwave assisted extraction of iodine and bromine from edible seaweed for inductively coupled plasma-mass spectrometry determination*. Talanta, 2009. **79**(3): p. 947-952.
28. Kumar, K.S., K. Ganesan and P.V.S. Rao, *Antioxidant potential of solvent extracts of Kappaphycus alvarezii (Doty) Doty – An edible seaweed*. Food Chemistry, 2008. **107**(1): p. 289-295.
29. Zhao, Y., J. Wu, D. Shang, J. Ning, Y. Zhai, X. Sheng and H. Ding, *Subcellular distribution and chemical forms of cadmium in the edible seaweed, Porphyra yezoensis*. Food Chemistry, 2015. **168**: p. 48-54.
30. Sundbæk, K.B., I.D.W. Koch, C.G. Villaro, N.S. Rasmussen, S.L. Holdt and N.B. Hartmann, *Sorption of fluorescent polystyrene microplastic particles to edible seaweed Fucus vesiculosus*. J Appl Physiol, 2018.
31. Liu, D., J.K. Keesing, Z. Dong, Y. Zhen, B. Di, Y. Shi, P. Fearn and P. Shi, *Recurrence of the world's largest green-tide in 2009 in Yellow Sea, China: Porphyra yezoensis aquaculture rafts confirmed as nursery for macroalgal blooms*. Marine Pollution Bulletin, 2010. **60**(9): p. 1423-1432.

32. Hay, C.H. and P.A. Luckens, *The Asian kelp Undaria pinnatifida (Phaeophyta: Laminariales) found in a New Zealand harbour*. New Zealand Journal of Botany, 1987. **25**(2): p. 329-332.
33. Wang, L., J.Y. Oh, H.S. Kim, W. Lee, Y. Cui, H.G. Lee, Y.-T. Kim, J.Y. Ko and Y.-J. Jeon, *Protective effect of polysaccharides from Celluclast-assisted extract of Hizikia fusiforme against hydrogen peroxide-induced oxidative stress in vitro in Vero cells and in vivo in zebrafish*. International Journal of Biological Macromolecules, 2018. **112**: p. 483-489.
34. Fernandes, F., M. Barbosa, D.M. Pereira, I. Sousa-Pinto, P. Valentão, I.C. Azevedo and P.B. Andrade, *Chemical profiling of edible seaweed (Ochrophyta) extracts and assessment of their in vitro effects on cell-free enzyme systems and on the viability of glutamate-injured SH-SY5Y cells*. Food Chem Toxicol, 2018. **116**: p. 196-206.
35. Kang, J.Y., M.N.A. Khan, N.H. Park, J.Y. Cho, M.C. Lee, H. Fujii and Y.K. Hong, *Antipyretic, analgesic, and anti-inflammatory activities of the seaweed Sargassum fulvellum and Sargassum thunbergii in mice*. Journal of Ethnopharmacology, 2008. **116**(1): p. 187-190.
36. Lee, J.-B., Y. Ohta, K. Hayashi and T. Hayashi, *Immunostimulating effects of a sulfated galactan from Codium fragile*. Carbohydrate Research, 2010. **345**(10): p. 1452-1454.
37. Lee, S.A., S.-M. Moon, Y.H. Choi, S.H. Han, B.-R. Park, M.S. Choi, J.-S. Kim, Y.H. Kim, D.K. Kim and C.S. Kim, *Aqueous extract of Codium fragile suppressed inflammatory responses in lipopolysaccharide-stimulated RAW264.7 cells and carrageenan-induced rats*. Biomedicine & Pharmacotherapy, 2017. **93**: p. 1055-1064.

38. Wang, L., W. Lee, J. Oh, Y. Cui, B. Ryu and Y.-J. Jeon, *Protective Effect of Sulfated Polysaccharides from Celluclast-Assisted Extract of Hizikia fusiforme Against Ultraviolet B-Induced Skin Damage by Regulating NF- κ B, AP-1, and MAPKs Signaling Pathways In Vitro in Human Dermal Fibroblasts*. *Marine Drugs*, 2018. **16**(7): p. 239.
39. Chemists, A.A. and W. Horwitz, *Official methods of analysis*. Vol. I. 15th ed. AOAC, Arlington, VA, 1990.
40. Chandler, S.F. and J.H. Dodds, *The effect of phosphate, nitrogen and sucrose on the production of phenolics and solasodine in callus cultures of solanum laciniatum*. *Plant Cell Reports*, 1983. **2**(4): p. 205-208.
41. Heo, S.-J., S.-C. Ko, S.-H. Cha, D.-H. Kang, H.-S. Park, Y.-U. Choi, D. Kim, W.-K. Jung and Y.-J. Jeon, *Effect of phlorotannins isolated from Ecklonia cava on melanogenesis and their protective effect against photo-oxidative stress induced by UV-B radiation*. *Toxicology in Vitro*, 2009. **23**(6): p. 1123-1130.
42. Kang, S.-M., S.-J. Heo, K.-N. Kim, S.-H. Lee, H.-M. Yang, A.-D. Kim and Y.-J. Jeon, *Molecular docking studies of a phlorotannin, dieckol isolated from Ecklonia cava with tyrosinase inhibitory activity*. *Bioorganic & Medicinal Chemistry*, 2012. **20**(1): p. 311-316.
43. Kraunsoe, J.A., T.D. Claridge and G. Lowe, *Inhibition of human leukocyte and porcine pancreatic elastase by homologues of bovine pancreatic trypsin inhibitor*. *Biochemistry*, 1996. **35**(28): p. 9090-9096.
44. Wang, L., B. Ryu, W.-S. Kim, G.H. Kim and Y.-J. Jeon, *Protective effect of gallic acid derivatives from the freshwater green alga *Spirogyra* sp. against ultraviolet B-induced apoptosis*

- through reactive oxygen species clearance in human keratinocytes and zebrafish*. *Algae*, 2017. **32**(4): p. 379-388.
45. Kang, M.-C., S.Y. Kim, Y.T. Kim, E.-A. Kim, S.-H. Lee, S.-C. Ko, W.A.J.P. Wijesinghe, K.W. Samarakoon, Y.-S. Kim, J.H. Cho, H.-S. Jang and Y.-J. Jeon, *In vitro and in vivo antioxidant activities of polysaccharide purified from aloe vera (Aloe barbadensis) gel*. *Carbohyd Polym*, 2014. **99**: p. 365-371.
46. Kim, S.-Y., E.-A. Kim, Y.-S. Kim, S.-K. Yu, C. Choi, J.-S. Lee, Y.-T. Kim, J.-W. Nah and Y.-J. Jeon, *Protective effects of polysaccharides from Psidium guajava leaves against oxidative stresses*. *International Journal of Biological Macromolecules*, 2016. **91**: p. 804-811.
47. United Nations Scientific Committee on the Effects of Atomic, R., J.-Y. Oh, I.P. Shanura Fernando and Y.-J. Jeon, *Potential applications of radioprotective phytochemicals from marine algae*. *Algae*, 2016. **31**(4): p. 403-414.
48. Sanjeewa, K.K.A., I.P.S. Fernando, K.W. Samarakoon, H.H.C. Lakmal, E.-A. Kim, O.N. Kwon, M.G. Dilshara, J.-B. Lee and Y.-J. Jeon, *Anti-inflammatory and anti-cancer activities of sterol rich fraction of cultured marine microalga <italic>Nannochloropsis oculata</italic>*. *Algae*, 2016. **31**(3): p. 277-287.
49. Kang, N., S.-Y. Kim, S. Rho, J.-Y. Ko and Y.-J. Jeon, *Anti-fatigue activity of a mixture of seahorse (Hippocampus abdominalis) hydrolysate and red ginseng*. *Fisheries and Aquatic Sciences*, 2017. **20**(1): p. 3.
50. Lee, S.-H., C.-I. Ko, Y. Jee, Y. Jeong, M. Kim, J.-S. Kim and Y.-J. Jeon, *Anti-inflammatory effect of fucoidan extracted from Ecklonia cava in zebrafish model*. *Carbohyd Polym*, 2013. **92**(1): p. 84-89.
51. Ahn, G., S.J. Bing, S.-M. Kang, W.-W. Lee, S.-H. Lee, H. Matsuda, A. Tanaka, I.-H. Cho, Y.-J. Jeon and Y. Jee, *The JNK/NFκB pathway is required to activate*

- murine lymphocytes induced by a sulfated polysaccharide from Ecklonia cava*. Biochimica et Biophysica Acta (BBA) - General Subjects, 2013. **1830**(3): p. 2820-2829.
52. Ahn, G., W. Lee, K.-N. Kim, J.-H. Lee, S.-J. Heo, N. Kang, S.-H. Lee, C.-B. Ahn and Y.-J. Jeon, *A sulfated polysaccharide of Ecklonia cava inhibits the growth of colon cancer cells by inducing apoptosis*. EXCLI journal, 2015. **14**: p. 294-306.
53. Lee, J.-H., H.-H. Kim, J.-Y. Ko, J.-H. Jang, G.-H. Kim, J.-S. Lee, J.-W. Nah and Y.-J. Jeon, *Rapid preparation of functional polysaccharides from Pyropia yezoensis by microwave-assistant rapid enzyme digest system*. Carbohydr Polym, 2016. **153**: p. 512-517.
54. Choi, E.-Y., H.-J. Hwang, I.-H. Kim and T.-J. Nam, *Protective effects of a polysaccharide from Hizikia fusiformis against ethanol toxicity in rats*. Food Chem Toxicol, 2009. **47**(1): p. 134-139.
55. Choi, E.-Y., H.-J. Hwang and T.-J. Nam, *Protective effect of a polysaccharide from Hizikia fusiformis against ethanol-induced cytotoxicity in IEC-6 cells*. Toxicology in Vitro, 2010. **24**(1): p. 79-84.
56. Jeong, S.C., Y.T. Jeong, S.M. Lee and J.H. Kim, *Immune-modulating activities of polysaccharides extracted from brown algae Hizikia fusiforme*. Bioscience, Biotechnology, and Biochemistry, 2015. **79**(8): p. 1362-1365.
57. Chemists, A.o.O.A., *Official methods of analysis of the Association of Official Analytical Chemists*. Vol. 1. 1990: The Association.
58. Kang, S.-M., K.-N. Kim, S.-H. Lee, G. Ahn, S.-H. Cha, A.-D. Kim, X.-D. Yang, M.-C. Kang and Y.-J. Jeon, *Anti-inflammatory activity of polysaccharide*

- purified from AMG-assistant extract of Ecklonia cava in LPS-stimulated RAW 264.7 macrophages. Carbohydr Polym, 2011. 85(1): p. 80-85.*
59. Wang, L., M.-J. Jo, R. Katagiri, K. Harata, M. Ohta, A. Ogawa, M. Kamegai, Y. Ishida, S. Tanoue, S. Kimura, S.-C. Lee and Y.-J. Jeon, *Antioxidant effects of citrus pomace extracts processed by super-heated steam. LWT, 2018. 90: p. 331-338.*
 60. Wijesinghe, W.A.J.P., Y.J. Jeon, P. Ramasamy, M.E.A. Wahid and C.S. Vairappan, *Anticancer activity and mediation of apoptosis in human HL-60 leukaemia cells by edible sea cucumber (Holothuria edulis) extract. Food Chemistry, 2013. 139(1): p. 326-331.*
 61. Kim, E.-A., S.-H. Lee, C.-i. Ko, S.-H. Cha, M.-C. Kang, S.-M. Kang, S.-C. Ko, W.-W. Lee, J.-Y. Ko, J.-H. Lee, N. Kang, J.-Y. Oh, G. Ahn, Y.H. Jee and Y.-J. Jeon, *Protective effect of fucoidan against AAPH-induced oxidative stress in zebrafish model. Carbohydr Polym, 2014. 102: p. 185-191.*
 62. Heo, S.-J., W.-J. Yoon, K.-N. Kim, G.-N. Ahn, S.-M. Kang, D.-H. Kang, A. affan, C. Oh, W.-K. Jung and Y.-J. Jeon, *Evaluation of anti-inflammatory effect of fucoxanthin isolated from brown algae in lipopolysaccharide-stimulated RAW 264.7 macrophages. Food Chem Toxicol, 2010. 48(8): p. 2045-2051.*
 63. Lee, S.-H., C.-I. Ko, G. Ahn, S. You, J.-S. Kim, M.S. Heu, J. Kim, Y. Jee and Y.-J. Jeon, *Molecular characteristics and anti-inflammatory activity of the fucoidan extracted from Ecklonia cava. Carbohydr Polym, 2012. 89(2): p. 599-606.*
 64. Fernando, I.P.S., J.-W. Nah and Y.-J. Jeon, *Potential anti-inflammatory natural products from marine algae. Environmental Toxicology and Pharmacology, 2016. 48: p. 22-30.*

65. Kim, K.-N., Y.-J. Ko, M.-C. Kang, H.-M. Yang, S.W. Roh, T. Oda, Y.-J. Jeon, W.-K. Jung, S.-J. Heo, W.-J. Yoon and D. Kim, *Anti-inflammatory effects of trans-1,3-diphenyl-2,3-epoxypropane-1-one mediated by suppression of inflammatory mediators in LPS-stimulated RAW 264.7 macrophages*. Food Chem Toxicol, 2013. **53**: p. 371-375.
66. Kim, K.-N., H.-M. Yang, S.-M. Kang, D. Kim, G. Ahn and Y.-J. Jeon, *Octaphlorethol A isolated from Ishige foliacea inhibits α -MSH-stimulated induced melanogenesis via ERK pathway in B16F10 melanoma cells*. Food Chem Toxicol, 2013. **59**: p. 521-526.
67. Yang, H.-M., Y.-M. Ham, W.-J. Yoon, S.W. Roh, Y.-J. Jeon, T. Oda, S.-M. Kang, M.-C. Kang, E.-A. Kim, D. Kim and K.-N. Kim, *Quercitrin protects against ultraviolet B-induced cell death in vitro and in an in vivo zebrafish model*. Journal of Photochemistry and Photobiology B: Biology, 2012. **114**: p. 126-131.
68. Kim, E.-A., S.-Y. Kim, J. Kim, J.-Y. Oh, H.-S. Kim, W.-J. Yoon, D.-H. Kang and S.-J. Heo, *Tuberatolide B isolated from Sargassum macrocarpum inhibited LPS-stimulated inflammatory response via MAPKs and NF- κ B signaling pathway in RAW264.7 cells and zebrafish model*. Journal of Functional Foods, 2019. **52**: p. 109-115.
69. Heo, S.-J., S.-C. Ko, S.-M. Kang, S.-H. Cha, S.-H. Lee, D.-H. Kang, W.-K. Jung, A. Affan, C. Oh and Y.-J. Jeon, *Inhibitory effect of diphlorethohydroxycarmalol on melanogenesis and its protective effect against UV-B radiation-induced cell damage*. Food Chem Toxicol, 2010. **48**(5): p. 1355-1361.

70. Lee, S.-H., J.-S. Han, S.-J. Heo, J.-Y. Hwang and Y.-J. Jeon, *Protective effects of dieckol isolated from Ecklonia cava against high glucose-induced oxidative stress in human umbilical vein endothelial cells*. *Toxicology in Vitro*, 2010. **24**(2): p. 375-381.
71. Yang, X., S.-M. Kang, B.-T. Jeon, Y.-D. Kim, J.-H. Ha, Y.-T. Kim and Y.-J. Jeon, *Isolation and identification of an antioxidant flavonoid compound from citrus-processing by-product*. *Journal of the Science of Food and Agriculture*, 2011. **91**(10): p. 1925-1927.
72. Fernando, I.P.S., K.K.A. Sanjeewa, K.W. Samarakoon, W.W. Lee, H.-S. Kim and Y.-J. Jeon, *Squalene isolated from marine macroalgae Caulerpa racemosa and its potent antioxidant and anti-inflammatory activities*. *Journal of Food Biochemistry*, 2018. **42**(5): p. e12628.
73. Shanura Fernando, I.P., K.K. Asanka Sanjeewa, K.W. Samarakoon, W.W. Lee, H.-S. Kim, E.-A. Kim, U.K.D.S.S. Gunasekara, D.T.U. Abeyunga, C. Nanayakkara, E.D. de Silva, H.-S. Lee and Y.-J. Jeon, *FTIR characterization and antioxidant activity of water soluble crude polysaccharides of Sri Lankan marine algae*. *Algae*, 2017. **32**(1): p. 75-86.
74. Kim, H.-S., W. Lee, J.-H. Lee, K.K.A. Sanjeewa, I.P.S. Fernando, S.-C. Ko, S.-H. Lee, Y.-T. Kim and Y.-J. Jeon, *Purification and Identification of an Antioxidative Peptide from Digestive Enzyme Hydrolysis of Cutlassfish Muscle*. *Journal of Aquatic Food Product Technology*, 2018. **27**(8): p. 934-944.
75. Suganuma, K., H. Nakajima, M. Ohtsuki and G. Imokawa, *Astaxanthin attenuates the UVA-induced up-regulation of matrix-metalloproteinase-1 and skin fibroblast elastase in human dermal fibroblasts*. *Journal of Dermatological Science*, 2010. **58**(2): p. 136-142.

76. Fisher, G.J., S. Kang, J. Varani, Z. Bata-Csorgo, Y. Wan, S. Datta and J.J. Voorhees, *Mechanisms of photoaging and chronological skin aging*. Archives of dermatology, 2002. **138**(11): p. 1462-1470.
77. Longstreth, J., F. De Gruijl, M. Kripke, S. Abseck, F. Arnold, H. Slaper, G. Velders, Y. Takizawa and J. Van der Leun, *Health risks*. Journal of Photochemistry and Photobiology B: Biology, 1998. **46**(1-3): p. 20-39.
78. Tanaka, K., J. Hasegawa, K. Asamitsu and T. Okamoto, *Magnolia ovovata extract and its active component magnolol prevent skin photoaging via inhibition of nuclear factor κ B*. Eur J Pharmacol, 2007. **565**(1): p. 212-219.
79. Ryu, B., B.-N. Ahn, K.-H. Kang, Y.-S. Kim, Y.-X. Li, C.-S. Kong, S.-K. Kim and D.G. Kim, *Dioxinohydroeckol protects human keratinocyte cells from UVB-induced apoptosis modulated by related genes Bax/Bcl-2 and caspase pathway*. Journal of Photochemistry and Photobiology B: Biology, 2015. **153**: p. 352-357.
80. Pathak, M.A. and D.L. Fanselow, *Photobiology of melanin pigmentation: Dose/response of skin to sunlight and its contents*. Journal of the American Academy of Dermatology, 1983. **9**(5): p. 724-733.
81. Wang, L., B. Ryu, W.-S. Kim, G.H. Kim and Y.-J. Jeon, *Protective effect of gallic acid derivatives from the freshwater green alga Spirogyra sp. against ultraviolet B-induced apoptosis through reactive oxygen species clearance in human keratinocytes and zebrafish*. ALGAE, 2017. **32**(4): p. 379-388.
82. Katiyar, S.K., B.M. Bergamo, P.K. Vyalil and C.A. Elmetts, *Green tea polyphenols: DNA photodamage and photoimmunology*. Journal of Photochemistry and Photobiology B: Biology, 2001. **65**(2): p. 109-114.

83. Pallela, R., Y. Na-Young and S.-K. Kim, *Anti-photoaging and photoprotective compounds derived from marine organisms*. *Marine drugs*, 2010. **8**(4): p. 1189-1202.
84. Adil, M.D., P. Kaiser, N.K. Satti, A.M. Zargar, R.A. Vishwakarma and S.A. Tasduq, *Effect of Emblica officinalis (fruit) against UVB-induced photo-aging in human skin fibroblasts*. *Journal of Ethnopharmacology*, 2010. **132**(1): p. 109-114.
85. Thomas, N.V. and S.-K. Kim, *Metalloproteinase inhibitors: status and scope from marine organisms*. *Biochemistry research international*, 2010. **2010**.
86. Athukorala, Y., K.-N. Kim and Y.-J. Jeon, *Antiproliferative and antioxidant properties of an enzymatic hydrolysate from brown alga, Ecklonia cava*. *Food Chem Toxicol*, 2006. **44**(7): p. 1065-1074.
87. Sanjeeva, K.K.A., I.P.S. Fernando, S.-Y. Kim, H.-S. Kim, G. Ahn, Y. Jee and Y.-J. Jeon, *In vitro and in vivo anti-inflammatory activities of high molecular weight sulfated polysaccharide; containing fucose separated from Sargassum horneri: Short communication*. *International Journal of Biological Macromolecules*, 2018. **107**: p. 803-807.
88. Ahn, G.-N., K.-N. Kim, S.-H. Cha, C.-B. Song, J. Lee, M.-S. Heo, I.-K. Yeo, N.-H. Lee, Y.-H. Jee, J.-S. Kim, M.-S. Heu and Y.-J. Jeon, *Antioxidant activities of phlorotannins purified from Ecklonia cava on free radical scavenging using ESR and H₂O₂-mediated DNA damage*. *European Food Research and Technology*, 2007. **226**(1): p. 71-79.
89. SHAHIDI, F., J. KAMIL, Y.-J. JEON and S.-K. KIM, *ANTIOXIDANT ROLE OF CHITOSAN IN A COOKED COD (GADUS MORHUA) MODEL SYSTEM*. *Journal of Food Lipids*, 2002. **9**(1): p. 57-64.

90. Baird, L. and A.T. Dinkova-Kostova, *The cytoprotective role of the Keap1–Nrf2 pathway*. Archives of Toxicology, 2011. **85**(4): p. 241-272.
91. Loboda, A., M. Damulewicz, E. Pyza, A. Jozkowicz and J. Dulak, *Role of Nrf2/HO-1 system in development, oxidative stress response and diseases: an evolutionarily conserved mechanism*. Cellular and Molecular Life Sciences, 2016. **73**(17): p. 3221-3247.
92. Kim, K.-N., Y.-J. Ko, H.-M. Yang, Y.-M. Ham, S.W. Roh, Y.-J. Jeon, G. Ahn, M.-C. Kang, W.-J. Yoon, D. Kim and T. Oda, *Anti-inflammatory effect of essential oil and its constituents from fingered citron (*Citrus medica* L. var. *sarcodactylis*) through blocking JNK, ERK and NF- κ B signaling pathways in LPS-activated RAW 264.7 cells*. Food Chem Toxicol, 2013. **57**: p. 126-131.
93. Ko, S.-C. and Y.-J. Jeon, *Anti-inflammatory effect of enzymatic hydrolysates from *Styela clava* flesh tissue in lipopolysaccharide-stimulated RAW 264.7 macrophages and in vivo zebrafish model*. Nutr Res Pract, 2015. **9**(3): p. 219-226.
94. Cheong, S.H., H.-W. Yang, E.-Y. Ko, G. Ahn, W. Lee, D. Kim, Y.-J. Jeon and K.-N. Kim, *Anti-inflammatory effects of trans-1,3-diphenyl-2,3-epoxypropane-1-one in zebrafish embryos in vivo model*. Fish & Shellfish Immunology, 2016. **50**: p. 16-20.
95. Asanka Sanjeeva, K.K., Y.-j. Park, I.P. Shanura Fernando, Y.-S. Ann, C.-I. Ko, L. Wang, Y.-J. Jeon and W. Lee, *Soft corals collected from Jeju Island inhibits the α -MSH-induced melanogenesis in B16F10 cells through activation of ERK*. Fisheries and Aquatic Sciences, 2018. **21**(1): p. 21.

96. Ko, S.-C., S.-H. Cha, S.-J. Heo, S.-H. Lee, S.-M. Kang and Y.-J. Jeon, *Protective effect of Ecklonia cava on UVB-induced oxidative stress: in vitro and in vivo zebrafish model*. J Appl Physiol, 2011. **23**(4): p. 697-708.
97. Kang, G.-J., S.-C. Han, Y.-S. Koh, H.-K. Kang, Y.-J. Jeon and E.-S. Yoo, *Diphlorethohydroxycarmalol, Isolated from Ishige okamurae, Increases Prostaglandin E2 through the Expression of Cyclooxygenase-1 and -2 in HaCaT Human Keratinocytes*. Biomolecules & therapeutics, 2012. **20**(6): p. 520-525.
98. Yeo, I., Y.-J. Lee, K. Song, H.-S. Jin, J.-E. Lee, D. Kim, D.-W. Lee and N.J. Kang, *Low-molecular weight keratins with anti-skin aging activity produced by anaerobic digestion of poultry feathers with Fervidobacterium islandicum AW-1*. Journal of Biotechnology, 2018. **271**: p. 17-25.

ACKNOWLEDGEMENT

First and foremost, I would like to express my most sincere thanks and gratitude to my supervisor, professor You-Jin Jeon, Department of Marine Life Sciences, Jeju National University, Jeju, Korea. He is always kindly guidance, help, and understanding me. And his high academic level and wonderful life experience encouraged me to keep moving forward. During my Ph.D. course period in Jeju National University, I have adored my supervisor as a great advisor. It is really my great honor as a student supervised by him.

In addition, I would like to thank my parents, family members, and all of my relatives for their love, care, and support. I want to thank my parents for their effort to take good care of me since birth. They at their best tried to give me all the finest things that they can afford, for my well-being.

Secondly, I would like to extend my thanks and gratitude to Dr. Yong Li, Changchun University of Chinese Medicine, Changchun, China. Thanks for him kindly recommending me to working under Prof. You-Jin Jeon. Also, I would like to thank Prof. Zhihong Wang, Prof. Peng Yu, Dr. Ye Wang, Dr. Na Li, Changchun University of Chinese Medicine, Changchun, China, and Prof. Guirong Zhang, Jilin University, Changchun, China. Thanks for their help, believe and the academic guidance. In addition, I would like to extend my thanks and gratitude to Prof. Xiaoting Fu, Prof. Haijin Mou, Prof. Hong Lin, Ocean University of China, Qingdao, China. Thanks for their trust and help in my career.

Thirdly, I would like to thank my colleagues, Dr. WonWoo Lee, Dr. BoMi Ryu, Dr. Min-Cheol Kang, Dr. Ji-Heyok Lee, Dr. Ju Young Ku, Dr. Eun-A Kim, Dr. Jea Young Oh, Dr. Nalse Kang, Dr. Shanura Fernando, Dr. Seo Young Kim, Dr. Hyun Soo Kim, Ms. Hye-Won Yang, Mr. Geon Jun Je, Mr. Ji Min Hyun, Ms. Jin Hwang, Mr.

Hyogeun Lee, Mr. Asanka Sanjeewa, Mr. Thilina U. Jayawardena, Ms. Hurini Fernando, Mr. Yoon Teak Kim, Mr. Hyoung Ho Kim, Mr. Baro Kim, Mr. H.H. Chaminda Lakmal, Mr. Yulin Dai, Mr. Yunfei Jiang, Ms. Xining Li, and Ms. Yu An Lu. Thanks for their help in my research work and my daily life in Korea.

Last but not least, I would like to express my grateful appreciation to my Chinese friends which know each other in Korea. Namely Sheng Piao, Xin Zhang, Jiamei Cui, Bowei Yan, Zhenyu Zhong, Wenhao Shi, Xiateng Hu, Fengkai Wang, Mengyan Fang, Ye Tian, and Sujuan Jin; Shuo He, Mengke Chang, Zetian Wang, Yi Li, Tian Hang, and Xiaoxuan Huang; Meishan Piao, Guoqing Wang, Hui Liu, Yue Yin, Peiyan Wu, Heli Wang, and Liyuan Jing; Zhen Liu, Hao Yu, Ya Zhang, Lei Song, Yang Zhao, Bo Zhao, Zhifang Zuo, Hongyu Li, Aoxuan Zhen and others. Thanks for their accompanying me and for the unforgettable times and memories in this foreign land.

Thanks a lot.

Lei Wang

Jeju National University

Republic of Korea

February, 2019